GIS-Based Modeling of Shallow Groundwater Potential in Arid Regions under changing Climate and Future Water Demands: a case study of Al-Madinah, Saudi Arabia.

Ohood Ayid Alharbi

PhD

University of York

Environment and Geography

February 2024

Abstract

Investigating water resources in arid regions is essential for managing water scarcity's unique challenges in these environments. GIS and remote sensing approaches have been applied here to model and analyse three main aspects: mapping potential groundwater zones, assessing climate change impacts, and examining future water needs under socio-economic scenarios.

A fuzzy-frequency ratio model and a logistic regression model successfully delineated the potential groundwater zones. An ensemble of models performed well (Best model AUC = 0.943). Soil type was the most important factor in driving both models. The spatial distribution of very high potential groundwater areas in Al-Madinah is primarily compatible with volcanic lava areas with Lithosols and Calcic Yermosols soils.

Assessing climate change under IPCC RCPs scenarios (2021-2100, RCP4.5 and RCP8.5) revealed that the temperature and Reference Evapotranspiration (ET0) rate of Al-Madinah is expected to continue to increase although rainfall may also increase by around 18.74% or 22.81 mm (2081-2100, RCP8.5) compared to 1970-2018. Such an increase might not have a pronounced effect on enhancing groundwater availability due to raising temperature (2°C) and ET0 (359.70 mm) with a higher probability of drought events indicated by the Standardised Precipitation Evapotranspiration Index (SPEI). Increases with higher water accumulation opportunities are predicted at 2081-2100 (RCP8.5). However, changes in potential groundwater zones using the Topographic Wetness Index (TWI) weighted by Rainfall are expected to show a small quantitative increase with the greatest addition of suitable potential zones also estimated for 2081-2100 under RCP8.5 (logistic regression = 19296km²)

Analysing water needs in Al-Madinah city under the Impact of Population, Affluence, and Technology (IPAT) model confirmed that population was the most important factor in explaining water consumption trends. Water demand is projected to increase by up to 28% under IPCC_ SSP scenarios. These findings should aid in developing water resources management strategies and sustainable decision-making.

TABLE OF CONTENTS

List of Figures

List of Tables

Acknowledgements

First and foremost, I am grateful to ALLAH for health and well-being and for providing me with the strength and perseverance to complete this thesis.

Completing this PhD thesis has been a monumental undertaking, and I am profoundly grateful to many individuals and institutions that have supported me along the way. I would like to express my deepest appreciation to my supervisors, Dr Colin McClean and Dr Marco Sakai, for their unwavering support, guidance, and feedback throughout my PhD journey. Their expertise, patience, and encouragement have played a pivotal role in moulding and refining this academic work. I am very grateful to Dr Colin for his technical support in my study and for teaching me, particularly in coding in R.

I take this opportunity to express gratitude to the Ministry of Environment, Water and Agriculture in Saudi Arabia for providing the necessary data. I would also like to acknowledge the Ministry of Education in Saudi Arabia, represented by King Abdulaziz University, for the scholarship and generous financial support that allowed me to realize my academic aspirations with determination and ambition.

To my beloved family, my husband and my kids, words cannot sufficiently convey the depth of my appreciation for your endless love, understanding, and sacrifices. Your persistent belief in me and your motivation has been a constant source of strength. I am incredibly grateful for your unwavering support. I extend my heartfelt thanks to all those who have helped me with this thesis, directly or indirectly and enriched my academic journey. I sincerely appreciate your contributions to this milestone in my academic journey.

Declaration

I declare that this thesis is a presentation of original work, and I am the sole author. This work has not previously been presented for an award at this, or any other, University. All sources are acknowledged as References.

List of Abbreviations

ASAR	Arid-Semi Arid Region
BCM	Billion Cubic Meters
BLR	Binary logistic regression
CMIP6	Climate Model Intercomparison Project
ET0	Reference Evapotranspiration
FAO	The Food and Agricultural Organization
FL	Fuzzy Logic
FR	Frequency Ratio
GASTAT	General Authority for Statistics
GCM	Global Climate Model
GDP	Gross Domestic Product
GDP_PC	Gross Domestic Product Per Capita
GIS	Geographic Information System
GWPZ	GroundWater Potential Zones
IPAT	Impact of Population, Affluence, and Technology
IPCC	Intergovernmental Panel on Climate Change
LULC	Land Use/Land Cover
MCDA	Multi-Criteria Decision-Making method
MCM	Million Cubic Meter
MEIMR	Ministry of Energy, Industry and Mineral Resources
MEWA	Ministry of Environment, Water and Agriculture
MOMRA	Ministry of Municipal and Rural Affairs
MWE	Ministry of Water & Electricity
OLS	Ordinary Least Squares
PLS	Partial Least Squares
PPM	Parts Per Million
RCP	Representative Concentration Pathways
RF	Random Forest
ROC-AUC	The Area Under Curve of the Relative Operating Characteristics Curve
RS	Remote Sensing
SAGIA	Saudi Arabian General Investment Authority
SEM	Simple Ensemble Mean
SPEI	Standardised Precipitation Evapotranspiration Index
SPI	Stream Power Index
SSPs	Shared Socio-economic Pathways
SWPC	Saudi Water Partnership Company
TWI	Topographic Wetness Index
VIP	The variables' importance in the projection

Chapter 1 Introduction

1.1 A brief overview of global groundwater

Water is the most prevalent liquid on the earth's surface at 71%, where 97.5 % is oceans, and freshwater constitutes only 2.5%; it was estimated that about two-thirds are lakes, ice caps and glacier conditions and one-third is groundwater resources (Margat and Van der Gun, 2013). Generally, groundwater is present in aquifers located in subsurface geological formations that store and transmit water (Margat and Van der Gun, 2013). The groundwater system could be categorised by hydraulic state comprising unconfined aquifers without impermeable layers, confined aquifers located between impermeable layers and semiconfined aquifers, as well as classified geologically including, for example, karst aquifers, alluvial aquifers and volcanic aquifers (Margat and Van der Gun, 2013 ; Smith et al., 2016). Moreover, groundwater could be classified based on depth below the Earth's surface into deep groundwater in thousands of meters and shallow groundwater at a few hundred meters; this location often impacts the potential replenishment or recharge rates combined with geological conditions, which in turn categorises as groundwater resources into renewable and non-renewable groundwater (UN, 2022 ; Margat and Van der Gun, 2013).

In the context of human utilization of groundwater, nearly half of the world's drinking water supply is sourced from groundwater, and about 43% of the water used for agricultural irrigation is derived from groundwater (Smith et al., 2016). Global groundwater extraction is estimated at 26% of total freshwater withdrawal; the rate has tripled and is expected to increase to 1-2% annually (Van Der Gun, 2012). This extraction varies widely across countries and regions; about two-thirds of the global extraction was contributed by Asia in 2010. India led the rankings with an annual groundwater extraction of 251 km^3, while Saudi Arabia secures the eighth position with 23 (km^3/year) (Van Der Gun, 2012).

Consequently, the United Nations projects that by 2025, about two-thirds of the global population will experience an extreme scarcity of fresh water and around half of the world's population will reside in regions characterized by increased water stress (FAO, 2007). Therefore, the limited availability of groundwater as well as its various benefits for human activities highlight

the need to introduce sustainable management strategies, especially in arid and semi-arid regions that are facing the challenges of water scarcity and limited accessible freshwater resources. These challenges are often viewed as highly driven not only by shifts in global climate (Green, 2016) but also by increasing population pressures and socio-economic changes (Hanasaki et al., 2012b). Water resource systems always have complicated characteristics such as that involve intricate associations between surface water and groundwater (Margat and Van der Gun, 2013). Thus, decision-making, and sustainable management require a sophisticated spatial methodology.

1.2 Water Resource Challenges in Saudi Arabia

The kingdom of Saudi Arabia is located between 16.5–32.5 N and 33.75–56.25 E in the arid climate area. It is characterized by low annual precipitation that is between 100 and 200 mm, with no existing permanent surface water such as rivers or lakes (MWE, 2012). Saudi Arabia has also experienced rapid development in both social and economic aspects and also in population growth rates. According to General Authority for Statistics in Saudi Arabia GaStat (2022) population has reached 31,552,510 in 2020 with a population growth rate of about 4.5%. The United Nations UN (2019) also has projected that the population will continue growing to reach approximately 44 million in 2050 along with rising living standards and urbanization in most cities in the KSA. This accelerating growth has led to further pressures on water demand in all domains; domestic, industrial, and agricultural. The government has faced a significant challenge in meeting these burgeoning water demands. The water consumption of domestic chores has increased substantially in KSA from 1,800 Million Cubic Meter (MCM) in 2000 to 3,150 MCM in 2017 (MEWA, 2017a), with an expected rise to about 3,512 MCM and 5,219 MCM in 2030 and 2050 receptively (MWE, 2012), (Figure 1-1). The Kingdom of Saudi Arabia falls into severe water deficiencies according to the water scarcity index of UNESCO (Ouda, 2013). In 47 years Saudi Arabia might not have any groundwater resources, caused by over consuming (Almoslut, 2015).

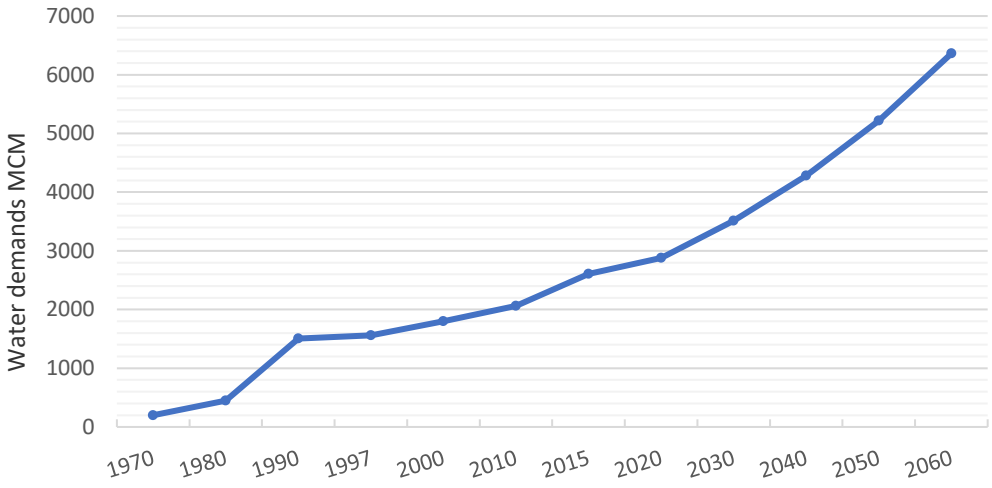

Source: adapted from (MWE, 2012)

Figure 1-1 Growth of Municipal Water demands and future expectations in Saudi Arabia from 1970 to 2060

Generally, the water supply in Saudi Arabia relies on two significant water resources. Firstly, those that come from the conventional sources that involve non-renewable represented in deep groundwater aquifers, and renewable sources that comprise shallow groundwater and limited surface water from rainfall accumulated in some areas (Ouda, 2013). Secondly, water resources using advanced extraction techniques such as desalinated seawater and treated wastewater (MWE, 2012 ; AlAwad, 2018).

The conventional sources, groundwater constitutes an essential natural water source in Saudi Arabia. The aquifer catchment areas often exist in two types of bed that were categorised depending upon hydraulic parameters, areal extension, and their thickness (MEIMR, 2018), which are deep confined aquifers comprise of principal aquifers and secondary aquifers, as illustrated in Table 1-1 and Figure 1-2, and shallow unconfined groundwater aquifers. These aquifers are associated clearly with the geological structure of the country. Geologically, Saudi Arabia is classified into two major geologic units: the Arabian Shelf in the eastern part; and the Arabian Shield in the western part (Figure 1-3) (Al-Ibrahim, 1991 ; Zaidi et al., 2015 ; MWE, 2012). The Arabian Shelf includes eight of the principal aquifers in with confirmed reserves of 253,000

BCM (Billion Cubic Meters) and potential reserves of over 700,000 BCM (MWE, 2012 ; Al-Rashed and Sherif, 2000 ; Closas and Molle, 2016), Moreover, shallow alluvial aquifers or renewable groundwater are mainly found in the considerable valleys draining in the Arabian Shield area (Al-ahmadi and El-Fiky, 2009).

Table 1-1. Groundwater reserves in the Principal Aquifers and Secondary Aquifers with estimated annual recharge and total dissolved solids.

Aquifer name	Total Reserve (MCM)[a]	Annual Recharge (MCM)	Thickness (m)	Total dissolved solids (Ppm)[b]
Principal Aquifer				
Wasia-Biyadh	590,000 – 740,000	480	600	900-10,000
Saq	277,000 – 290,000	310	400-1200	300-3,000
Wajid	220,000 – 255,000	104	200-900	500-1200
Tabuk	205,000 – 210,000	455	500-950	200-2500
Umm Er Radhuma	188,000 – 190,000	406	300-700	2,000-5,000
Minjur-Dhruma	180,000 – 182,000	80	400	1,100-20,000
Neogene	130,000	290 - 360	NA[C]	2,400-4,000
Dammam	25,000 – 45,000	200	NA	2,600-6,000
Secondary Aquifers				
Al-Jilh	113,000 – 115,000	60	± 326	3,800-5,000
Al-Jauf and Sakaka	100,000	95	~ 400	400-5,000
Al-Khuff	30,000	132	99.3	3,800-6,000
Aruma	85,000	80	141.5	1,600-3,000
the upper Jurassic	NA	NA	NA	NA
lower Cretaceous	NA	NA	NA	NA
Basalts and Wadi Sediments	NA	NA	NA	NA
Total	2,185,000 - 2330000			

(MCM)[a]: million cubic meters (ppm)[b]: parts per million. NA[C]: Not Available data.

Source: adapted from (MWE, 2012 ; Al-Rashed and Sherif, 2000 ; Abderrahman, 2002 ; Al-Ibrahim, 1991)

Excessive groundwater extraction could highly affect water quality deterioration, such as increased salinity levels (Al-ahmadi and El-Fiky, 2009). As shown in Table 1-1 the main aquifers of groundwater in Saudi Arabia variation in total dissolved solids (TDS) concentration in groundwater, ranging from 300 to more than 10,000 parts per million (ppm); water containing approximately less than 1000 to 1500 ppm and sometimes to 4000 ppm of TDS is typically categorized as good water quality, having a low concentration of dissolved solids (Al-Rashed and Sherif, 2000 ; Al-ahmadi and El-Fiky, 2009). While groundwater with TDS exceeding 15,000 ppm

is considered poor water quality with very high dissolved solids, which is unsuitable for drinking or irrigation without proper treatment (Al-Rashed and Sherif, 2000).

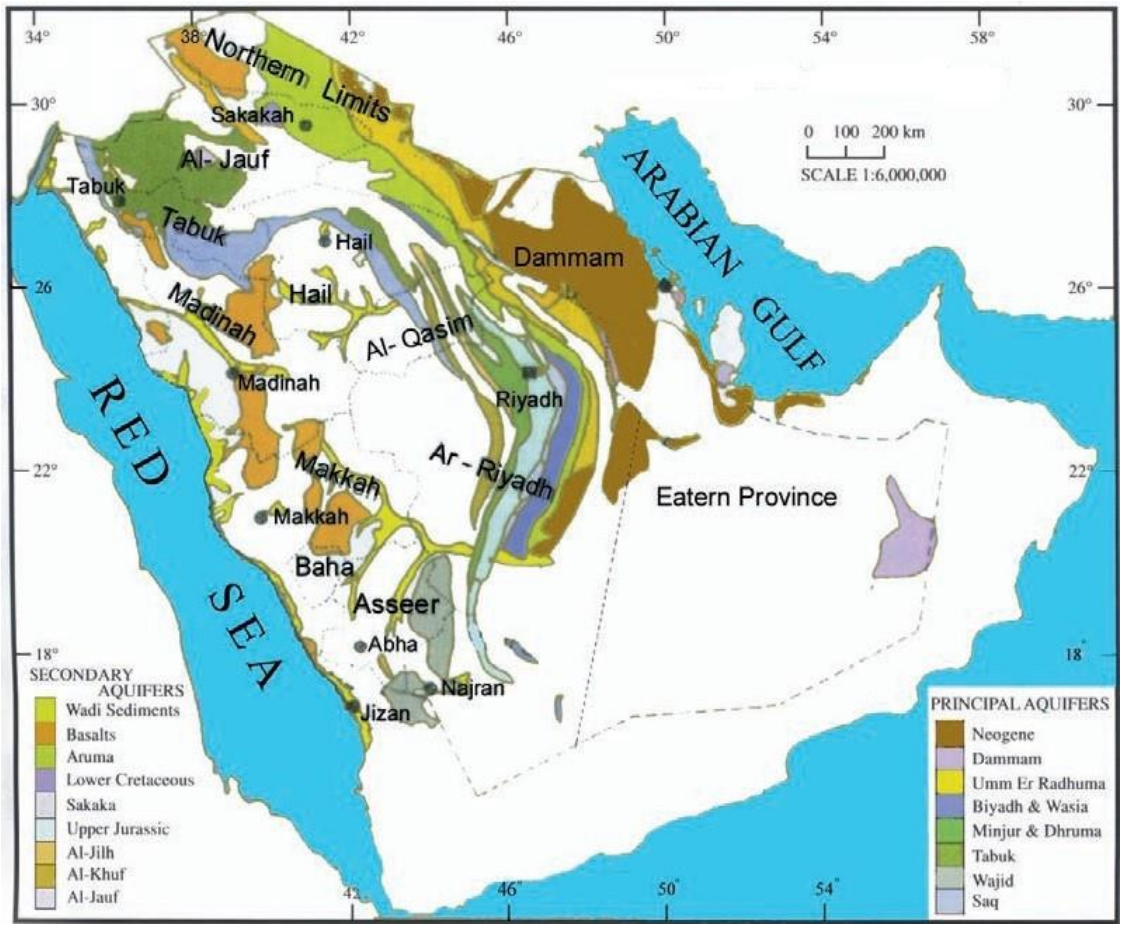

Source: (Abderrahman, 2002)

Figure 1-2. Groundwater reserves in the Principal Aquifers and Secondary Aquifers

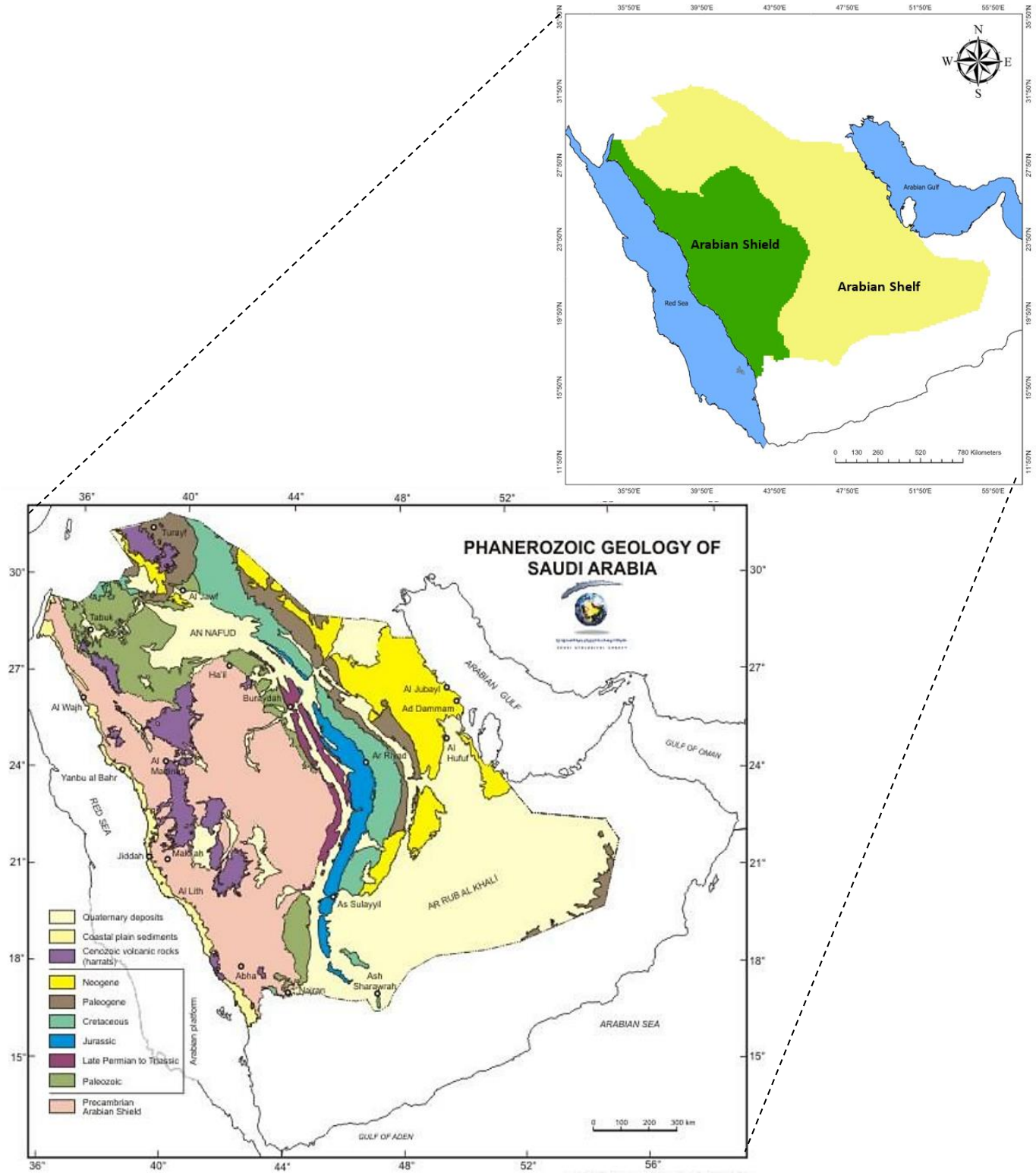

Source: (SGS, 2018)

Figure 1-3. The main geological features of the Arabian Shelf and Arabian Shield in Saudi Arabia

The Ministry of Agriculture and Water, MAW (1984) and Abderrahman (2002) state that the Basalts layers, Wadi Sediments and alluvial aquifers could be considered as the main store of renewable groundwater resources in Saudi Arabia, and they are recharged by rainfall-runoff water. According to MWE (2012), these aquifers reserve roughly 84000 (MCM) with an estimate recharge rate of 1,196 (MCM) annually. The alluvial deposits' thicknesses range from around 20 to 200 m with a width varying from a few hundred meters to many kilometers; also, the dissolved solids in the alluvial aquifers were estimated at around 250 and 4000 (ppm) which indicated the water has good quality (Al-Rashed and Sherif, 2000).

The recharging of this groundwater type often occurs from rainfall and discharge through the valleys, although surface runoff in Saudi Arabia is limited caused by sporadic rainfall events, with low volumes in some seasons and higher evaporation rate (MWE, 2012 ; Amin et al., 2016). Nevertheless, there are valuable amounts of surface water that could be produced by rainfall in short duration, which creates flash floods (Al-Rashed and Sherif, 2000) particularly, in the mountainous areas in the west and southwest part where these areas experience high precipitation with relatively regular runoff compared to other regions of KSA (Zaharani et al., 2011 ; MEIMR, 2018). According to FAO (2009), as cited in Zaharani et al. (2011), the volume of surface water reached about 2.2 km^3/year. Therefore, several projects have been developed to acquire more benefit from these surface waters by the Ministry of Environment, Water and Agriculture (MEWA). 509 dams were constructed in valley channels across the KSA and these currently store about 2084 MCM, the dams also have various purposes ranging from flood control, through aquifer recharge to irrigation usages and water supply in general, and over 60% (329) of these dams have been built in order to augment and recharge aquifers with an estimated capacity of 683.7 MCM (MEWA, 2018a ; MEIMR, 2018).

The non-conventional water supplies in Saudi Arabia can be divided into desalinated seawater and treated or reclaimed wastewater. In terms of desalinated water, Saudi Arabia is viewed as the biggest generator in the world, accounting for 18% of the total global production, and desalinated water contributed approximately of 61% to 63% of municipal use between 2015 to 2017, providing nearly 1,835 to 2,175 MCM/yr during same period (Alnajdi et al., 2019 ; GaStat, 2018a). According to Saline Water Conversion Corporation SWCC (2014), there are around 24

desalination plants constructed on the coast of the Red Sea and six plants on the coast of the Arabian Gulf, (Figure 1-4). Furthermore, there are also around 91 wastewater treatment plants in the big cities that have produced good quality treated water (Ghanim, 2019 ; GaStat, 2018a ; MEWA, 2018a). In spite of the fact that there is an average of roughly 4.562 MCM³ per day of wastewater treated in 2018, only a small fraction 0.826 MCM³ per day, around 18.11% has been used for purposes such as industry usages, agricultural irrigation and roadside afforestation.

The largest portion (around 54%) of domestic or municipal requirement is provided by desalination water 2175 MCM in 2017 and 2137 MCM in 2018 while groundwater resources have satisfied the remaining water needs at 975 MCM and 1255 MCM in 2017 and 2018 respectively (MEWA, 2018a).

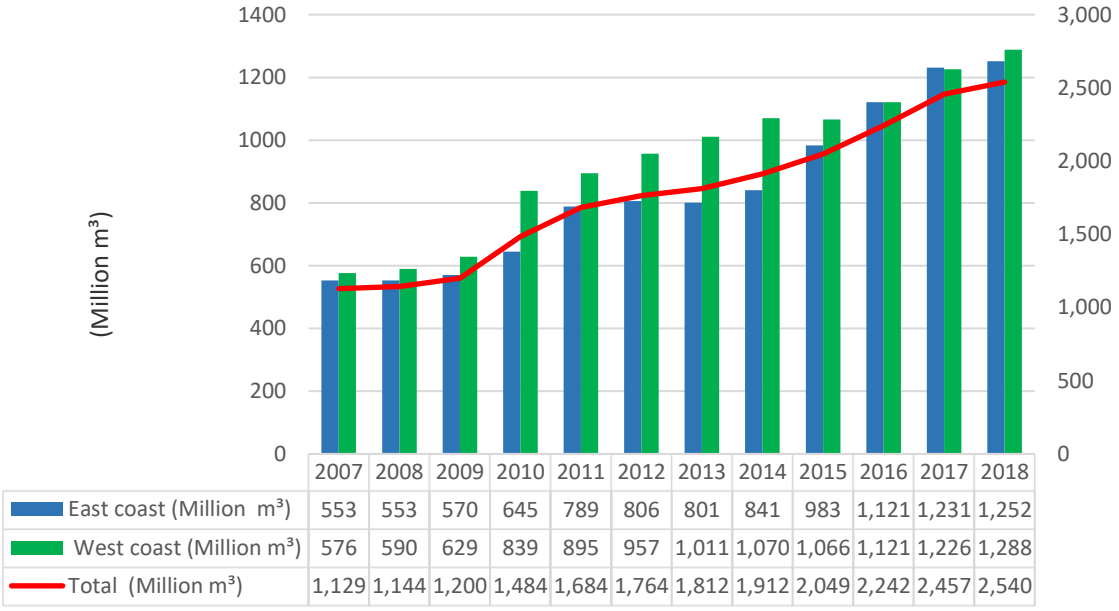

	2007	2008	2009	2010	2011	2012	2013	2014	2015	2016	2017	2018
East coast (Million m³)	553	553	570	645	789	806	801	841	983	1,121	1,231	1,252
West coast (Million m³)	576	590	629	839	895	957	1,011	1,070	1,066	1,121	1,226	1,288
Total (Million m³)	1,129	1,144	1,200	1,484	1,684	1,764	1,812	1,912	2,049	2,242	2,457	2,540

Source: adapted from (SWCC, 2019)

Figure 1-4. Production of seawater desalination in Saudi Arabia 2007 – 2018. The figure illustrates the quantities of water produced in Million m³ from desalination plants on the western coast of the Red Sea and the eastern coast of the Arabian Gulf in KSA.

Drinking water was 69% from desalinated water and 31% from non-renewable groundwater in 2017, while in 2018 non-renewable groundwater supplies had increased to around 37% and desalinated water accounted for 63%, (Figure 1-5) (MWE, 2012 ; GaStat, 2018b). Moreover, industrial growth in Saudi Arabia has been increasing since 1980; primarily, due to oil discovery

and production. Generally, industrial needs from water are considered smaller than the water demands for domestic purposes and some manufacturing also demands special water quality (Chowdhury and Al-Zahrani, 2013a ; Abderrahman, 2000).

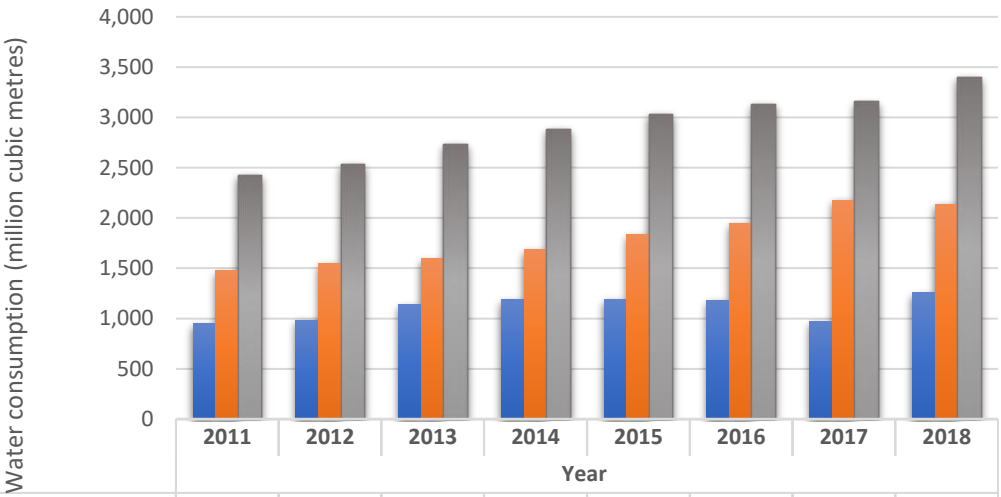

	2011	2012	2013	2014	2015	2016	2017	2018
Groundwater	947	981	1,137	1,189	1190	1182	975	1255
Desalinated water	1,476	1,546	1,594	1,685	1,835	1,947	2,175	2,137
Total	2423	2527	2731	2874	3025	3129	3150	3392

Source: adapted from (MEWA, 2018a)

Figure 1-5. The quantity and sources of water consumed by municipal sector in 2011 - 2018.

The Ministry of Water and Electricity MWE (2012) and Ministry of Environment ,Water and Agriculture MEWA (2019) reported that Industrial water requirement rose from about 56 MCM in 1980 to 450 MCM in 2000 and 977 MCM in 2015. It also is expected to develop to 1,024 MCM and 1,948 MCM in 2020 and 2050 respectively, (Figure 1-6). Water desalination mainly satisfies these water needs (50% of the total demand), and the remaining are met by groundwater resources as well as recycled effluent (Abderrahman, 2000). Since 2001, the Saudi Authority for Industrial Cities and Technology Zones (MODON) has been responsible for drawing the plans for providing water for all industrial cities in the Kingdom of Saudi Arabia. Consequently, MODON established treatment plants to reclaim industrial wastewater for every industrial area for 35 cities in Saudi Arabia (MODON, 2017) .The total capacity of all these treatment plants has reached 108,000 m^3/day (MODON, 2017).

Although the KSA is characterized as a desert climate, there are several regions where conditions support agricultural activities. The government provides farmers with financial support, low-cost water, fuel, and electricity. Therefore, cultivated lands have experienced massive increases from less than 0.4 million hectares in 1971 to 1.62 million ha in 1991, which decreased slightly to 1.07 million ha in 2007 (MEIMR, 2018 ; Chowdhury and Al-Zahrani, 2013a).

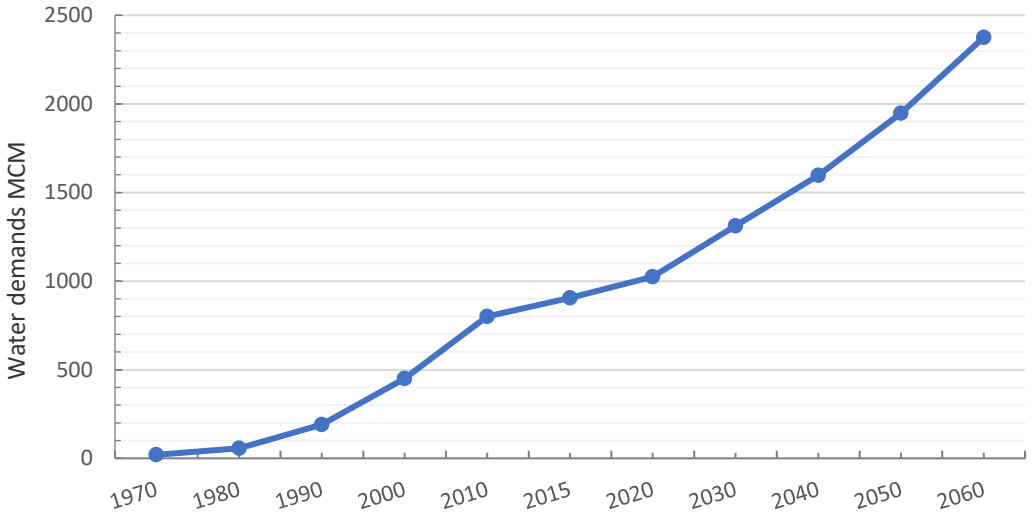

Source: adapted from (MWE, 2012)

Figure 1-6 Growth in industrial water demands and future expectations in Saudi Arabia in MCM/year.

However, recently, according to the Ministry of Agriculture, the agricultural areas had been estimated at around 13.8 million hectares in 2017 and cereals, fodder, date fruits, and vegetables are the main products in Saudi Arabia (GaStat, 2017). Consequently, water demand for the agricultural sector in KSA is the largest demand at about 82.2% of the total water from all sources and around 65% of total freshwater use, compared to municipal use of 13.5% and industrial use of 4.3% of the total water consumption (Figure 1-7) (MEWA, 2018a ; Alamri and Reed, 2019). About 1,850 MCM of water was consumed in 1980, which rose to 11,200 MCM and 14,700 MCM in 2000 and 2010, respectively (Zaharani et al., 2011). Moreover, irrigation depends massively on non-renewable groundwater resources with an average use of 8,300 MCM / year and other

irrigation water comes from surface and renewable water resources at around 6,750 MCM / year (MWE, 2012). In addition, the total number of wells drilled, which extract non-renewable groundwater have increased from 26,000 in 1982 to 236,849 wells drilled in 2018, which irrigate about 85.9% of total cultivated areas (GaStat, 2018b). Treatment wastewater was also utilised to irrigate cultivated fields with date palm and forage yields on approximately 9000 ha near Riyadh city, consuming about 146 MCM (Abderrahman, 2000).

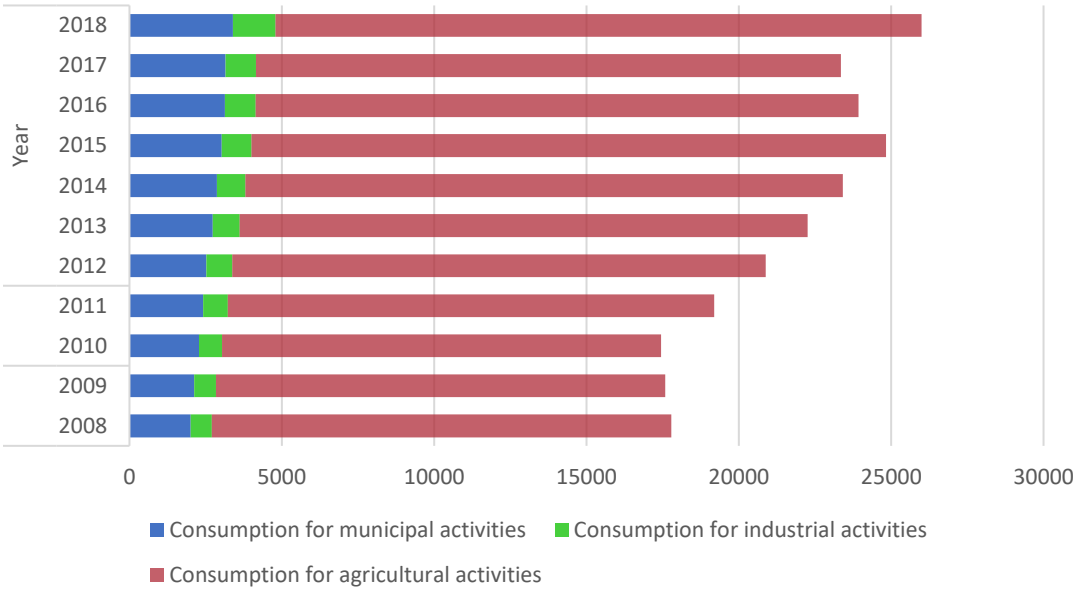

Source: adapted from (MEWA,2018, MEWA,2015)

Figure 1-7 Water consumption by sector (municipal, industrial, and agricultural) in Saudi Arabia in 2010-2018

In general, the water demand in Saudi Arabia has risen annually. There was an average yearly increase in water requirement between 2000 and 2005 of 1.7%, from around 20,740 MCM to about 22,480 MCM (Odhiambo, 2016). MEWA (2019) has estimated (25,992 MCM) an average increased water demand from desalination water and groundwater of approximately 8% in 2018. Therefore, this combination of circumstances of the scarcity of water resources and high water demands in all sectors would produce a complex set of challenges that have potentially far-reaching consequences on the environment, climate, and economy in the country.

1.3 The research questions and objectives

As a result of increased consumption and concerns of the potential depletion of non-renewable groundwater, sustainable management for groundwater resources in Saudi Arabia has become essential. Therefore, research is needed on the conservation of groundwater resources, as well as the assessment of potential sites for renewable groundwater. Such research would aim to help mitigate pressure on existing water resources and to move towards improving water security in Saudi Arabia.

Accordingly, determining potential sites that have a good groundwater potential in the Arabian Shield is one of the essential goals of the sustainable development plan of MEWA in Saudi Arabia (SWPC, 2019 ; MWE, 2015). Moreover, the National Water Strategy 2030 of Saudi Arabia aims to sustainably reform the water sector by developing renewable groundwater and surface water resources as well as improving water demand management in all uses, therefore, there is an urgent requirement for an integrated approach to identifying natural sources such as renewable groundwater sources along with the assessment of the variation of water demand under social and economic scenarios (MEWA, 2018b). Al-Madinah is a good location for applying such an integrated approach because it climatically represents one of the important arid regions. Additionally, although it is the fourth largest city in the Kingdom of Saudi Arabia (UN-HABITAT, 2019a) and has religious and economic significance in the Arab and Islamic world, it has received scant attention in the research literature on the management of groundwater or water resources sustainability under the impacts of climate change, population change, urbanization and GDP scenarios.

The delineation of the potential groundwater zones is usually conducted by the traditional approaches such as geophysical operations and drilling, which are time consuming and expensive (Rahmati et al., 2014 ; Alahmadi, 2019). Therefore, over the past decade, Remote Sensing (RS) and Geographic Information System (GIS) approaches have been increasingly applied for natural resource management and sustainable utilization that enhance decision-making, as well as these techniques have capacities of analysis for combining spatial information from multiple types to generate new insights (Manap et al., 2012).

Therefore, this study aims to contribute to sustainable groundwater management in an arid-semi arid region (ASARs) represented in Al-Madinah City through the application of RS and GIS approaches to determine potential groundwater zones, an essential starting point for the successful implementation of groundwater protection and management programs. Moreover, optimal groundwater management requires that the potential zones should be examined under external factors that might affect groundwater or other water resources, including climate change impacts as well as population growth, urbanization, and GDP increases.

This study will address the following research questions:

1. Where are the potential groundwater zones located in Al-Madinah region?
2. Which factors have the most impact on determining potential groundwater locations?
3. How could climate change impact on these potential groundwater zones?
4. What are the possible effects of population and GDP on water demand?

Accordingly, to answer these research questions, we need to solve the following objectives.

1. to develop a methodological framework for mapping potential groundwater zones in Al-Madinah by using GIS approaches.
2. Spatial analysis of climate changes under future scenarios and potential effects on potential groundwater zones in Al-Madinah.
3. Analysis of future water demands in Al-Madinah using the modified IPAT model under different socio-economic scenarios.

1.4 Thesis structure

The thesis structure is summarised in Figure 1-8 which also displays the topics presented and addressed in each of the next chapters.

Chapter 2 focuses on exploring the current status of water supply and demand in the Study Area. Reviewing and evaluating relevant methodologies of mapping potential groundwater zones and conditioning factors and the suitable criteria to input into the suitability model. Moreover, it

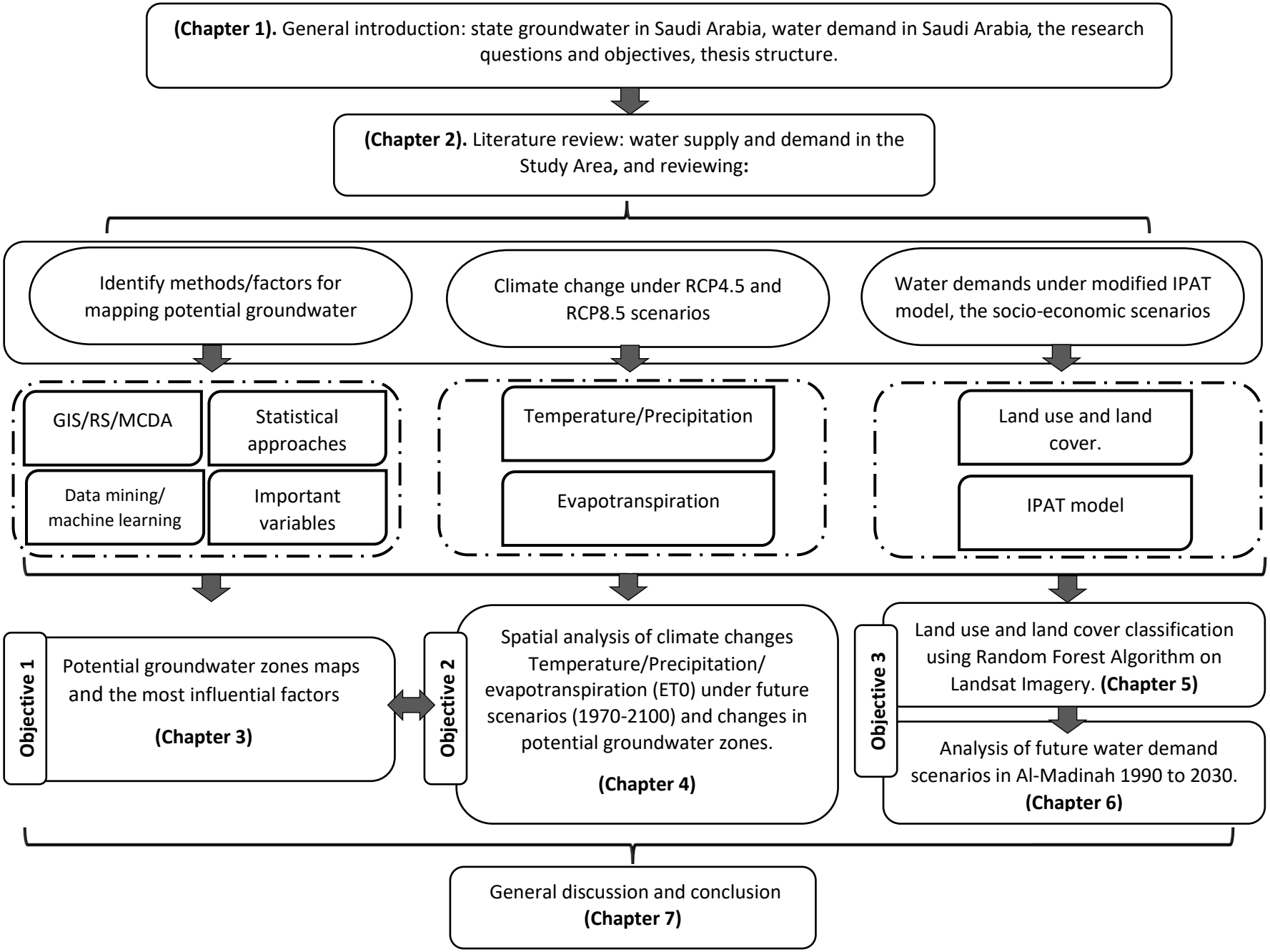

Figure 1-8. Thesis structure outlines the main topics presented and addressed in each chapter.

presents studies related to climate change to understand climatic variables of temperature, precipitation and evapotranspiration that considerably affect the hydrological system. The IPAT model application and its applicability in the water field have also been reviewed. This chapter identifies the research gap related to the methods used in general or the possible contribution to the knowledge for each objective.

Chapter 3 identifies the potential groundwater zones and the most influential factors by comparing two methods. The fuzzy logic-frequency ratio approach and logistic regression modelling approach; the models' accuracy also has been validated.

Chapter 4 analyses the spatial and temporal distribution of the climate changes in temperature, precipitation, and potential evapotranspiration (ET0) during the historical period (1970-2018) and under RCP4.5 and RCP8.5 future scenarios (2021-2100). Potential drought condition helps highlight the climatic water balance in the study area. Potential changes in the potential groundwater zones are then considered using a novel approach based on integrating the topographic wetness index (TWI) with rainfall.

Chapter 5 develops three land use/land cover maps for the study area in different years by applying the random forest algorithm to Landsat imagery.

Chapter 6 analyses the future water demand scenarios in Al-Madinah from 1990 to 2030 by employing the adapted environmental impact (I) of population (P), affluence (A), and technology (T) (IPAT) model under various demographic, economic and technological assumptions.

Finally, Chapter 7 provides a general discussion of all the objectives and findings and highlights the main thesis contribution, the possible Limitations, and implications. It also concludes with the recommendations extracted.

Chapter 2 literature review

The Kingdom of Saudi Arabia has an arid climate caused by its position in the desert climate zone, which is marked by limited water supplies with the absence of permanent rivers or lakes. More than 70% of water supplies come from groundwater extraction, whether from renewable or non-renewable water resources (Al-Ibrahim, 1991 ; Bob et al., 2014). Therefore, sustainable development programs have become required to preserve groundwater that is viewed as a valuable resource of irrigation and drinking water in Saudi Arabia. Conducting groundwater-based research is deemed as one of the effective tools to establish such programs. In addition, groundwater governance is a complex process where its effectiveness is affected by natural and human factors (Llamas et al., 2006). The concept of sustainable management of groundwater could be examined from many perspectives including, socioeconomic pathways, ecological and hydrological sciences, legal and institutional and policy aspects (Llamas et al., 2006).

This study attempts to investigate the groundwater resources of arid and semi-arid (ASARs) lands by examining three main aspects that comprise mapping potential groundwater zones, the possible impacts of climate change on these zones and the future water demand under different socio-economic scenarios. Therefore, this chapter reviews the various relevant literature to these areas along with the water supply status of the Al Madinah study area.

2.1 The current status of water supply and demand in the Study Area

Al- Madinah City-region is located in the western part of the Kingdom Saudi Arabia, as shown in Figure 2-1, where extends geographically between 24 °28″ N latitudes and 39° 36″ E longitude (Gutub, 2013) with an area of 14376 km². The study area is geologically part of the Arabian Shield, with its rocks dating to the Precambrian era. Moreover, the rocks of Arabian Shield are classified into two types are layered and plutonic; layered rocks comprise from metavolcanics and metasedimentary rock whereas the plutonic rocks consist of two sets are the older diorite set and the younger syn- and post-tectonic granitic set (Subyani and Al-Ahmadi, 2011). In General, Al-Madinah comprises three principal parts. Firstly, lava plateaus of basaltic rocks that are termed locally (Harrats) and are widely spread in the east, west and south side (Gutub, 2013 ; Alahmadi, 2019). This basalt structure contains a vital aquifer. Secondly, alluvial deposits that include poorly

sorted sand and gravels. Finally, the rocky outcrops in the western and northern area, which exist as massifs of several kilometres or as isolated outcrop in a few meters (Gutub, 2013 ; Al-Shaibani et al., 2007 ; Alahmadi, 2019).

The basin of Al-Madinah was formed as a result of a long Tectonic development during Late Precambrian and the Tertiary to the Quaternary period. This influenced the drainage system and hydrogeology of Al-Madinah. The main direction of the drainage system was toward the north in the Tertiary period, and in the Quaternary period, this direction changed to poured into the Red Sea along the Najd strike-slip faults' trend, from SE to NW (Bamousa et al., 2012). The Wadi Qanah–Al-Hamd watershed is considered as the regional valley that the valleys of Al-Madinah are part of . There is a parallel drainage system in the study area that flows from SE to NW. The Wadi Qanah–Al-Hamd watershed includes three sub-basins: Wadi Al-Aqiq, Wadi Malal, and Wadi Bat'han watersheds. Al-Aqiq valley enters Al-Madinah from the south, which has had a trellised drainage pattern and Internal drainage system. The valley's recharging area located in about 150 km south of Al- Madinah, where the Wadi An-Naqi valley pours into the Al-Aqiq valley. Parallel with Wadi Al-Aqiq at approximately 50 km from the west of Al-Madinah; the Wadi Malal situated that also has a trellised drainage pattern. In addition, there are tributaries Ar-Ranona, Bat'han, and Al-Mabouth wadis that flow through Al-Madinah City from South to North and formed the Wadi Bat'han watershed, which has overall radial drainage pattern. (Bourouba, 2016 ; Bamousa et al., 2012).

The water resources in the city of Al-Madinah are similar to most cities on the western side of Saudi Arabia, involving conventional and non-conventional water sources. The conventional sources are renewable groundwater resource as well as some surface water accumulated from rainfall. The non-conventional water sources include desalinated seawater and treated wastewater or reclaimed water (MWE, 2012). In terms of the groundwater resource, the area lies on two distinct hydro-geological systems that are on basalt flows of Harrat Rahat in the south part, and old sub-basaltic geology of alluvial deposits along with sedimentary rocks located in the beds of valleys and in the ancient basins, which extend from the south-east towards the north parts (Gutub, 2013 ; El Maghraby, 2014b).

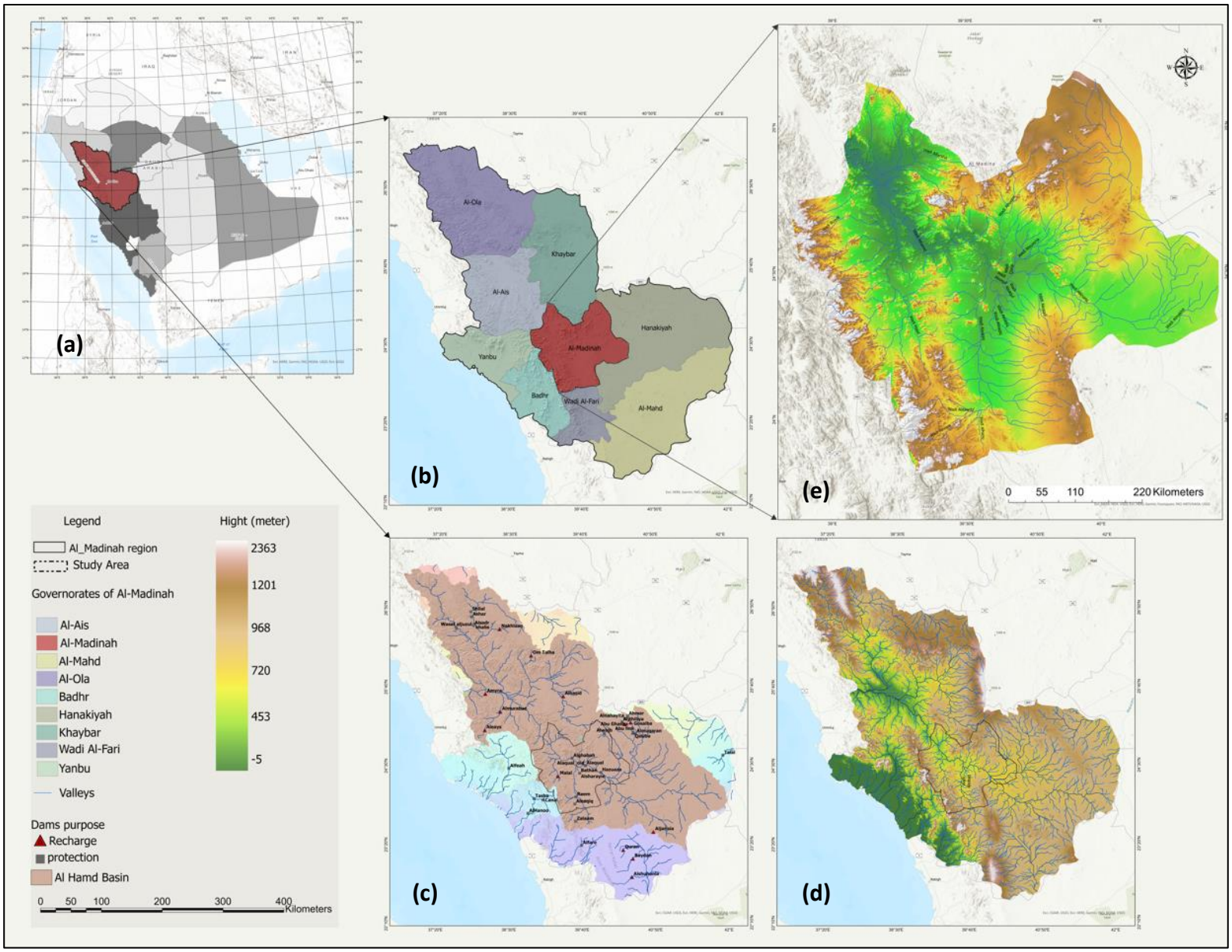

Figure 2-1. The information of Al-Madinah city location, figure shows the location of Al-Madinah City in Saudi Arabia (a) and Al-Madinah administrative area (b). (c) display the Al-Madinah City location based on the Al Hamad basin and the main valleys and dams in Al-Madinah administrative area. (d) and (e) demonstrates the terrain and elevations in regions.

Firstly, the largest basaltic aquifer in Saudi Arabia is located under Harrat Rahat, where its northern part extends to the south of Al-Madinah city as shown in Figure 2-2, which is locally named Harrat Al-Madinah (Mansouri et al., 2022). The basalts of northern Harrat Rahat returns to the Tertiary and Quaternary age that covered about 2000 km^2 with an estimated basaltic and saturated layer thickness of around 300m and 60m, respectively (Al-Shaibani et al., 2007 ; Mansouri et al., 2022).The groundwater was mainly discovered over marl and clay caused by basalt weathering (El Maghraby, 2015). Moreover, this reservoir system is classified as varying between not confined systems due to the existence of some free water table and the semi-confined system caused by the spread of some impermeable layers that do not allow rainfall water to cascade between the rocks (El Maghraby, 2015 ; Mansouri et al., 2022). However, the recent lava was characterized by a relatively high permeability system, where its transmissivity was estimated at around 260 m^2/day, with the average storativity being about 3×10^{-3}.(El Maghraby, 2015).

Secondly, the alluvial aquifer belongs to the Quaternary era and is comprised of clay, sand, and gravel caused by Tertiary/Quaternary basalts' erosion operation (El Maghraby, 2015). The basaltic flow covered the alluvial aquifer on the southern side of study area, which constituted the sub-basaltic aquifer (Khashogji and El Maghraby, 2012). Moreover, the alluvial deposits' thickness was estimated to range from a thin layer of a few centimetres to several meters of around 19 m, and the saturated thickness was characterized as changeable caused by bedrock topography variance (Khashogji and El Maghraby, 2012 ; Gutub, 2013). The fractured and weathered bedrock covered by alluvial deposits has contributed primarily to transmitting and storing groundwater (Khashogji and El Maghraby, 2012). Al-Madinah's hydrology is greatly affected by the spread of valleys, which are the main element for recharging groundwater of shallow alluvial aquifer, thus; the valleys' alluvium is considered the main product of the aquifer, particularly with highly permeable alluvial deposits in the most valleys channels at the Arabian Shield (Bob et al., 2014 ; Al-ahmadi and El-Fiky, 2009).

According to Al-Shaibani et al. (2007), in the early 1970s, the extraction from aquifer started, and three wellfields were built between 1990 and 2000 in order to provide the Al-Madinah area with water that produced an average of 43,000 m^3 per day in 1992. Gutub (2013) stated that the

volume of groundwater stored in the sub-basaltic alluvium was estimated at about 750 x 10^6 m^3 in 1980. Moreover, there is about 1053 groundwater wells within populated urban areas of Al-Madinah (Alahmadi, 2019) as well as the groundwater level was estimated to range between 535 and 595 m whereas the depth of water fluctuated from 30 m to slightly higher than 91 m below ground surface (El Maghraby,2014).

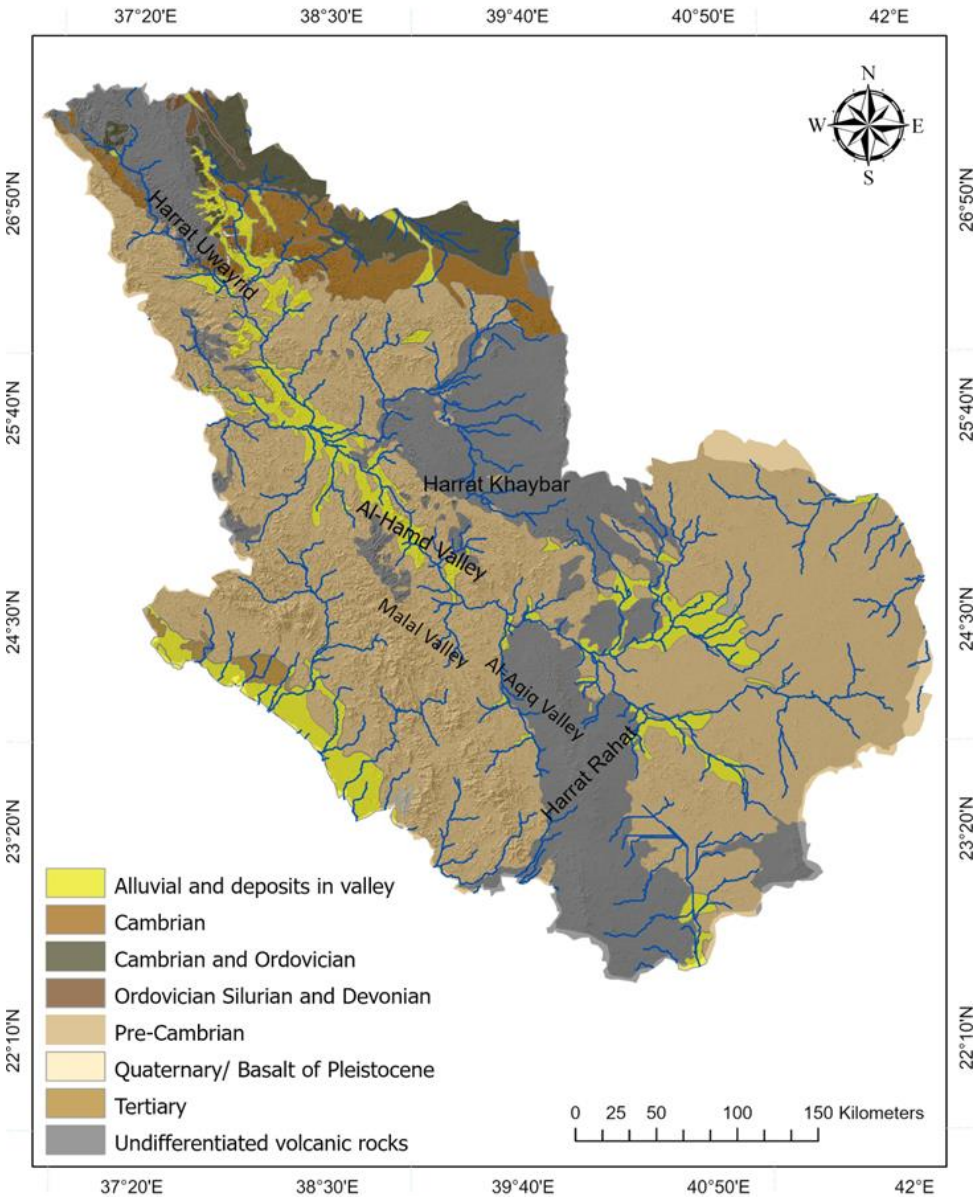

Figure 2-2. Geological map of the Al-Madinah region.

El Maghraby (2014a) and Khashogji and El Maghraby (2012) highlighted that the rainfall and flash floods, which might occur in the rain season, is regarded as the primary source to recharge aquifer as well as some the underground flow from the bordering areas, and the annual recharge rate was estimated by between 7 and 14.6 mm from the rainfall. Furthermore, many dams were constructed on valleys, for protecting from flash floods risks or for recharging the groundwater reservoirs (Gutub, 2013). MEWA (2018a; 2017a) points out that at the end of 2018, there were about 41 dams in the Al-Madinah area with the total storage capacity around 112,815 MCM, one dam with 854,322 MCM has been built for drinking water purposes and 40 dams (111,961 MCM) for recharging underground water. Bathan dam is considered as one of the most important dams in Al-Madinah city; it was constructed on Wadi Bathan to protect the urban area from floods with a storage capacity of 500,000 million cubic metres (MCM) (Al-Turki, 1995). This reservoir water was used for recharging the aquifer and for domestic and agricultural purposes (Al-Turki, 1995).

The first amount of desalinated water that Al-Madinah obtained was about 21,600 m^3/d in 1981 ,which developed steadily as a result of growing water need (Gutub, 2013). Recently, most drinking water in Al-Madinah city has been supplied from the Yanbu desalination plant, which is in the southwest, 250km away on the Red Sea (Gutub, 2013). It supplied Al-Madinah with approximately 214 and 237 MCM in 2018 and 2019 respectively (MEWA, 2019).

Wastewater is regarded as the only water resource that will increase as population is growing with more significant potential for efficient reuse. Some restrictions have been applied by the Ministry of Water and Electricity (MWE) related to not using such water in domestic purposes. In 2018 the percentage of reused treated water has increased to 51.31 % with three sewage treatment plants have been implemented in Al-Madinah area (MEWA, 2018a). Treatment wastewater has been confined for irrigate non-edible crops. The average amount of reused water in 2014 was around 2,958 m^3/ day that is equivalent to only 1% of the total average amount of treated water 220,000 m^3/ day (MWE, 2014).

Some Saudi cities might encounter more water supply challenges than others. For instance, Riyadh, Makkah, the Eastern Province, and Al-Madinah cites are the most heavily consuming cities, which consume more than 80% of the total (MEWA, 2018b). Al-Madinah is ranked fourth as an urban agglomeration and population size in the Kingdom of Saudi Arabia (UN-HABITAT,

2019a) and also has formed religious importance in the Islamic world as well as the economic significance associated with agricultural products in Saudi Arabia.

Economically, the most contribution to Al-Madinah's Gross domestic product (GDP) was gained from the industry sector by about 33% of the total Gross domestic product, (Figure 2-3) (MCCI, 2017) where the industrial area has been built on nearly 17 km² toward the southwest. It involves around 237 factories, which manage numerous manufactures activities such as electronic, metal, plastic, medical equipment and food industries (Modon,2019) as well as Al-Madinah province contributes about 7% of the total GDP of Saudi Arabia (UN-HABITAT, 2019a).

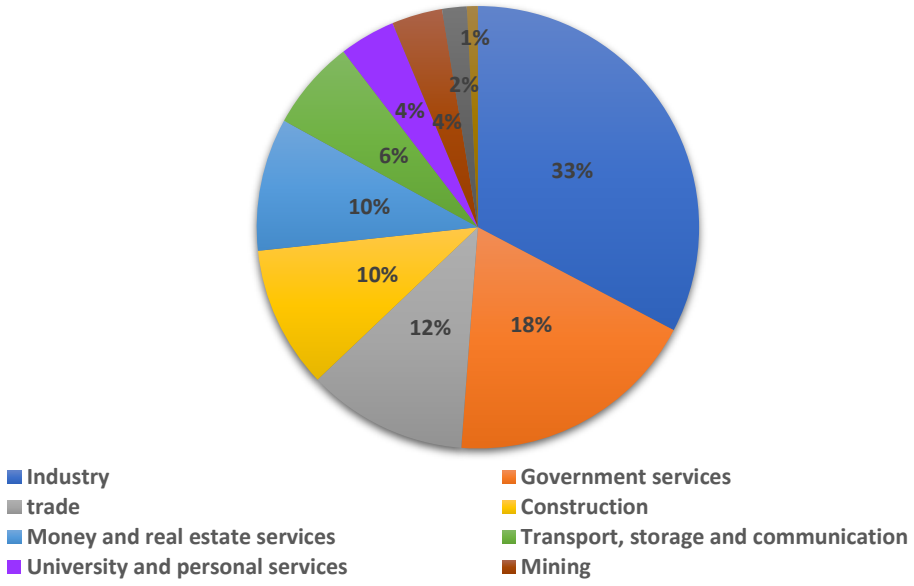

Source: (MCCI, 2017)

Figure 2-3. The contribution of the economic sectors to GDP of the Al- Madinah in 2017.

Generally, although Al-Madinah generated 23% of its budget from own-source revenue in 2017, these incomes only represent a total of 35% from the actual budget of Al-Madinah, and it remains dependent on the central budget and other financial resources provides by the government as analogous as of all Saudi cities (UN-HABITAT, 2019a). Therefore, Al-Madinah domestic product, similar to the rest of Saudi cities, is affected by oil prices. Figure 2-4 exhibited the GDP from 1990 -2020 that increased dramatically in most period's years with a noticeable reduction in 2009, 2016 and 2020, where the rate growth plummeted considerably by -4.1 in 2020. The highest GDP expansion was in the years 2012 and 2015 this was not only in Al-Madinah but also in the whole

of Saudi Arabia where the total GDP growth rate reached about 5.41 and 4.11 in 2012 and 2015 respectively.This increase is attributed to the oil sector contributed significantly where its income grew to about 6%, which was higher than in previous years (Matabadal, 2012 ; SAMA, 2020).

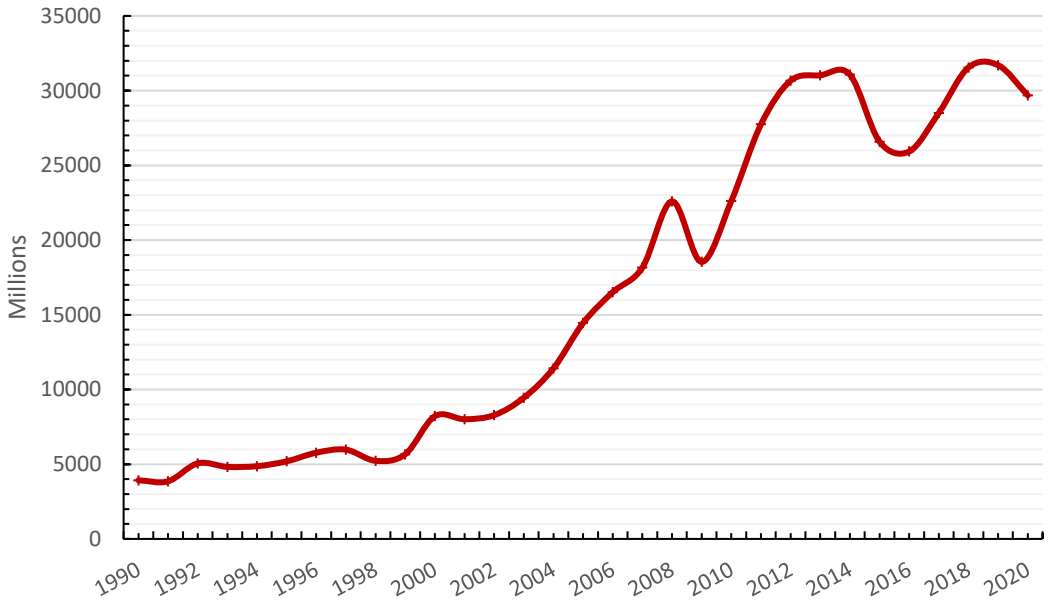

Source: (GaStat, 2020)

Figure 2-4. Gross domestic product (GDP) in Al-Madinah region 1990-2020

On the contrary, GDP had declined caused of retracting oil price in 2009, 2016 and 2020 (Lopez-Ruiz et al., 2019) where the oil sector is considered the primary economic source that GDP is associated with all the cities of the Kingdom of Saudi Arabia. Moreover, the GDP per capita was around 25,243 and 24,929 USD in 2012 and 2014 with mean household income 30,208 and 20,482 USD, respectively (UN-HABITAT, 2018 ; 2016).

Al-Madinah has experienced accelerated economic and industrial developments accompanied by significant growth in population, which in turn led to in a higher demand for freshwater. Moreover, as a result of being Al-Madinah region having no permanent rivers or lakes, groundwater is counted as a valuable water resource in the area (Bob et al., 2014 ; Ghanim, 2019). It estimated that about 92% of water requirement for agriculture purposes was covered from groundwater (Ghanim, 2019). Al-Madinah province is considered one of the most important agricultural lands in KSA growing many types of crops. The total cultivated area was estimated at

27,165 thousand hectares in 2009, which increased to around 83.99 thousand hectares in 2017; 86.51% of these agricultural lands are irrigated from groundwater (GaStat, 2017 ; Abbas, 2013). Grapes, dates and fodder had the largest cultivated area with around 3105 ha, 2485 ha, 18576 ha respectively, their consumption from total water requirement in the study area reaching of nearly 8.6, 76.8, and 8.4% respectively (Abbas, 2013).

According to MWE (2015) and MEWA (2018a), water consumption for municipal purposes in Al-Madinah city accounted for 174 MCM/year in 2015 with an average about 231 L/d Per Capita water demand, whereas in 2018 increased to about 204 MCM/year only for household consumption from the total annual usage that was about 240 MCM/year, equivalent approximately 674,157 Thousand/day. Water consumption, increased about 5% to 252 MCM/year in 2019 (Figure 2-5). Demand is expected to around 281 MCM/year (800 Thousand m^3/d) 2025, (SWPC, 2019, 2020). Furthermore, there is an additional burden on the water supply during the Hajj (pilgrimage) and Umra seasons, when Al-Madinah experiences an increase of population.

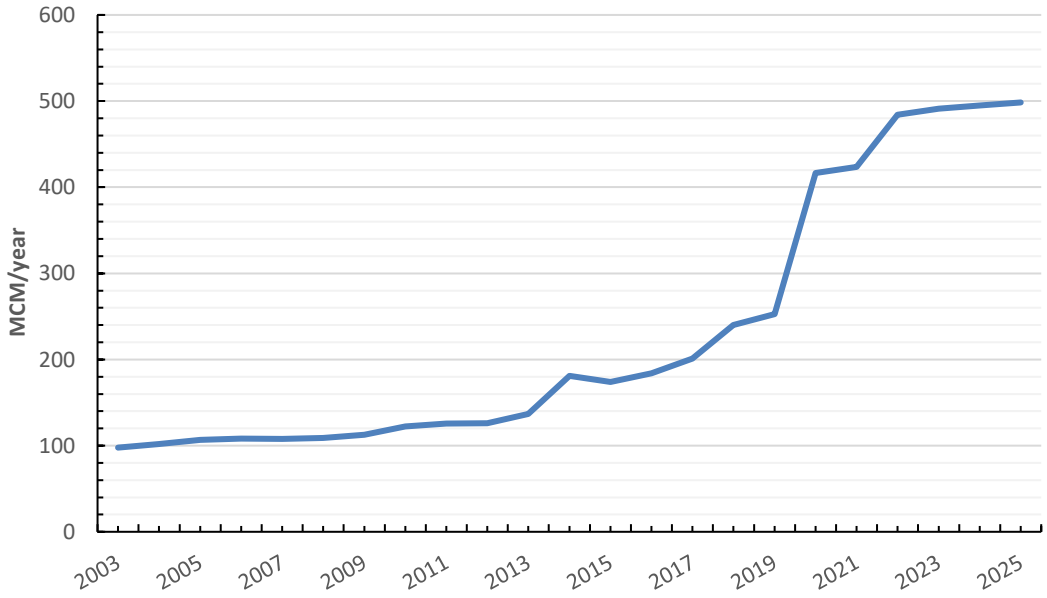

Source: adapted from (MWE, 2013, 2014 ; MEWA, 2019 ; SWPC, 2019)

Figure 2-5. Water Consumption in Al-Madinah 2003 – 2025

The SWPC (2019) calculated that water demand in Hajj season reached 6.4 million m^3 in 2019 with prediction of rise to 8.8 MCM in 2025.The water consumption for Umrah was estimated at 0.2 million m^3 /d in 2019 with a predicted to 0.6 million m^3 /d in 2025. Additionally, the treatment plant in Al-Madinah has a production capacity to accommodate about 12000 cubic m/day (MODON, 2016). The industrial area of the city is supplied with 5000m^3/day by both treated wastewater and desalinated water (MODON, 2019). The reclaimed water consumption has increased dramatically from about 22,000 m^3/day in 2012 to by 61,528 m^3/day in 2015 for the manufacturing activities that located inside industrial cities (MEP, 2014 ; MODON, 2016) (Figure 2-6). According to the Ministry of Economy and Planning, MEP (2014), the average growth in water use for industrial purposes was 5,8% between 2009 and 2014, and an increase in the future is expected due to industrial growth.

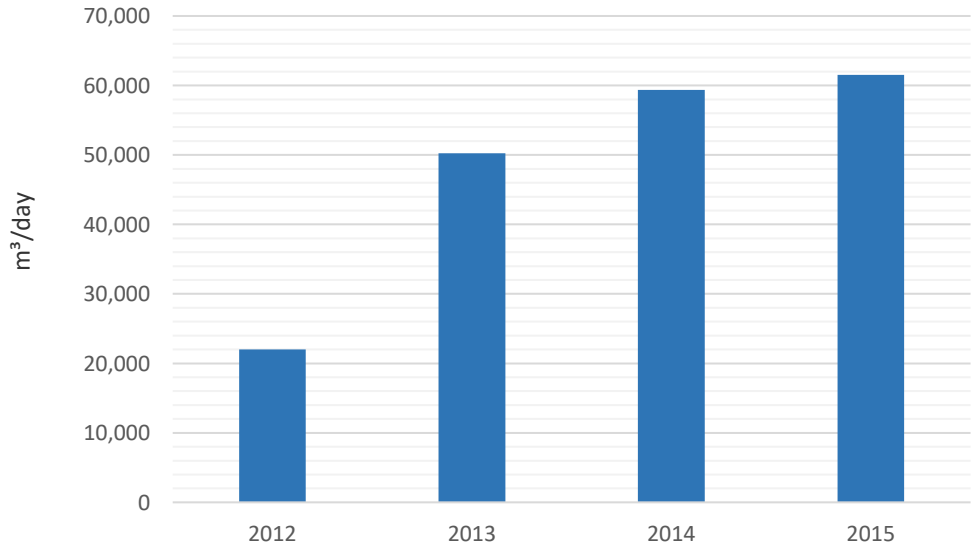

Source: adapted from (MEP, 2014 ; MODON, 2016)

Figure 2-6. The reclaimed water consumption in industrial cities (2012-2015)

Generally, it is reported by Gutub (2013) that although Al Madinah region has good quality groundwater, it had moved in terms of drinking water resources, from complete reliance on groundwater to almost total dependence on desalinated water (Figure 2-7). Such alteration might be caused by the long term aims of sustainable development goals of the Ministry of

Environment, Water and Agriculture (MEWA). These target to supply urban areas by about 90% desalinated water and 10% groundwater and surface water by 2030. They also want to identify the potential sites that have a good groundwater potential in the Arabian Shield, which in turn may help to compensate the groundwater table that has experienced over-exploitation in the past years (SWPC, 2019 ; MWE, 2015), the groundwater level has diminished throughout the last 25 years by about 10 m caused by the total discharge of 2 × $10^3 m^3$, exceeding the recharge amount (Alghamdi et al., 2020). The groundwater stocks within the aquifer have been measured as 5.7×10^3 m^3 (Alghamdi et al., 2020).

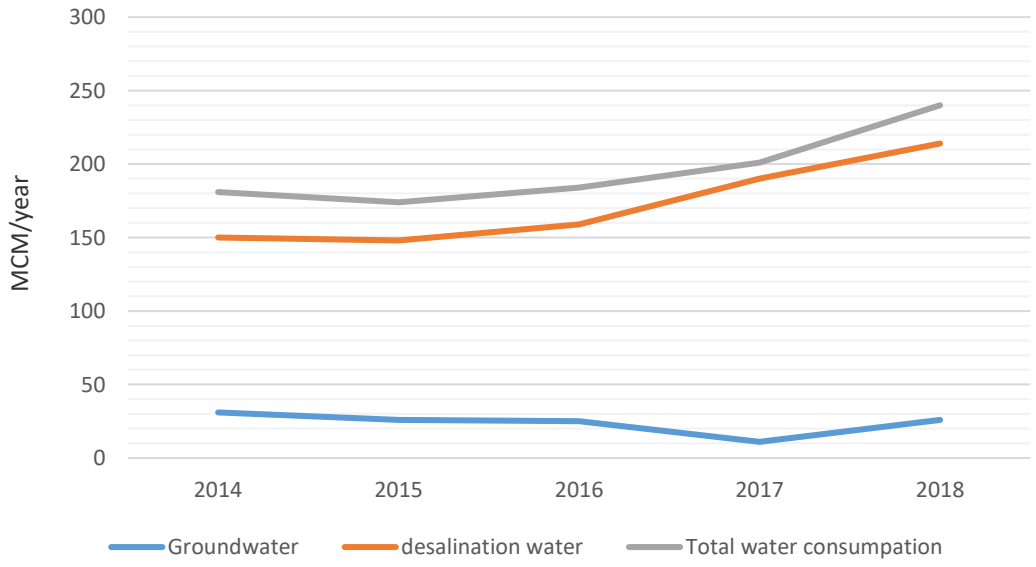

Source: adapted from (MEWA, 2018a, 2019 ; MWE, 2014)

Figure 2-7. The quantity and sources of water consumed in Al-Madinah (2014-2018 /MCM)

2.2 mapping potential groundwater zones

In arid and semi-arid countries, a vital starting point for enhancing groundwater management is mapping available or potential groundwater locations. This type of knowledge would be a beneficial step in producing reasonable visions and plans. For example, when planning future land-use consideration needs to be given to what activities would be acceptable in relation to

potential groundwater zones, which should be compatible with such a natural resource and does not have any contaminated risk (Smith et al., 2016 ; Lamichhane and Shakya, 2019b).

Although there has been limited groundwater research in the Arab world, which accounted for just about 3.3% of global research productivity (Zyoud and Fuchs-Hanusch, 2016), there are some reasonable efforts from Arab countries that have applied advanced techniques and methodologies for supporting groundwater management system. However, the majority of this work investigated the chemical assessment of groundwater quality, along with some work on measuring its quantity (Zyoud and Fuchs-Hanusch, 2016). Mapping potential groundwater appears less common in the current Arab research world. Furthermore, the development of a good framework to demarcate the possible zones to manage such sites' sustainability has not been covered enough by existing research at the global level.

In practice, various methods and criteria through multiple disciplines have been applied to delineate potential groundwater zones. This requires an effective comparison of their performance along with an assessment of the impacts of the factors used in the spatial suitability model of groundwater zones. Therefore, developing a successful model to predict the potential locations of groundwater demands a thorough review and analysis of directly relevant previous studies published in scientific journals in recent decades. In the present study, the literature review included 53 studies that have been analysed regarding methods and criteria used to map potential groundwater zones.

At the global scale, a considerable literature has been produced about the theme of groundwater maps. These have applied methods involving multidisciplinary collaboration as well as the possibility of integration within a GIS environment. Generally, these methods can be divided into three categories: multicriteria decision making that usually includes geographic information system (GIS) with remote sensing (RS); bivariate and multivariate statistics approaches, and data mining/machine learning approaches.

2.2.1 Multicriteria decision making with geographic information system (GIS) and remote sensing (RS)

Multi-Criteria decision-making methods often refer to methods that select the best solution from many alternatives as well as supporting a prioritization within the group of alternatives (Adiat et al., 2012 ; S. Dhiman and Deb, 2020). They have the capability to operate with quantitative and qualitative factors (Balioti et al., 2018). Examples of the literature that used an integrated method of geographic information system (GIS) with remote sensing (RS) include Shimpi et al. (2019) ; Ferozur et al. (2019) ; Nasir et al. (2018) ; Kumar et al. (2016) ; Arnous (2016) ; Elewa and Qaddah (2011). Results revealed that using the MCDA technique effectively combined many physical, hydrological, and anthropogenic factors for the delineation the potential groundwater zones in map format.

Approaches within MCDA include the use of the analytic hierarchy process (AHP) as well as multivariate statistics and data mining/machine learning methods. Therefore, both Benjmel et al. (2020), Nithya et al. (2019), Pinto et al. (2015), Roy et al. (2019) and Adiat et al. (2012). Have used such approaches finding acceptable to good model performance for predicting the probability of groundwater formation.

2.2.2 Statistical approaches

Statistical models have also been used. The most common examples of statistical methods, which were applied over the past two decades in GWPZ mapping and the GIS field comprise weights-of-evidence (WOE), logistic regression (LR), frequency ratio (FR), the certainty factor (CF) model, evidential belief function (EBF) and index of entropy (IOE) model.

WOE model is a Bayesian approach, which uses non-conditional and conditional probabilities (Arabameri et al., 2019a ; Ozdemir, 2011a). Khoshtinat et al. (2019) found the high prediction capability in GWP mapping in Sero Plain, Azerbaijan Province. Al-Abadi (2015) ; Ozdemir (2011a) also confirmed the power of WOE to predict prospective aquifer zones with high The Area Under Curve (AUC) prediction rates of above 0.8 in Iraq and the Sultan Mountains, Turkey, respectively. However, Chen et al. (2018) found other methods outperformed WOE in the Ningtiaota region

in China, the functional tree (FT) model's and logistic regression performance were more satisfying.

Logistic regression (LR) is considered an extension of the linear regression model that has the capability of resolving classification problems (Miraki et al., 2018). A statistical model is used to explain the relationship between the dependent and independent variables which can be both continuous and categorical (Miraki et al., 2018). Several studies have applied LR approach for environmental management purposes such as mapping potential groundwater zones. Arabameriet al., (2019a ; 2019b) revealed that the LR model had high accuracy prediction rate in the Shahroud and Damghan plain areas in Iran. Moreover, Ozdemir (2011a) also found that a LR model provided reasonable and good estimations when applied in the Sultan Mountains in Turkey. By contrast, Miraki et al. (2018) and Nampak et al. (2014) showed an acceptable performance of LR in Kurdistan province and Malaysia, respectively.

Frequency-ratio (FR) approaches viewed as a geospatial evaluation technique helping to measure statistical relationships among independent and dependent variables (Moghaddam et al., 2015 ; Sahoo et al., 2017 ; Ozdemir, 2011a). According to Manap et al. (2012), many researchers have recently applied a frequency ratio model with GIS to develop environmental models and identify groundwater sites after it has been widely used to assess landslide susceptibility and forest fire distribution. The FR model also is considered simply and straightforward in terms of preparing geospatial data, entering, calculating probabilistic relationships and understanding the results (Ozdemir and Altural, 2013 ; Lee et al., 2019).

Ozdemir (2011a) have investigated the predictive accuracy of frequency ratio for mapping potential groundwater springs with involving also logistic regression model and weights of evidence in the Sultan Mountains in Turkey. The results showed good prediction accuracy. Elmahdy and Mohamed (2014) ; Manap et al. (2012) ; Pourtaghi and Pourghasemi (2014) ; Oh et al. (2011) ; Razandi et al. (2015) ; Moghaddam et al. (2015) have confirmed the effectiveness of the frequency ratio model that revealed accuracy rates ranging from good to acceptable for prediction, and also the recent publication by Abdekareem et al. (2023), considered groundwater potential zones spatially in the Wadi Al Hamdh Watershed in Saudi Arabia using frequency ratio

and overlay analysis within the GIS environment. The results indicated that the frequency ratio technique showed good performance (AUC: 0.893).

In addition, the hybrid techniques could enhance the performance of the predictive capability of the models. For example, Al-Abadi et al. (2016) integrated the FR with the Index of entropy (IOE), which again provided good results, and prediction capability slightly increased when combined with an entropy index from 0.804 to 0.81 under the ROC-AUC curve.

However, Lee et al. (2019) examined FR at Goyang-si in South Korea and concluded that its accuracy rate did not exceed 0.68 (AUC), which is viewed as a poor prediction model for groundwater sites. This result might raise inquiry about the reasons that cause the weak frequency ratio model prediction, despite the fact that its success has been confirmed in many geographical regions and domains. Such findings could return to not giving sufficient consideration to selecting the influencing factors where the timber density, timber type and soil depth factors were entered in the model without a comprehensive interpretation of their impact on potential groundwater sites, which might negatively affect the model accuracy outcome. This was confirmed by the sensitivity analysis used in this study, where removing these variables increased the FR accuracy to AUC= 68.67, 68.51 and 68.77, respectively. Moreover, the boosted classification tree (BCT) model that was used and compared its results with FR in this study also had almost poor accuracy by ROC-AUC= 0.693. Thus, an extensive analysis of affected factors should be considered before running the prediction model.

The Evidential belief function (EBF) is a bivariate statistically model utilised to define the spatial integration based on the combination rule to build in uncertainty/belief by applying the Dempster–Shafer theory (Pourghasemi and Beheshtirad, 2014 ; Ghosh, 2021). Several studies such as Nampak et al. (2014), Pourghasemi and Beheshtirad (2014) and Tahmassebipoor et al. (2015) have proved that the evidential belief function (EBF) model was usefully implemented in potential groundwater mapping. Moreover, according to Ghosh (2021), developing the ensemble prediction models would provide new information that helps to sustainable management of natural resources; thus, integrating AHP with EBF in the lower Gangetic plain in the Indian state of West Bengal had the highest prediction accurateness by about AHP-EBF (ROC-AUC = 0.84) than the individual model the EBF (ROC-AUC = 0.83) and AHP (ROC-AUC = 0.76).

In summary, considering all of this evidence, it seems that a considerable amount of literature has been published on implementing and integrating bivariate and multivariate statistics to produce GWPZ. These studies certainly have played an essential role in enhancing sustainable groundwater management. It is expected that the statistical models' performance would not be equivalent because their mathematical concepts are running on different principles (Jaafari et al., 2019). Therefore, this difference does not necessarily mean the statistical models' performance to be unreliable or unhelpful. On the contrary from that, some statistical models can efficiently be used with the GIS environment as well as define the degree of correlation among parameters and the significance and contributions of each factor in mapping GWPZ (Jebur et al., 2015).

2.2.3 Data mining/machine learning

Recently, information and database technologies have experienced accelerated development allowing the development of new algorithms known as data mining and machine learning (Arabameri et al., 2019a). Data mining is knowledge discovery from complex databases or large amounts of data by applying computational, statistical or visual techniques (Mennis and Guo, 2009). Furthermore, Machine learning (Ml) could be defined as allowing a computer to learn from the data by using algorithms that combine computational and statistical approaches (Oladipupo, 2010). Generally, there are four types of tasks that Machine learning often offer, which are Supervised Learning, Unsupervised Learning, Semi-supervised learning and Reinforcement Learning (Muhamedyev 2015). Supervised machine learning relies on training data, and can be divided into two types, which are regression and classification. Classification often aims to separate the data where output is having defined labels, whereas the regression predicts a continuous-valued (Soofi and Awan, 2017 ; Oladipupo, 2010).

There is an overlapping between data mining and machine learning approaches where data mining might use machine learning algorithms to extract beneficial information or machine learning could use data resulting from mining, for example, in prediction models (Hüllermeier, 2005 ; Guruvayur and Suchithra, 2017). Thus, this section reviewed the literature by classifying these methods under one section named data mining/machine learning.

The literature on mapping groundwater has highlighted several data mining/machine learning methods, which include random forest (RF), Boosted Regression Tree (BRT), multivariate adaptive regression splines (MARS), Classification and Regression Tree (CART) and Fuzzy Logic (FL). The performance of these approaches in delineating groundwater has often been compared with the more traditional statistical methods such as logistic regression.

Classification and Regression Trees (CART) are algorithms that from trees (Naghibi et al., 2015 ; Hastie et al., 2009). The CART model could be divided based on the response variables into the classification tree and Regression tree algorithms. Both commonly uses boosting algorithms that assist its predictions performance and accuracy (Nolan et al., 2015). The boosting algorithms often aim to convert weak learner method to robust learners, by combining, for example, with statistical learning such as regression to improve prediction performance (Nolan et al., 2015). Consequently, Boosted Regression Tree (BRT) algorithms have shown promising results against both statistical methods, EBF and GLM (generalized linear model), as confirmed by Naghibi et al. (2015).

Random forest, based on CARTs, is a nonparametric technique consisting of multiple trees that could be developed based on randomly selected subsets from the original dataset (Naghibi et al., 2015 ; Rahmati et al., 2016). Naghibi and Pourghasemi (2015) and Naghibi et al. (2015) have evaluated the capability of three machine learning models, namely RF, BRT and CART, in two different regions in Iran in Beheshtabad watershed and the Koohrang watershed, respectively. The results indicated that all three machine learning techniques showed very good performance, by more than 0.86 AUC value in the Beheshtabad watershed. In contrast, although using almost the same influence factors in the Koohrang watershed, the random forest method had a lower performance (ROC-AUC = 0.71) than BRT and CART. This result was similar to Zabihi et al. (2016), who concluded that the RF technique had offered a fairly acceptable degree of prediction for the potential groundwater locations in North-Khorasan Province, Iran.

Naghibi et al. (2017a) and Chen et al. (2019) have combined Random Forest (RF) approaches with the Genetic Algorithm (GA) approaches at Khalkahl Region in Iran and at the Wuqi County in China. They concluded with a high accuracy model in mapping the potential groundwater zones and saw slight performance improvements in hybrid models. Miraki et al. (2018) combined

random forest (RF) with Random Subspace (RS) in Qorveh-Dehgolan plain in Kurdistan province, gaining an acceptable prediction model for the potential locations of groundwater. Similarly, Arabameri et al. (2019a) ; Arabameri et al. (2019b) and Rahmati et al. (2016) gained good results for ground water mapping using RF.

There are several models that have been designed for classification purposes or as dimensionality reduction techniques in machine learning (Velliangiri et al., 2019) and have been implemented in mapping groundwater zones, which exemplified mainly in Linear discriminant analysis (LDA), quadratic discriminant analysis (QDA), flexible discriminant analysis (FDA) and penalized discriminant analysis (PDA).

These four dimensional reduction techniques were compared by Naghibi et al. (2017c) with another six advanced data mining computing technique including boosted regression tree (BRT), random forest (RF), artificial neural network (ANN), K-nearest neighbour (KNN), multivariate adaptive regression splines (MARS), and support vector machine (SVM) models. Although the FDA approach exhibited the best performance among discriminant models in mapping groundwater sites, all discriminant models represented a lower prediction rate compared with other methods. This finding was also reported by Naghibi and Pourghasemi (2015), who applied KNN, and QDA models in the Khalkhal region, Iran, and the models had also acceptable performance prediction rates.

Although dimensionality reduction techniques (DRTs) effectively diminish computing time and the input number of variables, the main disadvantage is that the variability in the original data might be lost, as well as unsuitable for all types of data (categorical, continuous numerical data or mixed data types) that could need pre-processing (Ayesha et al., 2020).

Multivariate adaptive regression splines (MARS) is another common type of decision tree, which measures the type of relationship between the response factor and the influence factors by combining three methods of constructing splines mathematically, binary recursive partitioning and linear regression (Naghibi et al., 2017c). Zabihi et al. (2016) and Naghibi and Dashtpagerdi (2017) have delimited groundwater zones by the MARS method finding that the MARS had acceptable performances. However, Yousefi et al. (2020) have employed ensemble modelling,

where a number of machine learning approaches have been applied such as the multivariate adaptive regression spline with the support vector machine method (MARS-SVM). The resultant maps had a high predictive rate.

The Support Vector Machine (SVM) approach is also one of the methods can be optimized by integrating with Genetic Algorithms (GA) to select the optimal set of parameters. According to Chen et al. (2019), the SVM performance displayed a high improvement from ROC-AUC= 0.85 in original model to ROC-AUC= 0.94 in the optimized model. Moreover, the SVM method also proved the effectiveness and efficiency of forecasting to map the groundwater as solely model, which both have applied Naghibi et al. (2017a) ; Arabameri et al. (2019b) and Naghibi et al. (2017c), with estimated prediction ROC-AUC values ranging from 0.75 to 0.83.

Although fuzzy logic is based on the mathematical principles and theory of fuzzy sets to deal with uncertainty, it has been applied widely with mining data and machine learning methods (Hüllermeier, 2011) as well as it is regarded as a type of soft computing technique or artificial intelligence techniques tool that assists knowledge-driven discovery (Pradhan and Kim, 2014 ; Razandi et al., 2015 ; Aouragh et al., 2016 ; Roy and Saha, 2019 ; Nyimbili and Erden, 2020). The fundamental assumption of Fuzzy Logic theory is simulating human thinking in decision making particularly in complex and MCDM problems which are difficult to determine precisely in crisp numbers; this is achieved by considering degrees of truth or membership values (Zadeh, 1965 ; Dymova et al., 2021).

Rajasekhar et al. (2019) ; Mallick et al. (2019) ; Mohamed and Elmahdy (2016) ; Aouragh et al. (2016) and Roy et al. (2022), have employed fuzzy set theory, and membership degrees of each criterion has been allocated based on a matrix of pair-wise comparisons AHP for multi-criteria analysis that efficiently performed within a GIS environment, in India, Saudi Arabia, United Arab Emirates (UAE), Morocco. They have suggested such this model would be beneficial in semi-arid countries to improve groundwater management. The validation of resultant maps of both Rajasekhar et al. (2019) ; Mallick et al. (2019) and Mohamed and Elmahdy (2016) have demonstrated that the prediction accuracy ranged from acceptable to good model by ROC_AUC values 0.78, 0.81 and 0.89 respectively. However, the accuracy of the prediction model has not been demonstrated statistically by Aouragh et al. (2016) and Roy et al. (2022), and the results

have been validated by analysing well locations and water levels based on potential groundwater zones that indicated good compliance between water levels and high potential zones.

In addition, Mahmoud and Alazba (2016b) applied a similar validation approach based on extracting the relationship between the used groundwater wells and the resultant suitability maps alongside with field survey method, which also revealed there is a good agreement between the groundwater wells and high and very high potential areas in maps created by fuzzy logic (FL) method that has been used as a single model to delineate the possible regions of groundwater in Al-Riyadh province located at the central part of Saudi Arabia. Nevertheless, one of the issues that could emerge from such verification methodology is that it might be viewed as an inaccurate or unreliable approach, particularly with the lack of clarity on the method of a field survey referred to in the study. Moreover, the method used for identification of the Fuzzy Membership for the criteria needs more description and clarification because determining membership degrees in the fuzzy logic is considered one of the critical stages that could affect the validity of the results (Medasani et al., 1998).

Alahmadi (2019) delineated the aquifer boundaries by applying algorithms of spatial cluster modelling in R using the well's locations as the leading indicator for aquifer delineation. This study revealed that the groundwater wells showed cluster patterns toward the south, north, western, south, eastern, south, and central parts of the urban mass of Al-Madinah city. The potential limitation of this study might be that a comprehensive understanding of the phenomenon of groundwater boundaries needs to be made involving a broader scope of influential factors such as geological and hydrological factors.

Generally, some prior studies have shown that data mining or machine learning techniques offered more reliable performance compared with bivariate and multivariate models such as Naghibi et al. (2015). However, machine learning techniques are regarded as complicated processes requiring proficient knowledge of programming to be applied accurately (Jaafari et al., 2019).

2.2.4 Important variables for groundwater potential zones.

Numerous published study mapping groundwater successfully employed different methods and achieved high-performance (Mogaji and Lim, 2017). However, reviewing the literature revealed that no official guidelines have been suggested for the most critical factors affecting groundwater formation, such as the FAO (2003) guidelines to identify suitable areas for rainwater harvesting (RWH). Consequently, evaluating the variables that have been applied in groundwater potential assessments from the published literature is highly required. Moreover, the redundant factors used in mapping groundwater potential zones might cause erroneous outputs; thus, selecting the most relevant and effective parameters in modelling GWPZ could be challenging and needs a more in-depth review in the light of the nature of the study area and mechanisms of contributing variables. The commonly used variables included three main groups: geological features, hydrological and topographical elements, as well as land use/land cover and NDVI index aspects.

The literature review of the common influencing factors for delineating potential groundwater zones (GWPZ), is shown in Table 2-1. The studies reviewed have indicated that the most common criterion used to identify the potential groundwater zones is slope where it was used in about 94% of the literature, followed by land use/land cover (75.5%), drainage density (66%), lineament/faults density and Lithology (60% to 58%), topographic wetness index (TWI) (54%), soil (52.8%), distance from river/stream and plan/ profile curvature (47%), rainfall (45%), distance to faults (39.6%), geology and geomorphology from 33 % to 18.8%, elevation/altitude from 32% to 35.8%, slope aspect and stream power index (SPI) of around 26 %, and normalized difference vegetation index (NDVI) and distance to roads (15%), While the rest of the factors did not exceed 8% of the literature. These percentages are out of 53 of the studies reviewed.

Table 2-1 The conditioning factors that are used to map potential groundwater zones.

			CONDITIONING FACTORS																						
No	Author	Country	Altitude	Elevation	Crop intensity	Depth of wells	Distance from river/stream	Distance to faults	Distance to roads	Drainage density	Geology	Geomorphology	Groundwater level	Hydraulic conductivity (K)	land use/land cover	Lineament/faults density	Lithology	NDVI[a]	Plan/ profile Curvature	Rainfall	Recharge rate	Slope aspect	slope	soil	SPI[b]	TWI[c]
1	(Adiat et al., 2012)	Malaysia								●						●	●			●			●			
2	(Al-Abadi et al., 2016)	Iraq		●				●			●				●				●			●	●		●	●
3	(Al-Abadi, 2015)	Iraq	●			●		●	●		●				●								●			
4	(Abdekareem et al., 2023)	Saudi Arabia		●			●			●	●					●		●	●	●			●	●		●
5	(Al-Ruzouq et al., 2019)	UAE		●						●	●	●				●				●			●			
6	(Aouragh et al., 2016)	Morocco								●					●	●	●						●			
7	(Arabameri et al., 2019a)	Iran		●			●	●	●	●					●		●		●	●		●	●	●		●
8	(Arabameri et al., 2019b)	Iran		●			●	●	●	●					●		●	●		●		●	●	●	●	●
9	(Arnous, 2016)	Egypt								●						●	●		●	●			●			
10	(Benjmel et al., 2020)	Morocco					●	●		●						●			●				●			●
11	(Chen et al., 2018)	China	●					●	●						●		●	●	●			●	●	●	●	●
12	(Chen et al., 2019)	China		●				●	●								●	●	●	●		●	●	●	●	●
13	(Elewa and Qaddah, 2011)	Egypt								●						●	●			●			●			
14	(Elmahdy and Mohamed, 2014)	UAE	●							●						●	●		●				●			
15	(Ghosh, 2021)	India					●	●		●		●			●		●		●				●	●		
16	(Gupta and Srivastava, 2010)	India								●					●	●							●			
17	(Halder et al., 2020)	India					●			●	●	●	●		●	●							●	●		
18	(Khoshtinat et al., 2019)	Iran	●				●	●							●				●			●	●	●		
19	(Kumar et al., 2016)	Sri Lanka									●	●			●								●	●		

			CONDITIONING FACTORS																						
No	Author	Country	Altitude	Elevation	Crop intensity	Depth of wells	Distance from river/stream	Distance to faults	Distance to roads	Drainage density	Geology	Geomorphology	Groundwater level	Hydraulic conductivity (K)	land use/land cover	Lineament/faults density	Lithology	NDVI[a]	Plan/ profile Curvature	Rainfall	Recharge rate	Slope aspect	slope	soil	SPI[b]	TWI[c]
20	(Lee et al., 2019)	South Korea	●								●				●								●	●		
21	(Mahmoud and Alazba, 2016b)	Saudi Arabia								●	●	●			●	●	●			●			●	●		
22	(Mallick et al., 2019)	Saudi Arabia		●						●	●			●	●	●		●		●			●	●		●
23	(Manap et al., 2012)	Malaysia		●			●				●				●	●	●		●				●	●		
24	(Miraki et al., 2018)	Iran		●		●				●					●	●				●			●		●	●
25	(Mogaji and Lim, 2017)	Malaysia								●	●			●		●	●			●			●	●		
26	(Moghaddam et al., 2015)	Iran	●				●	●	●	●					●		●		●				●	●	●	●
27	(Mohamed and Elmahdy, 2016)	UAE	●					●									●						●	●		●
28	(Naghibi and Dashtpagerdi, 2017)	Iran	●				●	●							●	●	●		●				●		●	●
29	(Naghibi and Pourghasemi, 2015)	Iran	●				●	●							●	●	●		●				●		●	●
30	(Naghibi et al., 2015)	Iran	●				●	●		●					●	●	●		●			●	●			●
31	(Naghibi et al., 2017a)	Iran	●				●	●		●					●	●	●		●			●	●		●	●
32	(Naghibi et al., 2017b)	Iran	●												●		●	●				●	●		●	●
33	(Naghibi et al., 2017c)	Iran	●				●	●							●	●	●		●				●		●	●
34	(Nampak et al., 2014)	Malaysia		●						●					●	●	●	●	●	●			●	●	●	●
35	(Nasir et al., 2018)	Pakistan								●	●				●	●				●			●	●		
36	(Nithya et al., 2019)	India								●	●	●			●	●				●			●			
37	(Oh et al., 2011)	Korea		●			●									●							●	●		●

			CONDITIONING FACTORS																						
No	Author	Country	Altitude	Elevation	Crop intensity	Depth of wells	Distance from river/stream	Distance to faults	Distance to roads	Drainage density	Geology	Geomorphology	Groundwater level	Hydraulic conductivity (K)	land use/land cover	Lineament/faults density	Lithology	NDVI[a]	Plan/ profile Curvature	Rainfall	Recharge rate	Slope aspect	slope	soil	SPI[b]	TWI[c]
38	(Ozdemir, 2011a)	Turkey		●	●		●			●					●	●	●			●		●			●	●
39	(Pinto et al., 2015)	TimorLeste		●						●	●				●	●				●			●	●		
40	(Pourghasemi and Beheshtirad, 2014)	Iran	●				●	●		●					●	●	●		●			●	●			●
41	(Pourtaghi and Pourghasemi, 2014)	Iran		●			●	●	●						●		●		●				●		●	●
42	(Rahmati et al., 2014)	Iran								●						●	●			●			●			
43	(Rahmati et al., 2016)	Iran	●				●			●					●		●		●				●	●		●
44	(Rajasekhar et al., 2019)	India								●	●	●	●		●									●		
45	(Razandi et al., 2015)	Iran	●				●			●			●				●			●			●			●
46	(Razavi-Termeh et al., 2019)	Iran	●				●	●		●					●	●	●		●	●		●	●			●
47	(Roy et al., 2019)	India								●	●	●			●	●				●			●	●		
48	(Roy et al., 2022)	India		●			●			●					●				●	●			●	●		●
49	(Sahoo et al., 2017)	India		●	●					●	●	●	●		●			●		●	●		●	●		
50	(Shimpi et al., 2019)	India								●	●	●			●								●	●		
51	(Tahmassebipoor et al., 2015)	Iran	●				●			●					●	●	●		●	●			●	●		●
52	(Yousefi et al., 2020)	Iran		●			●	●							●	●	●			●		●	●	●		●
53	(Zabihi et al., 2016)	Iran	●				●	●		●					●	●	●		●			●	●			●

NDVI[a] = Normalized Difference Vegetation Index SPI[b] = Stream Power Index TWI[c] = Topographic Wetness Index.

In addition, most of the reviewed studies aimed to determine the factors that were most influential in predicting potential locations of groundwater. Several studies Chen et al. (2019) ; Elmahdy and Mohamed (2014) ; Khoshtinat et al. (2019) ; Lee et al. (2019) ; Naghibi and Dashtpagerdi (2017) ; Naghibi et al. (2015) ; Naghibi et al. (2017a) ; Naghibi et al. (2017c) and Pourghasemi and Beheshtirad (2014) have shown that the topographical factor of elevation/altitude was the most significant. Alternatively, Al-Abadi (2015) ; Moghaddam et al. (2015) and Mohamed and Elmahdy (2016) confirmed that the slope was the most important elements.

However, Al-Ruzouq et al. (2019) ; Mallick et al. (2019) ; Mogaji and Lim (2017) ; Roy et al. (2019) and Shimpi et al. (2019) find the most significant factors are geology structures. A strong relationship between lithology and potential groundwater has been reported in the literature by Adiat et al. (2012) ; Aouragh et al. (2016) ; Chen et al. (2019) ; Ghosh (2021) and Manap et al. (2012). Soil and lineament/faults density factors have demonstrated a highly positive association with groundwater occurrence according Halder et al. (2020); Oh et al. (2011); Gupta and Srivastava (2010) and Nithya et al. (2019). Similarly, drainage density variables with permeability and porosity features are associated with positively affecting recharging operation (Navane and Sahoo, 2017 ; Zakaria et al., 2016). Roy et al. (2022) stated that drainage density showed the highest importance.

In the literature, there is little indication that rainfall factor highly influences groundwater occurrence such as Elewa and Qaddah (2011) ; Pinto et al. (2015) ; Rahmati et al. (2014) and Yousefi et al. (2020) although there is a significant hydrological role of rainfall in arid and semi-arid regions in recharging groundwater. Furthermore, the topographic wetness index (TWI) that represents the influence of topography conditions on the possibility of surface runoff generation (Moghaddam et al., 2015). Miraki et al. (2018) reported the TWI played an essential role in detecting groundwater potential.

In addition, it has been indicated by Al-Abadi et al. (2016) ; Nasir et al. (2018) and Tahmassebipoor et al. (2015) that land use/land cover was the most important factor affecting soil moisture and potential groundwater zones, reflecting human activities and socioeconomic. In contrast, Naghibi

et al. (2017b) showed that the NDVI element significantly impacted groundwater occurrence based on three data mining algorithms applied in the Kashmar Region in Iran. Abdekareem et al. (2023) also confirmed that the NDVI index had the highest correlation with potential groundwater in their study area.

Moreover, several studies applied multiple methods in the same study area. According to Sahoo et al. (2017), although WOE and FR methods showed similar trends in groundwater maps for Hirakud, India, differences were found in the degree of attribute influence. The land use/land cover factor was the most effective in WOE while the soil was most important in FR. In contrast, Ozdemir (2011a) results have revealed stream power index (SPI) as important when using the LR model, while geology and plan curvature were the important factors in the WOE and FR models. These results differ from Pourtaghi and Pourghasemi (2014), who estimated that slope aspect was most important when employing a LR, distance to road most important for WOE and LULC factors most important for FR models when applied in the Birjand Township in Iran.

Naghibi and Pourghasemi (2015) demonstrated that topographical and geological features were more effective in machine learning models that were employed in the Beheshtabad Watershed in Iran, where altitude and distance from faults were most influential when using BRT and RF models, while the distance from faults and fault density factors where more important for a CART approach. Razavi-Termeh et al. (2019) in the Booshehr plain in Iran revealed that the most contributing parameters were considered similar where slope aspect and distance to river had the most importance based on FR-RF and EBF-RF models whereas slope angle and distance to river in CF-RF model.

Furthermore, Arabameri et al. (2019a) ; Arabameri et al. (2019b) have applied methods of similarity to ideal solution (TOPSIS), random forest, binary logistic regression, and the weight of evidence in two different regions in Iran. The results indicated that slope, LULC and elevation, respectively, had the most substantial effect on the Shahroud plain, whereas rainfall, elevation, and distance from the river, respectively, were considered influential in Damghan sedimentary plain. Showing that important factors can vary by study location as well as by methods.

Eventually, it seems that there is no obvious consensus about the best-performing methods and the most influential factors in mapping groundwater potential zones. Several factors might affect the accuracy of the models used, such as the mechanism of applying approaches, data quality and physiographic conditions of the study area. The selection of criteria is most often related to the availability and accessibility of data and the technical experience in preparing data for a study.

Given the variety of methods and variables used in assessing ground water potential in areas across the globe, work in this study will be guided by the sets of variables typically used along with exact data availability for the Al Madinah study area. The study will focus on two of the methods that are simple to apply and easy to interpret, a fuzzy logic with frequency ratio approach and a logistic regression approach, both of which have given useful results in the literature reviewed.

However, despite the apparent importance of some factors, excluding them from the present study could enhance the usefulness of outputs. The distribution of groundwater wells that are often used in suitability models as training and validation datasets, as will be used in present study, are likely to reflect the current human land use activities and therefore demand for groundwater resources than the actual distribution of potential groundwater resources. The wells are usually more related to urban areas and agricultural lands. Therefore, LULC variables are excluded in the present study.

Moreover, various studies have confirmed the correlation between Normalized difference vegetation index (NDVI) and groundwater, whether in investigating groundwater recharge areas or fluctuating groundwater levels by measuring vegetation's density responses in different time series duration. It is also thought that vegetation density plays an important role in obstructing surface runoff that leads to more time for the rainwater to infiltration into the ground as well as decreasing evapotranspiration rate (Seeyan et al., 2014 ; Huang et al., 2019 ; Parizi et al., 2020). However, once again, NDVI in the study area could be sensitive to land use activities such as irrigation rather than capturing more natural vegetation cover that completely depends on groundwater reservoirs. Therefore, NDVI is also excluded in the present study.

2.3 Climate change

2.3.1 Temperature and Precipitation

Climate change directly influences the availability of water resources where Zhang et al. (2016) assessed the impacts of land-use change and climate variability in the near future on the hydrological system, and the results showed that climate changes tend to affect the hydrological regimes more than land-use changes, particularly as the climate becomes drier in the future. Lamichhane and Shakya (2019a) used different climate change scenarios (RCP4.5 and RCP8.5) with the hydrological model of soil and water assessment tool (SWAT) in the Kathmandu Valley Watershed. They concluded that the hydrology system is primarily influenced by changes in climatic variables more than LULC variables. Shrestha et al. (2016) also evaluated groundwater resources in the Mekong Delta aquifer system under RCP4.5 and RCP8.5 scenarios utilising the WETSPASS model and MODFLOW for groundwater recharge and flow simulation, respectively. The findings indicated that although the rainfall amount is expected to increase in the wet season, it also will experience a decrease in the dry season, which is likley cause a potential decline in groundwater levels and storage in future.

Kahsay et al. (2018) have applied the Coordinated Regional Climate Downscaling Experiment (CORDEX) estimations of Representative Concentration Pathways (RCPs) of RCP 2.6 and RCP 4.5 scenarios to analyse the trends in groundwater recharge rates. The study revealed that the groundwater charging rate decreases by 1.3% to 3.4% under RCP 4.5 and RCP 2.6, respectively. This is caused by the reduction in the amount of rainfall along with the increase in temperatures and the rate of evaporation. Driouech et al. (2020) also used the CORDEX model data in the MENA regions. The results revealed an increase in warming by about 4 degrees in Morocco, Algeria, and the Arabian Peninsula under RCP 8.5, while under RCP 4.5, the expected increase was about 2 C. Future rainfall shows the opposite pattern. Moreover, the drought events, based on the SPEI index, are expected to be more intense and extensive than those using the SPI index. Therefore, drought hot spots are projected in the region at the end of the century, while the region's northern half would experience more drought events.

In Saudi Arabia, Amin et al. (2016) also considered RCP scenarios for 2050 and 2075. Their study revealed that the temperature would increase along with slightly decreasing mean annual rainfall

(1.5 %) under the RCP4.5 for 2050 and a 12–24 % decrease is predicted under RCP8.5. By 2075 the rainfall decreases will be 1.95 % and 15–27 % under RCP4.5 and RCP8.5 respectively. This study does not address the extent of the expected impact of climate change on water resources in Saudi Arabia. On the contrary, Tarawneh and Chowdhury (2018) investigated the influence of temperature and rainfall changes on future water resources in some regions of Saudi Arabia under RCP8.5, RCP6 and RCP2.6 scenarios. Their study is in accord with Amin et al. (2016) regarding the expectations of temperature (increasing trend in the whole of Saudi Arabia) under all scenarios, while it differs in terms of rainfall pattern predictions where Tarawneh and Chowdhury (2018) concluded that under scenarios RCP8.5 and RCP2.6 scenarios, the rainfall is expected to display variable patterns, while under RCP6 scenario is projected that Saudi Arabia might experience a reduction in the rainfall amount. However, in light of the limited availability and accessibility to high resolutions data required for running any hydrological model, this study reviews the effects of climate change on water resources from a broad review based on government reports and pieces of published research in the literature.

Almazroui (2013) simulated the future rainfall and temperature from 2021 to 2070 in Saudi Arabia using the UK Met Office Regional Climate Model PRECIS (Providing Regional Climates for Impacts Studies). The results indicated that future temperature shows a positive trend of around 0.65 ◦C per decade for almost the whole of Saudi Arabia, whereas the changes in rainfall are expected to vary from an increased amount in the coastal areas and the south-southwestern regions into the drought conditions in the northern and central parts.

Niyazi et al. (2019) aimed to observe the spatiotemporal variability in the groundwater resources of the Red Sea Coastal Aquifer utilising the Gravity Recovery and Climate Experiment (GRACE) data and Analysis of climate models of Tropical Rainfall Measuring Mission (TRMM). The results reported that the recharge rate was estimated at ~16% of rainfall amount. This is related to rising rainfall events with the annual recharge rates increasing around 2.7–4.9% by the end of the 21st century. In the same study area on the Eastern Red Sea coastal plain, Sultan et al. (2015) have investigated the impacts of climate change on hydrologic systems of the period from 2020 to 2100, employing TRMM measurements and Community Climate System Model (CCSM4) with the SWAT hydrological model. The results indicated that the northern and central watersheds would

experience increased precipitation that would lead to an increase in the rate of streamflow and potential recharge, such as in the Wadi Al-Hemd mainly located in Al-Madinah, whereas rainfall would decrease towards the southern watersheds.

The study also estimated that the average annual runoff volume in Wadi Al-Hamd from 1998 to 2010 was about 6.197×10^6 m³, with an annual rainfall of about 58mm. The potential recharge was computed at 12.5%, and initial losses were estimated to be around 54% during the same period. Although precipitation is expected to increase to 85mm at the end of the century with a potential recharge of about 27.7%, it is estimated to increase initial rains' losses to more than 58%.

In the literature, many hydrological models have been employed to determine the influence of climate change on groundwater, which requires varied daily historical records for precipitation and temperature as well as the runoff data that would assist in calculating recharge rate changes. However, the difficulties of accessing runoff data for a sufficient historical period prevented the application of such hydrological models in this study. Therefore, the Topographic Wetness Index (TWI) was weighted by the future precipitation (2021- 2100) under RCP4.5 and RCP8.5 scenarios and was applied to examine the future climate-driven impacts on the natural replenishment of groundwater (Chapter 4). The TWI assumptions could provide valuable information about the spatial distribution of moisture patterns and the locations where water highly tends to accumulate (Grabs et al., 2009) and shows the possible impact of climate changes in the future potential groundwater zones under both models.

2.3.2 Evapotranspiration

Predicting precipitation and potential evapotranspiration (ET0) would play an essential role in outlining the future vision of groundwater resources, particularly in ASARs countries with chronic water scarcity. Therefore, the estimated impact of climate change on quantifying ET0 and analysis of the future spatial and temporal variability of the variable would contribute to developing sustainable water management strategies. In addition, although evapotranspiration is considered the primary ingredient after the rainfall affecting the hydrological budget, accurately estimating quantified evapotranspiration is viewed as being highly difficult because of

the complicated associations between meteorological features and conditions of specific sites (Gharbia et al., 2018). In reviewing the literature, several studies have attempted modelling the spatial distribution of ET0 and examining the efficacy of ET0 methods, which vary in climatological parameters used as well as computational complexity (Feng et al., 2016). For example, ElNesr et al. (2010) and Elnesr and Alazb (2013) applied the Penman-Monteith formula in Saudi Arabia to estimate the daily ET0 from 1980 to 2008. The results indicated that January had experienced the lowest amount by around 5 mm/d, whereas July's largest was about 15 mm/d. Moreover, spatially, the southern region recorded the lowest quantity between November and February, while the western part registered the lower amount from March to October.

It also was detected that Saudi Arabia had a steady increase in ET0 over the study period by a daily average of 9.6 mm/d in 1980 to 10.5 mm/d in 2008. In addition, Elnesr and Alazb (2013) revealed that the ET0 amount had increased toward the east of Saudi Arabia, which might be associated with the concentration of oil industries in these parts that could impact the air temperature as well as rise in relative humidity caused by its location on the Arabian Gulf. Mahmoud and Alazba (2016a) also estimated actual evapotranspiration (AET) in the western and southern regions of Saudi Arabia from 1992 to 2014 based on RS data using the Surface Energy Balance Algorithm for Land Method (SEBAL) on MODIS. The Penman-Monteith method has been applied to calculate reference evapotranspiration, which required various data such as latitude and longitude of the station, elevation, air temperature (maximum and minimum), wind speed, relative humidity, daily sunshine hours and monthly rainfall. The results showed that the monthly AET amount gradually increased in months from January to April, whereas values experienced a reduction from May to December. Moreover, the highest value of ET0 was recorded in Al-Madinah Province, (2059-2405 mm/y) while the mean annual AET ranged from 414 to 1510 mm/y.

Mahmoud and Gan (2019) also applied the FAO Penman-Monteith method with remote sensing (MODIS-NDVI) and GIS techniques for estimating and spatial distributing ET0 and AET in the central region of Saudi Arabia from 1950 to 2013. The results indicated that the highest ET0 values were (January to March) and (November-December) as well as the annual ET0 amount had experienced an increasing tendency in the entire study area by about 2127 to 2460 mm/year

in the study period. While the annual AET was estimated to range from 1200 to 2900 mm/year, which had increased gradually in the crop-growing season (January to May).

Generally, the Penman-Monteith method or FAO-56 is difficult to implement due to the large number of meteorological data requirements that might not be measured frequently in many regions (Feng et al., 2016). Accordingly, Čadro et al. (2017) have applied the 12 ET0 methods to estimate ET0 at sixteen locations in Bosnia and Herzegovina for the period 1961–2015 and examined these methods to find alternative equations that require fewer meteorological parameters compared to the FAO-PM method. The findings showed that the adjusted Trajkovic (AHS_Trajk) method was the best alternative with low the root mean square difference (RMSD) from 0.15 to 0.24 mm/day. This method only needs temperature (maximum, minimum) and solar radiation. The study also concluded that the models based on temperatures had more accurate predictions than combined approaches.

Gharbia et al. (2018) have assessed the efficacy of six algorithms for ET0, which are Hargreaves & Samni, Thornthwaite, Hamon, Blaney-Criddle, Kharrufa and Oudin that have integrated with GIS in the Shannon River catchment, Ireland. The most accurate ET0 model was combined with GCM ensembles of climate change models to predict future change influences on ET0 amount in periods 2020, 2050 and 2080 under RCP 4.5 and RCP 8.5 scenario. The results have revealed that the Hamon was the highest performer with the lowest RMSE of 8.6 mm. The most significant increase in ET0 in the Shannon River catchment is expected to be under the RCP 8.5 scenario at the end of the century in 2080 by around 75.9 mm annually, which counted a growth of 13.5% compared to 2020.

In addition, it would be highly beneficial in water resources management to display climatic variability and the interactions between evapotranspiration and rainfall that directly impact the hydrological system and groundwater recharge. Therefore, the climatic water balance has been highlighted by several pieces of literature. Evapotranspiration is considered the primary component of modelling the water balance (Fisher and Pringle Iii, 2013), and it was calculated mainly by difference between climatic data that is precipitation and potential evapotranspiration that also reveals the potential water surplus or deficit (Faye et al., 2019). This is often used as indicator of drought. The Standardised Precipitation–Evapotranspiration Index (SPEI) was widely

utilised for monitoring drought conditions in multiple timescales (Pei et al., 2020). Abdullah (2014) ; Faye et al. (2019) ; Pei et al. (2020) ; Qaisrani et al. (2021) have applied the SPEI index to analyse the drought trend in arid-semi arid areas by applying various ET0 methods such as Hargreaves, Penman-Monteith and Thornthwaite. The results showed that the SPEI index successfully analysed drought events and provided further understanding of its trends, which would support the decision-making process in managing water resources. However, these studies would be more advantageous in the water resource sector if future predictions of water balance were considered.

This study aimed to analyse climate change for the elements of precipitation, temperature, and evapotranspiration under two representative concentration pathways (RCPs) RCP4.5 and RCP8.5 scenarios. Moreover, the impact of climate change on the potential zones of groundwater using a novel approach based on integrating the TWI index with rainfall, as well as the prediction of the future of ET0 and SPEI, will also be displayed in this study.

2.4 Water demands under modified IPAT model and the socio-economic scenarios.

The sustainable management of water resources also requires considering the socio-economic factors, population, urbanization, and GDP per capita variables that would increase demand and consumption rates and place more burden on arid-semi regions that suffer from water scarcity. In order to examine the water demand growth relationship with all those variables more accurately, the modified IPAT model (explained below) was utilised in this study.

Such an analysis needs to prepare, generate, and calculate the required data, whether from official authority sources or open-access data. Therefore, this section is divided into reviewing the modified IPAT model studies and developing Landuse/Landcover Classification maps for extracting urbanisation data required by the IPAT model.

2.4.1 Modified IPAT model

There are several approaches and software tools that have been used to predict future water demand. These approaches included software tools such as WEAP; and statistical models that involved regression analysis alongside time series modelling, applying the computational

intelligence models, as well as adapted methods such as the IPAT model (Ayt Ougougdal et al., 2020 ; Wang et al., 2017b ; Babel et al., 2006 ; Al-Zahrani and Abo-Monasar, 2015 ; Quéfélec and Allal, 2014).

The WEAP tool was produced by the Stockholm Environment Institute's US Center (SEI-US), it is designed to support planners in evaluating water supply policies and implementing proper strategies of water resources (Maliehe and Mulungu, 2017). In addition, this model has the capability of drawing a comprehensive framework of solving water resources problems based on various variables included economic-social, demographic and hydrological factors as well as examining it under future development scenarios (Sieber and Purkey, 2015). In the literature, Water Evaluation and Planning (WEAP) modelling have been applied by Ayt Ougougdal et al. (2020), Alemu and Dioha (2020), Amin et al. (2018) and Johannsen et al. (2016) to simulate the current water condition in the reference scenario that performs as the measure to compare the output of other scenarios to. It also predicts the water demands under different scenarios by using the socio-economic scenarios including variables such as population growth, living standards (HLS) and climate change scenarios as inputs for developing water demands scenarios. In contrast, Hocine Kiniouar et al. (2017) applied WEAP in Mediterranean Basin to produce five scenarios for examining water needs over 30 years by using variables of population growth, drinking water, and water consumption for crop and industrial purposes.

Furthermore, several statistical models have been used to efficiently develop water demand future scenarios, whether they have been applied individually or combined with further models such as time series approach. Regression analysis is considered the most common by employing linear forecast functions (Wang et al., 2017b). The regression models have been used by Li et al. (2017) to analyse water demands in Shanghai through three future scenarios that included variables of GDP and population growth to 2050. These analyses used the extrapolation from past trends, whereas Wang et al. (2017b) have developed a statistical model represented in a linear regression model to project domestic water demands in the Huaihe River Basin of China for the years 2020 and 2030 using variables of population growth, lifestyle changes, urbanisation, technological advances as well as climate change. Kamis (2012) also investigated the present and future domestic water demands for Jeddah City in three scenarios that representing high,

moderate and low cases for the population, and the Geometrical Progression method and the Arithmetic Methods have been used to generate the high and low growth rate of the population respectively. Ouda (2013) also had analysed historical data to develop three scenarios based on population growth rate, which were named optimistic, moderate, and pessimistic scenarios to project domestic, industrial, and agricultural water demands in Saudi Arabia from groundwater, surface water, desalinated water, and treated wastewater until 2030. The findings exhibited that water demand management actions are required in all sectors in Saudi Arabia to minimise gaps between future demand and supply.

Almutaz et al. (2012) also used historical records to produce a long-term forecast model for water demand in Riyadh city the capital of KSA, which included variables of income, household size and temperature in three scenarios. The results revealed that socio-economic factors and temperature are equally crucial for water demand. Additionally, forecasting using Time series analysis is considered as a statistical abstraction that enables the clarification of the change of water demand over time, whether in long-term or short-term models (Qi and Chang, 2011). Thus, Babel et al. (2006) generated a model based on the multivariate economic approach utilising multiple regression analysis and time series modelling with considering nine factors influence. The results reported that the population, water tariff, public education level, and average annual rainfall have a significant effect on domestic water demand as well as the length of data series that has impacts on the accuracy of the prediction model. Moreover, both of Ghiassi et al. (2008) and Al-Zahrani and Abo-Monasar (2015) combined Artificial Neural Networks and Time Series Models to predict future water demand in urban residential considering the effect of climatic variables. The results exhibited that such models had performed efficiently in estimating water needs.

In the literature review, the IPAT model, which refers to Environmental Impact (I) by Population Size (P), Affluence (A), Technology (T), or extended forms as STIRPAT and Kaya were widely used to measure human activities' environmental effect related to growth in carbon dioxide emissions as well as to determine driving factors. Both of Lin and Li (2020) ; Majeed et al. (2020); Li et al. (2015); Wang et al. (2017a); and Li et al. (2015) have investigated in general the relationship between carbon emission and population, affluence, and the urbanization by implementing the

STIRPAT model. the results revealed that urbanization level, production industry and population, respectively, were the primary factors of increasing carbon emission. Furthermore, Qin et al. (2019) ; Li et al. (2015); Gao et al. (2010) have generated scenarios based on the STIRPAT to 2025 and 2020 respectively, to predict the environmental load and growth of carbon emissions where the appropriate models were suggested after examination significance statistically.

Although these models featured by being more flexible and manageable to operate, there are limited attempts to adapt and apply them in water resources issues. Quéfélec and Allal (2014) have highlighted the developing water demand management employing the IPAT model combined with a sustainable energy model as well as creating trend and adaptation scenarios for water demand to 2050 in North Africa. These scenarios based on population, GDP, electricity for water and energy bill factors. The results indicated that under both scenarios demand for drinking and industrial water increases rapidly over the studied period. Moreover, Jin et al. (2016) have examined the main factors affecting the agricultural water footprint in Beijing. It applied the STIRPAT model using population, urbanization level, GDP per capita, Engel coefficient that related to income that is consumed on food, and total rural power. The results exhibited that expending on the food and urbanization has the most considerable positive impact on increased water consumption for agricultural purposes.

Generally, the principal benefit of conducting scenarios based on the IPAT or the STIRPAT models is that such scenarios not only enable the researcher to analyse and predict the relations between the environment and human activities but also identify the fundamental driving forces and the most influencing factor; this would help to suggest the improvement measures and appropriate protection for environment quality (Gao et al., 2010 ; Fan and Lei, 2015).

In addition, as a result of being that socioeconomic factors have been the most influential on the increase in water demand. Hanasaki et al. (2012b) developed water usage scenarios consistent with Shared Socioeconomic Pathways (SSPs) assumptions on the global scale, which included factors of potential industrial water and municipal water consumption demand and the agriculture-related factors that comprised irrigation area and efficiency, and crop intensity. According to water developed SSPs assumptions, about 39 to 55% of the population would live

under exceptional water-stressed conditions and scarcity by 2071–2100, which is expected to be caused by population growth and economic activities. Graham et al. (2018) also produced future water sector assumptions for all SSPs that mainly in water technology assumptions and investigated global water demands via the end of the century. The results showed that the technological change affects the water sector and would assist in minimizing the water demand to above 32% in 2100, as well as the low-income areas would be more likely the most influential drivers of future water demands resulting from improving the irrigation system.

Moreover, Alcamo et al. (2007) and Li et al. (2017) have investigated future water demand under the different socio-economic and climatic changes; and the factors of GDP and population growth, respectively. The findings revealed that income growth and increased GDP were more important factors associated with increased water consumption.

Therefore, based on reviewing previous studies, the main contribution of this objective is to understand future water demand in Al-Madinah in light of the city's future development plans by employing the adapted IPAT model to facilitate predicting future water consumption trends under various demographic, economic and technological assumptions. Furthermore, throughout searching in the relevant literature, no related article has been found to date that uses the IPAT model in Saudi Arabia as well as to predict the water demand in a significant city such as Al-Madinah. Additionally, the IPAT model has rarely been applied to the water demand domain, and this study would be a contribution to enriching the water discipline research.

2.4.2 Landuse/Landcover Classification

Several techniques have been developed to map LULC patterns changes using the remote sensing (RS) approaches and satellite data as well as GIS technology. These techniques have been categorized into supervised and unsupervised methods (Talukdar et al., 2020) where the supervised classification requires prior knowledge about the study area to collect training data (Mohammady et al., 2014). Recently, classification by applying machine learning and deep learning algorithms for mapping LULC have become more prevalent (Vali et al., 2020). Both of Thanh Noi and Kappas (2017) and Abdi (2019) have compared the performance of non-

parametric machine learning algorithms to classify LULC by using data from Sentinel-2. These classifiers included random forests (RF), deep learning (DL), extreme gradient boosting (Xgboost), k-Nearest Neighbor (kNN), and support vector machines (SVM) that achieved the highest overall accuracy in the LULC map.

Li et al. (2023) also applied remote sensing from Landsat imagery data and a hybrid machine learning framework for land cover classification to detect agricultural land expansion in Saudi Arabia over the past three decades (1990 to 2021). The findings indicate the method showed good classification accuracy. Moreover, a significant expansion of agricultural land has led to the depletion of groundwater resources in the country. In 1990, the central regions of Saudi Arabia included the majority of agricultural land. Over the period from 1990 to 2010, there was a minor decrease in field acreage, which was mainly linked to a policy targeting the reduction of wheat cultivation. Saudi Arabia experienced a stage of agricultural fluctuations followed by an agricultural uptick starting in 2021.

In addition, random forest (RF) has been applied by Halmy et al. (2015) and Zhang et al. (2017) on Landsat Thematic Mapper 5 data to produce high accuracy LULC maps for more than 80 % for Egypt and the Wuhan urban, respectively. Nurfadila et al. (2019) also obtained an overall accuracy of more than 90% in the LULC map of Enrekang Region by implementing the RF approach on Sentinel-2 Imagery along with spot satellite data 6 for validation. Furthermore, dynamic models such as cellular automata models were used widely to simulate spatial distribution and predict land-use changes with the possibility of taking into account the physical and socio-economic as drivers of LULC changes (Gidey et al., 2017). Thus, both Guan et al. (2011) ; Yagoub and Al Bizreh (2014) ; Gidey et al. (2017) employed the integration method between Markov and Cellular Automata Models, and the results showed that the LULC maps generated were with satisfactory accuracy and such the model was effective to predicting the future LULC.

Consequently, to adapt the IPAT model, the variables' time-series data have been collected and extracted from various sources. Furthermore, due to the lack of LULC maps covering the whole study area from 1990 to 2020, remote sensing and GIS technologies and satellite image data were employed to extract maps and complete the time series used in the present study. Moreover, the supervised classification Random Forest approach has been applied in the present study

because it offers better accuracy in LULC maps and is considered a flexible and easy to utilise the method, particularly is embedded as a tool in ArcGIS pro an environment.

2.5 Conclusion

These studies clearly indicate that improving water security and sustainable management in arid-semi arid regions requires not only exploring new freshwater sources, such as identifying further potential sites for renewable groundwater to help mitigate pressure on existing water resources, but also the examination of external factors that might affect groundwater or other water resources would be needed, which including the climate change's impacts as well as the potential driving factors such as population, urbanization and GDP that could highly raise consumption rates. Therefore, the present study would make an important contribution to the field of water resources by creating comprehensive models in three dimensions that could help provide insight into the effective management of groundwater resources in the arid-semi arid regions that included several essential considerations by employing novel and multiple sophisticated technologies. First, the methodological framework for delineating potential groundwater zones will be developed in a semi-arid region using the suitability models based on GIS technologies, remote sensing data and statistical models that have assisted in integrating the fuzzy logic method with frequency ratio and then comparing the logistic regression model. Secondly, climate change's impacts on potential groundwater zones would also be evaluated by a novel method based on TWI-Rainfall that might be suitable for arid areas that lack daily records of required meteorological elements. Thirdly, future water demand patterns under the modified IPAT model and the socio-economic scenarios that are infrequently used in the water field will be examined.

Chapter 3 Modelling Groundwater Potential Zones in Al-Madinah using the integration of Fuzzy Logic-Frequency Ratio methods and Logistic regression models.

Abstract

Groundwater is considered one of the essential natural resources globally, where it has been estimated that approximately one-third of the world population has become entirely dependent on groundwater. It is a primary source of fresh water as an alternative for deficiency of surface water. Demand for such resources is also increasing along with increasing population. Therefore, mapping potential groundwater zones (GWPZ) could help develop the sustainable management of groundwater resources, especially in arid and semi-arid areas. This study applies two approaches, one combining Fuzzy logic and frequency ratio methods and the other applying Logistic regression models, to examine potential groundwater zones for Al-Madinah city, located in western Saudi Arabia. The models were built based on geological, topographical, and hydrological factors, including soil, lithology, slope aspects, slope gradient, plan curvature, altitude, rainfall, topographic wetness index (TWI), stream power index (SPI), fault density and drainage density. The Area Under the Receiver Operating Characteristic Curves (ROC-AUC) were employed to validate and compare the performance of the models. The results indicated that the Fuzzy Gamma 0.97 method had a slightly higher performance than logistic regression, AUC = 0.943 and 0.885, respectively. The most relevant contributors to groundwater occurrence are soil, faults density, drainage density in the fuzzy logic approach and soil, drainage density, TWI_Rainfall in the logistic regression approach. The spatial distribution of very high potential groundwater areas in Al-Madinah is primarily compatible with volcanic lava areas. Finally, decision-makers could utilise these findings to improve conservation measures and sustainable groundwater management and consider these potential zones during future strategic LULC planning.

3.1 Introduction

Water is fundamental not only for human survival and ecosystems but also considered necessary for sustainable development and improving socio-economic activities (Hanasaki et al., 2012a ;

Ghosh, 2021). Water is one of the vital issues that numerous arid and semi-arid countries face; these areas are expected to suffer from scarcity of water resources or water stress currently or in the future, even if they do not suffer currently (Bates et al., 2008). The freshwater supplies from rivers, lakes and precipitation are characterised by uneven distribution geographically in these areas (Bates et al., 2008). Further additional pressure on water may be imposed by climate change, which means more of the global population may be exposed to risk of water scarcity (Bates et al., 2008). Therefore, groundwater plays an essential role in many of these arid and semi-arid areas as the only source of freshwater and the main water supply for meeting drinking and irrigation needs. It has been reported by Margat and Van der Gun (2013) that about 70% of global groundwater withdrawals were in arid and semi-arid regions that occupy about 30% of the Earth's inhabited surface.

Non-renewable groundwater, which is deep aquifers inside sedimentary basins, and renewable groundwater resources such as the shallow alluvial aquifers are considered the two main types of groundwater (Al-ahmadi and El-Fiky, 2009). Although renewable groundwater is not widely spread in arid and semi-arid countries, it is viewed as the only permanent local water source in countries devoid of surface water such as rivers and lakes (Margat and Van der Gun, 2013 ; Al-ahmadi and El-Fiky, 2009). In the twenty-first century, many renewable groundwater aquifers have been made more vulnerable to depletion because of over-abstraction (Margat and Van der Gun, 2013).

Therefore, these groundwater resources need to be managed sustainably. Recently, the development of remote sensing and GIS techniques has contributed to managing groundwater resources by mapping the current or potential suitable zones for groundwater (Rahmati et al., 2014). These efforts have employed methods such as statistical models, data mining/machine learning, and multi-criteria decision making.

It has been declared by United Nations World Water Development Report, UN (2022) that Saudi Arabia was among the countries that had the highest groundwater withdrawals in 2017. The scarcity of natural water supplies in the Kingdom of Saudi Arabia (Zaharani et al., 2011) are considered the principal motive not only to develop future strategies of the water sector in Vision 2030 based on sustainable water consumption but also to explore new renewable groundwater

sources (MEWA, 2018b). Therefore, mapping the potential groundwater is considered a pressing necessity to structure and establish a proper water management plan. Recently, remote sensing and geographical information system have been integrated with statistical methodologies and machine learning to generate spatial and temporal data related to predicting and suitability models (Rahmati et al., 2016 ; Arabameri et al., 2019a). This allowed the mapping of potential groundwater locations. However, there no full or agreement about which method has the most predictive accuracy (Arabameri et al., 2019a) or which methods are best for different settings. Consequently, the further experimentation and application of approaches that could be useful to mapping potential groundwater remains an opportunity good to enrich knowledge in this discipline.

Accordingly, the present study attempts to model groundwater potential in the semi-arid area of Al-Madinah city, western Saudi Arabia. This study will compare two methods of mapping potential groundwater zones: a Fuzzy Logic-Frequency ratio approach and a logistic regression model approach. The first approach has rarely been used in the field of groundwater mapping, whereas the second method is commonly utilised, eleven conditioning factors that would assist in the prediction of groundwater distribution are employed.

3.2 Methodology

Figure 3-1 represents the methodology used in this study, comprising multiple steps.

3.2.1 The Fuzzy Logic approaches.

Fuzzy Logic was introduced by Lotfi A. Zadeh in 1965 (Zadeh, 1965). The fundamental assumption of Fuzzy Logic theory is simulating human thinking in decision making, particularly in complex and MCDM problems that are difficult to determine precisely in crisp numbers; this is achieved by considering degrees of truth or membership values in the unit interval between 1 and 0 rather than applied two-valued Boolean logic, which is based on true/false or 1s and 0s (Zadeh, 1965 ; Dymova et al., 2021). Generally, Fuzzy logic is viewed as a generalization of classical set theory and also as an extension of Boolean logic that relies on the mathematical principles of fuzzy sets (Dernoncourt, 2013). A set can be defined as a grouping of elements with similar properties that represented members; in the classic set, element membership is determined by precise boundaries, which are used to include an element as a member of the set or not, where no partial

membership exist (Czogała and Łęski, 2000 ; Smithson and Verkuilen, 2006) and in classical logic, a membership function is expressed with the form

$$f_A(x) = \begin{cases} 1, if\ x\ \in A \\ 0, if\ x\ \notin A \end{cases} \qquad f_A(x):\ X \to \{0,1\} \qquad (1)$$

Where: $f_A(x)$ is the membership function of element x in set A (Czogała and Łęski, 2000 ; Aouragh et al., 2016)

However, it might be difficult to define a specific point that would categorize the elements according to their characteristics because elements could possess a property in varying degrees, which requires work with a degree of uncertainty (Zadeh, 2008 ; Smithson and Verkuilen, 2006). Therefore, Fuzzy logic effectively deals with such subjects where partial membership is allowed that indicates that elements can have varying degrees of membership within the set (Zadeh,1965).

The membership functions represent an essential role in fuzzy set theory, and it could be described by a graph that shows how much of each input variable is considered to be a member of set A, this graph is outlined to an interval scale between zero and one where the x-axis displays the universe of discourse, and the y-axis is the grade of membership between 0 and 1 (Zadeh, 2008 ; Smithson and Verkuilen, 2006). Furthermore, the fuzzy set A of universe X is defined by function μ (x) called the membership function of set A and is expressed mathematically as (Zadeh, 1965 ; Negnevitsky, 2005):

$$u_A(x): X \to [0,1] \quad \text{Where:} \qquad (2)$$

$$u_A(x) = I\ if\ x\ is\ totally\ in\ A;$$

$$u_A(x) = 0\ if\ x\ is\ not\ in\ A; \qquad 0\ < u_A(x) < I\ if\ x\ is\ partly\ in\ A$$

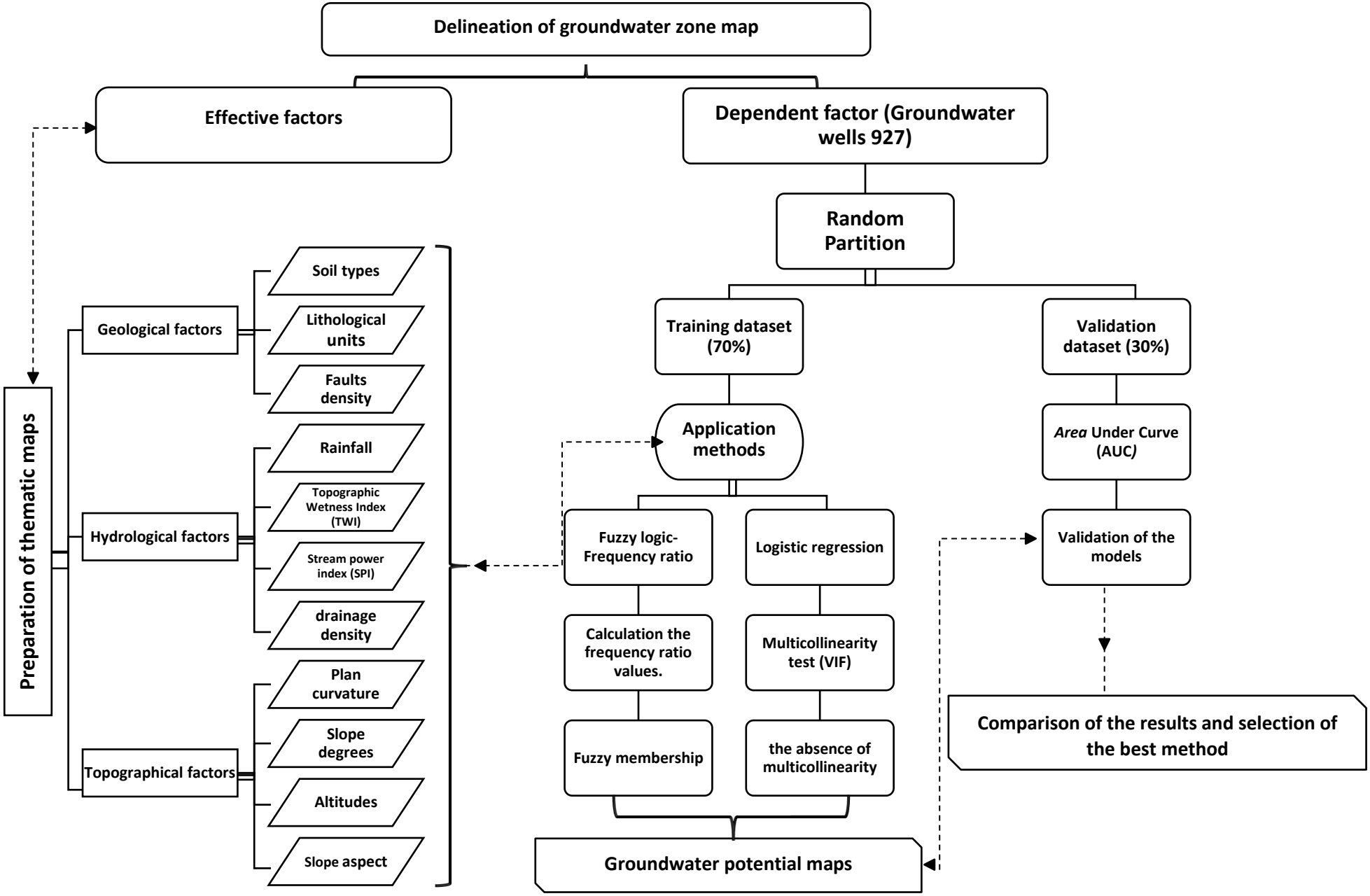

Figure 3-1. Flow chart of the methodology used in groundwater potential zones mapping in Al-Madinah province

In addition, there are some common or primary types of membership functions (MF) based on the shape of the curve formed by the insertion points, as illustrated in Figure 3-2, these types are named Triangular MF, Trapezoidal MF, Gaussian MF and the generalized bell MF (Talpur et al., 2017 ; Jang and Chuen-Tsai, 1995 ; Jain and Sharma, 2020). According to Sadollah (2018), extensive literature has indicated that a triangular MF has often been applied with the advantage of simplicity. The Gaussian MF was also been commonly employed due to its features of smoothness and concise notation (Sadollah, 2018 ; Jang and Chuen-Tsai, 1995). The degrees of membership in fuzzy logic is not subjected to specific guidelines and rules for their extraction; generally, experimentation, sufficient experience and the accumulation of knowledge would assist in identifying the appropriate form of MF (Medasani et al., 1998 ; Sadollah, 2018). However, these fuzzy membership shapes could be highly associated with subjective judgment issues in deriving the membership (Kritikos et al., 2015 ; GEMITZI et al., 2011).

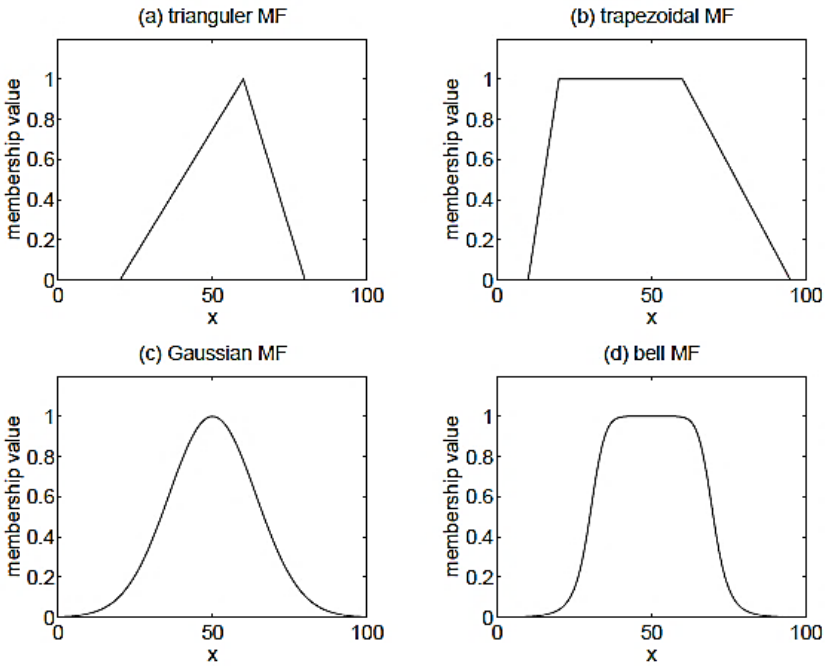

Source: (Jang and Chuen-Tsai, 1995)

Figure 3-2. The main shapes of membership functions

Consequently, membership degrees have experienced extensive attempts to develop more appropriate methods for estimating such values (Medasani et al., 1998). Therefore, the present study attempts to find the degrees of membership using the statistical Frequency Ratio approach.

Fuzzy logic and Geoinformation modelling

The process of representing geographical data and making decisions about geographical phenomena is often faced with uncertainty, where it may be very complicated to define a precise separation point or boundary separating the categories of any geographical phenomenon. An example is the classification of soil into units, as shown in Figure 3-3 related to the distribution of Yellow Latosol (YL) and Red Latosol (RL). Thus, using the uncertainty term and functions that exist in Fuzzy logic modelling is considered more appropriate than describing such issues as being data misrepresentation or error problems (Mironova, 2018).

Sui (1992) stated that several scientists have realized the insufficiency of the Boolean logic processes that is used widely in geographic information systems for spatial data modelling purposes, particularly with the development and prevalence of GIS in the 1980s as well as the emergence of an increasing need for uncertainty in human data related to the procedures of modelling and decision-making.

Buckley (1984) and Mironova (2018) indicated that the solution of the geographical problem commonly consists of a set of alternatives and criteria that might be vaguely understood or uncertain, therefore, producing degrees of priority and importance by the linguistic expressions such as 'low' or 'high' are more preferable, as well as the Fuzzy logic method viewed as an approach that could convert such descriptions into a numerical form for use in the spatial modelling processes.

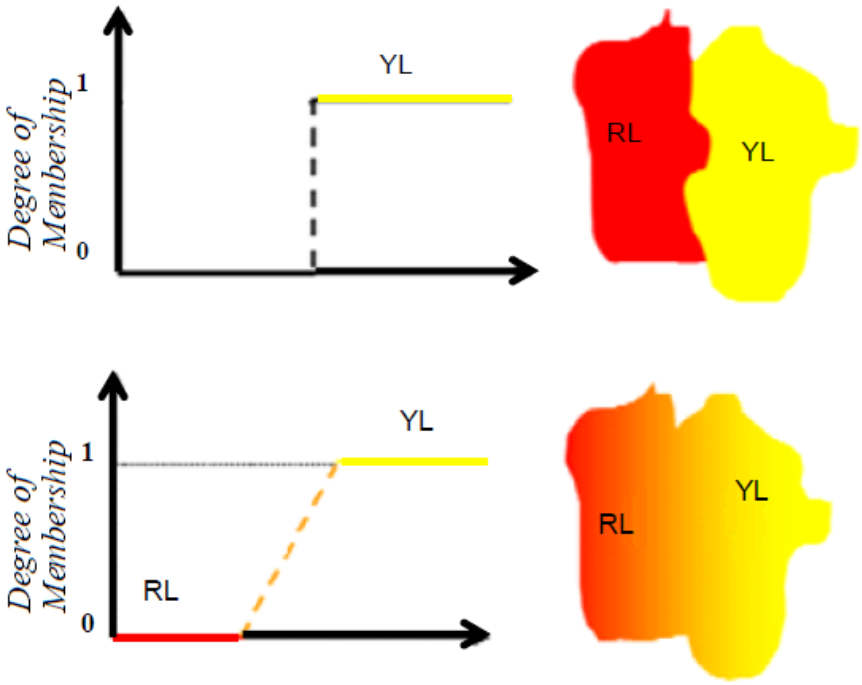

Source: *(Menezes et al., 2013)*

Figure 3-3 The membership degree in Fuzzy logic and classical logic. Distribution Yellow Latosol (YL) and Red Latosol (RL) under Boolean logic (above) and fuzzy logic (bottom)

The Multi-Criteria Decision Making (MCDM) has been utilised extensively in studies related to water management to improve the transparency of the decision process where MCDM work has used the fuzzy set (Hajkowicz and Collins, 2006). Furthermore, these approaches have integrated efficiently with GIS technique that allowed them to be applied spatially (Carver, 1991). Therefore, the definition of criteria' classes used and the characteristics of the phenomenon by values of membership is crucial to implement suitability models (ESRI, 2016b).

3.2.2 Fuzzy-Frequency ratio membership of conditioning factors

Here, the raster calculator of Spatial Analyst in ArcGIS Pro has been used to compute and generate fuzzy raster layers from input variables based on the frequency ratio method. In addition, several fuzzy operators included in ArcGIS Pro were employed to combine the fuzzy memberships of criteria used into a final suitability map. The fuzzified variables in the present study have been combined using various fuzzy overlay methods represented in Fuzzy-And, Fuzzy-OR, Fuzzy-Sum, Fuzzy-product, and Fuzzy-Gamma, as displayed in Table 3-1 (ESRI, 2016a). The

fuzzy gamma operator allows an output between the increasing trend of fuzzy SUM and the decreasing effect of fuzzy Product (Bonham-Carter, 1994 as cited in Srivastava et al. (2010). The fuzzy gamma operator has been examined with values of 0.50, 0.70, 0.80, 0.90, 0.95, 0.97, 0.98 and 0.99.

Table 3-1 Types of fuzzy operators

Operator	Equation	Explanations
AND	$U_{combination}=\min(U_A,\mu_B,\ldots)$	it represents the intersection function that defines the minimum values among all the membership degrees of inputted raster.
OR	$U_{combination}=\max(U_A,\mu_B,\ldots)$	it represents the union function that defines the maximum values among all the membership degrees of inputted raster.
PRODUCT	$U_{combination} = -\Pi_i^n = 1\ \mathcal{U}1$	It is based on multiplying each of the fuzzy membership values for all the entered raster, the output will be less than any of the input or equal to the smallest value.
SUM	$U_{combination} = -\Pi_i^n = 1(1- \mathcal{U}_i)$	it combined the fuzzy membership values of the inputted raster, and the output always is greater than or equal to the largest value of fuzzy membership value.
GAMMA	$U\text{combinatin} = (FuzzySum)^{y} * (FuzzyProduct)^{1-y} \quad Y^1[0 - 1]$	It is a combination between the fuzzy sum and fuzzy product, where both are raised to the power of gamma. The gamma 1 is closer to the type of fuzzy sum, whereas if the gamma value is zero, it is closer to the fuzzy product; γ is a number from<0, 1>interval that provides either fuzzy algebraic sum (γ=1) or fuzzy algebraic product (γ=0) (Roy and Saha, 2019).

Adapted from (ESRI, 2016a ; Alavipoor et al., 2016 ; Nyimbili and Erden, 2020)

3.2.3 The frequency ratio method

The frequency ratio is a bivariate statistical analysis approach that calculated the percentage probability of occurrence of a particular attribute (Oh et al., 2011). Geographically, it provides the possibility to estimate the relationship between dependent and independent variables based on the spatial distribution or that composed from multi-classified maps (Ozdemir, 2011a ; Sahoo et al., 2017). Accordingly, the frequency ratio computes the ratio of the area where the event has occurred to the total study area, particularly the concept the probabilistic theory that has included allows to assume that historical events affect future events if they occur under the same conditions (Oh et al., 2010). To determine is a site has a high or low chance of water availability,

the approach can be applied to the geological, hydrological, and topographic determinants that affect the formation of groundwater. The frequency ratio can be expressed as:

$$GWPI = \sum FR \qquad (3)$$

Where GWPI is groundwater potential zones index, and FR is the frequency ratio. FR is formulated as:

$$FR = \frac{\frac{N_{pix}(SX_i)}{\sum_{i=1}^{m} SX_i}}{\frac{N_{pix}(X_j)}{\sum_{j=1}^{n} N_{pix}(X_j)}} \qquad (4)$$

Where $N_{pix}\ (SX_i)$ represents the count of pixels containing groundwater wells in class i of parameter variable X, $N_{pix}\ (X_j)$ indicates the total number of pixels within parameter variable X_j, m is the number of classes in the parameter variable X_i, and n is the number of parameters in the study area (Regmi et al., 2013). Figure 3-4 displays the example of the main steps for extracting the frequency ratio for one class from raster data.

Firstly, collecting data about locations of groundwater wells for the whole study area, which is considered the main factor to calculate FR. Secondly, extracting the number of pixels for each class for factor A. Thirdly, representing the area of spatial overlap for areas of groundwater wells and areas of class 1 for factor A, where the higher ratio indicates there is a strong relationship between the places of groundwater wells and the given factor's attribute, which also could be used to predict for the future possibilities of the groundwater. Finally, the Frequency Ratio values were normalized within a range of 0 to 1 to generate the fuzzy membership values.

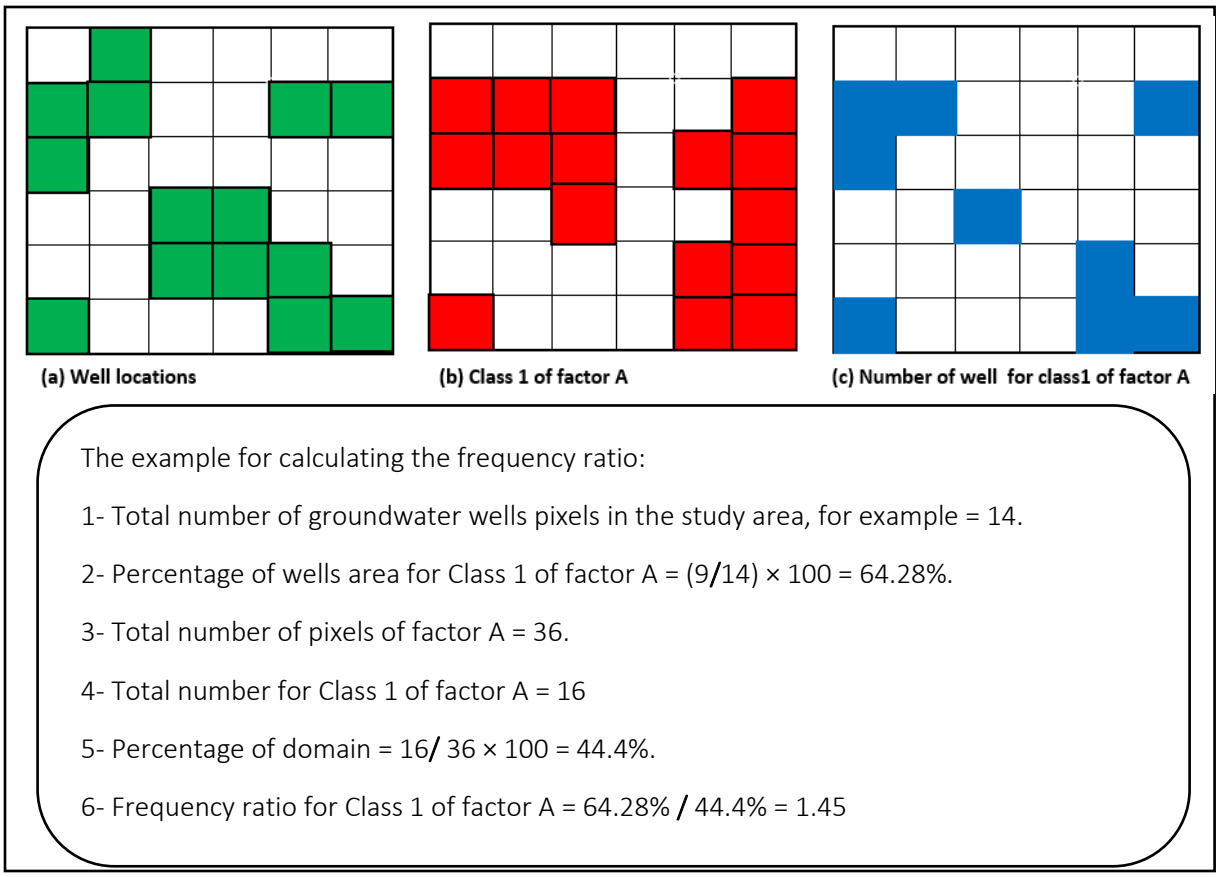

Figure 3-4.Diagram displaying the main steps for extracting the frequency ratio values.

3.2.4 Binary logistic regression (BLR) model

A logistic regression model is a statistical approach of regression analysis and one of the Generalized Linear Models family, which is applied to identify the relationship between binary responses (coded 0,1) of the dependent variable for estimating the probability of presence and absence based on a variety of independent variables that could be categorical, multiple ordinal and continuous or a mixture (Ozdemir, 2011a ; Roy and Saha, 2019). The general equation of logistic regression can be represented as follows:

$$P = \frac{1}{1 + e^{-z}} \quad (5)$$

$$Z = \propto + B_1 x_1 + B_2 x_2 + B_k x_k \quad (6)$$

Where p is the probability of an event that ranges between 0 and 1, whereas Z represent the linear function of the predictors, and $\propto$ is the intercept of the model, B_i denotes the coefficients of the independent variables x_1 to x_k (Kleinbaum and Klein, 2010 ; Du et al., 2017 ; Ozdemir, 2011b).

Moreover, the contribution of each independent variable to the probability value (P) can be estimated from the regression coefficients (Ozdemir, 2011a). The model estimates the probability of an event occurring which can be easily calculated as the odds ratios of independent variables. The odds ratio helps determine the extent to which predictor factors influence the likelihood of occurrence of the dependent variable (Hilbe, 2016). The odds ratio (OR) is the exponentiation of the variable coefficient (Kleinbaum and Klein, 2010 ; Hilbe, 2016) An odds ratio below 1 indicates that the probability of an event occurring decreases in that particular category compared to the baseline. Conversely, an odds ratio above 1 indicates that the probability of the event occurring increases in that category compared to the baseline. A value of 1 indicates no effect of the independent variable (Osborne, 2019). The continuous factors represented in percentages are often easier to interpret.; this could be using following formula:

$$OR\% = \left((exp(B) - 1) * 100\right) \qquad (7)$$

$exp(B)$ is the exponential of the coefficient B (Hilbe, 2016).

Therefore, the odds ratio besides the p. value has been used here to determine the most influential variables on groundwater formation. In the present study, the presence of 646 groundwater wells were used as the dependent variable along with 646 locations where wells are absence selected randomly within ArcGIS-Pro,(Figure 3-5). The independent variables included soil type, lithology, and slope aspect, as well as the continuous data comprised in fault density, drainage density, slope degree, The topographic wetness index (TWI)- rainfall index, Stream Power Index (SPI), plan curvature and altitude. The R and ArcGIS-Pro environments were used to enable the logistic regression modelling.

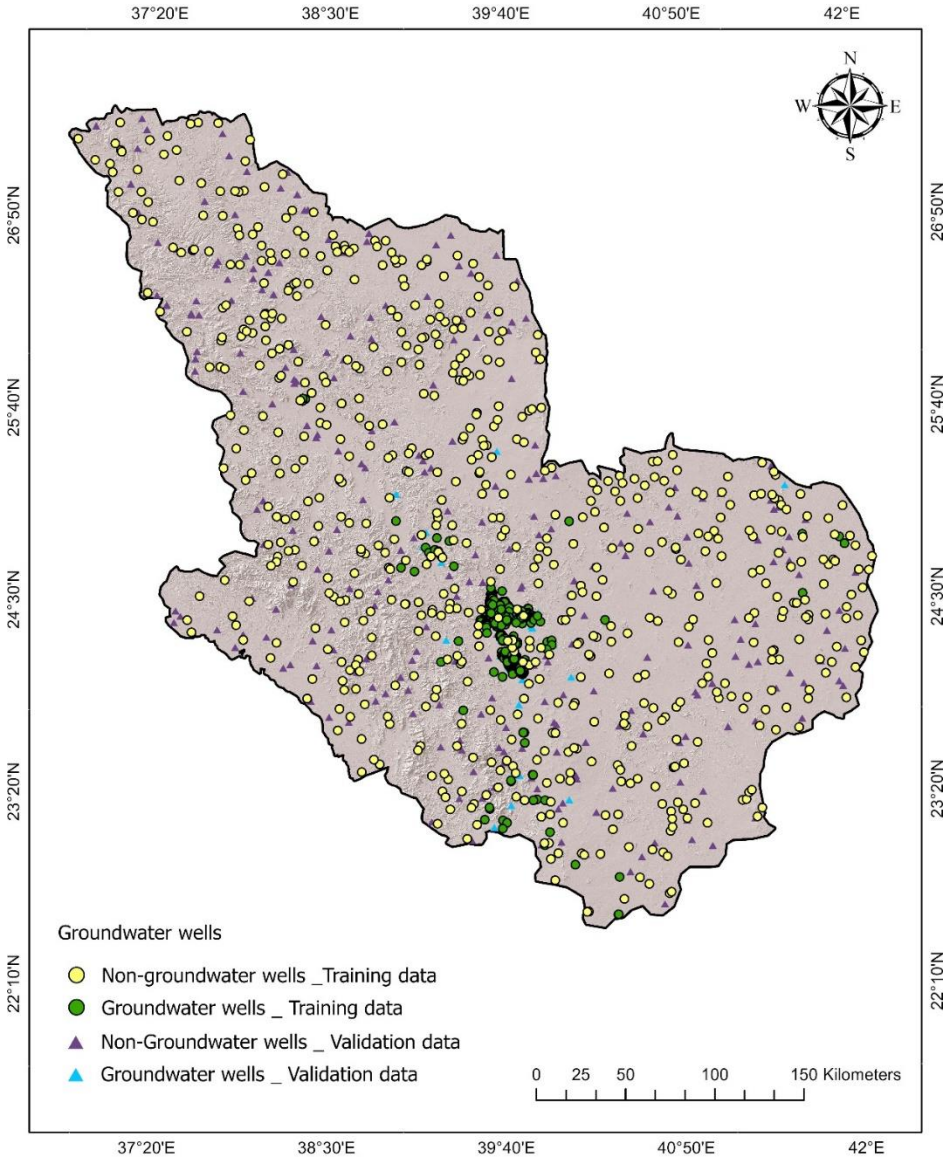

Figure 3-5 Spatial distribution of groundwater wells and non-groundwater wells.

3.3 Preparation of thematic maps

There are various control factors on groundwater formation and storage as well as replenishment operation that could vary considerably between regions (Mahmoud and Alazba, 2016b). Literature review informed the decision on which explanatory variables to use.

3.3.1 Geological factors

3.3.1.1 Soil type

Soil is considered an essential factor in delineating the potential groundwater zones because it impacts runoff and recharging groundwater as well as determines the magnitude of water-holding capacity according to its types and permeability level (Kumar et., al, 2016). The soil map of Al-Madinah, (Figure 3-6), was obtained from Al-Madinah Region Development Authority, and it covers six different soil types: Lithosols, Calcic Yermosols, Haplic Yermosols, Cambisols Chromic and Orthic Solonchaks. The lithosols that originated from sedimentary sandstones were very shallow with low capacity of water holding, and are poor for cultivation (De Pauw, 2002 ; Mahmoud and Alazba, 2016b).

In addition, Yermosols are generally aridic soils with clay accumulation, possibly developed during a period of wetter climate (Mahmoud and Alazba, 2016b). Al-Madinah contains two types of Yermosols, which are Calcic Yermosols and Haplic Yermosols that are very poorly developed, Calcic Yermosols soil is calcium-enriched subsoil and unsuitable for agriculture, whereas Haplic Yermosols require full irrigation for all agriculture practices (De Pauw, 2002). Moreover, the Cambisols Chromic consist of several rocky outcrops and mountains that cover large area in Al-Madinah. The Orthic Solonchaks are saline soils with badly drained states.

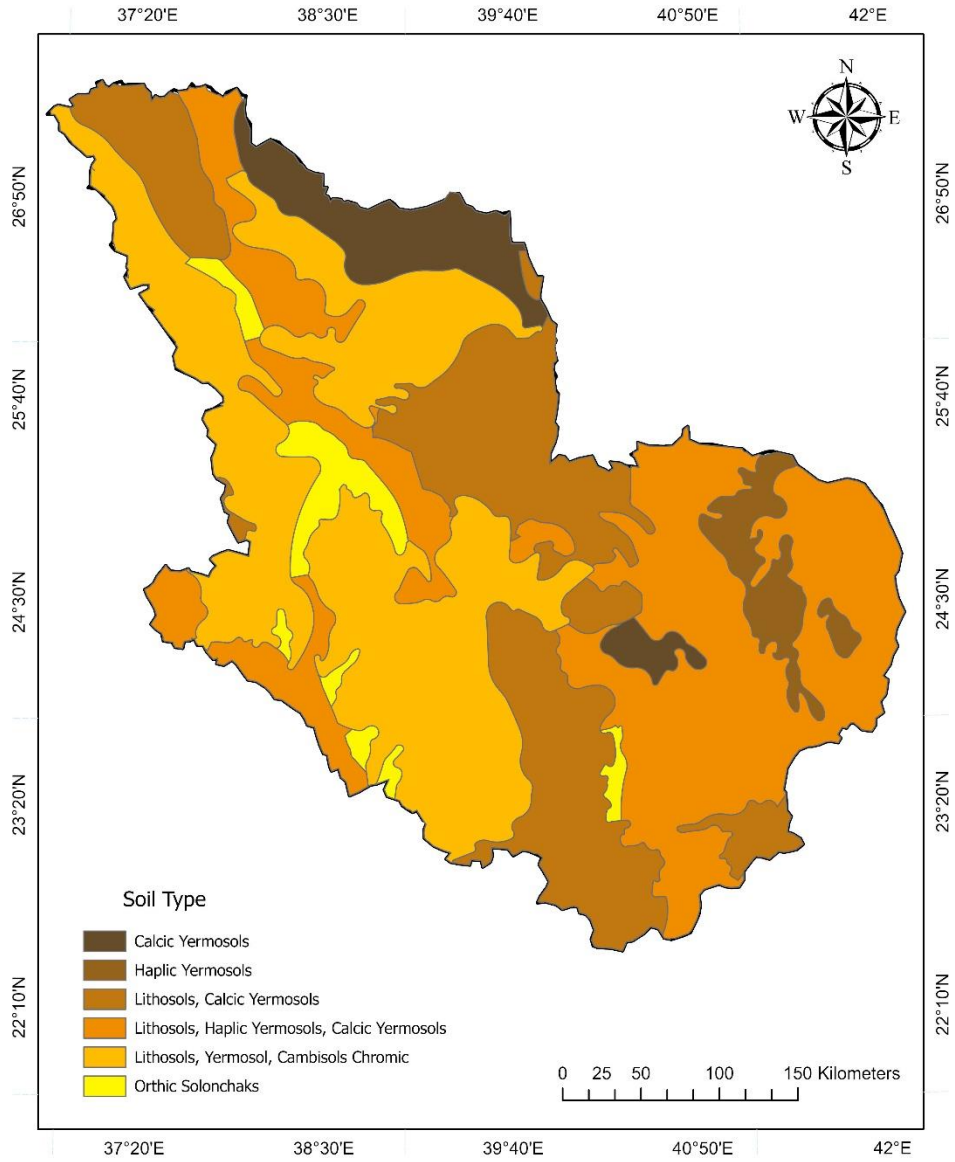

Source: adapted from (MMDA, 2020)

Figure 3-6. Soil types in Al-Madinah region

3.3.1.2 Lithology

Al-Madinah is considered as part of the Arabian Shield, with its rocks formed primarily since the Precambrian age, mostly from igneous and metamorphic rocks that also covered by volcanic lands (Powers et al., 1966). Therefore, lithology types of Al-Madinah could be divided into Igneous rocks, Metamorphic rocks, Polylithologic rocks, Sedimentary rocks and Surficial deposit or alluvial deposits. The Igneous rocks included many types (intrusive and extrusive) such as

granite, granodiorite, tonalite, gabbro and basalt. The lavas are often characterized by high permeability that allows groundwater to be stored (El Maghraby, 2014b). They cover about 43.9 % of the total area of Al-Madinah area, as shown in Figure 3-7.

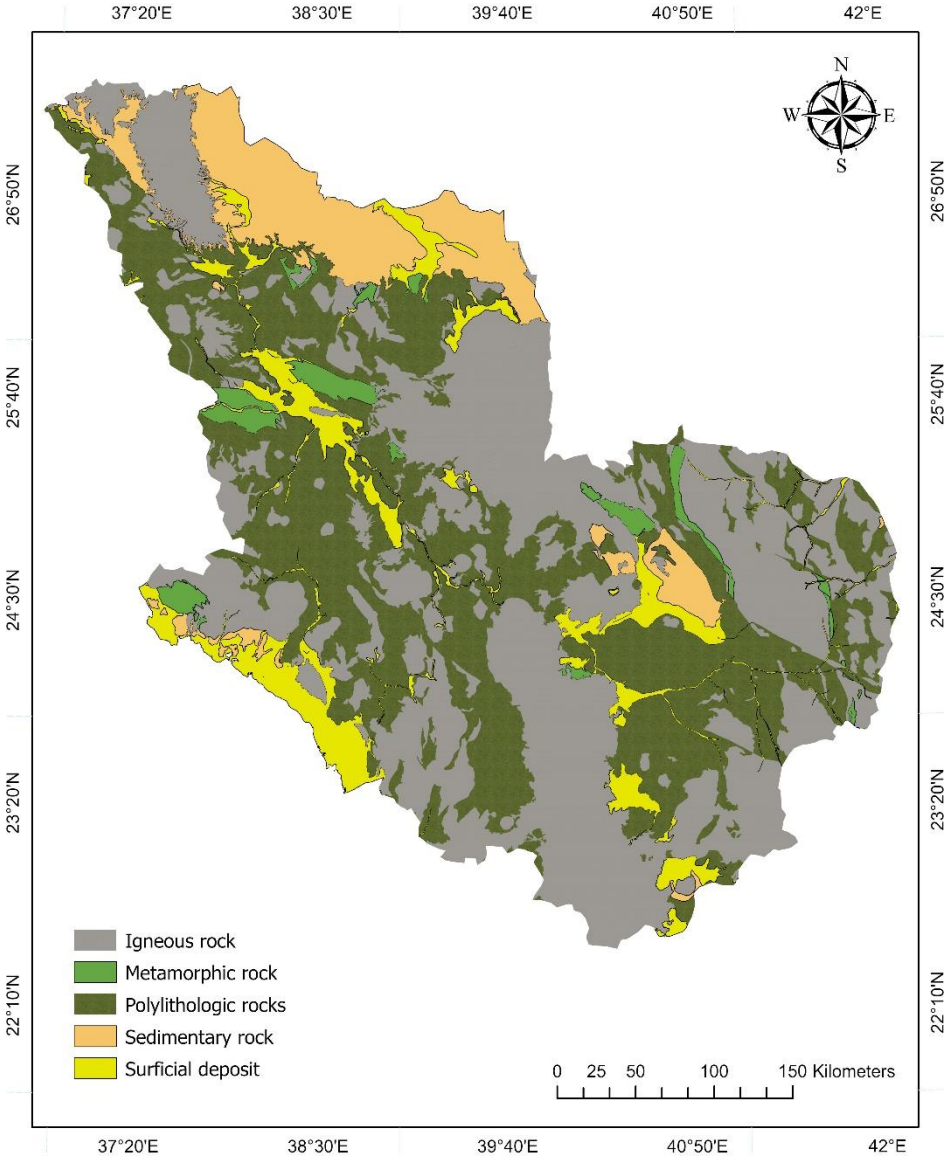

Source: adapted from (SGS, 2017b)

Figure 3-7. The main Lithological units of Al-Madinah region.

The lithological class of metamorphic rocks cover about 2.5% of Al-Madinah area. They comprises an aggregation of different rock types including rocks that have an igneous protolith such as

ortho-gneiss and ortho-schist, as well as some rocks that have a sedimentary protolith such as paraschis and paragneiss, which are medium-grained (Johnson, 2006). Moreover, polylithologic rocks included several groups of undivided volcanic and sedimentary rocks, from the Isamah formation, Siham group, Al Ays group, Tamran formation, Naslah formation, Suri formation, Ghamr group, Qahah formation and Mahd group (Johnson, 2006). These rocks covered around 35.6% of the Al-Madinah area. Volcanic and sedimentary rocks in some parts of the Arabian shield were described as having complexity and deformation (Johnson, 2006), which causes difficulty in identifying the water storage properties accurately. However, the database of groundwater wells in Al-Madinah, which has been used in the present study, revealed that about 196 wells, around 30% of the total wells, occurred over the polylithologic rocks, which indicates it has a good storage capability.

The sedimentary rocks in Al-Madinah involved the rocks from the Neogene period, Mesozoic and Palaeozoic sedimentary rocks, included, for example, sandstone, siltstone, and limestone where such these rocks are viewed as having the capability to store some water (Johnson, 2006 ; Fallatah, 2019). The sedimentary rocks cover about 9.5% of Al-Madinah area. In addition, Al-Madinah is covered by around 8.3% of Cenozoic surficial deposits, which contain soft clay deposits, sabkhah deposits (saline deposit), and wadi deposits and alluvial deposits where the wadi deposits are considered as the primary productive unit of the aquifer, and its thickness ranges from around 15m -19m to about 40m, with the maximum reaching around 50m in the centre of the wadi Al-Hamd area (Khashogji and El Maghraby, 2012 ; Bob et al., 2014 ; Al-Refeai and Al-Ghamdy, 1994).

3.3.1.3 Fault density

Al-Madinah is geologically a part of the Arabian Shield and consists of various types of faults perpendicular to the Red Sea and rifts parallel to the Red Sea coast. The Najd Fault System is considered as the main fault (Moore, 1979). The criterion of distance from faults or lineaments is essential in a hydrological investigation where the significant hydrologic zones are often located in the regions of linear formations (Benjmel et al., 2020). In addition, the faults have first been extracted by digitizing from the geological map of the study area. Subsequently, the faults

density was calculated using the line density analysis tool of ArcGIS pro software, which is based on drawing a circle around the centre of each cell after setting the search radius, and then each line within the circle is multiplied by the value of the population field, then the total is divided by the circle's area (ESRI, 2022b), (Figure 3-8).

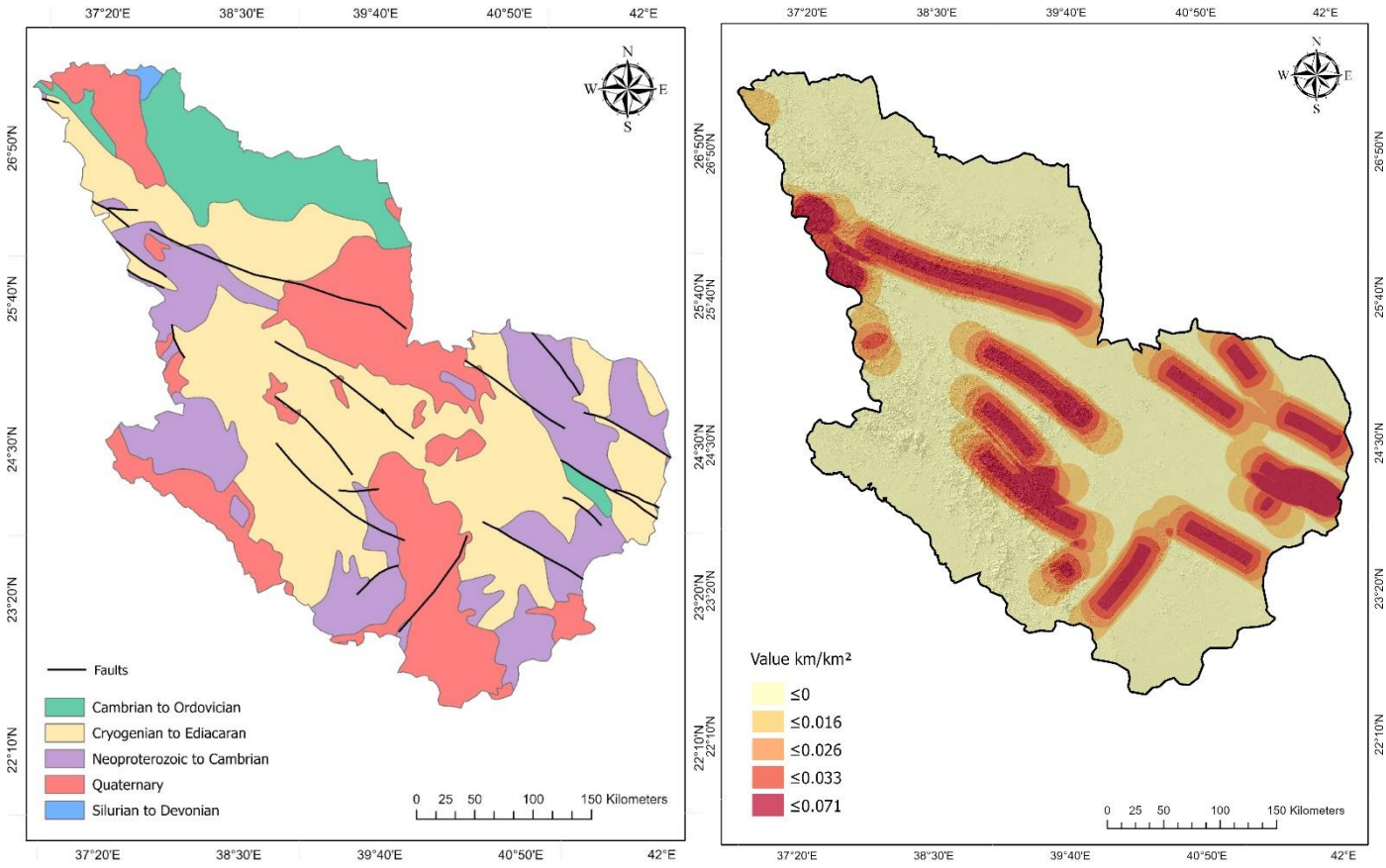

Figure 3-8. Geological map and fault density of Al-Madinah, figure shows Geological map of Al-Madinah (left) adapted from (SGS, 2017a), and fault density (right)

3.3.2 Hydrological and topographical factors

3.3.2.1 Rainfall

The precipitation is considered the major source of recharge for the groundwater of Al-Madinah. The baseline period data was selected from 1970 to 2018 from historical climate data in WorldClim (Fick and Hijmans, 2017). Analysis of these indicated that the annual average rainfall

of the region ranged from about 79.68mm to a maximum amount of around 121.74 millimetres. The Al-Madinah region's northern, northeastern, eastern, south, and south-eastern areas received the most rainfall during the historical period. The precipitation data used in this chapter are fully discussed in chapter four.

3.3.2.2 Topographic wetness index (TWI) and the Stream power index (SPI)

The TWI-Rainfall and SPI maps have been generated from Shuttle Radar Topography Mission (SRTM-30 DEM) by the r. watershed tool in QGIS using the multiple flow direction (MFD) method. Topography significantly influences the spatial variety of hydrological conditions by, for example, affecting exfiltration operation and soil moisture (Moore et al., 1991 ; Sørensen et al., 2005). The topographic wetness index (TWI) and Stream power index (SPI) are among the most critical factors used widely to map potential groundwater reservoirs. Generally, the TWI represents the association between slope degree and flow accumulation, the upslope area as a measure of water flowing towards a specific point, or in other words, it indicates the possible location that water tends to accumulate (Jaafarzadeh et al., 2021 ; Grabs et al., 2009). Consequently, the high TWI values may suggest a greater possibility of water accumulation due to a lower slope and substantial upstream area, whereas sites with a steep slope and lower upstream area will have low TWI value and have less opportunity for water collecting (B Riadi, 2018). TWI is defined as (Moore et al., 1991):

$$TWI = \ln (a/tan\, B) \qquad (8)$$

TWI in this study was calculated weighted by rainfall:

$$TWI = \ln (Rainfall * \alpha/tan\, B) \qquad (9)$$

where a is the cumulative upslope area draining to a point, and tan ß is the slope angle at the point. The TWI of Al-Madinah area ranges from 9.43 to 36.03, where the high values have compatible with the sinks and flows of valleys, as shown in the Figure 3-9.

The Stream power index (SPI) is a measure of the erosive power of water movement based on the hypothesis that discharge is proportionate to a particular catchment, and it is expressed by the following equation (Moore et al., 1991 ; Chen et al., 2018):

$$SPI = a \times tanß \qquad (10)$$

Where a is the upslope contributing area or flow accumulation, and ß is the local slope gradient.

The value of SPI and the risk of slope erosion would increase when the value of contributing area and gradient increase, as well as when the amount of water supplied from the upper area of the slope rises with water velocity increasing (Vijith and Dodge-Wan, 2019). The SPI values of Al-Madinah ranges between 1.50 to 22.10, as shown in the Figure 3-9. It was noted that about 40 % of the total study area has very low and low SPI values of around 1.50 to 2.20, whereas the high value of SPI of around 22 just represented about 19 % of the total area. Consequently, the high values indicated the areas that have great potential for erosion caused by existing steep slopes and flow accumulations areas (Vijith and Dodge-Wan, 2019). The high-value areas SPI are featured by an increased possibility for groundwater formation due to their likely higher water table (Tien Bui et al., 2019).

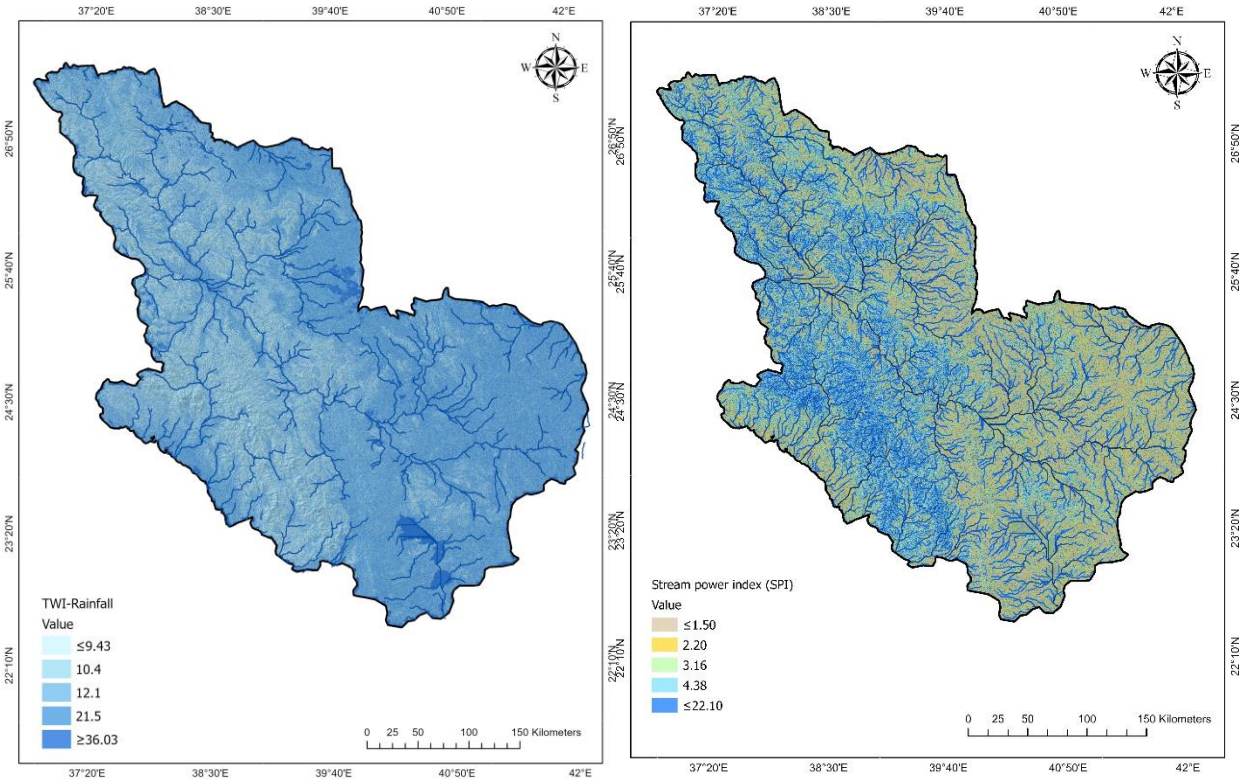

Figure 3-9. The TWI – Rainfall (left) and SPI units (right) of Al-Madinah.

3.3.2.3 Drainage Density

Drainage density is a potentially influential determinant in designating potential groundwater reservoirs, where high drainage density indicates increased surface runoff which in turn can affect the quantity of infiltrating rainwater, lower drainage density could increase the possibility of groundwater formation or enhance the recharging operation (Navane and Sahoo, 2017 ; Jaafarzadeh et al., 2021). In addition, the drainage density is usually associated with the permeability of soil and rocks where basins with high drainage density are characterized by impermeable soil, in contrast to basins with low drainage density being covered by more permeable soil and rock (Zakaria et al., 2016 ; Aldharab et al., 2019). Drainage density is usually estimated by defining the ratio of the length of the stream channel to the area of a drainage basin, it is expressed as (Strahler, 1967):

$$drainage\ density = stream\ length\ /\ basin\ area \quad (11)$$

In order to generate a drainage density map, firstly, the stream networks of Al-Madinah have been extracted from SRTM-30 DEM by hydrological tools in ArcGIS-Pro. The drainage density was then calculated using the line density analysis tool of ArcGIS-Pro software, which is mainly based on calculating the total length of all streams divided by the surface of a circle drawn around the centre of each cell using a search radius (Arabameri et al., 2019a ; Ozdemir, 2011a) to define the area around each point which will be included when estimating the density. This approach is considered a common method that has been applied by several studies such as (Jaafarzadeh et al., 2021 ; Arabameri et al., 2019a ; Nithya et al., 2019 ; Ferozur et al., 2019 ; Zabihi et al., 2016), all of which found reasonable results. The drainage density was classified by Smith (1950) into five textures categorise as shown in Table 3-2 (Aldharab et al., 2019 ; Zakaria et al., 2016). The drainage density values of Al-Madinah ranged between less than 0.74 to approximately 1.06 km/km², as shown in Figure 3-10, which in general means low drainage density and coarse drainage texture. These areas with lower drainage density often have good infiltration of water that would enhance the storage of groundwater (Zakaria et al., 2016).

Table 3-2. Drainage Density Classification

Drainage Density (km/sq.km)	Texture
< 1.24	Very Coarse
1.24-2.49	Coarse
2.49-3.73	Moderate
3.73-4.97	Fine
> 4.97	Very Fine

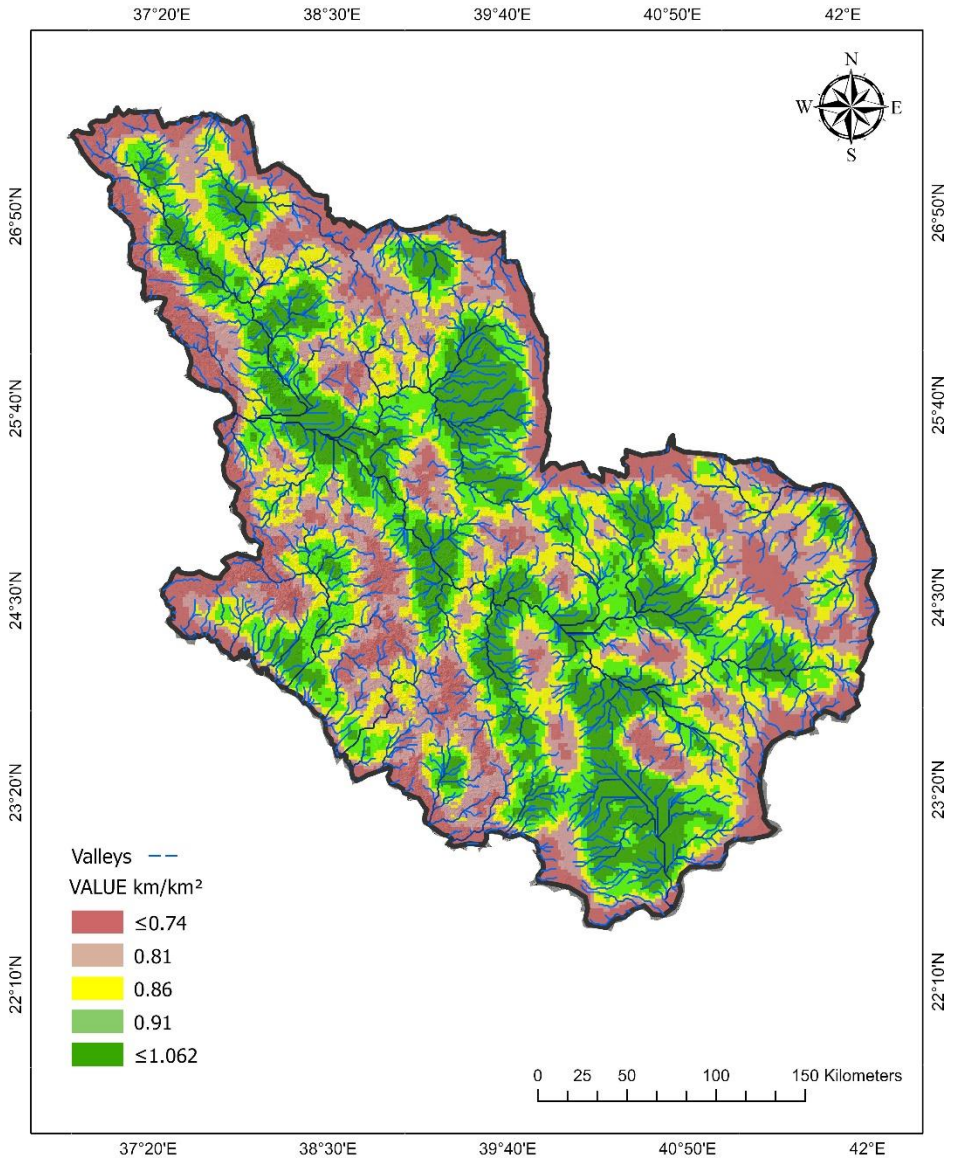

Figure 3-10. The drainage density units of Al-Madinah region.

3.3.2.4 topographic parameters

Topographical parameters such as slope, altitudes and curvature affect hydrological processes where the degree of slope and slope aspect control the surface runoff, drainage and infiltration process and consequently the groundwater recharge (Razavi-Termeh et al., 2019). The various altitudes could also produce diverse climates conditions, which would affect not only the amount of rainfall but also vegetation cover and soil types (Al-Abadi and Shahid, 2015 ; Al-Abadi et al., 2016). Moreover, the main influence of plan curvature on the hydrological process included the flow convergence and divergence and therefore impact on the surface flow speed (Razavi-Termeh et al., 2019).

Slope is considered one of the topographical parameters important that directly affects the rainfall infiltration process responsible for the formation and recharge of groundwater (Selvam et al., 2014). Al-Madinah area generally has gentle slopes of less than 6 degrees, which is estimated by around 71% of the total area, while steep slopes with 30 degrees or more did not exceed three per cent of the total area. Furthermore, the direction of the slopes (aspect) could mainly affect precipitation direction and the amount of moisture in the soil (Park et al., 2017). The aspect of Al-Madinah region is generally tended to the near zero aspect of flat areas toward the north, northwest, and west aspect, as shown in Figure 3-11.

3.4 Data classification methods

The present study's prediction model, Fuzzy Logic-Frequency ratio, requires reclassifying all data into categories, for example, five classes from very low to very high. Therefore, it is essential to understand the data used and consider the histogram of the distribution before setting a classification approach (Ravilious et al., 2020 ; Akgun et al., 2012).

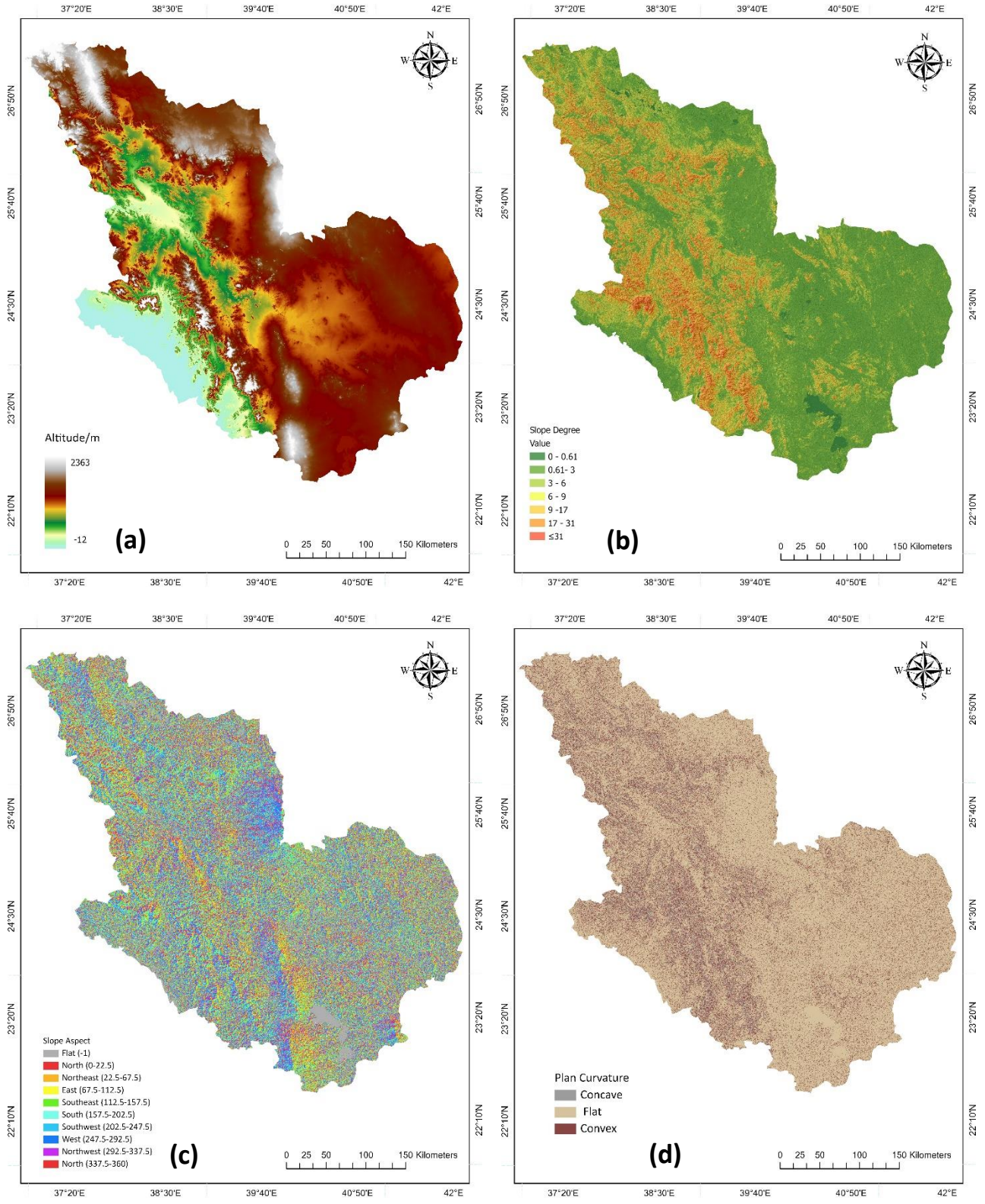

Figure 3-11. Topographical parameters of Al-Madinah, (a) altitudes, (b) slope, (c) slope aspect and (d) plan curvature.

ArcGIS has many classification methods include natural breaks (Jenks), quantile, equal interval, defined interval, manual interval, geometric interval, and standard deviation. Quantile classification is based on distributing the values into sets that include an equal number of values (ESRI, 2021). It is considered an ideal approach to rank data into gradual categories from very low to very high that allows to comparing between variables (ESRI, 2021 ; Ravilious et al., 2020).

The manual interval approach allows the thresholds between the categories to be based on external criteria (Ravilious et al., 2020). For example, slope gradient classes from FAO (2006) and the classification of plan curvature from Esri (2011), which have been utilised for slope degree data and plan curvature in the present study, as shown in Table 3-3. These classification schemes were most suitable for the present study data.

Table 3-3. Overview of factors used for mapping. groundwater potential zones

Factor	Range		classification method	justification
	Min	Max		
Soil, **Lithological units**	0	0	Soil Texture units and Lithological units	Al-Madinah Region Development Authority
Fault density	0	0.070	Quantile method	The data distribution on the histogram has been examined, which revealed that this factors group have positive or negative skewness; therefore, the classification methods of quantile or natural break could be most suitable to used (Ayalew and Yamagishi, 2005 ; Akgun et al., 2012), which help to isolate outlier values caused the skewness issue, as well as the, highlights the relative difference between features (Mitchell and Minami, 1999).
TWI_Rainfall	4.63	36.03		
SPI	-0.16	22.09		
Drainage density	0.13	1.06		
Altitudes	-5	2363		
Plan curvature	-41.11	46.77	Manual interval	‘’classified into concave (<1), flat (0), and convex classes (>1)’’ (ESRI, 2011).
Slope degree	0	> 31	Manual interval	Based on FAO slope gradient classes (Jahn et al., 2006)
Slope aspect	−1	360	-	‘’aspect is measured clockwise starting north at 0°. It returns as 360° north again’’

3.5 Models Validation

The accuracy and reliability of the resultant GWPZ maps were assessed using The Area Under Curve (AUC) of the Relative Operating Characteristics Curve (ROCs) is considered one of the most common approaches to validate the success rate accuracy and reliability of prediction model quantitatively (Morrison, 2005 ; Al-Abadi, 2015 ; Mohamed and Elmahdy, 2016). “ROC curves are two-dimensional graphs in which true positives (TP) rate is plotted on the Y axis and false positives (FP) rate is plotted on the X axis” (Fawcett, 2004).

The TP (sensitivity) and FP (1-specificity) indicate the correct predictions of groundwater wells, and the false predictions of groundwater wells, respectively (Manap et al., 2012). AUC values typically range from 0.5 to 1.0 where 0.90–1.0 indicate an excellent model, 0.80–0.90 good, 0.70–0.80 fair, 0.60–0.70 poor and 0.50–0.60 failure of the model (Gholami et al., 2019 ; Vakhshoori and Zare, 2016). In the current study, 70% of groundwater wells were used as a training dataset to generate the model and 30% as a test dataset to evaluate the model's prediction capability. The validation of the models is often performed by applying rates of success and prediction (Vakhshoori and Zare, 2016 ; Khoshtinat et al., 2019), using the training and test dataset, respectively.

According to Chung and Fabbri (2003), the success rate describes the model's goodness of fit, which is based on comparing the resultant prediction maps and the dataset of groundwater wells utilised in the modelling. In contrast, the prediction rate help to determine the predictive power of the resulting prediction maps (Pradhan and Kim, 2014 ; Manap et al., 2012) by comparing these maps and the distribution of groundwater wells that were not used to generate the model. The ROC curves of the present study were generated in SPSS and R.

The ROC curve also has been used to define the optimal cut-point value for classifying the possible areas into suitable and unsuitable zones of groundwater potentiality. This method selects the cut-point with the minimum distance from the left-upper corner of the unit square, which often has the highest sensitivity and specificity and accurately categorises most individuals (Unal, 2017). The present study used the threshold in the pROC package of R to finding the cut-off points.

3.6 Results

3.6.1 Application of Fuzzy-Frequency ratio membership of conditioning factors

The statistical analysis of the spatial relationship between the influencing factors and groundwater occurrence using the Fuzzy-Frequency Ratio model are shown in Table 3-4. Generally, the FR value greater than 1 indicate a strong relationship and vice versa (Moghaddam et al., 2015 ; Oh et al., 2011). Accordingly, in the geological factors, the highest weighted class was noted in the Lithosols, Calcic Yermosols soil type (3.49), followed by the low-density faults subclass and Igneous lithological unit with a measured frequency ratio of 3.47 and 1.41, respectively.

In terms of hydrological factors, the largest number of groundwater wells was found in the class of high drainage density category FR= 3.35. The highest class of the Topographic Wetness Index (TWI) weighted by rainfall variable gave FR = 1.25 were more likely to accumulate water. Despite the prominent role of the SPI factor in measuring the erosive power of water movement, the FR values calculated showed that the very low group has the highest FR 1.49. The lower altitude classes have higher FR values of 2.26 and 2.02. Low slope gradients had higher FR than steeper slopes, while flat plan curvature also had higher FR = 1.08 and associated with those, the flat aspect of areas had the highest FR of 1.62.

Finally, the highest weighted classes were noted in soil type (the Lithosols, Calcic Yermosols) followed by the low-density faults subclass, the high drainage density category, and the lower altitudes with the flat aspect revealed a higher relationship with potential groundwater events. These variables occupied the first five ranks in affecting groundwater occurrence.

3.6.2 Application of logistic regression (LR) model.

A statistical examination indicated that there was no multicollinearity among the independent variables (see Table S3-1 in appendix). As shown in Table 3-5, regression coefficients, odds ratio and p-values of the logistic regression analysis results indicated that the Lithosols, Calcic Yermosols and Lithosols, Yermosol, Cambisols Chromic soil types were statistically significant and had higher probabilities for groundwater than other categories (the reference category) by 496.5 and 99.9 times respectively. In addition, drainage density and TWI_Rainfall (positive coefficient)

were significance and had a high impact on the likelihood of groundwater well occurrence, where odds increased by around 2.43 and 1.89 times, respectively, when every one-unit increase in drainage density and the amount of rainfall, with all else equal.

The SPI index, slope degree, fault density and altitude variables also had significant negative relationships with groundwater wells' potential zones, with odds ratios of about 0.93, 0.88, 0.61 and 0.99, respectively. This means an additional increase of one unit in these variables is associated with a decrease of around 7%, 12%, 39% and 0.6%, respectively, odds of groundwater wells. The Northeast slope aspect also experiences a decline of about 0.42 times in the chances of groundwater wells occurring, equivalent to a 58% decrease, for each one-unit increase in Slope Aspect away from the Northeast direction.

Eventually, the most contributed factors to groundwater occurrence possibility under the logistic regression model were soil type (the Lithosols, Calcic Yermosols type, and Lithosols, Yermosol, Cambisols Chromic) followed by drainage density, TWI_Rainfall that associated positively, whereas the Northeast slope aspect and faults density negatively correlated with groundwater events occurring.

Table 3-4. Fuzzy membership values (FM) using frequency ratio (FR) method.

Factor	Factor classes	No. of groundwater wells	% of wells	No. of pixels in domain	% of domain	frequency ratio (FR) value	Fuzzy membership value
Geological factors							
Soil	Orthic Solonchaks	0	0.00	7308243	4.50	0.00	0.00
	Lithosols, Calcic Yermosols	516	79.84	37163300	22.90	**3.49**	1.00
	Haplic Yermosols	0	0.00	4872137	3.00	0.00	0.00
	Calcic Yermosols	0	0.00	9933020	6.12	0.00	0.00
	Lithosols, Haplic Yermosols, Calcic Yermosols	14	2.17	51459703	31.71	0.07	0.02
	Lithosols, Yermosol, Cambisols Chromic	116	17.98	51553494	31.77	0.57	0.16
Fault density	Very low > 0 - 0.016	362	56.05	97468643	60.06	0.93	0.27
	Low 0.016 - 0.026	226	35.10	16426191	10.12	**3.47**	1.00
	Medium 0.026 - 0.033	44	6.83	16054152	9.89	0.69	0.20
	High 0.033 - 0.070	9	1.39	16371767	10.09	0.14	0.04
	Very high ≤ 0.071	4	0.62	15969091	9.84	0.06	0.02
Lithological units	Polylithologic rocks	196	30.34	58241988	35.89	0.85	0.60
	Igneous rock	398	61.60	71137075	43.83	1.41	1.00
	Metamorphic rock	0	0.00	4142943	2.55	0.00	0.00
	Surficial deposit	52	8.07	13231223	8.15	0.99	0.70
	Sedimentary rock	0	0.00	15536661	9.57	0.00	0.00
Hydrological factors							
Topographic Wetness Index (TWI) + Rainfall	Very low 4.63 - 9.43	85	13.16	29811383	18.37	0.72	0.57
	Low 9.43 - 10.42	136	21.05	34302515	21.14	1.00	0.80
	Medium 10.42 -12.14	118	18.27	34922807	21.52	0.85	0.68
	High 12.14 -21.50	152	23.53	32131416	19.80	1.19	0.95
	Very high 21.50 -36.03	155	23.99	31121912	19.18	1.25	1.00
The Stream power index (SPI)	Very low -0.156 1.500	177	27.40	29823574	18.38	1.49	1.00
	Low 1.500 -2.198	203	31.42	35270025	21.73	1.45	0.97
	Medium 2.198 -3.158	133	20.59	35134730	21.65	0.95	0.64
	High 3.158 -4.380	68	10.53	31657397	19.51	0.54	0.36

Factor	Factor classes		No. of groundwater wells	% of wells	No. of pixels in domain	% of domain	frequency ratio (FR) value	Fuzzy membership value
	Very high	4.380-22.098	65	10.06	30388510	18.73	0.54	0.36
The drainage density	Very low	≤0.13- 0.74	10	1.55	31737129	19.64	0.08	0.02
	Low	0.74 - 0.81	6	0.93	32346046	20.02	0.05	0.01
	Medium	0.81- 0.86	68	10.54	32799696	20.30	0.52	0.15
	High	0.86 - 0.91	443	68.68	33093797	20.48	**3.35**	1.00
	Very high	0.91 – 1.062	118	18.29	31623978	19.57	0.93	0.28
Topographical parameters								
Plan curvature	Concave	-41.11 - -0.44	405	62.69	100559410	61.96	1.01	0.94
	Flat	-0.44 - -0.096	238	36.84	55342993	34.10	1.08	1.00
	Convex	-0.096 -46.77	3	0.46	6387289	3.94	0.12	0.11
Slope degree	Flat	0 - 0.61	103	15.94	17201093	10.60	1.50	1.00
	Gentely sloping	0.61 - 3	387	59.91	75890365	46.76	1.28	0.85
	Sloping	3 -6	130	20.12	22855685	14.08	1.43	0.95
	Strongly sloping	6- 9	17	2.63	8506225	5.24	0.50	0.33
	Moderately steep	9 - 17	5	0.77	17150994	10.57	0.07	0.05
	Steep	17 - 31	4	0.62	17397056	10.72	0.06	0.04
	Very steep	> 31	0	0.00	3287491	2.03	0.00	0
Altitudes	Very low	-5 - 646	292	45.20	32500534	20.03	**2.26**	1.00
	Low	646 - 872	262	40.56	32509438	20.03	2.02	0.90
	Medium	872 - 967	82	12.69	32687031	20.14	0.63	0.28
	High	967 -1097	7	1.08	32315840	19.91	0.05	0.02
	Very high	1097 - 2363	3	0.46	32261916	19.88	0.02	0.01
Slope aspect	Flat	-1	55	8.49	8515140	5.25	**1.62**	1.00
	North	0- 22.5-360	90	13.89	18751364	11.56	1.20	0.74
	Northeast	22.5 - 67.5	61	9.41	18869808	11.63	0.81	0.50
	East	67.5 - 112.5	61	9.41	18379500	11.33	0.83	0.51
	Southeast	112.5 - 157.5	60	9.26	19064196	11.75	0.79	0.49
	South	157.5 - 202.5	58	8.95	19623970	12.10	0.74	0.46
	Southwest	202.5 - 247.5	73	11.27	20709110	12.77	0.88	0.55
	West	247.5 - 292.5	90	13.89	19401416	11.96	1.16	0.72
	Northwest	292.5 - 337.5	100	15.43	18903077	11.65	1.32	0.82
			646	**100**				

Table 3-5 The coefficients of all variables in the logistic regression model

*The Estimate column represents the regression coefficients for explanatory variables. The 'St. Error'' is the standard deviation of the coefficient variables. Z-value examines the coefficient if it is statistically different from zero and is obtained by the regression coefficient divided by the standard error. The Pr(>|z|) column is the p-value that indicates the statistical significance level of factors at $p < 0.05$, and OR (EXP) is the exponential of coefficients or the odds ratio.

	Estimate	Std. Error	z value	Pr(>|z)	OR (EXP)
(Intercept)	-16.6400	2.1500	-7.7380	< 0.05	0.0001
(Soil) Lithosols, Calcic Yermosols	6.2080	1.0910	5.6880	**< 0.05**	**496.47**
(Soil) Haplic Yermosols	-13.3500	1121.00	-0.0120	0.9905	0.000
(Soil) Calcic Yermosols	-13.3400	707.700	-0.0190	0.9850	0.000
(Soil) Lithosols, Haplic Yermosols, Calcic Yermosols	1.4100	1.1180	1.2610	0.2074	4.095
(Soil) Lithosols, Yermosol, Cambisols Chromic	4.6050	1.0840	4.2490	**< 0.05**	**99.962**
(Rocks) Igneous rock	0.0580	0.2340	0.2480	0.8044	1.059
(Rocks) Metamorphic rock	-17.3700	1369.00	-0.0130	0.9899	0.000
(Rocks) Surficial deposit	0.1284	0.3572	0.3590	0.7193	1.137
(Rocks) Sedimentary rock	-17.0700	641.100	-0.0270	0.9788	0.000
(Slope Aspect) Flat	0.0256	0.4953	0.0520	0.9588	1.026
(Slope Aspect) North	0.2830	0.4118	0.6870	0.4919	1.327
(Slope Aspect) Northeast	-0.8558	0.3851	-2.2220	**0.0263**	**0.425**
(Slope Aspect) Northwest	0.3544	0.3896	0.9100	0.3629	1.425
(Slope Aspect) South	-0.3709	0.4018	-0.9230	0.3560	0.690
(Slope Aspect) Southeast	-0.2204	0.4203	-0.5240	0.6001	0.802
(Slope Aspect) Southwest	-0.1666	0.3908	-0.4260	0.6698	0.846
(Slope Aspect) West	0.0703	0.3882	0.1810	0.8562	1.073
Plan Curvature	0.2375	0.2515	0.9440	0.3450	1.268
TWI_Rainfall	0.6393	0.1024	6.2440	**< 0.05**	**1.895**
SPI index	-0.0778	0.0450	-1.7310	**< 0.05**	**0.925**
Slope degree	-0.1267	0.0262	-4.8460	**< 0.05**	**0.881**
Faults Density	0.00004	0.0000	-4.5130	**< 0.05**	**0.616**
Drainage Density	9.0580	1.3080	6.9270	**< 0.05**	**2.434**
Altitudes	-0.0049	0.0005	-9.6600	**< 0.05**	**0.995**

3.6.3 Validation of groundwater potential zones maps

The accuracy assessment of GWPZ maps use the AUC values for the ROC Curve (see Tables S3-2, S3-3 and Figures S3-1, S3-2 in appendix 2). The Gamma operators' fuzzy overlay performed better in both success and prediction rates, than the other methods. The Gamma 0.97 had the highest AUC, in both the success and the prediction rates, 0.963 and 0.943, respectively. In contrast, the

Fuzzy_Or and Fuzzy_Sum models had poor AUC values between 0.569 and 0.553. The logistic regression model showed that the success-rates AUC was 0.946, whereas the prediction-rates AUC was 0.885 (Figure 3-12).

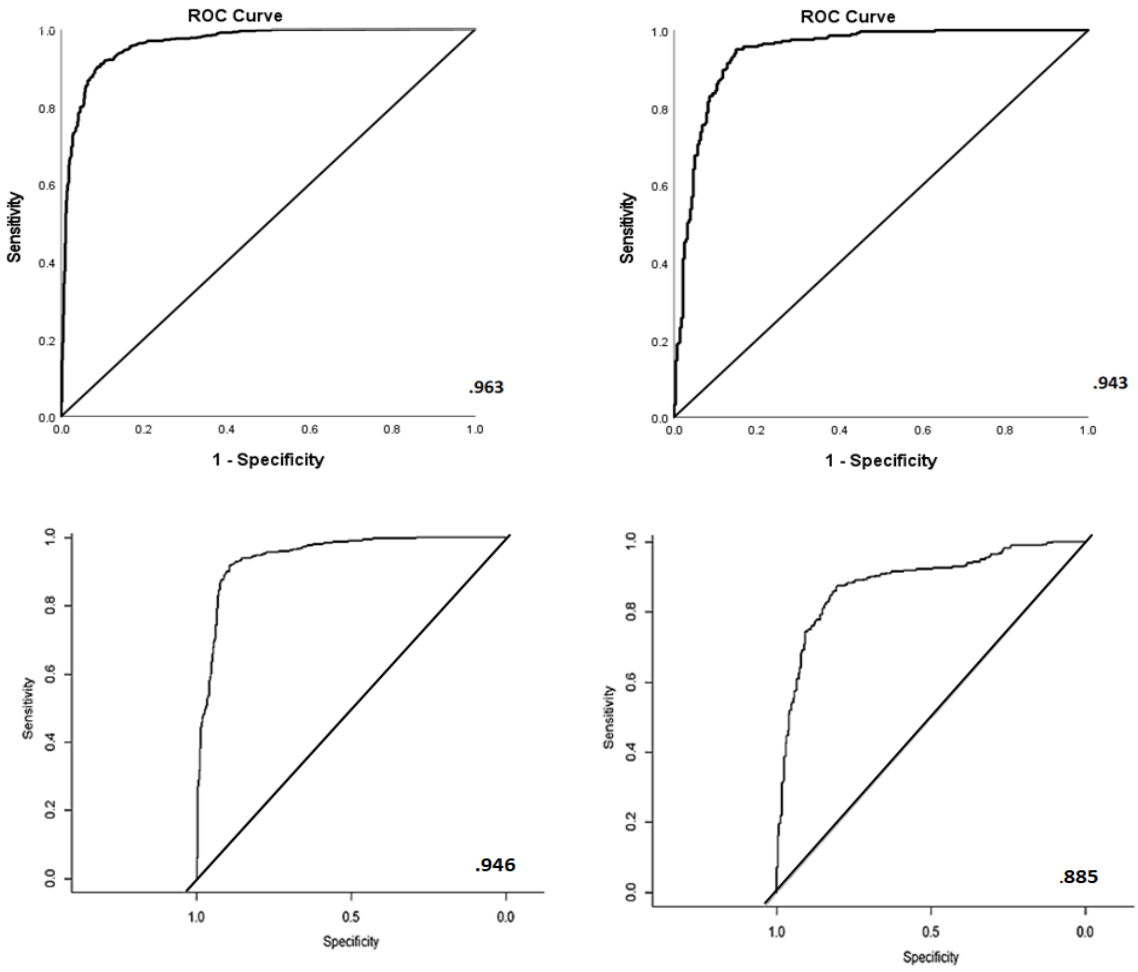

Figure 3-12. AUC curve for the success rate (Left), the predictive rate (Right) of Fuzzy-Gamma 0.97 (the top) and of logistic regression model (bottom).

Both models Fuzzy-Gamma 0.97 and logistic regression have correctly identified 271 and 256 wells as having groundwater potential (true positives, Sensitivity 0.87 and 0.85) and 241 and 237 locations as not having groundwater potential (true negatives, Specificity 0.96 and 0.905). However, most of the incorrectly predicted wells were located in areas covered by lava and have similar geological formations (Figure 3-13), which could indicate that the model may not be

capturing the influence of these factors on groundwater potential in those specific situations. This also may result from the limited data availability regarding the wells' location in these areas.

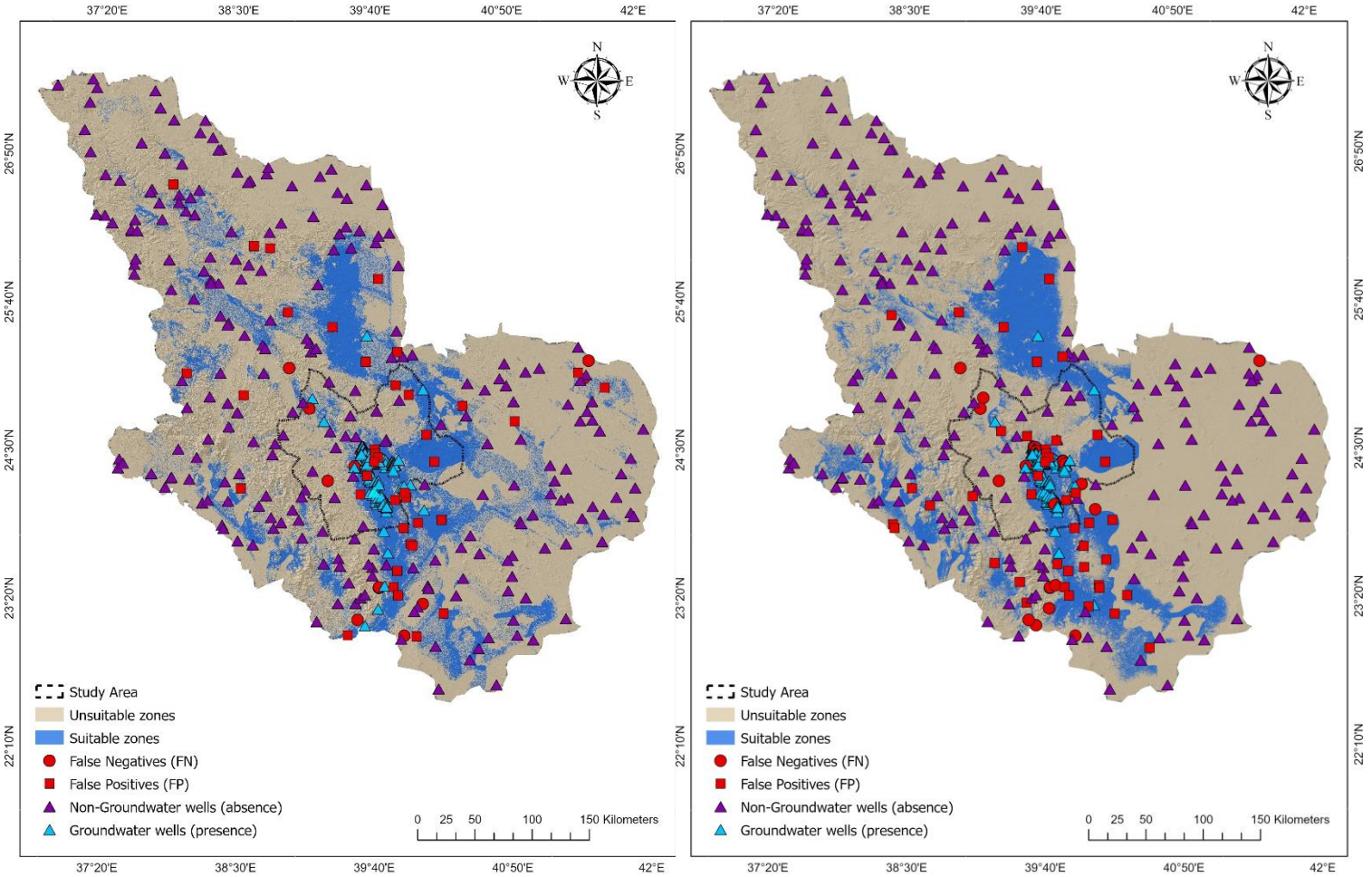

Figure 3-13. The spatial distribution of validation groundwater wells with potential groundwater zones, Fuzzy-Gamma 0.97 (Left) and of logistic regression model (Right). The figure shows the groundwater wells (presence) represent the True Positives (TP) and non-groundwater wells (absence) represent True Negatives (TN) locations where the model correctly identifies them as such. False Positives (FP) locations where wells are absent, but the model incorrectly predicts the presence of wells and False Negatives (FN) locations where wells are present, but the model incorrectly predicts the absence of wells.

3.6.4 The distribution of potential groundwater zones

The distribution of potential groundwater areas under the different suitability classes, are shown in Figure 3-14, Figure 3-15 and Figure 3-16. They reveal that 80.37% to 83.04% of Al-Madinah province are predicted to be unsuitable zones of groundwater potentiality under both the Fuzzy Gamma 0.97 and logistic regression models, Unsuitable areas are generally located toward the

east of Al-Madinah province (Al-hanakiyah and Mahd Al-Dahab cities), and also towards the southwest near Wadi Al-Fari.

In comparison, the very high potential zones ranged from 19.63 % to 16.96% of the total Al-Madinah area under both the Fuzzy Gamma 0.97 and logistic regression models. These suitable areas mainly cover the central and northwestern areas of Al-Madinah province. These areas include stream valleys and the volcanic hills in the south and east of Al-Madinah city that also extended to the north to Khaybar city. Between 3.77% and 3.15% of these highly suitable potential zones are be located in Al-Madinah city, representing about 38.07% and 31.78% of the total Al-Madinah city area and extending over about 14376 km².

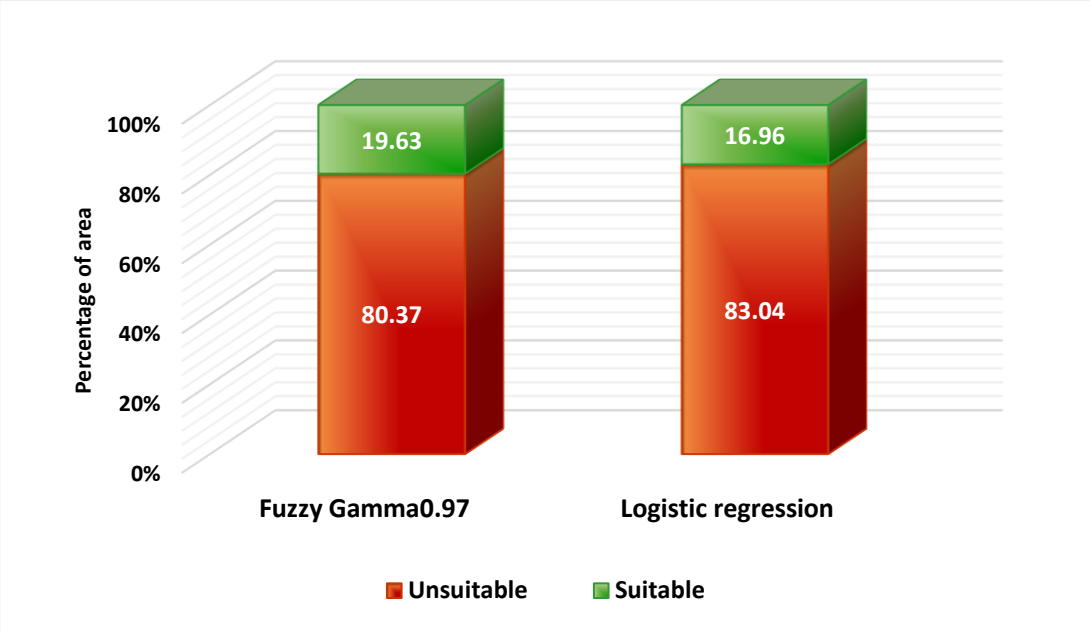

Figure 3-14. Distribution of potential areas under different the suitability classes.

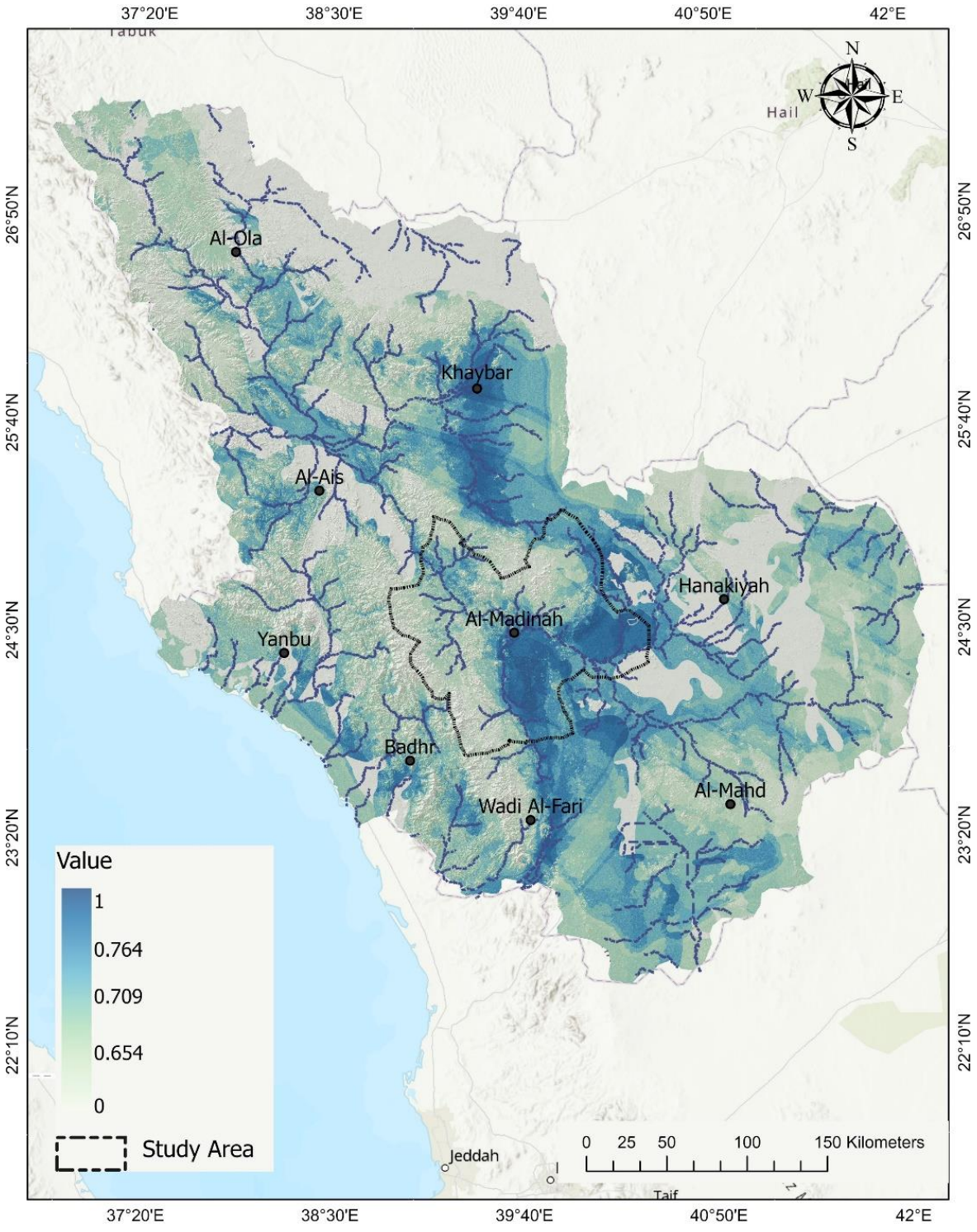

Figure 3-15. Potential groundwater zones map using the Fuzzy-Frequency ratio (Gamma 0.97) model. The figure illustrates the spatial distribution of the suitability of potential groundwater zones, with values closer to 1 indicating higher suitability and values closer to 0 indicating lower suitability.

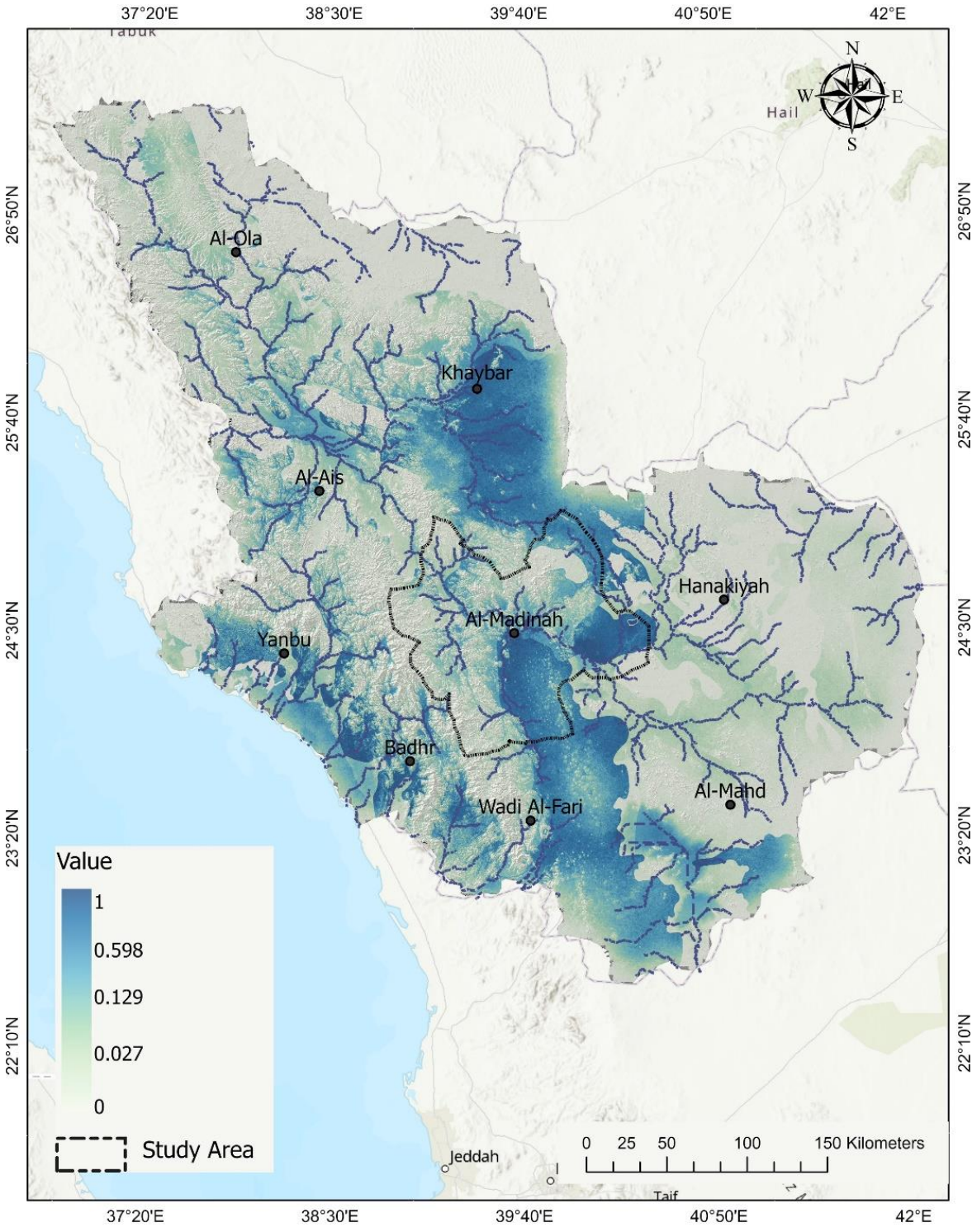

Figure 3-16. Potential groundwater zones map using logistic regression model. The figure illustrates the spatial distribution of the suitability of potential groundwater zones, with values closer to 1 indicating higher suitability and values closer to 0 indicating lower suitability.

3.7 Discussion

Identifying the potential groundwater zones based on the presence of groundwater wells and GIS-based models can be considered an essential domain and mechanism for sustainable water resources management, particularly in arid and semi-arid regions that suffer from scarcity of water (Tien Bui et al., 2019 ; Razavi-Termeh et al., 2019). The main contribution of this study is represented in comparing two methods, which are Fuzzy Logic-Frequency ratio and logistic regression, where the first one was rarely employed, whereas the second was commonly utilised in the field of groundwater mapping.

There is an absence of applying the integrated Fuzzy Logic-Frequency Ratio method in the groundwater mapping field, although it was successfully applied in other fields, such as Landslide hazards by Anbalagan et al. (2015) ; Kumar and Anbalagan (2015) ; Gholami et al. (2019), gully Erosion susceptibility by Roy and Saha (2019) and flood susceptibility assessment by Sahana and Patel (2019). Therefore, the present study findings could be compared with published studies that applied Fuzzy Logic and Frequency Ratio methods, whether as a single or ensemble model with another technique. For example, Rajasekhar et al. (2019) found that Fuzzy logic showed a fair or acceptable prediction model under the ROC_AUC curve. This model assigned the fuzzy membership values of influencing factors according to the experts' judgment. Moreover, the both Ozdemir (2011a) ; Manap et al. (2012) ; Mohamed and Elmahdy (2016) ; Al-Abadi et al. (2016) ; Chen et al. (2019) and Abdekareem et al. (2023) have indicated that the frequency ratio's performance ranged from a good to an excellent model based on the ROC_AUC technique.

However, Fuzzy logic performance increased to be a good model by combining with other models, such as AHP method that conducted by Mahmoud and Alazba (2016b); Rajasekhar et al. (2019) and Halder et al. (2020). This model successfully predicted the potential groundwater areas, which were validated by the ROC curve or a survey of groundwater levels. The results of the present study are consistent in that the ensemble models had a high performance in prediction by about 0.943 for the fuzzy logic-frequency ratio method. Nevertheless, the AHP method was criticised as it might be more exposed to subjectivity judgment when calculating weighting factors (Oguztimur, 2011), contrary to the frequency ratio technique that prevents this by statistically analysing the spatial relationship between the influencing factors and

groundwater occurrence. In addition, the distribution of groundwater wells used in models as training and validation datasets might reflect the current land use than the actual distribution of all groundwater resources, especially since the wells are usually more related to urban areas and agricultural lands; however, the frequency ratio method involved the probabilistic theory allowed to consider that historical events affect future events if they occur under the same conditions limit such problems. Generally, a comparison of the present study's findings with those studies confirmed that the Fuzzy-Frequency ratio model also had an excellent performance.

Logistic regression has been applied in diverse areas for environmentally sustainable management and showed observable differences in the prediction performance values. Chen et al. (2018); Miraki et al. (2018); and Nampak et al. (2014) revealed that the performance of logistic regression ranged from poor to fair in the prediction of potential groundwater, whereas Arabameri et al. (2019a) ; Ozdemir (2011a) ; Park et al. (2017) have shown the LR had efficiency in developing a good model under ROC-AUC curve in mapping groundwater. The findings of the current study accord with the effectiveness of LR (ROC-AUC= 0.885) in defining possible groundwater zones.

The comparison of the two models applied showed some similarities regarding the most important factors to determining the potential zones that included soil units, drainage density, slope aspects and faults density. In contrast, altitude contribute to the Fuzzy Logic-Frequency Ratio model more, while TWI_Rainfall factors was more important in the logistic regression model.

Accordingly, the soil types and their permeability contributed the most to both models. Soil texture significance is attributed to directly affecting the hydrological system in terms of surface runoff and infiltration; hence, groundwater recharge, storage and the amount of aquifer yield (Al-Abadi et al., 2016 ; Kumar et al., 2016 ; Khoshtinat et al., 2019). This result is in accord with Oh et al. (2011) ; Sahoo et al. (2017) ; Rajasekhar et al. (2019) ; Lee et al. (2019) ; Arabameri et al. (2019b) ; Halder et al. (2020) who all revealed that the soil variable was the most influential on groundwater occurrence probability. However, this differs from the findings presented by Rahmati et al. (2014) ; Pinto et al. (2015) and Yousefi et al. (2020), who showed that the most influential was the rainfall factor. Mohamed and Elmahdy (2016) ; Mahmoud and Alazba (2016b)

; Naghibi and Dashtpagerdi (2017) ; Nithya et al. (2019) ; Al-Ruzouq et al. (2019) and Roy et al. (2019) all indicated that slope, geomorphology, altitude, lineament density, geology and Lithology, respectively, were the most important elements on occurring potentially groundwater.

This inconsistent pattern might return to the mechanism of data analysis methods utilised; however, a more likely possible justification could be the diverse geographical and geological nature and socioeconomic status of the study areas that have different influential factors causing groundwater.

This could seem evident in the models used in the present study. For example, under the fuzzy logic model, most factors contributed to different degrees of membership, whether in categories or continuous data, to predict the possibility of groundwater occurrence. In contrast, the logistic model often determines the best predictors or relationships by statistical methods, such as considering the P. Value that is commonly used to select which variables could be included or excluded in the prediction model (Ozdemir, 2011b ; Chen et al., 2018). For instance, most lithology units contributed positively under the fuzzy-frequency ratio method, whereas all lithology units were not statistically significant in the logistic model, although in the literature, the lithology units highly impacted groundwater formations.

Spatial analysis of the results of the FR-FL and LR techniques applied in Al-Madinah indicates that the very high potential zones did not exceed 20% in either model. This result may be explained by the fact that Al-Madinah is topographically characterized by the high mountainous terrain and hills that cover most parts of the northern, southern, and western areas, which range from 800 to 1500 m and could reach above 2000m in some parts of the region (Metwaly et al., 2021 ; El Maghraby, 2014b). About 40% of the Al-Madinah area is occupied by heights above 900 m that are considered unsuitable for groundwater formations. Consequently, limiting the available space. A study published recently by Abdekareem et al. (2023), also demonstrated that only a minor area, about 8%, of the Al-Hamdh Watershed provided a good possibility for groundwater, where Al-Madinah city expands into of the Al-Hamdh basin. However, the prediction of this minor suitable area might have been influenced by including the distance from streams factor into the suitability model. Over three-quarters of used groundwater wells are within 500m of the Al

Hamdh Valley; thus, the predicted potential groundwater distribution closely resembles the wells used as the training data.

The very high potential zones in both models are primarily places where volcanic lava occurs in the northern and northwestern parts of the region, as well as in the central areas of Al-Madinah city. These predicted zones are share similarities with some of the expected potential groundwater zones predicted by Alahmadi (2019) and Abdekareem et al. (2023). These include the urban area of Al-Madinah City toward the central, south, eastern-south, north and western-south parts where according to Alahmadi (2019) clusters of groundwater wells in these areas may indicate the location of the aquifer. Abdekareem et al. (2023) also revealed that good zones were within500 m from Wadi Al-Hamdh in the farming regions around the watershed's north, northwest, and southern parts. However, the estimation of the high possibility of groundwater zones under the present study models varies from these two studies in considering complex effect aspects of geological, hydrological, and topographical, as well as excluding any factor that could restrict the examination into small areas such as around streams networks or urban areas. This broader approach allowed a more comprehensive understanding of the predicted potential of groundwater.

Generally, suitable areas are characterised by Lithosols, Calcic Yermosols soil with medium permeability ranging from 1.5 to 5.1 cm/hr.(MAW, 1985) that also cover igneous rocks largely formed from basaltic rocks that have high potential to hold the groundwater (particularly in the northern Harrat Rahat basaltic in the south of Al-Madinah (Al-Shaibani et al., 2007)). This result might reflect those of Metwaly et al. (2021) and Gutub (2013) who also estimated that most of Al-Madinah groundwater is encountered within the alluvial deposits and the highly permeable volcanic rocks that are considered the main hydrogeologic water-bearing units in Al-Madinah area. High potential groundwater formation zones showed good association with areas with a good drainage density texture (0.86 to 0.91). These textures are considered a useful system to infiltrate water to enhance groundwater storage. They extended into the main basins in Wadi Al-Hamd and its sub-basins as well as Al Aqiq and Malal. These results seem to be consistent with those of Subyani and Al-Ahmadi (2011) findings that revealed that the drainage density of the

five main catchments of Al-Madinah region, which are Mastorah, Marij, Safra, Fara'a and Al Aqiq, varied from 0.75 to 1.46 km-1, which indicates a permeable topography with moderate runoff potential.

The methods applied here show what can be achieve with quite limited input data. Ideally, more data on ground water availability would be accessible in addition to the limited number of well records used here. However, the high the AUC values suggest useful predictive models. further studies on potential groundwater zone maps combined with fieldwork to verify groundwater levels or water depth will need to be undertaken, especially in arid and semi-arid regions with insufficient records of monitoring groundwater levels.

3.8 Conclusion

Mapping groundwater provides valuable spatial insights that not only help to inform decision-making, such as for land use planning and management, but also improve understanding of current patterns of water availability. This could contribute to sustainable development efforts and the conservation of groundwater resources. However, the intricate dynamics of groundwater resources in challenging environments such as arid regions require considering geological, hydrological, and topographical variations. Fortunately, the evolution of remote sensing and GIS technologies have allowed the integration of diverse data with systematic analysis to enhance the accuracy of groundwater maps.

GIS supported the development of the methodological framework for mapping, analysing multi-criteria problems, and making decisions spatially and statistically in the current study. Integrated Fuzzy Logic with Frequency ratio has effectively estimated an area's potential groundwater resources. Based on the calculated AUC, the Fuzzy-Gamma 0.97 had a slightly higher performance than logistic regression, However, the essential influential factors under both models are similar.

The present study can inform such work for any arid regions with deficient water resources that experiences the similar climatic and population conditions. The study shows the importance of establishing databases that include all used and permitted wells by local authorities along with

recording quantities of extracted water and monitoring water levels that would support additional forecasting models. These results could positively contribute to improving sustainable groundwater management in the Al-Madinah region if they are considered in development plans and future changes to Land Use/Land Cover (LULC) in the area.

These resultant maps by both models serve as a foundational dataset for the subsequent analysis in Chapter 4. The models generated in Chapter 3 will be used alongside the topographical wetness index weighted by future rainfall (TWI-Rainfall) in Chapter 4 to assess the implications of future climate changes (2021- 2100) under RCP4.5 and RCP8.5 scenarios on potential groundwater zones. The TWI-Rainfall will also be employed to evaluate the suitability of sites of 14 dams established for recharging potential groundwater. This would help visualize and quantify projected changes and provide valuable insights into groundwater systems under future climate scenarios.

Chapter 4 Spatial analysis of climate changes under future scenarios and potential implications on predicted groundwater zones in Al-Madinah province

Abstract

Climate change significantly affects water resources through shifts in temperature, rainfall, and evapotranspiration patterns, as well as causing the distribution and intensity of precipitation and water availability to change. In the future, this may exacerbate the challenges of water scarcity in arid and semi-arid regions.

The global climate model (GCMs) results summarized by the WorldClim database have been used to analyse and model the historical (1970-2018) and future (2021-2100, RCP4.5 and RCP8.5) precipitation, temperature, and potential evapotranspiration (ET0) patterns under different IPCC RCPs scenarios for the Al- Madinah region, Saudi Arabia. The Hargreaves algorithms for ET0 and a standardised precipitation evapotranspiration index (SPEI) show the impacts of scenarios on potential water resources by displaying the temporal pattern of drought events and the water surplus and deficit cases. The Topographic Wetness Index (TWI) was weighed by future precipitation to show spatial changes in potential groundwater zones.

The temperature and ET0 variables are shown to have experience an increasing trend over the past period. This trend is expected to continue in the future period. A slight increase in rainfall (20.49% or 25mm, total of 147mm) and higher water accumulation opportunity is predicted by 2081-2100 under RCP8.5. Such an increase might not have a pronounced effect on enhancing the availability of groundwater due to raising the temperature that is projected to be around 2°C along with higher ET0 (Average: 182.47 mm/month; Total: 2189 mm/year) in the same period. The SPEI index revealed wetter conditions form 1970-2000 compared to the later period 2001-2018, which was characterized drought conditions. By 2081-2100 under both scenarios, drought events become longer in duration and of higher intensity.

These climate change implications should be highly beneficial in planning for existing water resources and contributing to developing future precautionary strategies to face the risks of exposure to drought and severe water shortages.

4.1 Introduction

The integrated management of groundwater requires understanding the potential impacts of future climate change; these impact could lead more challenges for water management (Jiménez et al., 2014) by affecting the hydrologic cycle. Changes in rainfall amount, temperature and the average of water vapour could bring adverse effects in diminishing the surface streamflow (Jia et al., 2019 ; Jiménez et al., 2014). Climate impact might also include extreme weather events leading floods or droughts (Jia et al., 2019 ; Jiménez et al., 2014). According to Portmann et al. (2013), the direction of changing renewable groundwater recharge correlates linearly with global temperature and it is expected that an additional 1-4% of global land area would experience 30% to 70% decreases in groundwater recharge resources, when the average global temperature increases by one degree Celsius.

General Circulation Models (GCMs) and the IPCC Representative Concentration Pathways (RCPs) scenarios are widely used to investigate potential future climate changes. Although such models involve some uncertainty, they still beneficial for estimating future climatic conditions (Portmann et al., 2013 ; Shrestha et al., 2016). Therefore, applying adaptation measures to assist in developing efficacious groundwater management strategies to meet the challenges of climate change requires considering the future climate change scenarios.

The Kingdom of Saudi Arabia, as one of the arid and semi-arid regions (ASARs) of the globe, has experienced rapid development, not only in social and economic aspects but also in population growth rates. This accelerating growth has led to imposing further pressures on water demand in all domains: domestic, industrial, and agricultural (Ouda, 2013). The government has faced a significant challenge on meeting such water demands (Ouda, 2013). The renewable groundwater aquifers constitute an essential natural water source in Al-Madinah province that rely on rainfall as the primary source of natural replenishment. Therefore, an understanding of the of variation in precipitation, temperature and evapotranspiration under global climate change scenarios would be valuable to improve different mitigation and adaptation measures that might help in water resource management.

This chapter aims to use the global climate models (GCMs) from the WorldClim database to identify the current trends in the baseline period (1970- 2018) and future predictions for temperature and precipitation. This also allows the extraction of the evapotranspiration patterns under RCP4.5 and RCP8.5 scenarios (2021-2100). Possible implications of climate variability on groundwater potential zones in Al-Madinah province can therefore be assessed.

4.2 Data and methodology

The present study employs climate models that were introduced by the Intergovernmental Panel on Climate Change (IPCC) assessment reports (Kim et al., 2013). These applications are components of the Coupled Model Intercomparison Project (CMIP), which display future climate predictions for agreed to what was termed representative concentration pathways (RCPs) that reflect different a set of greenhouse gas concentration and emissions pathways and involve four scenarios: RCP4.5, RCP6, RCP2.6 and RCP8.5 (Tarawneh and Chowdhury, 2018). In addition, these scenarios were also combined with Shared Socio-economic Pathways (SSPs) in SSP126, SSP245, SSP370 and SSP585, which represent sustainable development path (SSP1), the intermediate path (SSP2), the regional competition path (SSP3), and the traditional fossil fuel-based path (SSP5). The data of CMIP6 has been downscaled and calibrated from CRU-TS-4.03 by the Climatic Research Unit, University of East Anglia, using WorldClim 2.1 for bias correction (WorldClim, 2020).

This study used predictions of the precipitation and temperature in two scenarios high-emissions (RCP8.5) and medium stabilization (RCP4.5). These data have been designed in monthly means for 20-year periods that could be divided into near future (2021-2040), far future that includes mid-century (2041-2060 and 2061-2080), and end-century (2081-2100). They have a spatial resolution 2.5 minutes or of about ~21 km^2 at the equator (Harris et al., 2014 ; Fick and Hijmans, 2017).

4.2.1 Precipitation and Temperature

In the present study of Al-Madinah province, the baseline period data was selected from 1970 to 2018 from historical climate data in WorldClim. The monthly values of future total precipitation (mm), maximum temperature (°C) and minimum temperature (°C) have been derived from four

global climate models (GCMs) named BCC-CSM2-MR, CNRM-CM6-1, CanESM5 and IPSL-CM6A-LR. These GCMs models were selected because they are commonly used. The models' performances were acceptable, despite there being a small bias in estimations (McSweeney et al., 2014). Bias indicates the deviations of simulated climate models from observed climate data; whether outlier values have an increase or decrease trend, these models could represent future changes with some error (McSweeney et al., 2014). In the present study, the simulated model shows slight decreases in precipitation in most months compared to observed historical data, while the temperature data was more consistent. Generating dependable climate projections requires correcting these models to eliminate the potential negative effect on the model's accuracy.

The Simple Ensemble Mean (SEM) approach was used, which is based on calculating the mean of a group of GCM models outcomes, as shown in the Figure 4-1, Figure 4-2 and Figure 4-3 ; this method would assist in mitigating the uncertainty inherent in the models and therefore enhancing the future predictions' reliability (Jose et al., 2022 ; Ahmed et al., 2020).

Identifying the accuracy of gridded GCMs outputs (precipitation and temperature) also requires comparing them with observational data. The observed data (1973 - 2018) was collected from The General Authority of Meteorology, and Environmental Protection and Ministry of Environment, Water and Agriculture stations, which have codes 40430, 40439, M001, M002 and M004. These observational data have been used as a comprehensive reference document that represents the baseline (Historical) climate of the study area as well as to validate the gridded temperature and rainfall data from Worldclim. Additionally, the Pearson's correlation coefficient and linear regression (R^2) have been used to verify the Worldclim historical rainfall and temperature data with the observational data.

In a subsequent stage, in the present study, following from the analysis in chapter 3, the Topographic Wetness Index (TWI) applied in that chapter was weighted by the future precipitation (2021- 2100) under RCP4.5 and RCP8.5 scenarios. This allows the investigation of the possible impact of climate changes on the future potential groundwater zones by using climate forecasts in the suitability models developed in Chapter 3. It was also applied to examine the future climate-driven impacts on the natural replenishment of groundwater by evaluating

the sites of dams established for groundwater recharge purposes for 14 dams in the Al-Madinah province. Values are extracted from the raster maps (TWI-Rainfall maps and Flow Accumulation) within GIS-Pro environment.

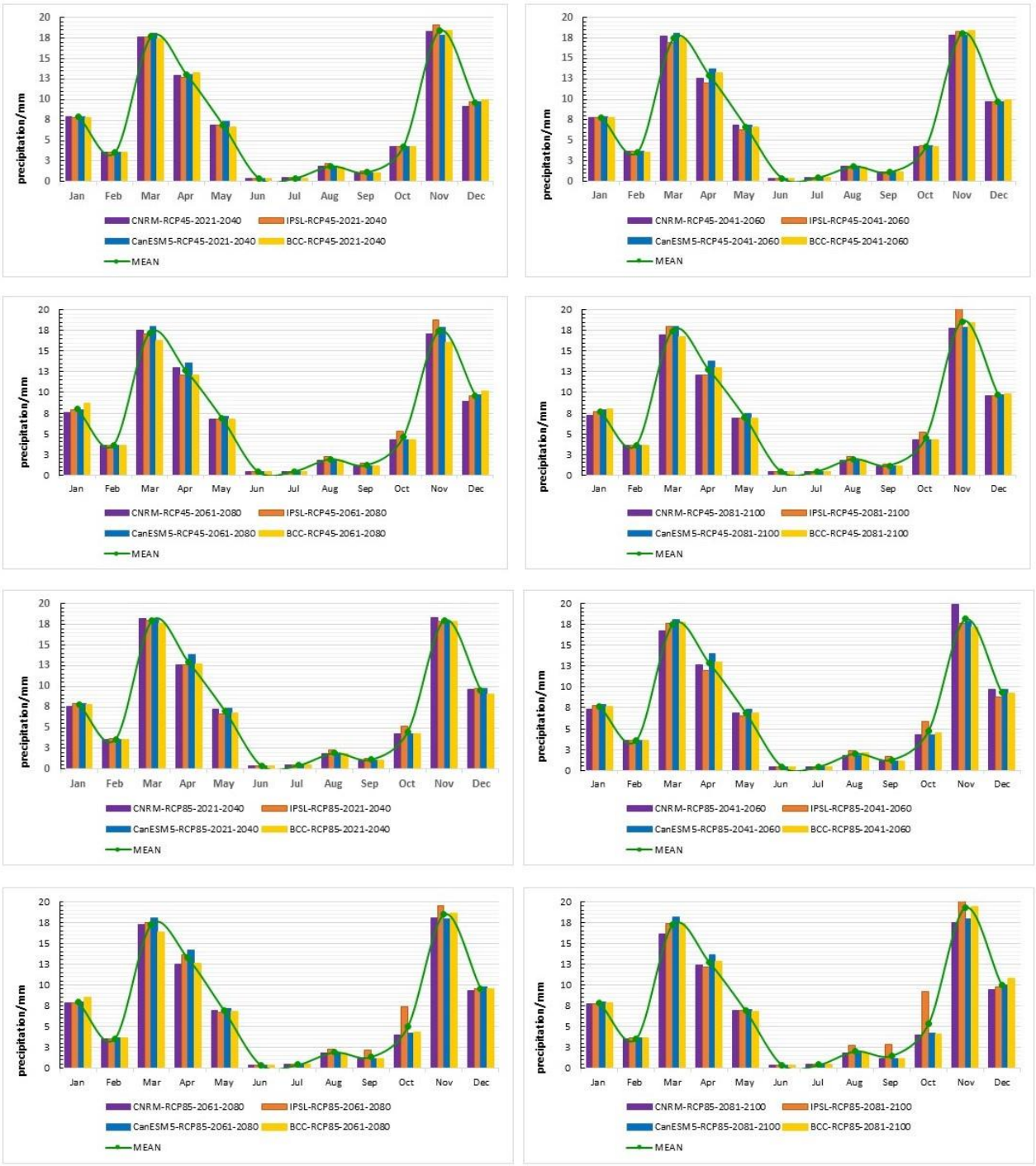

Figure 4-1 Comparison between monthly future precipitation projections (2021-2100) of four global climate models (GCMs) under RCP4.5 and RCP8.5 scenarios: BCC-CSM2-MR, CNRM-CM6-1, CanESM5 and IPSL-CM6A-LR. The line represents the mean of ensemble models.

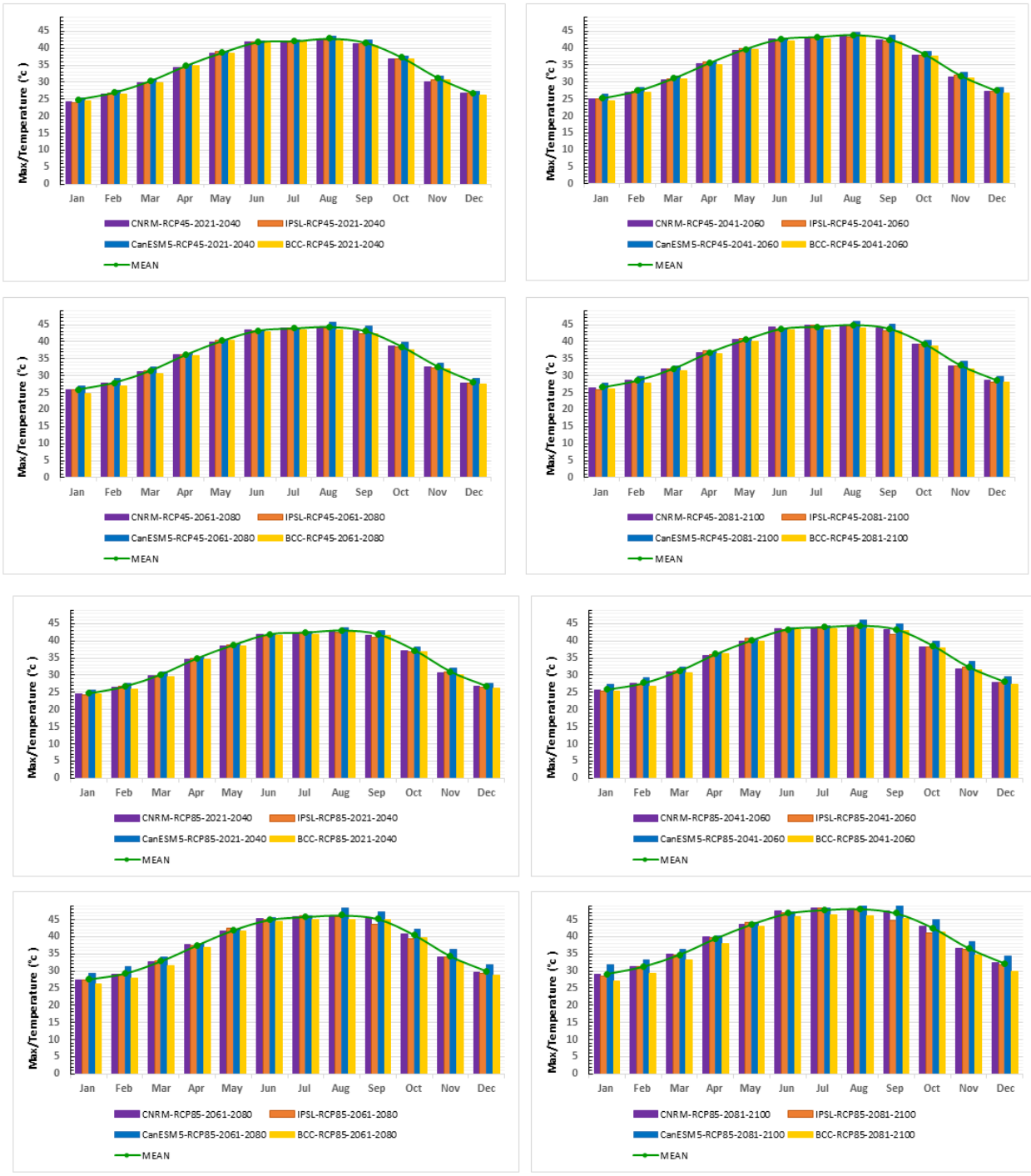

Figure 4-2 Comparison between monthly future maximum temperature (°C) projections (2021-2100) of four global climate models (GCMs)under RCP4.5 and RCP8.5 scenarios: BCC-CSM2-MR, CNRM-CM6-1, CanESM5 and IPSL-CM6A-LR. The line represents the mean of ensemble models.

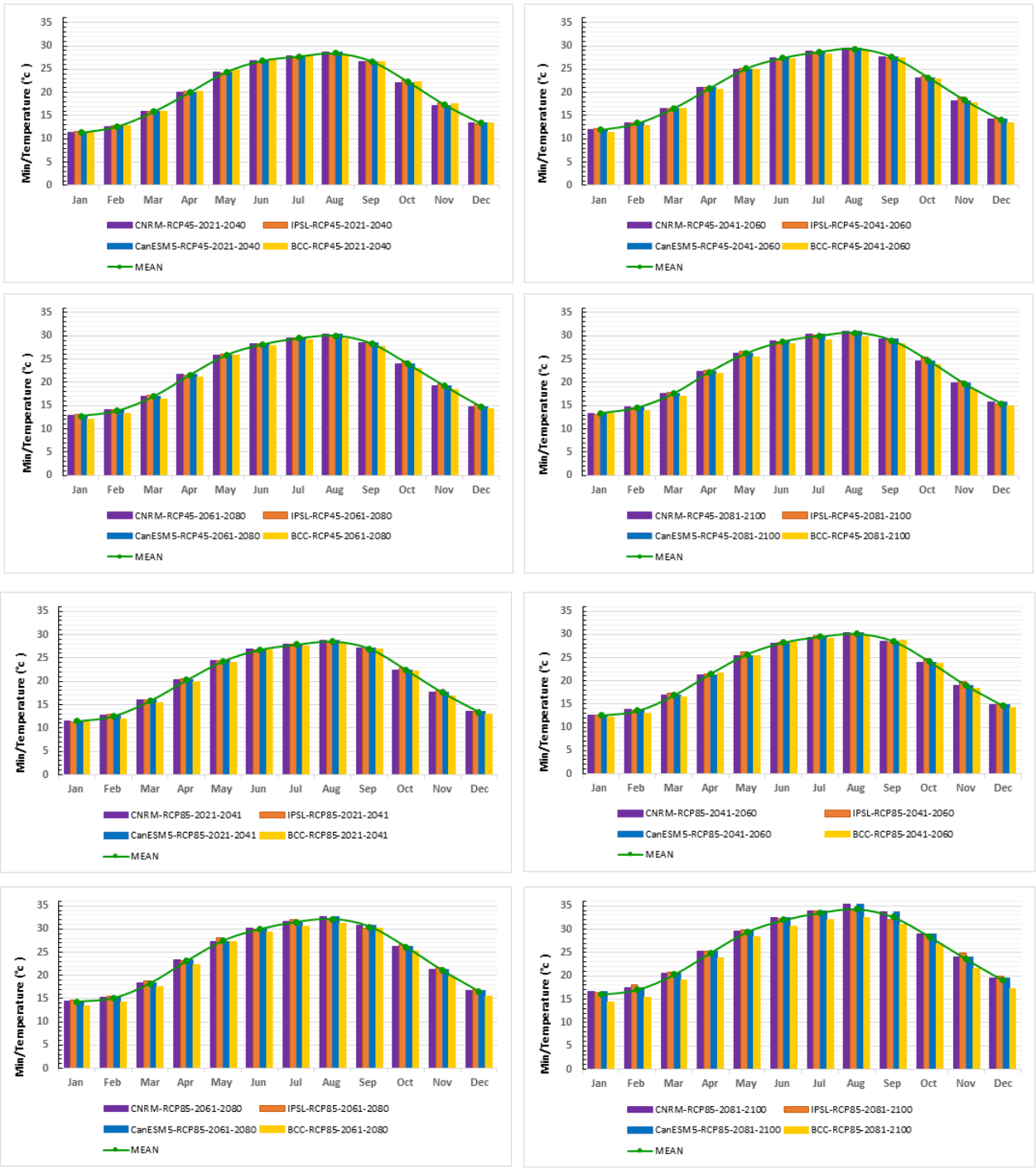

Figure 4-3 Comparison between monthly future minimum temperature (°C) projections (2021-2100) of four global climate models (GCMs)under RCP4.5 and RCP8.5 scenarios: BCC-CSM2-MR, CNRM-CM6-1, CanESM5 and IPSL-CM6A-LR. The line represents the mean of ensemble models.

4.2.2 The reference evapotranspiration

The reference evapotranspiration layer is not available in the WorldClim datasets. However, many models and equations have been formulated that help in estimating evapotranspiration. These equations differ in terms of data requirements, and climatic variables, as well as complexity (Gharbia et al., 2018). The most prominent of these methods, are Penman-Monteith, Priestley-Taylor, Makkink, Blaney-Criddle and Hargreaves (Gharbia et al., 2018). The Hargreaves approach is chosen in the present study due to its requirement of fewer variables, the minimum and maximum temperature and extraterrestrial radiation (Ra) (Čadro et al., 2017). All these variables are available in the WorldClim dataset.

In the present study, the available meteorological data for evaporation was from 1973 to 2009, usually measured by stations of the Ministry of Environment, Water and Agriculture (MEWA) using the evaporation pan method that represented the potential evaporation. The reference evapotranspiration (ET0) was also calculated by the Hargreaves approach based on two groups of data, which are the observed data of the minimum and maximum temperature (1973-2018) and the climate data from the WorldClim dataset (1970-2018). These two groups have been calculated by two different methods to compute the ET0 within the R environment using the SPEI and raster packages. The observed data (1973-2018) have been analyzed by applying the SPEI package to calculate the ET0 values. In contrast, the WorldClim dataset (1970-2018) has been processed by the raster package as well as the libraries rgdal and geosphere to extract the ET0-related maps. The code used is adapted from codes created by Spencer (2013b) ; (2013a), Hargreaves equation applied is expressed as:

$$ETo = 0.0023\ (0.408)\ (T_{mean} + 17.8)\ (T_{Max} - T_{Min})^{0.5}\ R_a \qquad (1)$$

Where Eto is Evapotranspiration Potential (mm /month); 0.0023 is an empirical coefficient used for unit conversion that also includes the kRs as an adjustment factor for solar radiation, and 0.408 is a factor to convert MJ M^{-2} to mm. Tmax = maximum air temperature (°C), Tmin = minimum air temperature (°C), Ra = extra-terrestrial radiation in mm/day (Fisher and Pringle Iii, 2013 ; Čadro et al., 2017).

Calculating the ET0 rates allows better monitoring of water resources in Al-Madinah by integrating the evapotranspiration estimations with the precipitation data. Consequently, the standardised precipitation evapotranspiration index (SPEI) is considered a beneficial index to show the impacts on the hydrological system and water resources by displaying the temporal pattern of drought events as well as providing a good understanding of the water surplus or deficit cases during the period in investigated (Faye et al., 2019 ; Qaisrani et al., 2021).The SPEI is formulated based on the monthly climatic water balance and is usually represented by calculating the difference between precipitation and evapotranspiration (Abdullah, 2014), monthly climatic water balance over a specified time period (D_i) is calculated:

$$D_i = Pi - PET_i \qquad (2)$$

Where P_i stands for the amount of precipitation, and PET_i represents Potential Evapotranspiration for the same month '*i*'. The negative value between quantities of rain and ET0 often indicate an existing rainfall deficit (RD) whereas surplus (RS) occur when rainfall is more than evapotranspiration (Feng et al., 2016).

The SPEI index included the aggregation of D_i values in different timescales, such as 1-month or 6-month periods. This aggregation is then converted into standardizing values using the log-logistic distribution that represents how many standard deviations a D_i value is from the mean of the log-logistic distribution. This provides a consistent method for comparing and interpreting drought or wet conditions across different periods and regions, The mathematical representation of the probability density function for the log-logistic distributed variable is as follows:

$$f_{(x)} = \frac{\beta}{\alpha}\left(\frac{x \backsim \gamma}{a}\right)^{\beta-1}\left[1 + \left(\frac{x \sim \gamma}{a}\right)^{\beta}\right]^{-2} \qquad (3)$$

where α, β, and γ are scale, shape, and origin parameters respectively (Vicente-Serrano et al., 2010 ; Qaisrani et al., 2021). The Log-logistic distribution adopted for standardizing the D series for all time scales is given by:

$$f_{(x)} = \left[1 + \left(\frac{a}{x} - y\right)^{\beta}\right]^{-1} \qquad (4)$$

F (x) value is then transformed to a normal variable by means of the following approximation:

$$SPEI = w - \frac{c_0 + c_1 w + c_2 w^2}{1 + d_1 w + d_2 w^2 + d_3 w^3}$$

Where P= 1-f(x), and w is given by

$$w = \begin{cases} \sqrt{-21n}(P) & if\ p \leq 0.5 \\ \sqrt{-21n}(1-p) & if \geq 0{,}5 \end{cases}$$

where C_0, C_1, C_2, d_1, d_2, and d_3 are constants equal to 2.515517, 0.802853, 0.010328, 1.432788, 0.189269, and 0.001308, respectively (Vicente-Serrano et al., 2010) . Moreover, the drought and moisture conditions would be identified via the SPEI values as displayed in Table 4-1. These values range from positive meaning wet conditions to negative values that exhibit drought events, while the SPEI value indicates the event's intensity (Mohammed and Algarni, 2020). Therefore, drought years were identified with the threshold values of -1 (Driouech et al., 2020 ; McKee et al., 1993).

Table 4-1 The degree of drought and moisture in SPEI

SPEI values	Conditions
SPEI≤-2	Extreme drought
-2<SPEI≤-1.5	Severe drought
-1.5<SPEI≤-1	Moderately drought
-1<SPEI≤1	Near Normal
1<SPEI≤1.5	Moderately wet
1.5<SPEI≤2	Severely wet
SPEI≥2	Extremely wet

The SPEI includes multiple timescales that exemplify different types of droughts. Short timescales are more suitable for detecting meteorological drought and agricultural drought which are (1-3 months averages) and (3, 6 months averages) the long time scales often used for hydrological drought and water resources that average (12 to 24 months averages) (Pei et al., 2020 ; Abdullah, 2014 ; Faye et al., 2019). In order to produce the SPEI index for the study area, the values of historical ET0 (1970- 2018) and future (2021-2100) have been extracted from the maps generated

based on the Worldclim database utilising the climate stations locations in Al-Madinah, which are 40430, 40439, M001, M002 and M004.

4.3 Results

The linear regression plots can be seen in Figure 4-4 for the historical period (1970-2018), a correlation coefficient of 0.936 was found between the observed monthly mean rainfall and the historical rainfall data form Worldclim. Pearson correlation coefficient showed significant agreement in most of the months between the temperatures from observational datasets and Worldclim data (1970-2018), with most coefficient higher than 0.98.

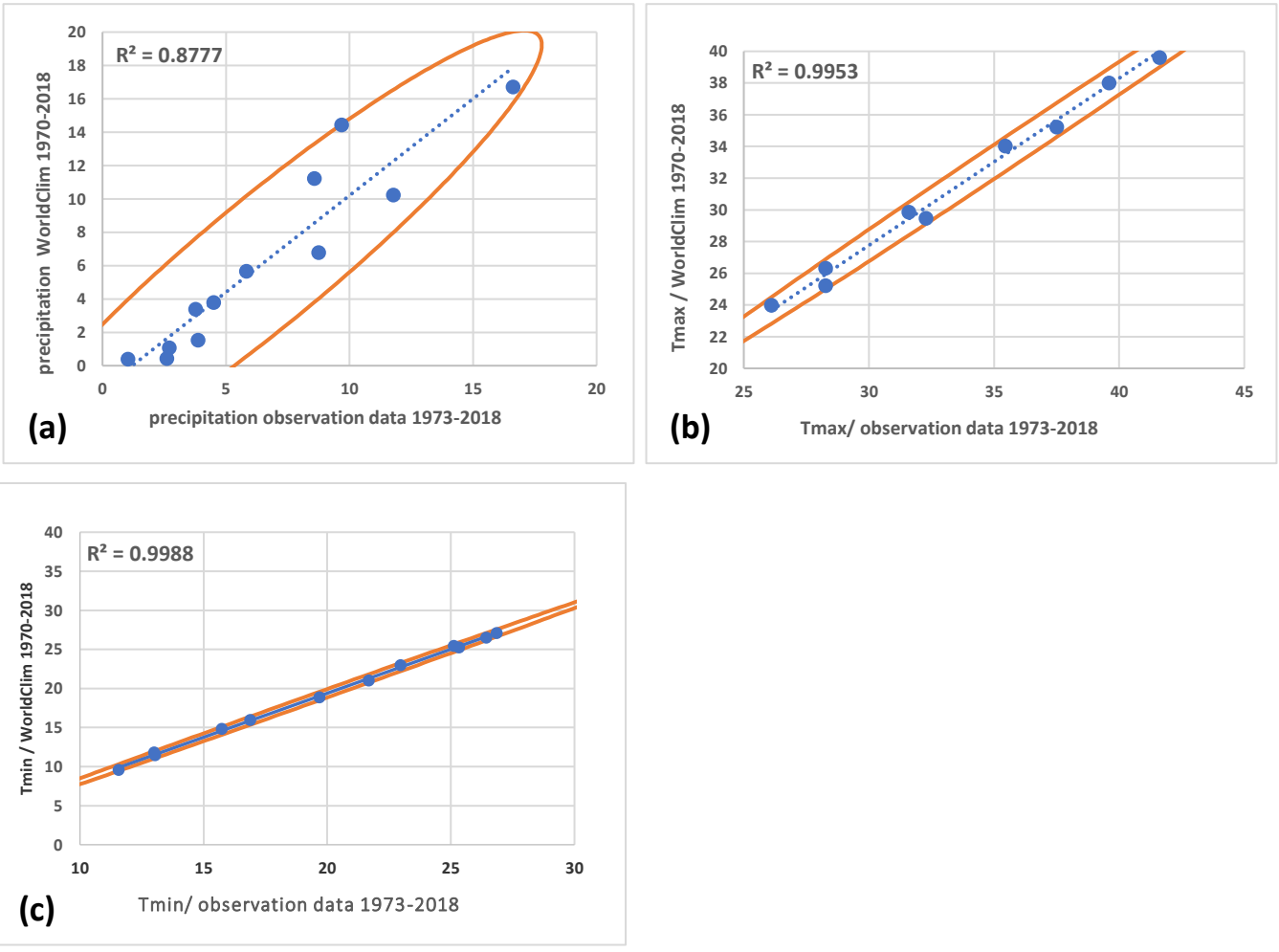

Figure 4-4. The correlations between the monthly averages of the observed and the Worldclim historical data for precipitation (a) and maximum temperature (b) minimum temperature (c).

4.3.1 Precipitation in Al-Madinah province

The analysis of annual rainfall data (1973-2018) showed fluctuations in precipitation in Al-Madinah Province through of 44 years (Figure 4-5). The annual average rainfall of the region ranged from about 75.15 mm to a maximum amount of around 151 mm. The years 1982 and 1993 were the wettest with 116 to 151 mm while 1973,1977 and 1978 were the driest years with less than 10 mm.

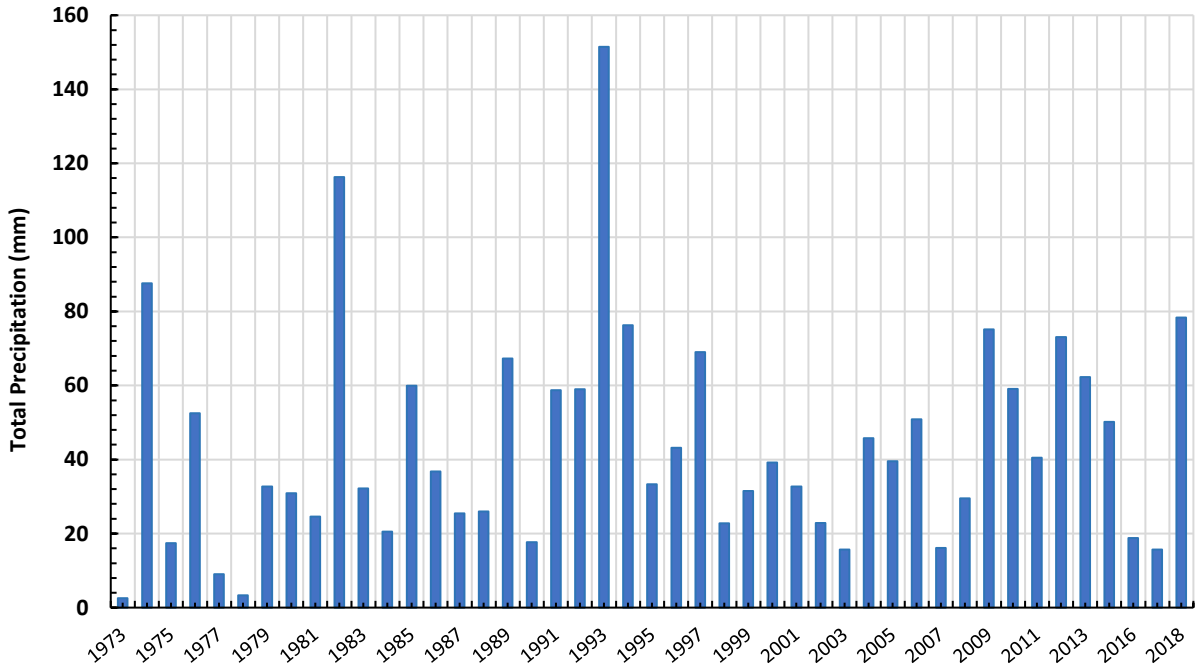

Figure 4-5. Total Precipitation (mm), annual data in AL-Madinah region 1973- 2018

The comparison of observed precipitation data (1973 - 2018) with the Worldclim's historical rainfall data has indicated a slight decrease in precipitation amount (122mm). Although the climate data from Worldclim shows slight increase in precipitation in March and April compared to observed data, the monthly rainfall patterns are very similar in most months. The lowest rainfall amount, for example, was recorded in June and July, while the heaviest precipitation rates were in March, April, November, and December, as shown in Figure 4-6. The period from 2001 to 2018 experienced a significant decrease in rainfall by about 28% compared to the period from 1970 to 2000, (Figure 4-7).

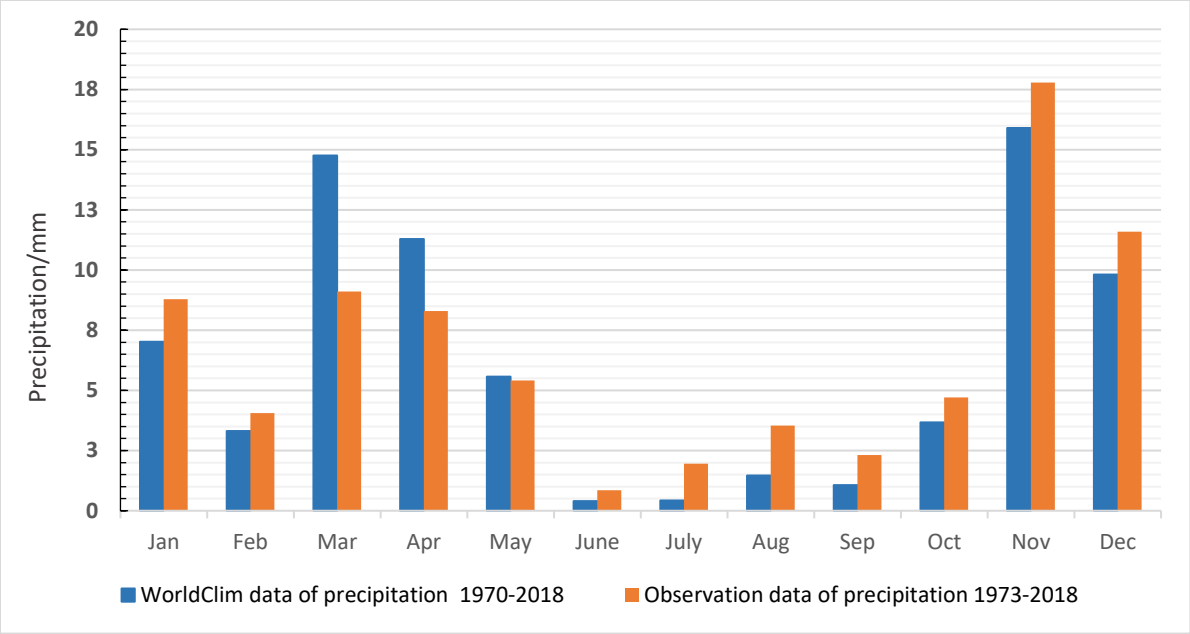

Figure 4-6. Comparison of the monthly mean of precipitation between observed data and the WorldClim dataset for the baseline period (1970-2018).

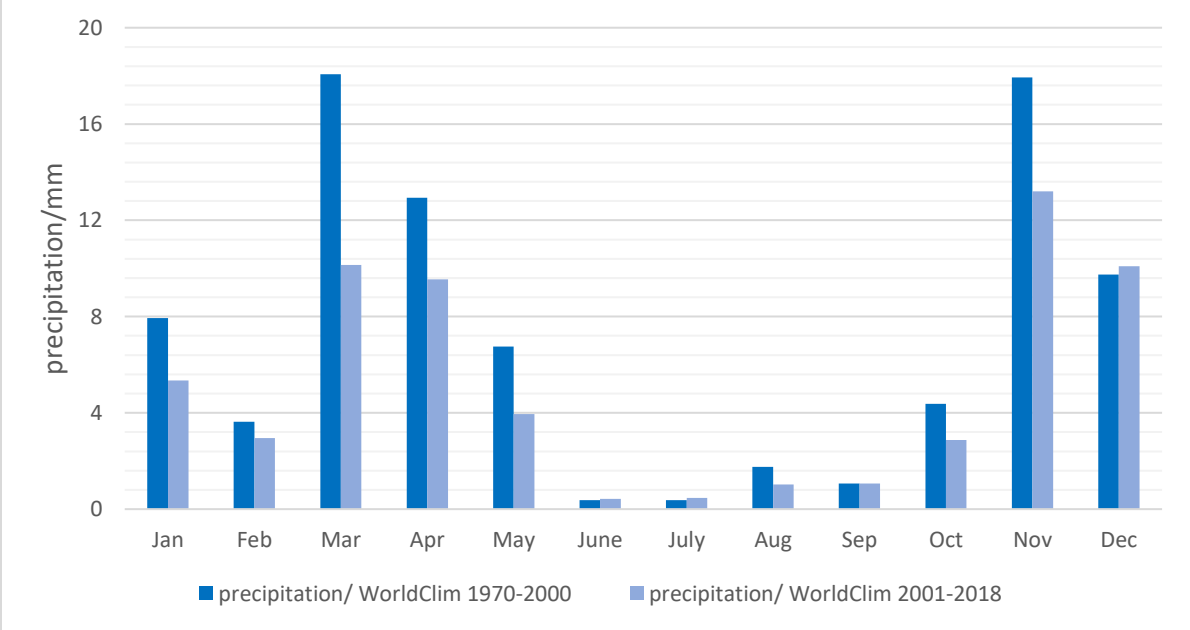

Figure 4-7. The comparison of precipitation amounts between the period (1970- 2000) and (2001- 2018)

Furthermore, the northern, northeastern, eastern, south, and southeastern areas in Al-Madinah province received the most amount of total rainfall during the historical periods 1970 -2018 and almost in all months, as shown in Figure 4-8 and Figure 4-9.

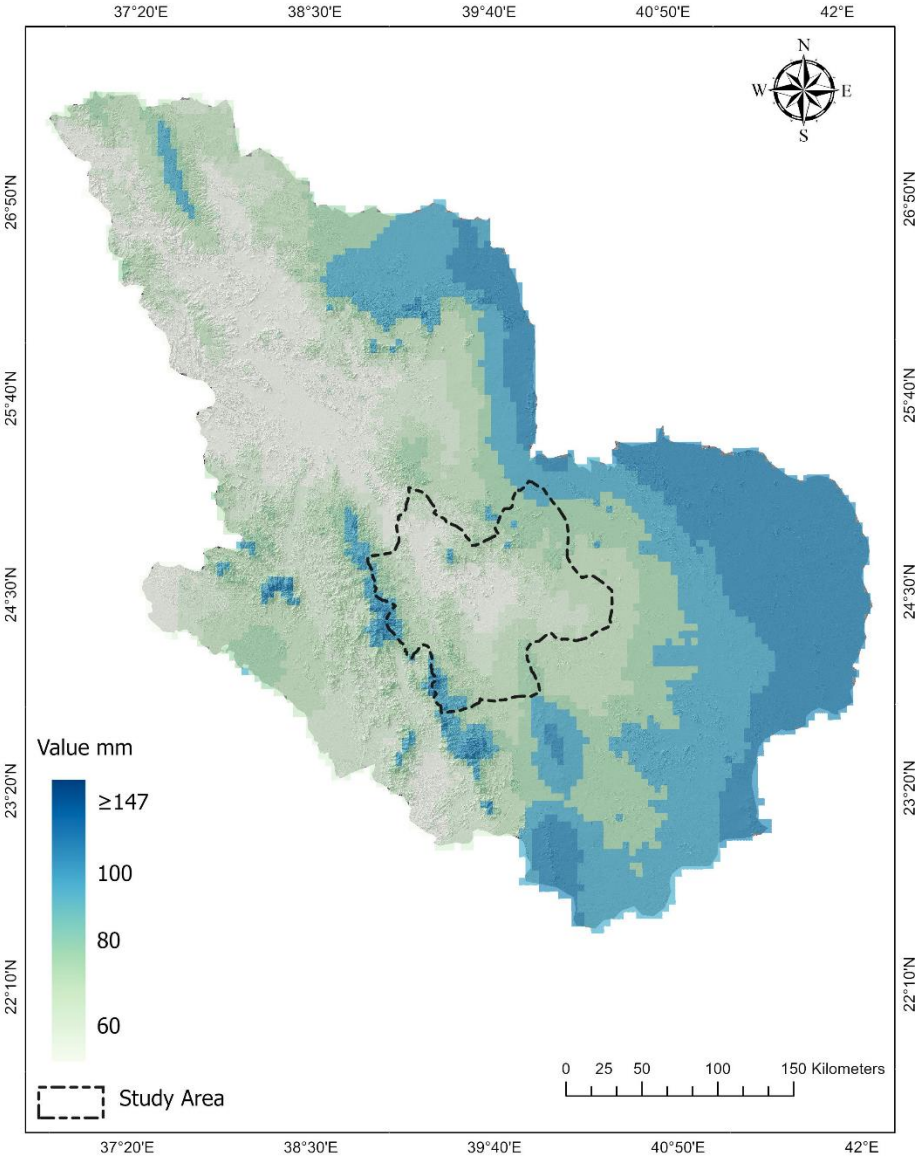

Figure 4-8. The distribution of annual average precipitation in Al-Madinah region (1970-2018) the Worldclim data.

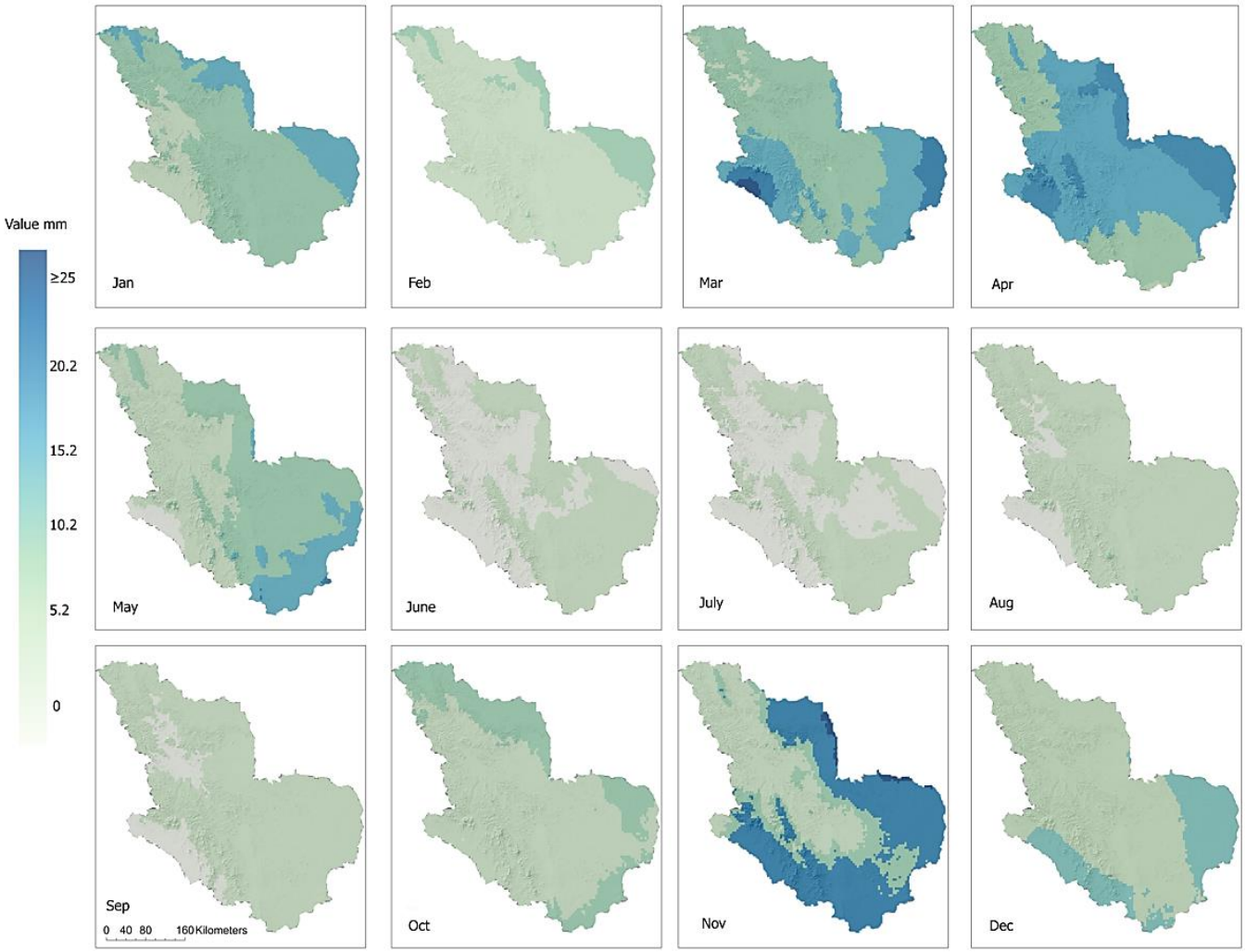

Figure 4-9. Average monthly rainfall distribution in Al-Madinah region (1970-2018), most areas in Al-Madinah province experienced high rainfall in April, whereas higher rainfall concentrations in November were in the northern, northeastern, eastern, south, and southeastern parts.

4.3.2 Future precipitation under climate change scenarios.

The comparison of the baseline period (1970- 2018) with future predicted precipitation under the RCP4.5 and RCP8.5 scenarios (2021-2100), averaged, shows an expected increase of between 18.74%, or 22.81 mm. However, there are small variations between different scenarios and future periods. Under the RCP4.5 scenario the rainfall rates are expected to be 145.5 mm in the period 2021-2040, lower in the mid-century by (2041-2060 and 2061-2080 periods) and higher again by the end of the century (2081-2100). Contrastingly, the RCP8.5 scenario exhibited higher

rainfall increasing until the 2081-2100 period, when the percentage increase will reach 1.73% or 2 mm compared to other periods. Therefore, 2081-2100/ RCP8.5 is predicted to have higher rainfall increases by 20.5% or 147 mm compared to 122 mm in the baseline period (Figure 4-10).

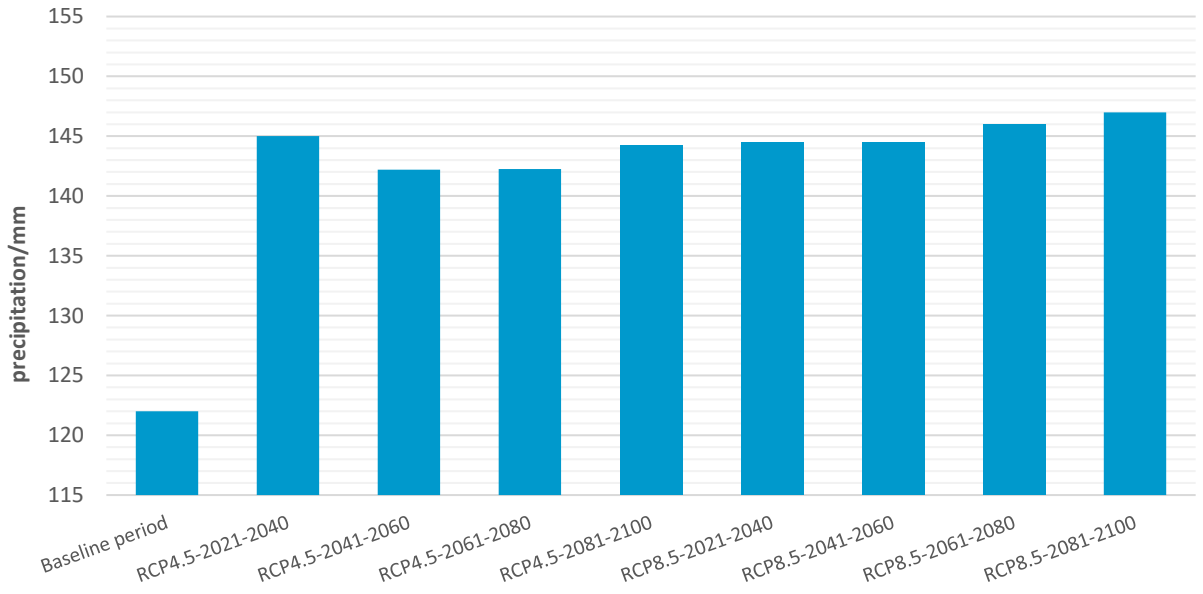

Figure 4-10. The future precipitation of Al-Madinah region under the RCP4-5 and RCP8-5 scenarios (2021-2100) compared to the baseline period.

Seasonally, as shown in Figure 4-11 the spring season of March and April is the wetter season in Al-Madinah. The projections also show the highest quantity of rainfall will occur in November (17.45 mm to 19.29 mm) under both scenarios. The baseline period value was around 15.9 mm, which represents about 21.3% of the total rainfall in the baseline period. In addition, the projections show trends towards drier conditions with an increase in the length of the dry season summer (June, July, August) that will overlap with autumn months September and October in particular. Moreover, the maximum average of summer rainfall will not exceed more than 0.91mm -0.96 mm for all periods under RCP4.5 and RCP8.5, respectively. Further, the driest summer season is expected to be in RCP45-2041-2060 with less than 0.90 mm. Generally, little change in rainfall pattern is apparent between the baseline and the future predictions, although there is a slight variation between scenarios and prediction periods.

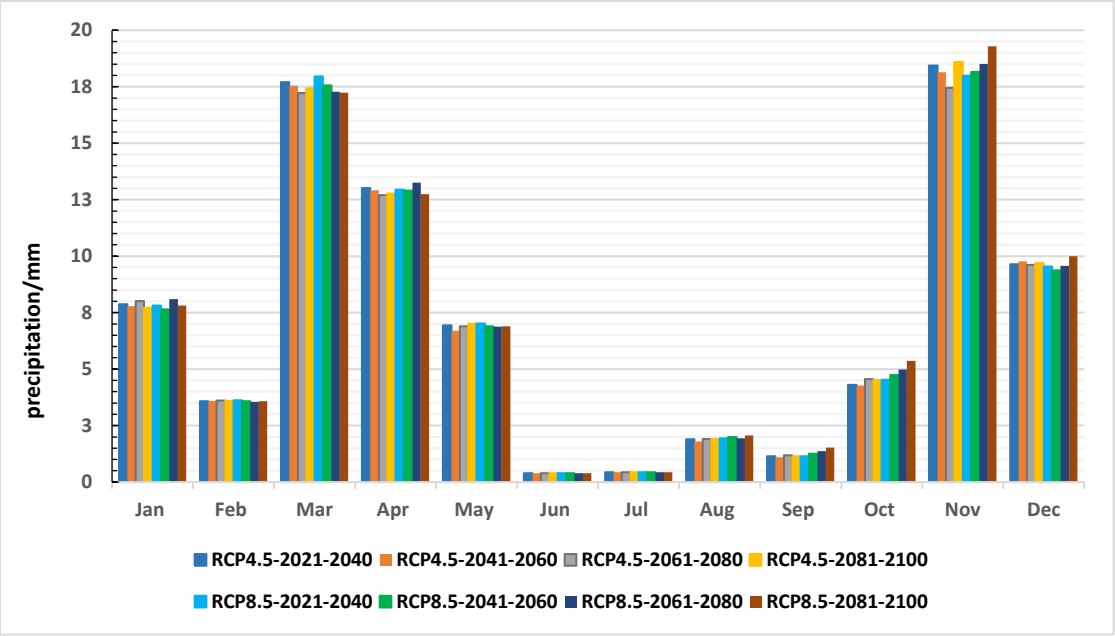

Figure 4-11. The future monthly mean of precipitation of Al-Madinah region under the RCP4-5 and RCP8-5 scenarios (2021-2100).

Generally, the spatial distribution of rainfall (mm) in the future climate models projections, as presented in Figure 4-12 has revealed that the northern, eastern, and southern areas will be more prone to changes in rainfall with a slight increase in the amount of rain under both RCP4-5 and RCP8-5 scenarios. Moreover, under RCP8-5, the rainfall variations will be more noticeable in the south and the maximum western regions, particularly at the end century (2081-2100). The rainfall changes in Wadi Al-Hamd indicated that it would experience a slight increase in rainfall throughout the future periods under both scenarios, most of the increase is expected to be under RCP4-5 at 2041-2060, and by the end-century (2081-2100).

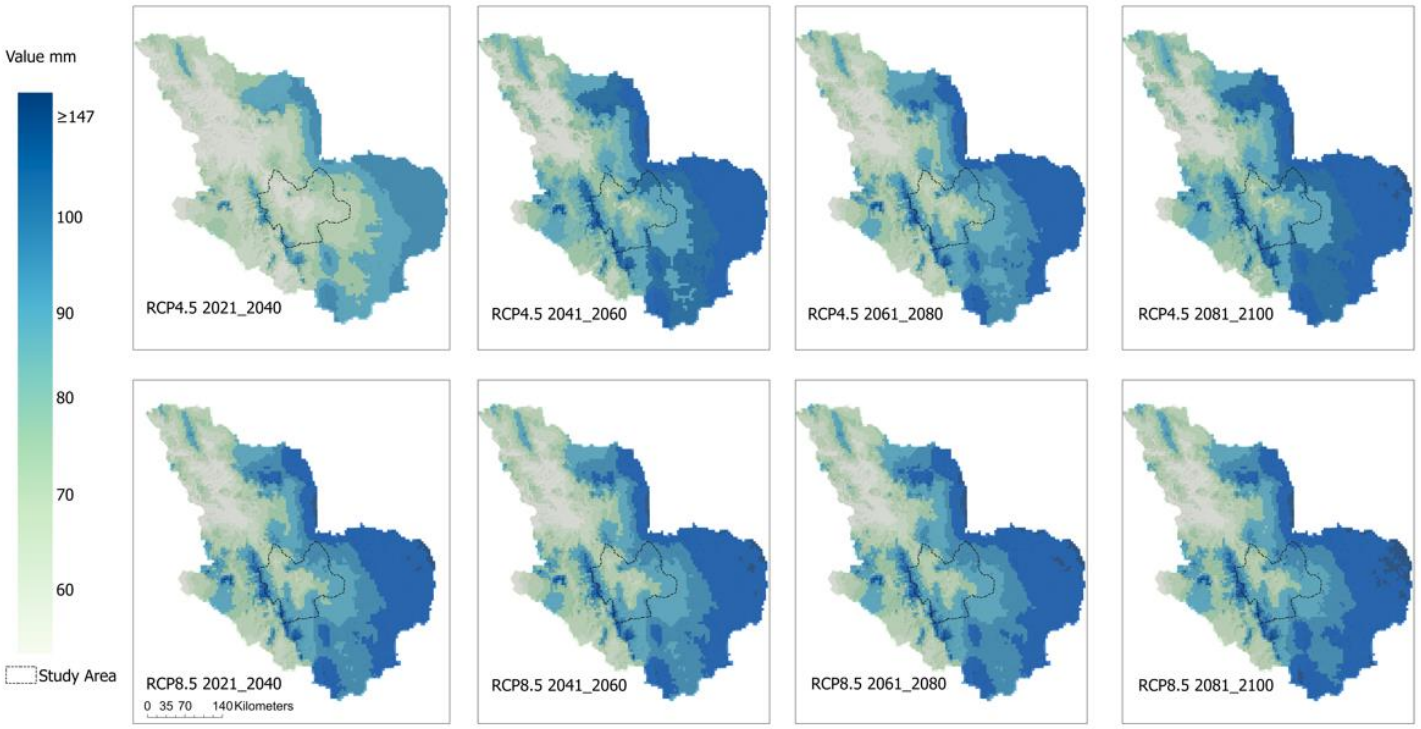

Figure 4-12. The spatial changes of precipitation (mm) in Al-Madinah region under the RCP4-5 and RCP8-5 scenarios (2021-2100).

4.3.3 Temperature in Al-Madinah province

The observed monthly temperature from 1973 to 2018 revealed that the annual mean temperature in Al-Madinah was 27.73˚C with a maximum of 35.60˚C and a minimum of 19.89˚C. The temperatures of the Worldclim dataset almost achieved a similar temperature range with a minor difference where the annual mean was 26.45 ˚C, and maximum (33.67˚C) and minimum (19.22˚C). The summer (June, July, August) as well as September are the hottest months, with the average maximum temperature from the Worldclim data around 40.47˚C, which is slightly lower than the stations' data, which was about 42.05 ˚C. The coldest months of the year were recorded in December, January, and February, with the mean maximum being around 25.17˚C and a minimum of around 10.94˚C, which were also smaller than observed temperatures by about +2˚C as shown in Figure 4-13.

.

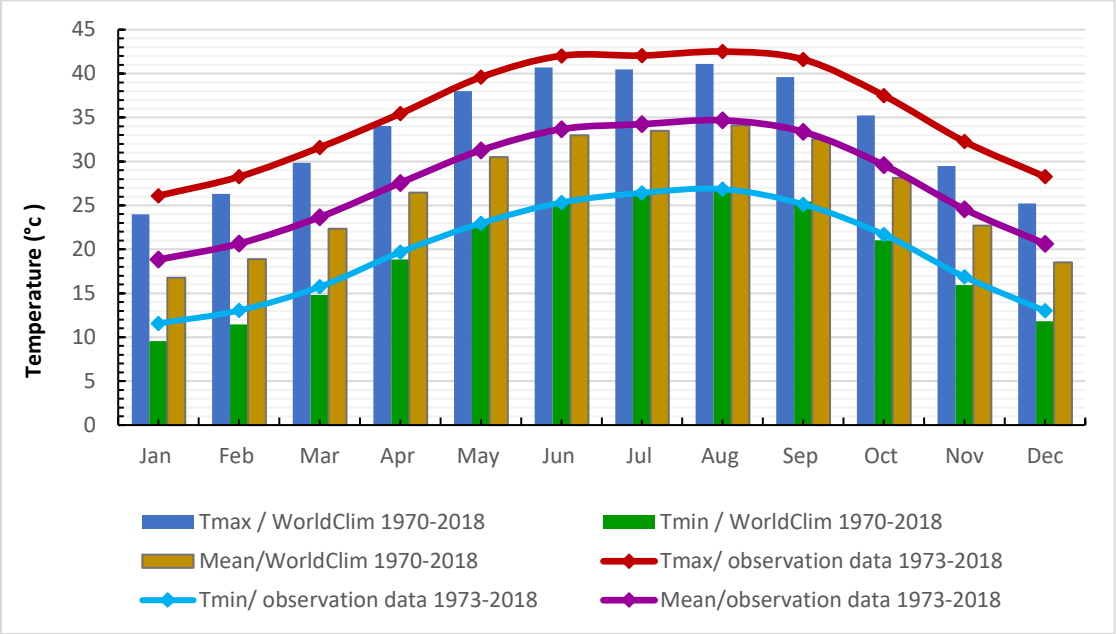

Figure 4-13. Monthly maximum, minimum and mean temperature in Al-Madinah 1970-2018

The spatial distribution of the mean maximum and minimum temperature (˚C) in Al-Madinah region from 1970 to 2018 indicated that the southeast to northwest parts, as well as the eastern side were the hottest temperature areas in Al-Madinah region. Most of these areas cover the Al-Hamd basin from the southeast to the furthest northwest direction, as shown in Figure 4-14. The high-temperature rate reached more than 36 ˚C and 22 ˚C in maximum and minimum temperature (˚C), respectively.

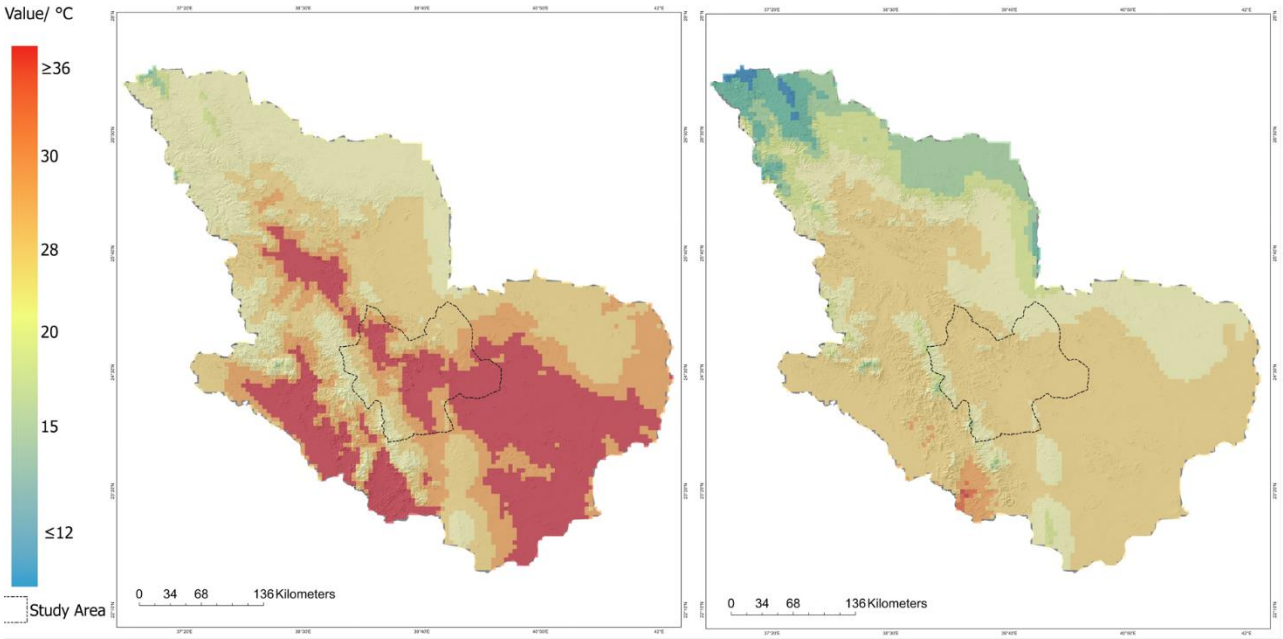

Figure 4-14. The spatial distribution of the mean maximum (left) and minimum (right) temperature (˚C) in Al-Madinah region (1970-2018).

4.3.4 Future temperature under climate change scenarios

The mean temperature predicted under all RCP4.5 and RCP8.5 scenarios showed an increasing trend compared to the baseline average annual temperature (1970-2018). The temperature is also expected to increase every month under both scenarios. The increases will continue for each of the Worldclim periods. RCP4.5 shows quite a linear increase, while RCP8.5 shows accelerating increases across the periods, as displayed in Figure 4-15 and Figure 4-16.

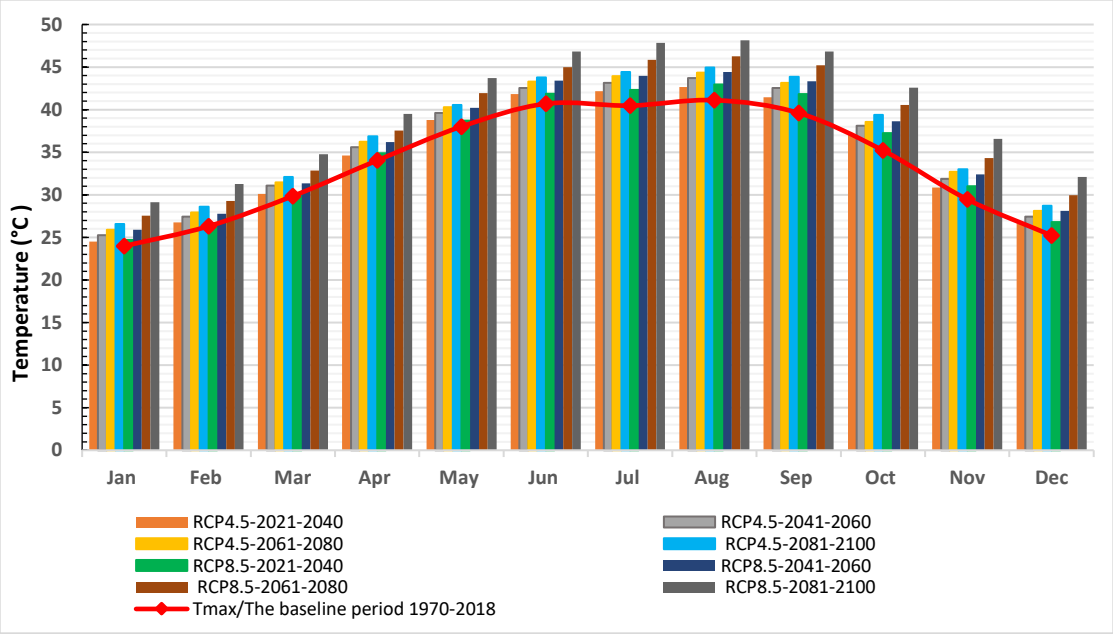

Figure 4-15. The Max- temperature (˚C) in the future climate projection under RCP4-5 and RCP8-5 scenarios.

The future spatial distribution of the mean temperature (˚C) in Al-Madinah region has revealed the continuing rise in temperatures in the Wadi al-Hamd basin area, which extends from the southeast to the northwest and occupies most of the area of Al-Madinah region. An average temperature that is above 36˚C is predicted to cover more than three-quarters of Al-Madinah's area by the end of the century (2081-2100) under the RCP8.5 scenario (Figure 4-17).

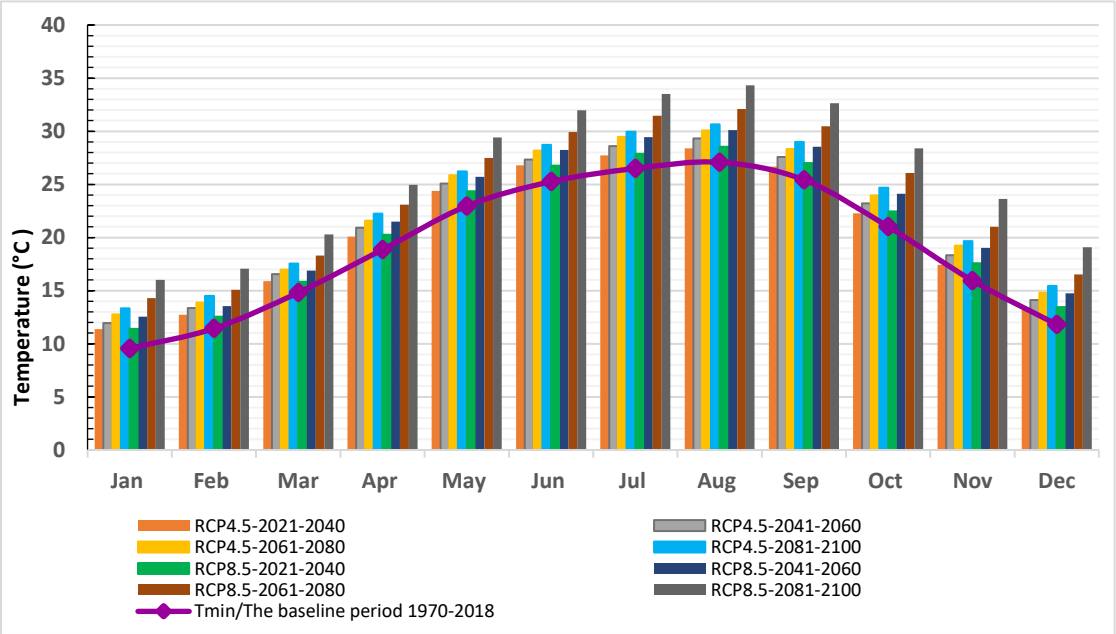

Figure 4-16. The Min-temperature (˚C) in the future climate projection under RCP4-5 and RCP8-5 scenarios.

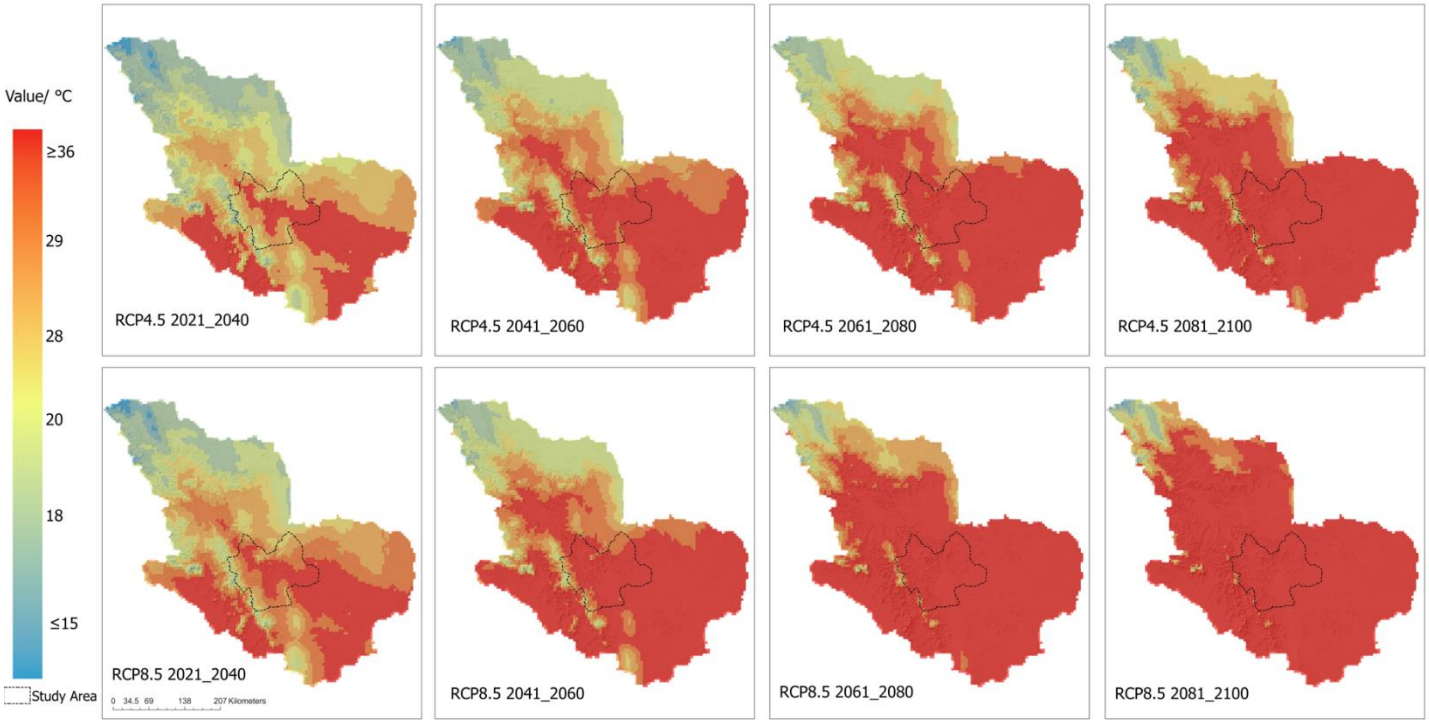

Figure 4-17. The future spatial distribution of the mean temperature (˚C) in Al-Madinah region (2021-2100) under RCP4-5 and RCP8-5 scenarios.

4.3.5 The reference evapotranspiration in Al-Madinah province

Linear regression was applied to all previous evaporation observations measured by the EVP-Pan approach (1973-2009), ET0- observed data (TMin and TMax 1973-2018) and ET0-WorldClim data (1970-2018). The results indicated strong agreement between all measures of evaporation, as shown by high R^2 values in Figure 4-18.The regression coefficients also show that the Worldclim estimates follow observed data closely by 0.9, although they mainly slight underestimate. The evaporation pan data although showing the same pattern as the EVP measures are consistently higher, as indicated in Figure 4-19.

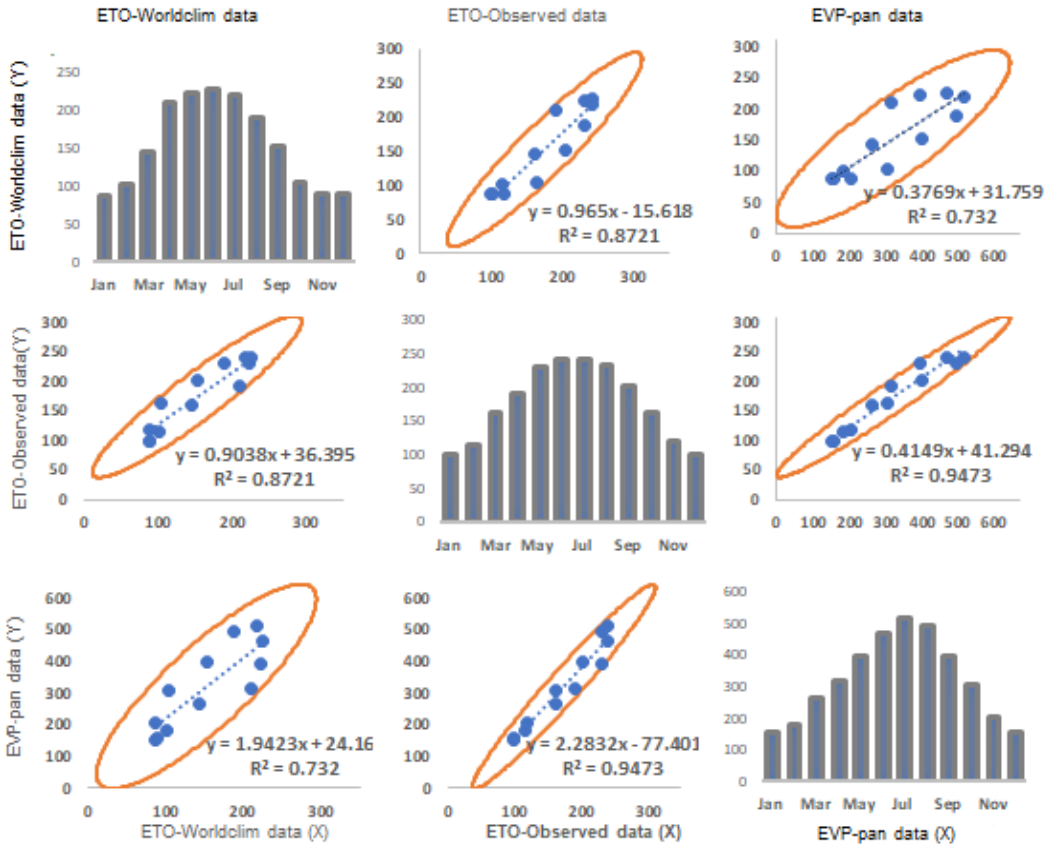

Figure 4-18. Scatterplot Matrix of EVP-Pan, ET0-Observed data and ET0-Worldclim data in Al-Madinah (1970-2018), show the direction of correlations between variables and the diagonal displays the histogram of the distributions of different datasets.

Measured evaporation by all techniques indicated that the highest amounts occurred during the summer (June, July, August), whereas the lowest rates were recorded in the winter months in

December and January with November, as displayed in Figure 4-19 and Figure 4-20. In addition, in the spatial distribution of ET0 rates, an increase is often towards the middle, eastern, and southeast parts. On the contrary, the lower amounts prevailed in the north and northwestern areas. Moreover, the annual evapotranspiration rates of Al-Madinah show substantial amounts of increase across the years, ranging from 1866.57 to 1991.7 mm/year (Figure 4-21).

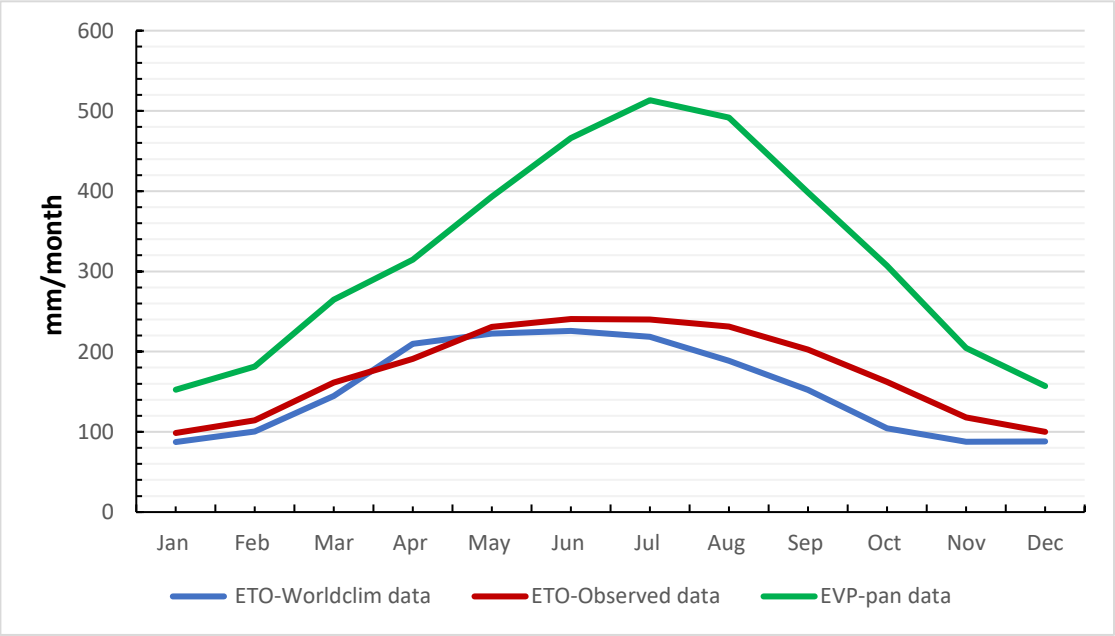

Figure 4-19. The comparison between the average monthly EVP-Pan data, ET0 observed data and ET0-Worldclim data in Al-Madinah (1970-2018)

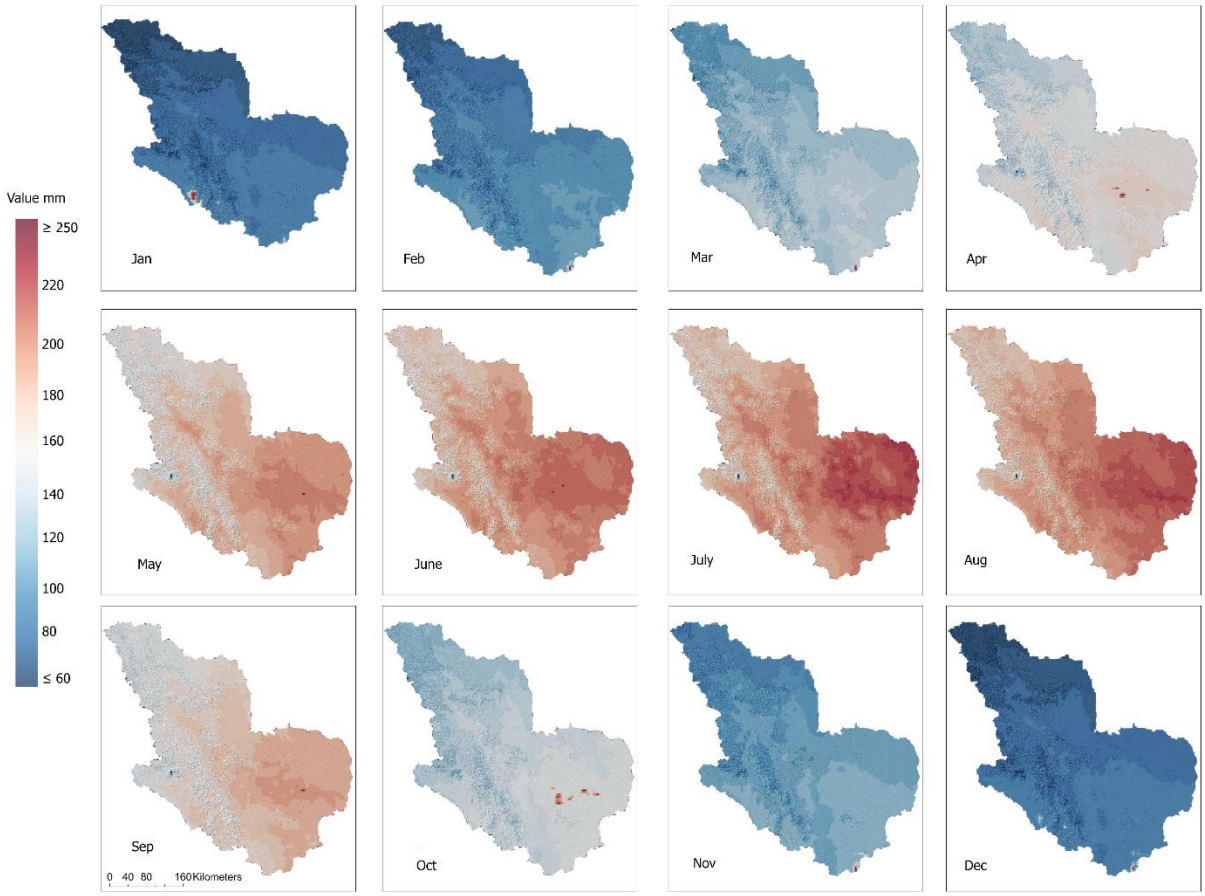

Figure 4-20. The spatial distribution of monthly averaged ET0 in Al-Madinah (1970-2018)

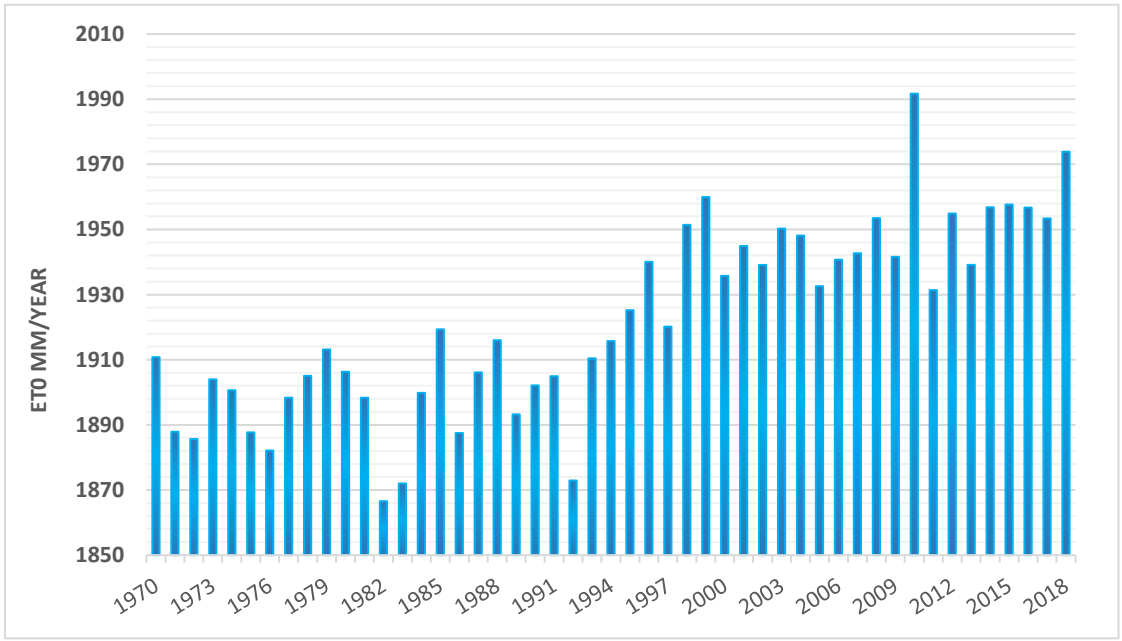

Figure 4-21. The annual evapotranspiration rates from ET0-Worldclim database for Al-Madinah (1970-2018)

Furthermore, the comparison between the monthly rainfall and ET0 during the years from 1970 to 2018 in Al-Madinah region, as shown in Figure 4-22 revealed that the ET0 rate was higher in all months than the amount of rainfall, which could result in a negative climatic water balance or water deficiency.

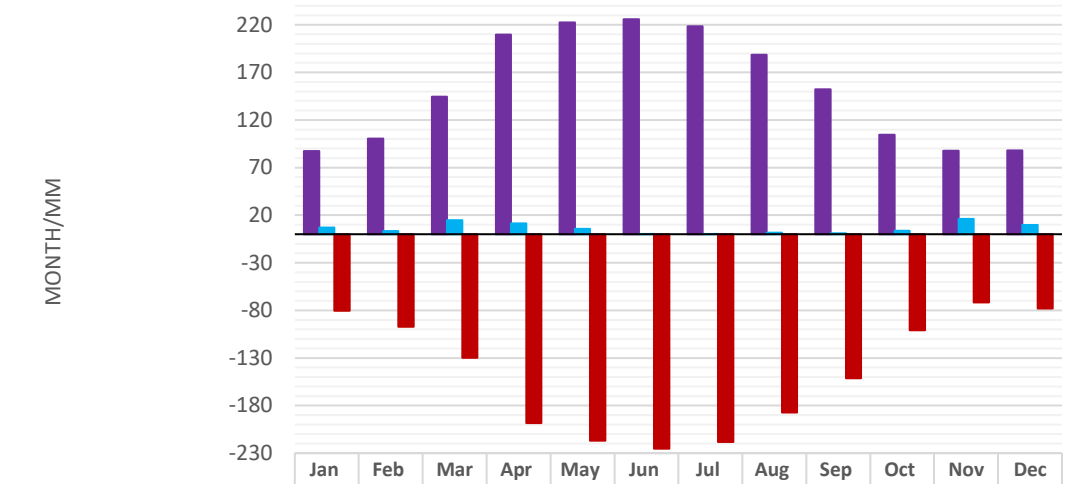

	Jan	Feb	Mar	Apr	May	Jun	Jul	Aug	Sep	Oct	Nov	Dec
ETO-Worldclim data	87.3	100.5	144.7	209.6	222.5	225.8	218.6	188.6	152.4	104.5	87.6	88.0
Precipitation-WorldClim data	7.0	3.3	14.8	11.3	5.6	0.4	0.4	1.5	1.1	3.7	15.9	9.8
climatic water balance	-80.3	-97.2	-129.9	-198.3	-217.0	-225.4	-218.1	-187.1	-151.3	-100.8	-71.6	-78.2

Figure 4-22. The monthly average climatic water balance (precipitation minus evapotranspiration) in Al-Madinah (1970-2018).

The SPEI findings, show the same pattern as EVP across time, with years since 2000 being drier than the last part of the 20th century, (Figure 4-23). Approximately 14.3% of the study period was characterized by wet conditions, while about 20.4% experienced dry occurrences.

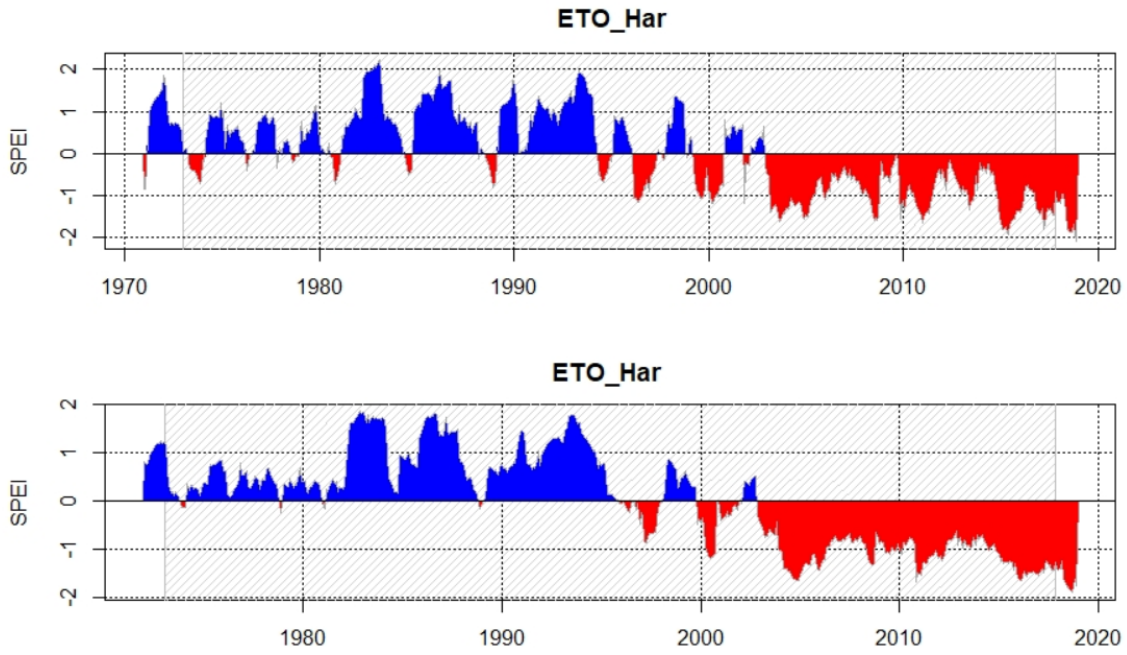

Figure 4-23. The SPEI in Al-Madinah region from 1970 to 2018 at 12-Month (above) and 24-Month (bottom) * Red colour represented drought situations with negative values, and blue colour symbolised wet conditions with positive values.

4.3.6 Evapotranspiration (ET0) under climate change scenarios.

The estimated evapotranspiration is expected to increase gradually for most of the year for all periods under RCP4.5 and RCP8.5 scenarios compared to the baseline (1970-2018). The increases are predicted to be slightly greater for later periods at the end of the century in 2081-2100 and more extreme scenarios. For example, under the RCP8.5, it is projected that the ET0 will show a higher trend by about 8.91% to 19.6% from the base period in the duration of 2021-2040 to 2081-2100, respectively, 162.86 mm/year to 359.70 mm/year respectively.

Moreover, the expectations indicate a substantial increase in the ET0 rates in the summer months of June, July and August, with the highest increase of 18.93% (40 mm) in the 2081-2100 period under the RCP8.5. In contrast, the winter months (December, January, February) are projected to display the smallest increase in evapotranspiration amount in 2021-2040 under RCP8.5, about 4.41% (4mm), which will rise by 16.92% (15.56 mm) at the end of the century under the same RCP8.5 scenario. The spring season, April and May, are projected to show slight

declines in ET0 amounts by up to 5% (9.7 mm) at the end of the century in 2081-2100 under the RCP8.5 scenario compared to the baseline, (Figure 4-24).

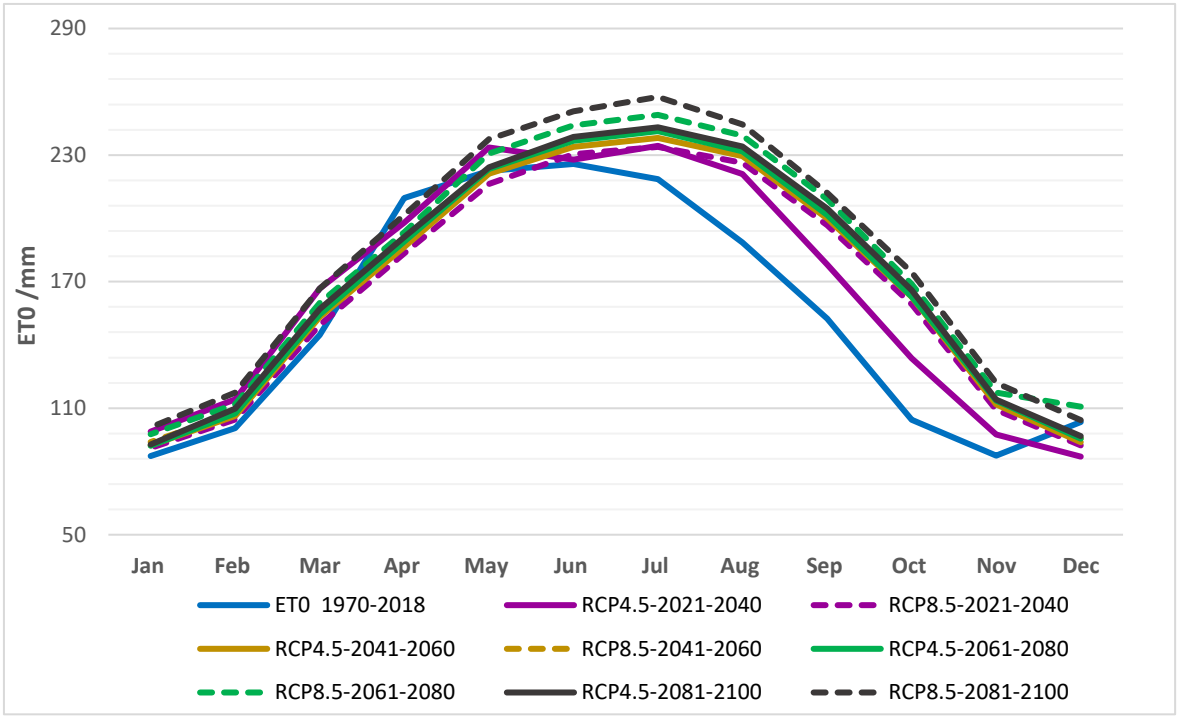

Figure 4-24. Projections of average evapotranspiration (ET0)/mm, in Al-Madinah under RCP4.5 and RCP8.5 scenarios from 2021 to 2100.

The spatial distribution of average evapotranspiration (ET0)/mm in Al-Madinah, is illustrated in the Figure 4-25. Under both the RCP4.5 and RCP8.5 scenarios an increase in ET0 amount towards the east and southeast areas was observed. 2081-2100 under the RCP8.5 scenario is estimated to experience the maximum increase of ET0 were values are predicted to exceed 200mm/month.

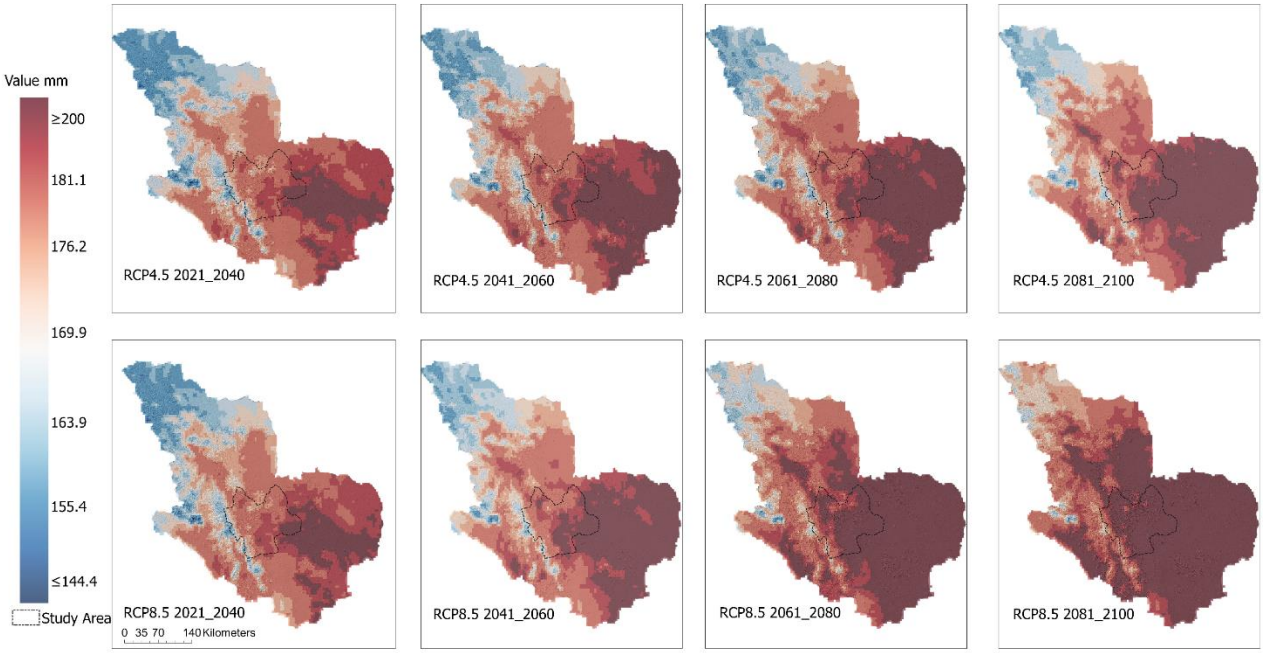

Figure 4-25. The spatial distribution of average evapotranspiration (ET0) mm/month, in Al-Madinah under RCP4.5 and RCP8.5 scenarios from 2021 to 2100.

The future drought projections under SPEI-12 and SPEI-24 revealed that at the end of the century (2081-2100) under both scenarios, RCP4.5 and RCP8.5, are expected to experience the highest intensity of drought events. The lengthiest duration of drought is projected to extend between periods (2061- 2080) to (2081-2100) under RCP.8.5. Al-Madinah will also experience slightly wetter conditions in the near future (2021-2041) as well as the 2041-2060 period under both scenarios and time scales, are displayed in the Figure 4-26.

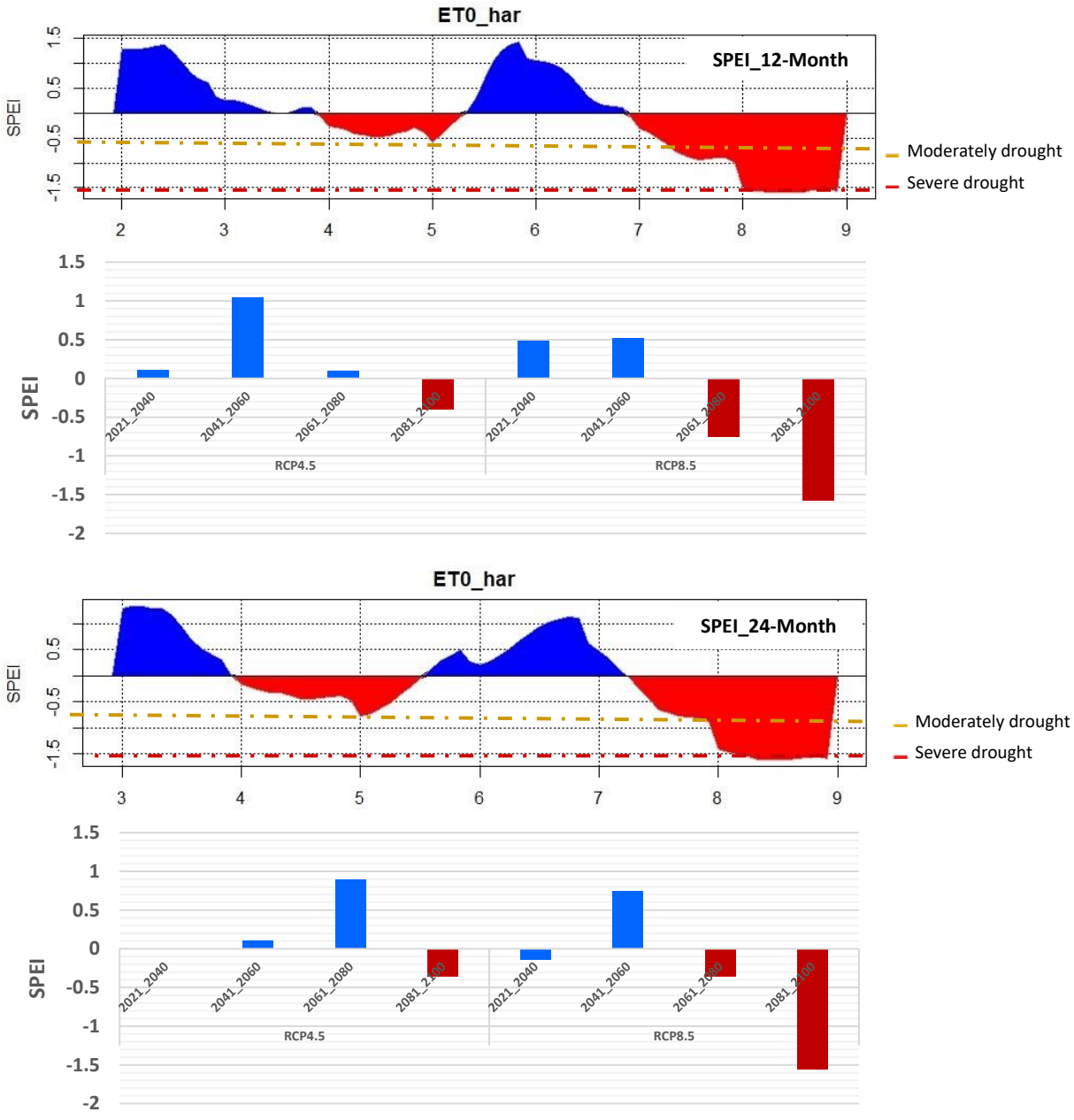

Figure 4-26. The SPEI in Al-Madinah region under RCP4.5 and RCP8.5 scenarios at 12-Month (above) and 24-Month (bottom) * Red colour represented drought situations with negative values, and blue colour symbolised wet conditions with positive values. The numbers on the x-axis refer to the future periods under RCP4.5 and RCP8.5. The charts show a noticeable increase in drought events at the end of the century into the severe drought conditions under RCP8.5, whereas it is expected to moderate drought at the end of the century under RCP4.5.

4.3.7 Changes in potential groundwater zones under RCP4.5 and RCP8.5 scenarios

The evaluation of potential groundwater zones using future precipitation accumulation conditions under RCP4.5 and RCP8.5 scenarios in the Fuzzy-Gamma 0.97 and the logistic regression models showed differing results. Only slight changes were detected applying Fuzzy-Gamma 0.97 model, whereas the logistic regression model revealed larger changes in the potential zones compared to the baseline period.

Additionally, the changes in the size of possible lands are predicted to show a small quantitative variance throughout all future intervals under both models. Under the Fuzzy-Gamma 0.97 model, the greatest addition of potential groundwater areas (139.79 km²) is estimated for 2081-2100 under RCP8.5 scenarios in Al-Madinah region, with around 17.65 km² in Al-Madinah City. These additional areas are expected to be accompanied by a loss of 127 km² that transitions into unsuitable zones. Thus, the total gain was estimate at areas at 12.76 km² in Al-Madinah area with about 5.09 km² in Al-Madinah City. The highest loss of suitable areas is estimated in the mid-century (2061-2080) under the RCP4.5 scenario, where sites becoming unsuitable will exceed the area of zones gaining suitability (Figure 4-27).

Changes were more noticeable in the logistic model results. The very high potential areas were estimated to increase to between 22.49% and 22.67% of the total area of Al-Madinah region, compared to the baseline period that extent of 16.95% of the total area. The higher increase for new area of groundwater suitability was predicted as the near future (2021-2040) and the end of the century (2081_2100) under both the RCP4.5 and RCP8.5 scenarios by approximately (19322km² and 19296km², respectively). Predictions suggested that about 4000 km² will be located in Al-Madinah city. The area gained was shown to be slightly higher towards the end of the century under the RCP8.5 scenario (8294km²) compared to the RCP4.5/2021-2040 period (8277km²). Similar to the Fuzzy-Gamma 0.97 model, the logistic regression results show that the mid-century (2061-2080) under the RCP4.5 will experience notable losses in areas in suitable areas, as illustrated in Figure 4-28.

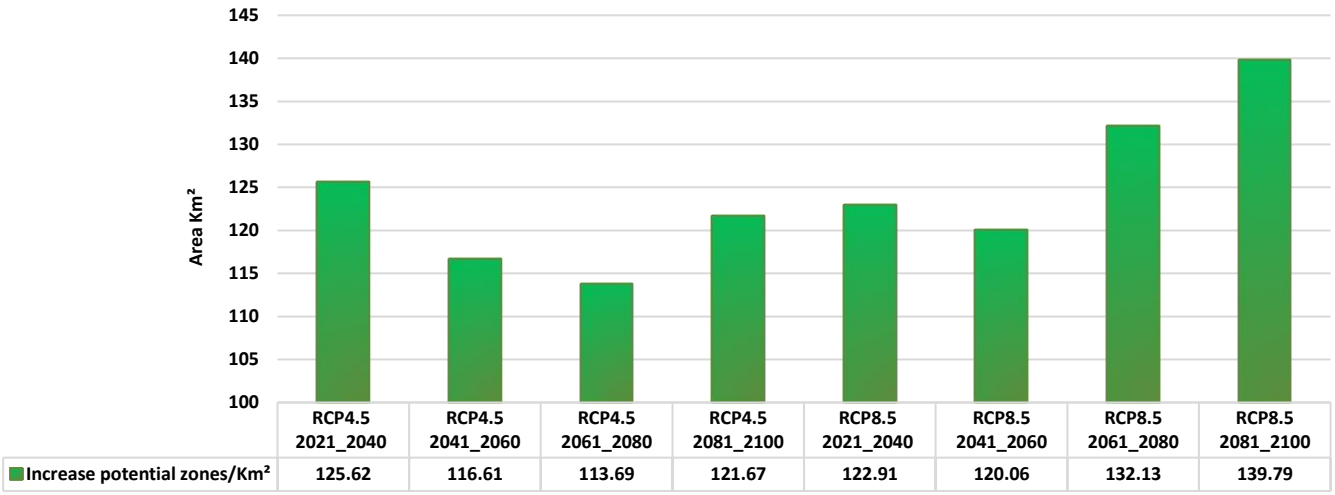

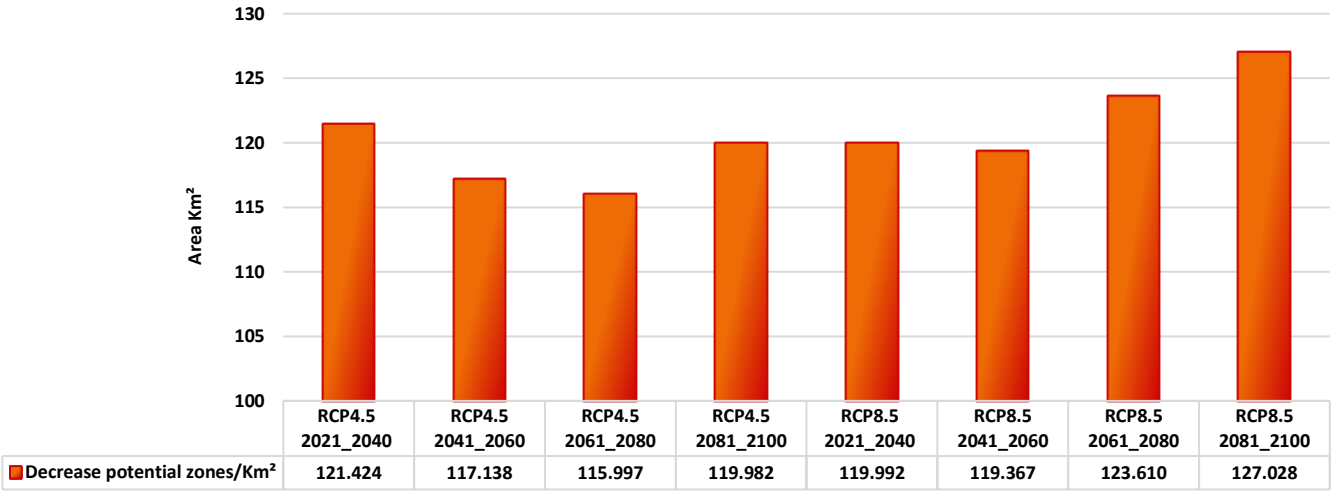

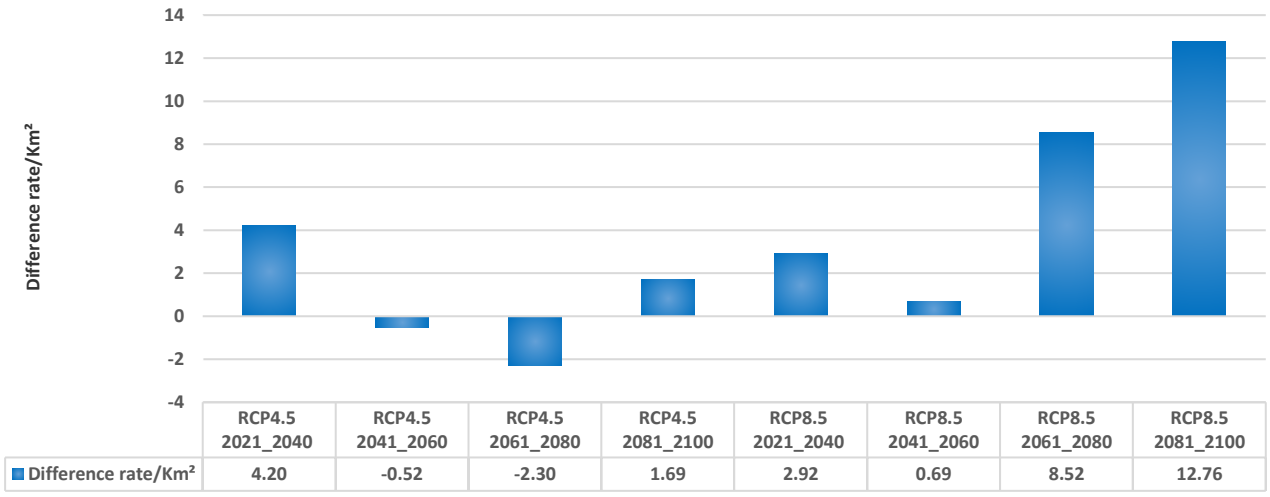

Figure 4-27. Projected changes in potential groundwater zones in the Fuzzy gamma 0.97 model under RCP4.5 and RCP8.5 scenarios and TWI weighted by future precipitation. The figure illustrates the quantitative variance of new areas gained and areas lost in square kilometers

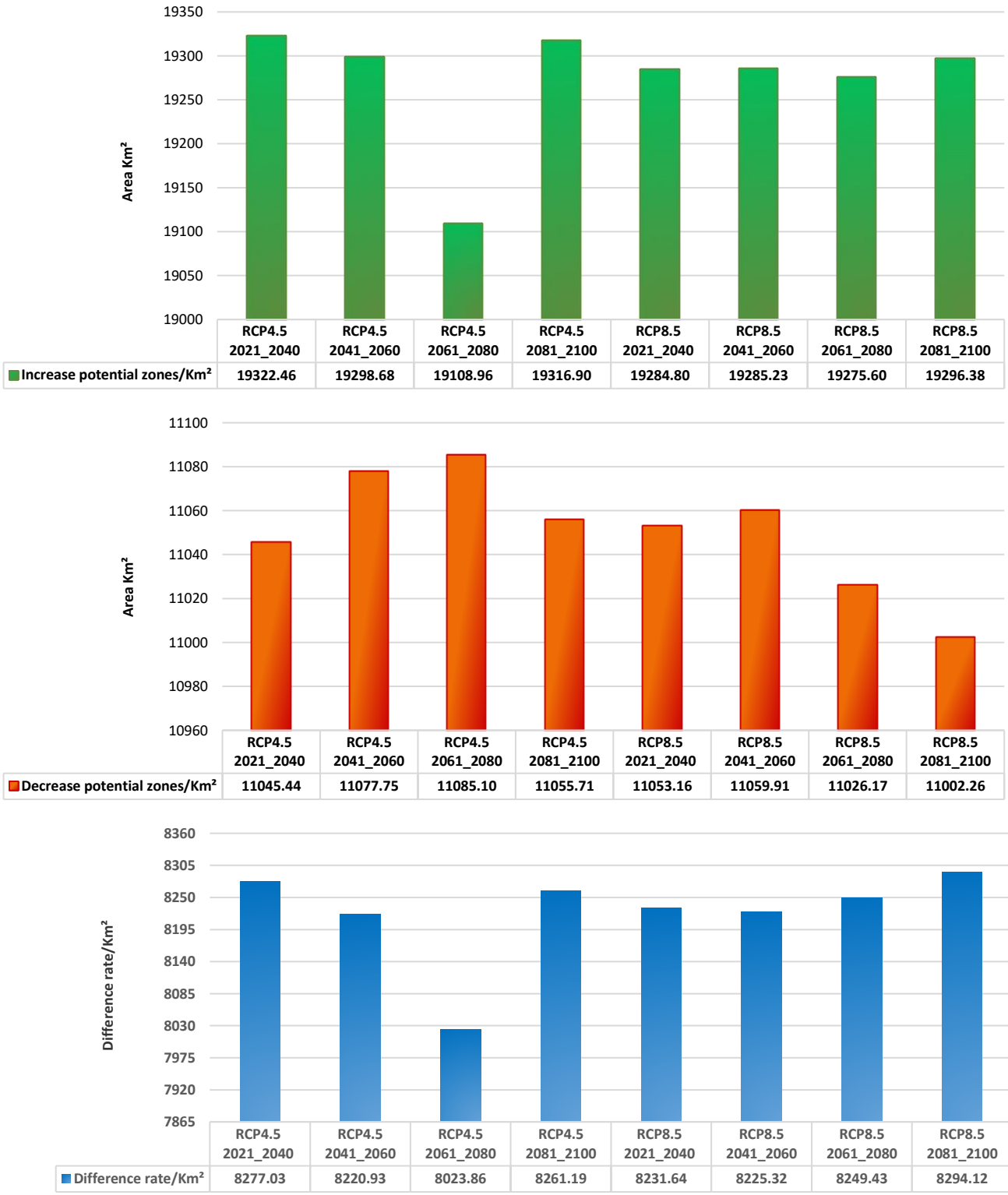

Figure 4-28. Projected changes in potential groundwater zones in the logistic regression model under RCP4.5 and RCP8.5 scenarios and TWI weighted by future precipitation. Th figure illustrates the quantitative variance of new areas gained and areas lost in square kilometers.

In terms of spatial changes, the analysis of the Fuzzy-Gamma 0.97 model showed that an average total of 28373 km² of potentially suitable lands for groundwater showed no changes in all future periods. These sites are highly compatible with the lava flows covering the north and south areas, as well as on some valleys extending towards the northwest, as illustrated in Figure 4-29.

The logistic regression model also revealed that 13558 km² (9.30 %) of the area was expected to remain unchanged as suitable areas , again primarily compatible with the lava areas and on some of the valleys. In contrast, 11002.26 km² (7.50%) of the Al-Madinah region area was predicted to become unsuitable. These areas were on the edges of the lava areas (e.g. Harrat Khaybar), which extends in the north of the Al-Madinah region, as well as the far south of Harrat Rahat to the south of Al-Madinah city (Figure 4-30).

4.3.8 The evaluation of the dam locations

The evaluation of 14 dams used to recharge groundwater in Al-Madinah under the TWI_Rainfall variable has indicated that the dams of Baydan, Abu Hunk, Qasiba and Nakhlaan received the highest rainfall in the baseline period (1970-2018) with average runoff, which was recorded from 2018 to 2021, about 520,868 m³; 24,378 m³; 61726.24m³ and 63868.8m³, respectively (MEWA, 2022). These dams also have a good opportunity for flow accumulation. They are located on Igneous rock and Lithosols, Calcic Yermosols soil with an average permeability of about 1.5 to 5.1 cm/hr. In addition, these dams under the RCP4.5 and RCP8.5 scenarios are projected to receive almost the same amount of rainfall in all future periods.

The dams of Al-Eays, Al-murabae, Al-hasid and Abu Ghasha had shown a very high potential to accumulate rainfall in the baseline period as represented in Figure 4-31, where the average runoff volume was about 355456.4 m³, 329474.6 m³; 77926.5 m³ and 45,936 m³, respectively (MEWA, 2022). Igneous rock beds and polylithologic rocks characterize these dams with two groups of soil: Lithosols, Calcic Yermosols soil unit and Lithosols, Yermosol, Cambisols Chromic soil types, whose permeability was estimated by about 1.5 to 5.1 and 5.1 to 15 cm/hr, respectively. Moreover, the rate of potential accumulation based on the TWI_Rainfall index is projected to increase noticeably under the RCP4.5 scenarios in the near future period (2021-2040), mid-century (2041-2080), and at the end-century (2080-2100).

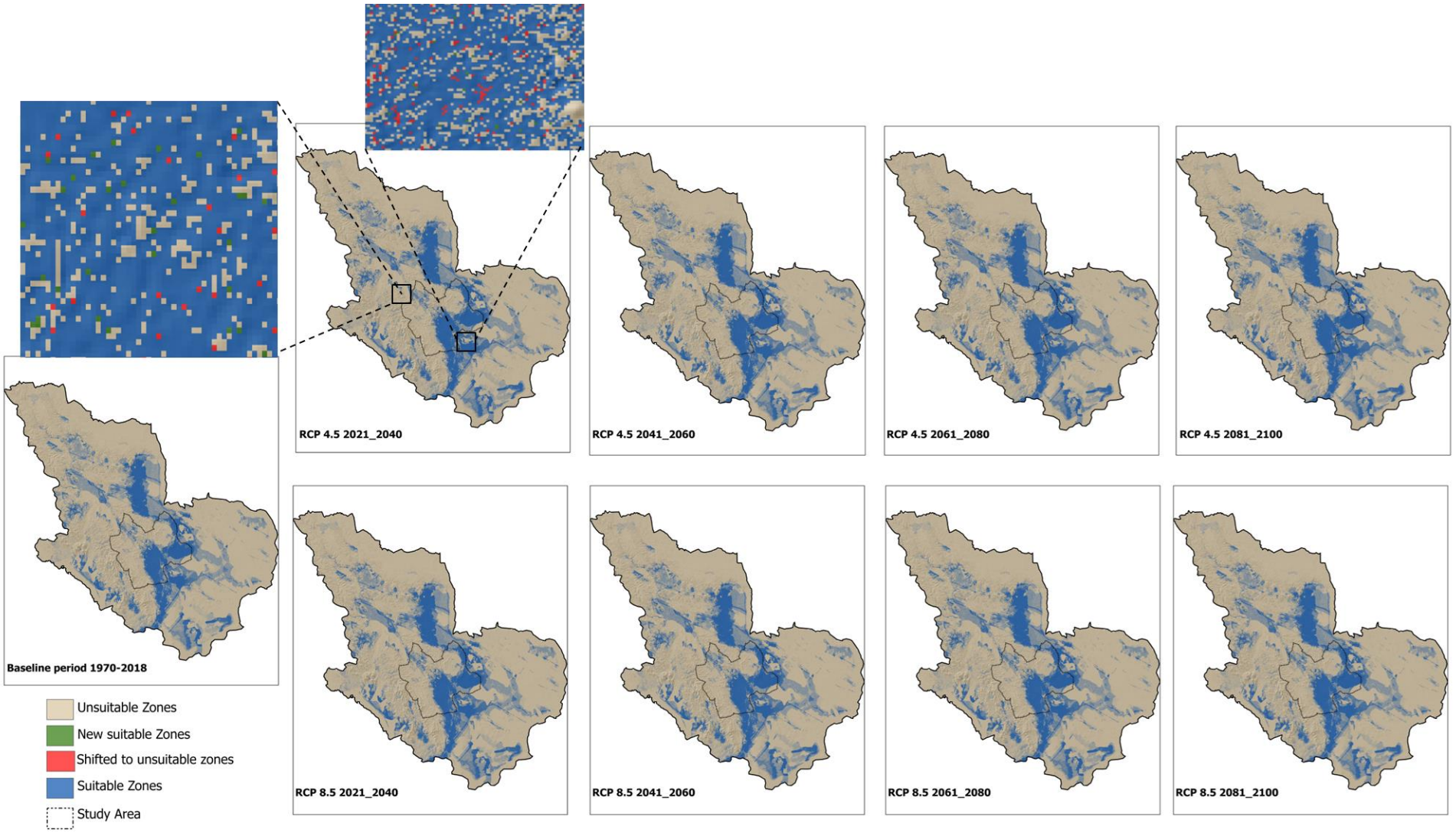

Figure 4-29. The spatial distribution of potential areas under different suitability classes in Al-Madinah under RCP4.5 and RCP8.5 scenarios from 2021 to 2100 in Fuzzy-Gamma 0.97 model.

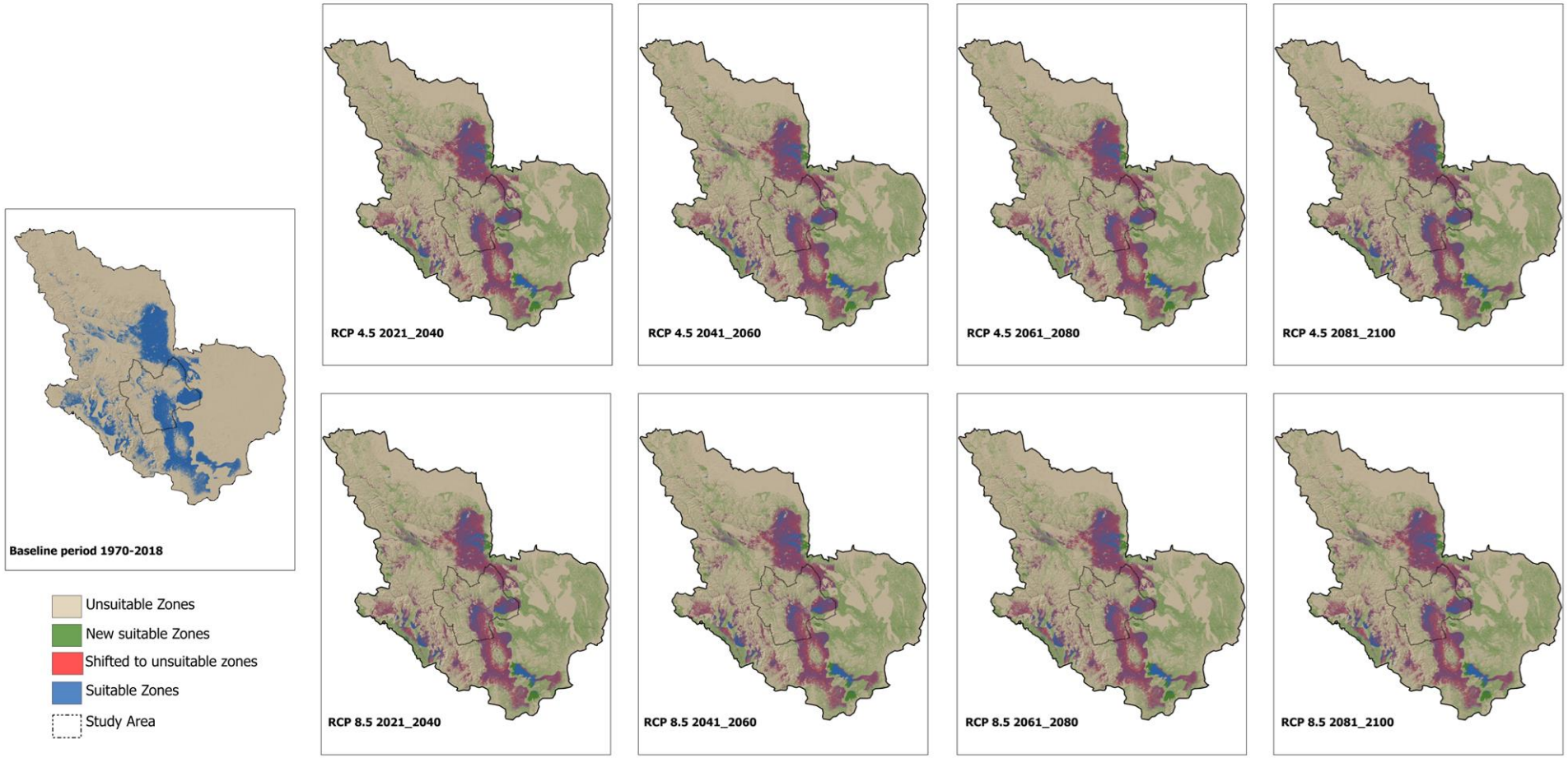

Figure 4-30. The spatial distribution of potential areas under different suitability classes in Al-Madinah under RCP4.5 and RCP8.5 scenarios from 2021 to 2100 in the logistic regression model.

The findings have indicated that the expected groundwater potential zones under Fuzzy logic 0.97 and logistic regression models are highly likely to recharge by rainwater stored on some dams with good locations. For example, the dams of Abu Hunk, Al-Eays, Al-murabae, Al-hasid and Alsalhania that have considerable potential for rainfall accumulation were constructed in suitable places for the groundwater areas under both models. However, Nakhlaan, Baydan and Abu-Ghasha dams are expected to recharge the potential groundwater areas under the Fuzzy logic 0.97 model, whereas the Malal dam would recharge the possible regions of the south-west of Al-Madinah city under the logistic regression model.

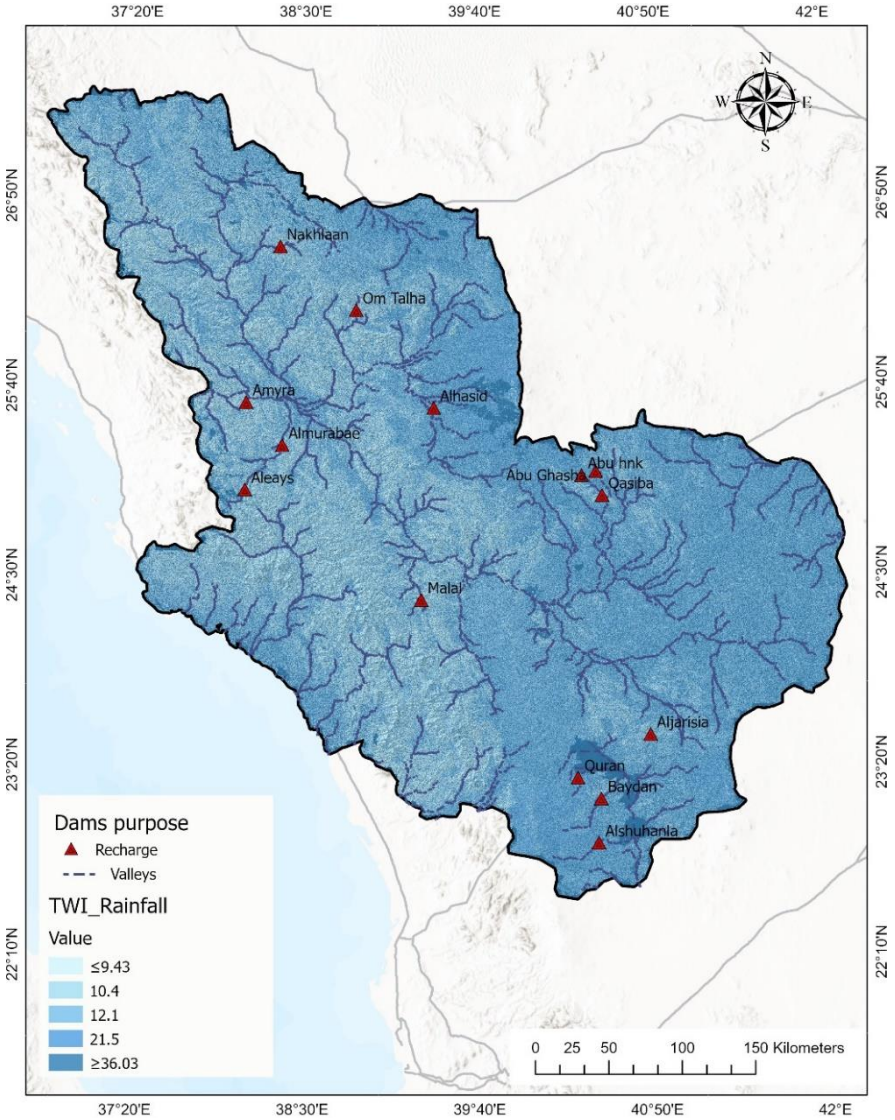

Figure 4-31.The recharge dams and topographic wetness index weighted by rainfall in baseline periods (1970-2018).

4.4 Discussion

Climate change and variability can have a negative effect on groundwater availability, ecosystems, and society (Shrestha et al., 2016). This is likely to be more visible in arid-semi and arid countries such as Saudi Arabia, particularly on the renewable or shallow groundwater aquifers (Arabia, 2005), such as those of Al-Madinah province, which rely on rainfall as the primary source of replenishment. Therefore, the evaluation of future precipitation, temperature, and evapotranspiration (ET0) trends under global climate change scenarios are considered an essential component in groundwater management and are likely to play a key role in mitigating any possible adverse consequences of climate change.

This study confirmed the usefulness of the Global climate models (GCMs) projections and the Representative Concentration Pathways (RCPs) to simulate and project climate changes as well as to understand the impact of climate processes on water resources. These models have also been applied by several other studies, such as Zhang et al. (2016) ; Lamichhane and Shakya (2019a) ; Kahsay et al. (2018) ; Amin et al. (2016) ; Shrestha et al. (2016), shown that these databases highly assisted in generating future climate change scenarios and efficiently have combined with various tools to estimate the impact of climate change on water resources.

The analysis of the historical period showed that the trend of precipitation in Al-Madinah fluctuated, although the period from 2001 to 2018 experienced a significant decrease in rainfall compared to the period from 1970 to 2000. This might be attributed to some flash flood and extreme weather events during the period of 1970–2000, where the climatic station of Al-Madinah recorded four flood events in 1984,1987,1991 and 1998 (Hermas et al., 2015) as well as some intense rainfall reported in Yanbu and Al-Madinah city in November 1992 and 2000.

With regard to the simulation data, simulated temperatures corresponded more with observational datasets than rainfall data. Furthermore, all measures of evaporation showed good agreement, although the estimated evapotranspiration (ET0) exhibits some variance compared to the observed EVP-Pan data. Consequently, there was a high level of confidence in their reliability to use in this study.

There are similarities between the historical trend results of ET0 in Al-Madinah in this study compared to those concluded by Elnesr and Alazb (2013), who investigated the ET0 rate by applying the Food and Agricultural Organization (FAO) Penman-Monteith (PM) method in 29 meteorological stations distributed all over Saudi Arabia for the period 1980 to 2008. The findings revealed the highest amount of ET0 in the summer and lowest in the winter in the country's entirety. The annual evapotranspiration rates of Al-Madinah showed high values (1991mm/year) that were also reported by Mahmoud and Alazba (2016a) and were slightly higher (ranging from 2059 to 2405mm/year during 1992–2014). These values are often expected in arid and semi-arid regions such as Saudi Arabia. For example, the ET0 amount of the central regions (Riyadh, Al-Qassim, Hail provinces) was estimated to be above 2100mm/year from 1950 to 2013 (Mahmoud and Gan, 2019). These regions mostly experience marginally hotter temperatures than Al-Madinah.

Moreover, an increase in the future temperature in Al-Madinah under both scenarios, RCP4.5 and RCP8.5, would influence the evapotranspiration rate. The prediction of an increase was about 8.9% by 2021-2040 periods under both scenarios; this was similar to Abbas (2013) who suggested, that evaporation was estimated to rise about 5% by 2050 in Al-Madinah region.

The future GCMs simulation models predicted that the annual precipitation would increase by an average of 18.74% (22.81 mm). Under the RCP 4.5 scenario, a notable increase is expected in 2021-2040 and the end of the century in 2081-2100. However, the precipitation amount has been estimated to drop slightly (2.27%) during the mid-century (2041-2060 and 2061-2080), which is a similar result to that of Amin et al. (2016), who reported that a potential decrease of 1.5 % through most of KSA under the RCP 4.5. Contrastingly, under the RCP 8.5 scenario, the present study's outcomes could be contrary to that of Amin et al. (2016), who found a decreasing trend of annual rainfall towards the 2050s, this study projected that all periods would have more rainfall under the RCP 8.5 scenario . Generally, the results of the current study are consistent with the findings of Alsarhan et al. (2016), who concluded that the average annual precipitation is predicted to increase by about 10 – 20 mm in most regions of KSA by the 2030 to 2080 period. This study also agrees with Almazroui (2013), who stated that rainfall patterns in most regions of Saudi Arabia are expected to show positive trends between 2021–2050.

In addition, the temperature will potentially rise steadily under both RCPs, with an average of about one degree Celsius per 20-year period in the near future (2021-2040) and the mid-century (2041-2060 and 2061-2080), with a more noticeable increase of around two degrees Celsius by end-century (2081-2100), in most months. These results agree with those obtained by Driouech et al. (2020), who concluded that the warming trend on the Arabian Peninsula is predicted to be larger under RCP8.5 (4°C increases) than the RCP4.5 scenario (2 °C increases), an almost similar finding was also reported by Tarawneh and Chowdhury (2018), who estimated that the temperature is likely to rise gradually under RCP8.5 to around 1.3–1.6C and 2.1–3.7C by 2025–2044 and 2045–2064 periods, respectively, to reach a high point in 2065–2084 by increasing by 3.2–3.8C. Although the results of these studies are in general accord with the present study, the difference in exact values changes can be attributed to the study area (most other studies look at Saudi Arabia), as well as differing climate models being used, including Regional Climate Models (CORDEX-MENA domain and CCSM4 model).

The evapotranspiration rate is known to respond to temperature rise. Consequently, the present study's estimation of future evapotranspiration patterns was highly compatible with temperature trends, which are expected to increase gradually towards the end-century 2081-2100. This study's projected trend in evapotranspiration agrees with the estimates of Alsarhan et al. (2016), which concluded that evapotranspiration would be higher in Saudi Arabia by end of 2080 periods.

Seasonally, Al-Madinah will be expected to experience slight growth in the average precipitation in winter by 2081-2100 under RCP8.5. This accords with Alsarhan et al. (2016) ; Almazroui et al. (2020) and El-Rawy et al. (2023) findings, which showed that the amount of winter precipitation in Saudi Arabia is expected to rise slightly by the end century. However, it was predicted that KSA will likely experience no precipitation in winter 2030, except the southwest area will receive about 100 -200 mm (Alsarhan et al., 2016). This finding is contrary to the present study, which has concluded that Al-Madinah winter precipitation will experience a slight growth in the 2021-2040 period under RCP45 and RCP8.5 scenarios. Moreover, the wintertime temperature values in Al-Madinah region are projected to show a warmer pattern, especially at the end of the century 2081-2100 under both scenarios. This warming pattern is predicted to increase the ET0 rate in

the wintertime compared to the baseline period from 91.95mm to the highest rate by about 100mm and 107.5mm at the end of century 2081-2100 under RCP4.5 and RCP8.5 scenarios, respectively. However, such a rate of ET0 is still considered the lowest ET0 amount in Al-Madinah seasons. This condition also would be similar to the winter across the Kingdom (Alsarhan et al., 2016).

Despite the fact that the spring season (March to May) is the rainy season in Al-Madinah, it is projected to experience a gradual increase in mean temperatures during all periods under both RCPs. Accordingly, the ET0 rates would be influenced by these weather conditions, with the biggest increase expected at the end of the century (2081-2100) by 5% under the RCP8.5 scenario. This result is consistent with Alsarhan et al. (2016) estimations, which reported that the ET0 rate of Al-Madinah region is projected to increase slightly in the springtime, around 2% by 2080, more than other areas located in the southeast and southwest parts of Saudi Arabia. Furthermore, the projections revealed that November would continue to receive the highest rainfall amount under both RCPs. The autumn rain is often associated with thunderstorms in Al-Madinah, which is caused by the influence of the extension of the Sudanese Low (Hafez and Miraj, 2013). The most frequent flash flood events were recorded in November not only in Al-Madinah region but also in many regions in Saudi Arabia (Alsarhan et al., 2016), which could potentially recur in the future. The autumn season is projected to experience less ET0 than springtime and summer. Therefore, winter and autumn rains may be more significant to the water resources in Al-Madinah, particularly in November and January.

The government's constructed about 40 dams in Al-Madinah; 14 dams for recharge to groundwater and 26 dams for protecting residential areas from floods may be useful developments. The expectations also indicate that the summer season would be longer with increased aridity and temperature conditions under both RCPs scenarios, accompanied by the highest estimation of the ET0 amount in Al-Madinah under all periods in both scenarios.

Al-Madinah could face drought events and water deficiency challenges caused by the increased ET0 rate with reduced rainfall, negatively affecting the hydrological and water resources. The analysis of historical data for meteorological droughts by the SPEI index showed Al-Madinah was characterised by wetter conditions in the last third of the 20th century (1970-2000) than in the

last half, which experienced more drought cases. These results are in agreement with those obtained by The National Centre of Meteorology in Saudi Arabia NCM (2019), which applied the Precipitation Index (SPI) to monitor drought situations (1985 to 2019 in 12-month); the findings have confirmed that there were moderate and severe wet conditions covering most parts of Saudi Arabia in the period 1985 to 1997, with fluctuations and frequent dry conditions from 1999 until 2018. Amin et al. (2016) also confirmed that the KSA experienced extreme drought events from (January) 2000 to (July) 2013 using the SPI index, whereas Almazroui (2019) concluded that applying the SPI index from 1978 to 2017 indicated that the drought occurred typically from June to September in Saudi Arabia, as well as October despite it being a transition month, October experienced drought conditions for around 29 years out of 40 years used in the study.

Moreover, the United Nations (2015) report about extreme climate indices for the Arab Region pointed to the dry periods increasing by the end of the century (RCP8.5/2081-2100), obviously in the western and northern parts of the Arabian Peninsula. This finding was confirmed by the present study, where it is projected that drought events in Al-Madinah, located in the western Arabian Peninsula, will be the lengthiest duration and highest intensity under both scenarios RCP4.5 and RCP8.5 by (2081-2100). According to Alsarhan et al. (2016), the more vulnerable areas to desertification by 2080 are expected to be in the regions situated in the northwest of Saudi Arabia, where Al-Madinah extended.

The escalating temperatures and changing patterns of potential evapotranspiration (ET0) in arid regions associated with low rainfall amounts would create complex challenges related to contributing to water resources depletion, excessive stress on soil moisture and precipitation accumulation possibilities, which could compromise groundwater recharge and diminishing the potentially suitable areas to store the shallow groundwater over time. In the present study, the weighted TWI index by rainfall offered more sensitivity to variations in precipitation change impact that helped evaluate groundwater potential zones in Al-Madinah under both RCPs.

Although the potential sites in Al-Madinah will experience more noticeable alterations in spatial distribution pattern than in quantitative size throughout all future intervals under both RCPs compared to the baseline period, the majority of the expected zones are likely to receive

recharge primarily from rainwater accumulated in strategically positioned dams. The most noticeable changes are represented in the emergence of new suitable areas in remote locations distant from current residential areas, while some areas near established population centres are expected to become less suitable. One of the most important areas in Al-Madinah city that are projected to be impacted by the alterations of accumulation precipitation patterns alongside a temperature rise and ET0 are the valleys that extend towards the northwest along Wadi Al-Hamd, which are not only classified as a highly suitable places for groundwater wells but also contain most of the agricultural areas in Al-Madinah city. These areas have been included in the local authority's plan to expand agricultural areas by 2030. Therefore, such changes in the area's suitability for groundwater extraction would greatly affect future irrigation methods, as well as could lead to increased pressure on water requirements, necessitating additional resources that come at a higher cost, such as wastewater treatment and desalination. Conversely, the expectations of new suitable zones for groundwater in the southwestern of Al-Madinah centre correspond with the suggested development in the local plan to utilize them for agricultural purposes.

Finally, understanding the potential implications of climate change on shallow groundwater in arid and semi-arid regions is strongly required. Nevertheless, according to Green (2016), quantitatively measuring the magnitude and direction of groundwater change can be challenging due to data availability limitations. In the present study, the difficulties of accessing runoff data for an acceptable historical period prevented the application of hydrological models, which have been used widely for estimating the influence of climate change on groundwater, especially the recharging rates. Therefore, to examine the future climate-driven impacts on the potential groundwater zones, the Topographic Wetness Index (TWI) was weighted by the future precipitation (2021- 2100) under RCP4.5 and RCP8.5 scenarios. However, the combined method between the prediction of future precipitation patterns with the topographic wetness index (TWI) was highly beneficial in mapping groundwater's spatial distribution and detecting potential temporal and spatial changes in the groundwater locations over future periods under RCP4.5 and RCP5.8 scenarios. Moreover, although it is difficult to ideally evaluate and optimise dam locations separated from the integrated view of the influential hydrological and physical factors, the use

of the rainfall accumulation factor might contribute to drawing a general assessment of the dams' locations in light of the limited data available in the study area. Therefore, further work is required to investigate the viability of Al-Madinah dams' locations.

This study provided good insights into understanding precipitation, temperatures and Evapotranspiration (ET0) patterns as well as the expected potential impacts of climate change under RCP scenarios on groundwater zones in Al-Madinah; however, groundwater recharge in arid and semi-arid regions such as Al-Madinah is mainly reliant on extreme rainfall occurrences, which often create runoff that is accumulating in recharge zones retained by dams. Therefore, these extreme events are complex and would likely not be fully captured by analysing average precipitation and evapotranspiration (ET0) values employed in the current study. For example, this could imply uncertainty and limitations by underestimating the contribution of these episodic, localized recharge processes by extreme rainfall events. Accordingly, to gain a precise understanding of how climate change affects groundwater replenishment in arid regions, future research should analyse historical rainfall data to identify trends in extreme events and their relationship to groundwater recharge, as well as develop models that can simulate the effects of extreme rainfall on runoff and recharge at sufficient spatial and temporal scales. These models also should be validated and improved by collecting field data on groundwater levels, soil moisture, runoff amounts, and recharge processes.

In summary, temperature, rainfall, and ET0 each played distinct roles in controlling water resources. Understanding these natural settings was essential to highlight the potential impacts of climate change under RCP scenarios on groundwater zones in arid and semi-arid regions such as Al-Madinah. However, identifying and addressing the impacts of human activities are also essential for developing effective water management strategies and ensuring the long-term resilience of water systems in the face of growing population pressures, urbanization, and economic development; these driving factors will be discussed in detail in the forthcoming chapters. By integrating these aspects, the broad picture of water resources will emerge, informing strategies for sustainable management in the face of evolving environmental and societal pressures.

4.5 Conclusion

This chapter has presented a comprehensive overview of understanding the anticipated impacts of climate change under RCP scenarios on groundwater zones. Al-Madinah. It is expected that a slight increase in rainfall coupled with rising temperatures and Evapotranspiration (ET0) rates will be more noticeable under RCP 8.5 at the end of the century than in RCP 4.5 scenarios. Therefore, although this slight increase in rainfall is beneficial to contribute to some replenishment of groundwater sources to some extent, it might not entirely counterbalance and compensate for the escalated evapotranspiration rates brought about by raised temperatures. These changes in climatic conditions are also projected to influence the suitability of potential groundwater zone locations, which displayed relatively stable and less variation over all future periods under the Fuzzy-Gamma 0.97 model than the logistic regression model.

Although there are some areas that are considered suitable for groundwater extraction that might experience decreased suitability due to these climatic shifts, the changes in distribution patterns that potential groundwater zones in Al-Madinah would experience may be important to further research by using more aspects, such as future land use and land cover, and mapping water demand. Addressing these challenges also requires comprehensive water management strategies that can adapt to the changing climate patterns, which will be essential in mitigating the potential impact of these climate-induced shifts on water resources, particularly in arid or semi-arid areas experiencing water stress.

Chapter 5 Land use and land cover classification using Random Forest Algorithm on Landsat Imagery over Al-Madinah City

Abstract

Land Use and Land Cover (LULC) maps are essential for water resource study in arid regions due to the unique challenges and environmental conditions present in these areas. This study employs the Random Forest supervised classification method to analyse Land Use and Land Cover (LULC) dynamics in Al-Madinah city. This aim was mainly related to identify built-up areas and agricultural lands and to estimate the rate of the change in these land uses over the period (1990 -2020). The random forest classifier has been applied to 1990, 2000, and 2020 Landsat images. The assessment of the classification's accuracy was conducted using the Kappa coefficient.

The results indicated an overall classification accuracy of more than 95% and the kappa coefficient (K) of 0.93 for all maps. Between 1990 and 2000, urban areas experienced a gradual expansion, increasing by around 44%. By 2020, urban development significantly accelerated, doubling the growth rate. In contrast, during the period from 1990 to 2000, there were fluctuations in growth in agricultural land, with a decline of 11% in cultivated areas. This trend was followed by growth of 19% by 2020.

These findings contribute to understanding the development of the LULC of Al-Madinah, which is essential for informed decision-making as well as formulating sustainable land use management plans that also help to be the cornerstone for predicting the potential future effects of LULC changes, such as the impact on trends of water demands.

5.1 Introduction

Effective Integrated water resource management necessitates a knowledge of land use and land cover changes, particularly the alterations in agricultural lands and residential areas that could cause an escalation in water demand (Wang et al., 2017b ; Fulazzaky, 2014). These changes in LULC patterns can also significantly influence groundwater quality, availability and recharge by impacting runoff and diminishing infiltration (Pande et al., 2018). Therefore, LULC maps are particularly crucial in water resources management in arid regions due to these environments' unique challenges and sensitivities related to water scarcity. In the present study, the

classification and mapping of the LULC of Al-Madinah was necessary to provide a foundational dataset for constructing the IPUAT model to predict the future water demand of Al-Madinah city. The main prevailing human activities and natural features of Al-Madinah include built-up areas, agricultural areas, lava lands, valleys and empty lands, and mountains and hills.

However, there is a lack of comprehensive LULC maps of the Al-Madinah City-Region scale. This areas includes Al-Madinah city with surrounding rural areas based on the development plan for the city by 2030, that established an urban growth boundary (UN-HABITAT, 2019a). Accordingly, adopting innovative solutions can enhance understanding of changes in these landscapes, such as implementing advanced remote sensing technologies using high-resolution satellite imagery combined with GIS techniques, which can facilitate the product of detailed LULC maps.

The Landsat satellites operated by NASA constitute a valuable resource for monitoring and studying the Earth's surface (Cohen and Goward, 2004). Landsat satellite imagery is employed widely for land use and land cover (LULC) mapping (Mohammady et al., 2014). These imagery features good moderate spatial resolution, covers large geographic scale area, and has multispectral bands, including visible, infrared, and thermal bands, suitable for detailed LULC analysis; Landsat images can also be integrated into cartographic modelling in GIS (Cohen and Goward, 2004) and are easily accessible from the United States Geological Survey (USGS) (Mohammady et al., 2014)

Various methodologies have been applied to delineate changes in Land Use and Land Cover (LULC) patterns. These methods are broadly classified into supervised and unsupervised approaches (Talukdar et al., 2020 ; Mohammady et al., 2014). These included, for example, machine learning, deep learning algorithms, cellular automata models and Random Forest. Many studies confirmed that Random Forest has high accuracy in classification tasks and can effectively manage complex and high-dimensional data in remote-sensing applications such as LULC maps (Nurfadila et al., 2019 ; Talukdar et al., 2020). The random forest classification approach is viewed as an effective image classification technique that could operate with segmented and other raster data sets (ESRI, 2020).

This chapter will focus on the classification of LULC for Al-Madinah using the Random Forest Algorithm on Landsat imagery for detecting changes across the period from 1990 to 2020. The inadequacy of historical data and maps related to LULC that cover the whole study area for Al-Madinah necessitates such a classification effort. This will allow to generation of the time series for changing patterns of urban and agricultural areas over the historical period, which will be used as an important input for modelling water demand in Chapter 6.

5.2 Methodology

5.2.1 Data acquisition

Landsat (4-5) Thematic Mapper-TM and Landsat (8) Operational Land Imager-OLI data have been employed to derive the land-use / land cover maps. These images have a resolution of 30m with 7 multi-spectral bands (Landsat 4-5) and 11 bands (Landsat 8) (Table 5-1), respectively. They allow selection base on zero cloud cover percentage, possible in areas of the Arbian Peninsula. The images covered 1990, 2000 and 2020 and were downloaded from USGS (https://ers.cr.usgs.gov/) through QGIS software. The combination of natural colour composite (RGB) Bands Red, Green, and Blue (Bands 4,3,2), as well as colour infrared composite (NIR-R-G) Bands Near-Infrared (NIR), Red and Green (Bands 5,4,2) have been used in classification process to distinguish LULC types.

Table 5-1 Details of Landsat images used for classification.

Satellite	Path/Row	Date of acquisition	Grid cell size (m)
Landsat (4-5) Thematic Mapper-TM	170 - 43	1990-03-03	30 m
Landsat (4-5) Thematic Mapper-TM		2000-09-06	
Landsat (8) Operational Land Imager-OLI		2020-02-02	

5.2.2 Random Forest classification method

The supervised image classification method adopted using the Random Trees classification technique, which is considered a machine-learning classifier introduced by Breiman (Naghibi et al., 2017c). Utilizing this method within ArcGIS Pro involves several steps presented in Figure 5-1, which shows the overall workflow of the study area's land use/cover classification. The present study identified five categories of LULC classes: built-up areas, agricultural areas, lava lands, valleys and empty lands, and mountains and hills in Al-Madinah city. This definition was established on an initial examination of the study area, which allowed the dominant classes to be defined.

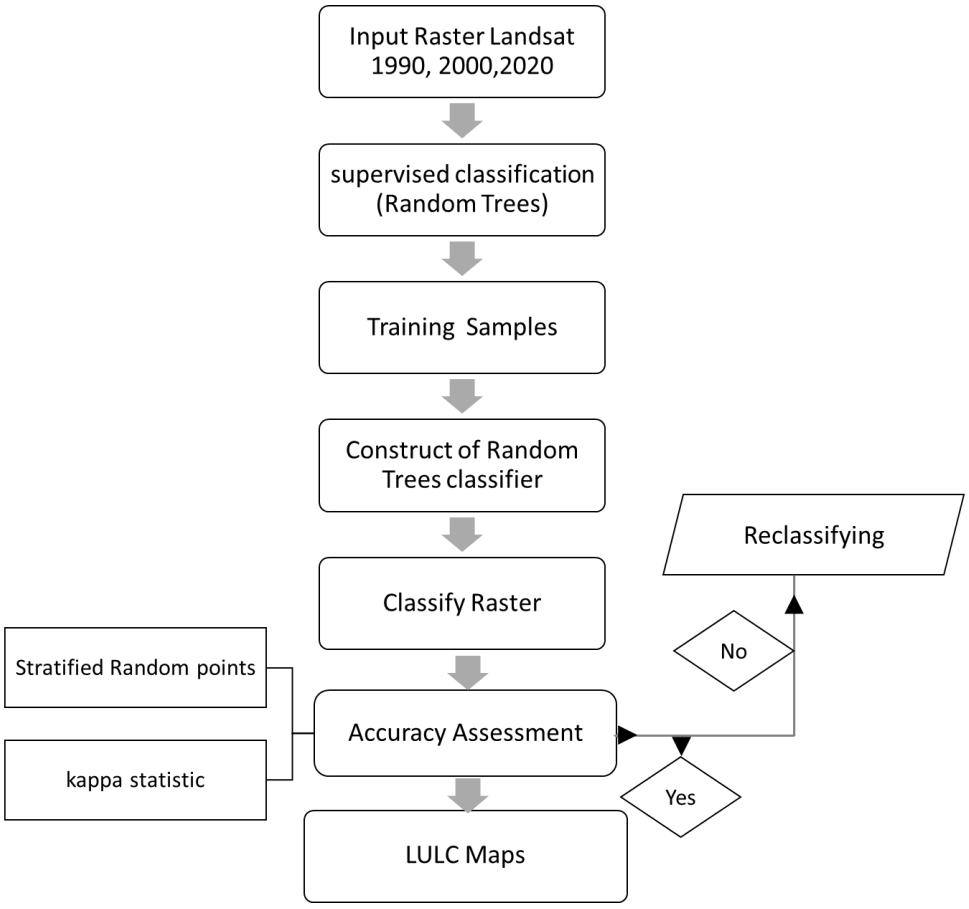

Figure 5-1 workflow of the land use/cover classification.

Accordingly, firstly, the simplicity and clarity resulting from a limited number of classes not only enhance the interpretability of the LULC map but also improve classification accuracy. Secondly,

to generate data suitable for the IPUAT model related water consumption, built-up areas, and agricultural lands are important LULC classes to distinguish from other areas. It should also be stated that the classification for 2010 was not performed due to relying on estimation data for adjacent years 2012 and 2015 that have the consistency of LULC patterns within the time series as well as were appropriate for research objectives and the IPUAT model.

The general steps to apply Random Trees classification in ArcGIS Pro comprise:

5.2.2.1 Collect Training Samples

The training sample file that can be either shapefiles or feature classes, is used to classify the dataset several times based on collecting random subsets of training pixels that result in various decision trees, which would help to make a final decision, as well as the selecting training samples and identifying categories typically based on the spectral response (ESRI, 2020). These training samples represent different land use and land cover classes, which allows instructing the Random Trees algorithm about the distinctive spectral attributes of each land cover category. In the present study, training samples were created manually by drawing polygons around representative areas of each class, such as built-up areas, agricultural lands, and lava, after the images were carefully visually interpreted. Training samples were randomly chosen by selection within each class to avoid bias, ensuring they accurately represented each class's spectral variability.

5.2.2.2 The Random Forest classifier

Involves two key parameters: the number of trees and tree depth. A greater number of trees generally leads to improved accuracy. The tree depth indicates the number of rules each tree can create to acquire a decision, representing how deeply the tree explores the data for complex patterns (ESRI, 2020).The present study setting has 50 trees and a tree depth of 30 in ArcGIS Pro, which is considered reasonable and a moderate number of trees that would provide stability and accuracy for classification LULC (Nadzri et al., 2023).

5.2.2.3 Accuracy assessment

A classification accuracy assessment is very important in remote sensing, as a final measure in the classification process to determine the extent of the accuracy of the classification in relation to training and test samples (Rwanga and Ndambuki, 2017 ; Rejaur Rahman and Saha, 2008). A confusion matrix was calculated, which allows the assessment of four accuracy measures: user's accuracy (commission error), producer's accuracy (omission error), as well as overall accuracy and it facilitates the calculation the Kappa coefficient, a measure of accuracy level taking into account both user and producer accuracy (ESRI, 2022a ; Rwanga and Ndambuki, 2017 ; Talukdar et al., 2020)

Commission Error represents the false positive rate in the classification the percentage of pixels that were classified into a specific land cover class but belong in reality to a different class. In contrast, the omission error reflects the rate of false negatives in the classification, representing the percentage of pixels genuinely associated with a specific land cover class but not identified as such during the classification process (ESRI, 2022a). The Cohen's Kappa Coefficient is a statistical model that measures the difference between the present agreement and expected agreement that could exist by chance; it calculates the agreement between the observed classification and the reference data or ground truth points(ESRI, 2022a ; Anthony J. Viera, 2005). The formula for Cohen's Kappa is:

$$k = \frac{p_0 \ - P_e}{1 \ - P_e} \qquad (1)$$

p_0 represent relative agreement between classification and training data (sum of agreements divided by total number of classifications.

P_e shows the expected agreement, representing the level of agreement that would be expected by random chance (which can be calculated from row and column totals in the confusion matrix).

The present study determined 521 ground truth points that are spatially distributed across the entire study area, The stratified random points method was used for selecting ground truth points. This method can consider the class size variation as well as the representativeness of the

variability within each land cover class. Moreover, different topographical maps were used to validate the land cover classification. The Cohen's kappa coefficient (κ) ranges from less than or equal to 1, where a value of 1 means perfect agreement and values less than zero indicate poor or less than chance agreement (Table 5-2) (Anthony J. Viera, 2005).

Table 5-2 Interpretation of Kappa

Kappa	Agreement
< 0	Less than chance agreement
0.01–0.20	Slight agreement
0.21– 0.40	Fair agreement
0.41–0.60	Moderate agreement
0.61–0.80	Substantial agreement
0.81–0.99	Almost perfect agreement

5.3 The results

The results of the accuracy assessment, as shown in Table 5-3, Table 5-4 and Table 5-5 revealed that the overall accuracy of classification was more than 95% in all years 1990, 2000 and 2020. The classification results for the built-up area over the studied years demonstrated high sensitivity with a Producer's Accuracy ranging from 0.90 (2020) to 0.95 (1990), which means effectively capturing 90% to 95% of true urban pixels. However, the User's Accuracy was 1 in 2020 compared to 0.75 in 1990. A 0.75 was the lowest accuracy LULC classification, which implies that a proportion (25%) of false positives indicate instances where non-urban pixels are misclassified as urban. In comparison, the classification model correctly identified every pixel in the agricultural land class across three images (1990, 2000,2020) as agricultural land by without any false negatives.

Table 5-3 the confusion matrix and accuracy assessment for LULC -1990 classification

* Rows represent actual land cover categories, while columns display the model's predictions aligned with ground truth data. The user's accuracy column shows false positives and the producer's accuracy column shows false negatives.

Class Name	Built up area	Valleys and Empty lands	Agricultural lands	Lava	Mountains and hills	Total	U_Accuracy	Kappa
Built up area	12	2	0	1	1	16	0.75	
Valleys and Empty lands	0	86	0	0	3	89	0.97	
Agricultural lands		0	10	0	0	10	1	
Lava	0	0	0	96	4	100	0.96	
Mountains and hills	0	1	0	9	296	306	0.97	
Total	12	89	10	106	304	521	0	
P_Accuracy	1	0.97	1	0.91	0.97	0	0.95	
Kappa								0.931

Table 5-4 the confusion matrix and accuracy assessment for LULC -2000 classification

Class Name	Built up area	Valleys and Empty lands	Agricultural lands	Lava	Mountains and hills	Total	U_Accuracy	Kappa
Built up area	15	1	0	0	0	16	0.93	
Valleys and Empty lands	0	86	0	0	3	89	0.97	
Agricultural lands	0	0	10	0	0	10	1	
Lava	0	0	0	93	7	100	0.93	
Mountains and hills	1	2	0	5	298	306	0.97	
Total	16	89	10	98	308	521	0	
P_Accuracy	0.94	0.97	1	0.95	0.97	0	0.96	
Kappa								0.937

Table 5-5 the confusion matrix and accuracy assessment for LULC -2020 classification

Class Name	Built up area	Valleys and Empty lands	Agricultural lands	Lava	Mountains and hills	Total	U_Accuracy	Kappa
Built up area	18	0	0	0	0	18	1	
Valleys and Empty lands	1	84	1	0	3	89	0.94	
Agricultural lands	0	0	11	0	0	11	1	
Lava	0	0	0	96	6	102	0.94	
Mountains and hills	1	2	0	6	292	301	0.97	
Total	20	86	12	102	301	521	0	
P_Accuracy	0.9	0.97	0.92	0.94	0.97	0	0.96	
Kappa								0.935

The kappa coefficient has indicated a very good agreement by 0.93 for all LULC maps, representing a high level of agreement beyond chance between the model's classifications and the ground truth data. Therefore, these reliable results of the classification of images would be beneficial for understanding LULC patterns in Al-Madinah city.

The classification maps are shown in Table 5-6 and Figure 5-2 showing that the mountains and hills class and lava fields class were the dominant forms of the land cover of the area by average accounting for 59% and 19% of the area. These were followed by valleys and empty lands with 17% of the whole study area. The built-up area and agriculture showed the smallest areas classified in all periods.

The growth rates for urban areas showed distinct patterns over the time intervals. Urbanization was observed to gradually increase between 1990 and 2000, where the built-up area increased by 43.53%. However, the subsequent period from 2000 to 2020 experienced an accelerated growth rate that showed a significant doubling of the built-up area. On the contrary, agricultural lands demonstrated fluctuations over the examined times, where land area experienced a decline between 1990 and 2000 by 11.3%, followed by a noticeable increase from 2000 to 2020 increase of 18.7%. Land covers represented in Lava, mountains, and valley beds have gradually decreased over the periods.

Table 5-6 Land-use/land-cover classification under different classes in study area

Class Name	Area in km² 1990	Percentage (%)	Area in km² 2000	Percentage (%)	Area in km ² 2020	Percentage (%)	Growth- km ²
Lava	2861.85	19.91	2861.47	19.90	2838.96	19.75	-22.89
Mountains and hills	8816.68	61.33	8793.43	61.17	8605.53	59.86	-211.15
Built-up areas	86.13	0.60	123.62	0.86	401.63	2.79	315.5
Valleys and Empty lands	2544.19	17.70	2537.88	17.65	2459.18	17.11	-85.01
Agricultural lands	66.82	0.46	59.27	0.41	70.37	0.49	3.55
Total	14375.6	100	14375.6	100	14375.6	100	-

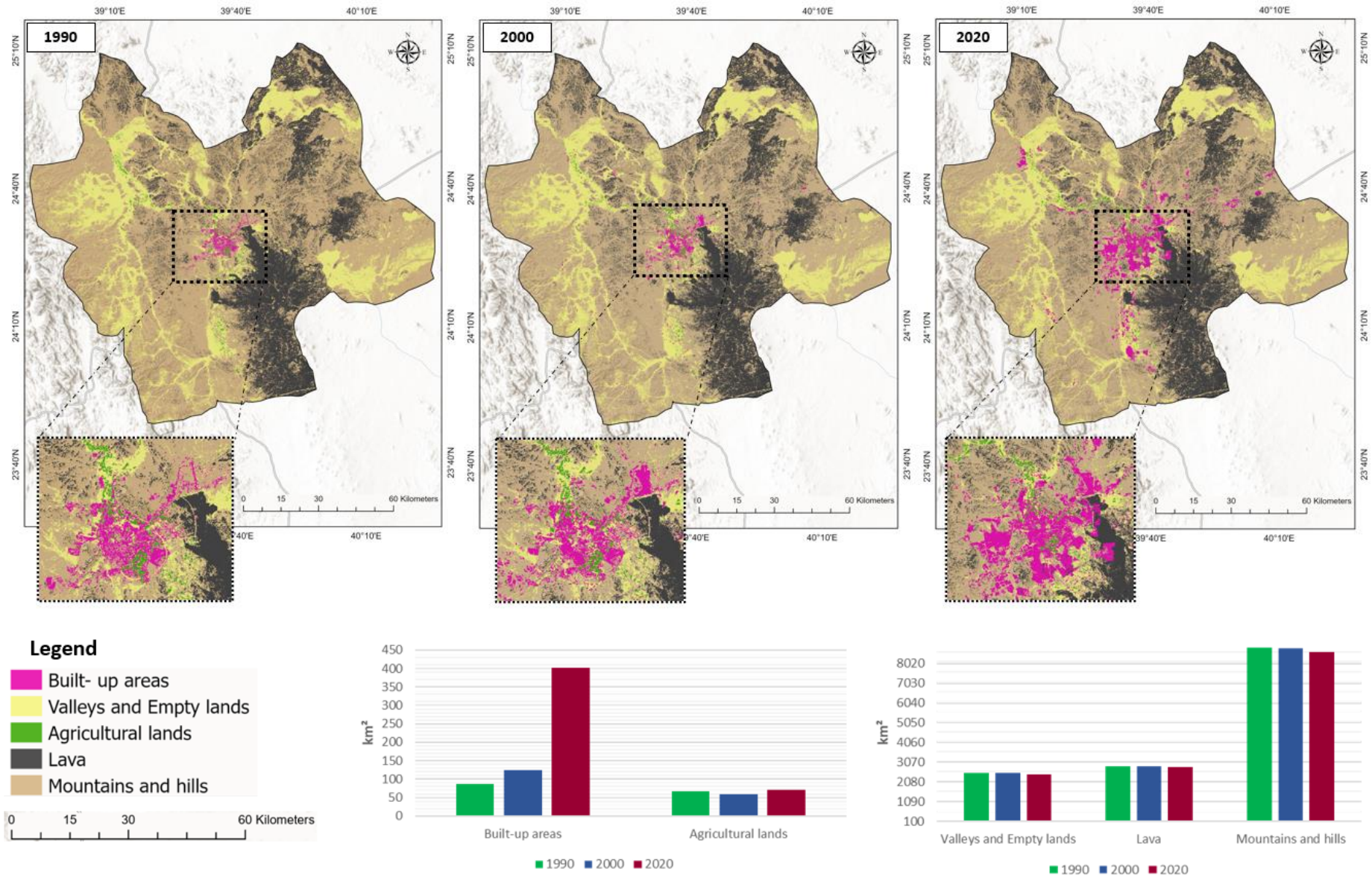

Figure 5-2 The changes in Land Use and Land Cover (LULC) patterns in Al-Madinah City over three decades (1990–2000–2020); the bar chart illustrates the corresponding changes in LULC amounts over time.

5.4 Discussion

The dominant prevailing forms of land cover in Al-Madinah were the mountains and hills class and lava fields, which comprised about 79% of the total area. These physical characteristics restricted the spatial accessibility of some human activities, such as settlement patterns and infrastructure development as well as influenced local land use planning.

The built-up area in this study represents the residential areas, commercial businesses, and industrial zones. There was a substantial increase in the settlement area in Al-Madinah, where the total built-up area was about (86.13 km², 0.60%;) (123.62 km²,0.86%) and (401.63 km², 2.79%) in 1990, 2000, and 2020, respectively. The lack of directly comparable studies addressing land use and land cover (LULC) changes in Al-Madinah city is notable. Thus, the present study presents some possible factors that contributed to these changes.

Al-Madinah Al-Munawara has experienced accelerated urban growth alongside increasing population since the 1970s (UN-HABITAT, 2019a). Urban expansion in Al-Madinah has been affected by several factors. Firstly, areas for urban development are constrained by surrounding mountains as well as the numerous steep valleys that determine the direction of urban growth (UN-HABITAT, 2018). Secondly, the religious importance of the area with annually pilgrimages, Umrah and Ramadan, where the city hosts more 8 million Muslim visitors per year (UN-HABITAT, 2019a). This has led not only to extensive investments in infrastructure but also providing the facilities such as hotels and other development in the commercial area that is surrounds the Prophet Holy Mosque in the city centre (Daqamseh, 2017).

The origin distribution for the built-up area, mainly the residential areas, had mostly grown around the Prophet Holy Mosque and along major roads through 1990. However, by 2000, substantial transformations had occurred, leading to the urban landscape shifting towards peripheral zones, distant from the central city ;these changes were driven by population growth and the implementation of expansion projects associated with the Prophet Holy Mosque (Alharbi, 2018). Consequently, residents who had previously inhabited the central zone were compelled to relocate to other areas within the city (Alharbi, 2018). This urbanization area

continued to increase until 2020, extending to the East, West, and Southwest. Between 1990 and 2020, this urban sprawl had mostly extended into dry valley beds (23.17% of the urban expansion), while nearly half of the total built-up area was established in the moderate terrains.

Furthermore, since 2000, a new group of urban communities developed outside the connected urban district of Al-Madinah in the far northwest, southwest and east. These expanded noticeably by the 2020 classification. According to the Urban Observatory of Al-Madinah and the Ministry Of Municipal And Rural Affairs Amana (2009), these new residential areas will be developed to constitute small cities that follow Al-Madinah administratively; these include Al-Furish, Al-Suwaidra, and Al-Mulaileh, a further three smaller suburbs are Abyar Al-Mashi, Al-Mundasa and Al-Awaina. These cities and villages have been planned for completion by the end of 2030 as part of the local development plan, the Greater Al-Madinah project.

This local development plan mainly aimed to expand the built-up area in Al-Madinah to 745.95 km² by 2030 (UN-HABITAT, 2019a). This indicates that the Urban area of the Al-Madinah area will increase by almost 54% compared to what existed in 2020. This expansion also includes investment lands with an area of 9.43 km², comprising the projects that the government funds for development (UN-HABITAT, 2019a). For instance, the Knowledge Economic City is considered an essential investment that will be constructed on 4.8 km² using an investment size reaching 7 billion US$ and offering around 20,000 new job opportunities (SAGIA, 2019). This would lead to an expansion in the urban areas, which would usually accompany an increase in the population.

In respect of the agricultural lands, these had diminished slightly by 2000 (59.27 km² from 66.82 km²), which is over an 11% drop. This result is in accord with the findings of Li et al. (2023), which indicated that a slight decline in agricultural acreages was noted between 1990 and 2010 in Saudi Arabia. This was attributed to alteration in some agricultural policies related to establishing restrictions on the cultivation of crops that have high water demands such as wheat production (Li et al., 2023). According to UN-HABITAT (2019a) Al-Madinah was estimated to have lost approximately 71.86 km² of vegetated areas between 1985 and 2010. This is equivalent of 2.87 km²/year. This decrease might have been caused by converting some agricultural lands, such as those in the central zone, to residential or commercial purposes (UN-HABITAT, 2019a).

The present study results seem consistent with those reasons, where the lost agricultural lands between 1990 and 2000 shifted into empty or white lands, then showed as built-up areas by 2020. This could be driven by increased urbanization and growing population pressure, often leading to converting agricultural lands into urban spaces or transforming into more lucrative urban uses. These lands have shown a slight increase by 2020. However, it is planned that cultivation lands should increase to around 91 km² by 2030, an increase of nearly 30% (UN-HABITAT, 2019a). Moreover, zones of potential arable lands and agricultural development areas have been proposed, which will account for 839 km² and 866 km² by 2030, respectively (UN-HABITAT, 2019a). These areas might have been identified as capable of supporting agriculture practices, often associated with factors of soil fertility, irrigation water resources, and climate suitableness for specific crops. These places are located towards the north and northwest, as well as the eastern regions of Al-Madinah city, which is confined between volcanic surfaces. The restriction of non-agricultural or urban development within these zones has been implemented to preserve these suitable zones for agricultural purposes. These actions are due to the agriculture sector playing a vital role in the local economy of Al-Madinah.

Generally, the agricultural land expansion developed towards the valley floor, comprising 24.58% of the expansion. Expansion on to moderate elevations accounted for 10.51% of the total agricultural area from 1900 to 2020. A considerable proportion of the farmlands are spread along the main valleys, such as Al-Hmad in the north and northwest, as well as Wadi Al-Aqiq in the south. This is due to the fertility of the alluvial soil within and around the valley. Furthermore, the distribution of agriculture areas coincided with groundwater well locations that are viewed as the primary source of irrigation water in and around Al-Madinah city.

Although the remote sensing data provided good information on land use and land cover in arid regions such as Al-Madinah, the limited availability of historical data or related studies in the literature could make it challenging to evaluate long-term trends of land use changes comprehensively. However, interpreting the possible reasons behind the LULC changes in the study area would help understand some urban expansion drivers, allowing for a more robust and comprehensive analysis of LULC dynamics in the future.

5.5 Conclusion

The application of the Random Forest classification in this study has extracted the LULC maps with good accuracy, which provided valuable insights into the dynamics of land use and land cover in an arid region such as Al-Madinah city over three decades. The dominant land cover classes were the mountains, moderately elevated terrains, and lava fields. These topographical features were crucial in shaping and influencing urban growth trends in the study area. The urban area demonstrated substantial and consistent expansion that outpaced the agricultural land growth. The observed fluctuation in agriculture might be driven not only by urban sprawl but also by the interplay with other factors, such as the impact of climatic conditions, which needs further investigation.

Analysing and interpreting the resultant LULC maps contributed not only to constructing the IPUAT model by extracting the data of built-up and agricultural lands but also to lay the groundwork for predicting future land cover dynamics. Understanding the past and present state of urban expansion and agricultural practices enables the extrapolation of trends, assisting in predicting potential changes. This proactive approach provides policymakers and stakeholders with essential information for formulating adaptive strategies and ensuring sustainable land use practices in the face of future evolving environmental and societal conditions in arid regions. Finally, this study would contribute to the existing body of knowledge by addressing a gap that reveals the absence of studies focusing on Land Use and Land Cover (LULC) changes within the Greater Al-Madinah project.

The good accuracy of the classified maps (1990, 2000, 2020) allowed us to understand the past and present state of land use and land cover changes focusing on urban expansion and agricultural practices, enabling the extrapolation of trends over three decades. This also achieved one of the main aims of this chapter, which represented enhancing the temporal resolution and providing the missing data needed for developing and analysing the IPUAT model in Chapter 6, where the data related to the built-up areas and agricultural lands was needed.

Chapter 6 Analysis of future water demands in Al-Madinah City (1990-2030) based on the modified IPAT model and the socio-economic scenarios.

Abstract

Arid regions such as Saudi Arabia are facing water scarcity and availability issues and experiencing growing pressure by rapid water consumption. Determining the main driving forces contributing to rising water demands and future water demand prediction are considered the cornerstone for developing a good sustainable management plan. Al-Madinah city was chosen as a case study. In this study, the population, affluence, and technology (IPAT) model has been modified to apply in the water sector to analyse water needs in Al-Madinah from 1990 to 2020 and examines factors including population, GDP-per capita, agricultural lands/GDP and built-up area/agricultural lands. In addition, socio-economic scenarios (SSPs) have been developed to predict water demands in Al-Madinah from 2020 to 2030. The results confirm that population was the most important in explaining water consumption trends. Moreover, water demand under all IPCC_SSP scenarios is expected to increase by between 17% to 28%. The scenarios of SSP3 and SSP4 are projected to experience an increase in water demands by an average of 25% and 26%, respectively. In contrast, the water demand is forecasted to be smaller under the SSP1 and SSP5 by around 20% and 17%, respectively. This evaluation could highly reinforce and improve sustainable water resource management strategies, which have recently become increasingly essential to face growing water challenges and demands.

6.1 Introduction

The accelerated development of global economies as well as the steady increase in urbanization rate and the population residing in cities have led to rapid increase in water consumption and caused a negative effect on the extent of water availability and quality (Liang et al., 2020 ; Zhao et al., 2014). Globally, the urban population grew from 29.6% in 1950 to 56.2% in 2020, which also is predicted to approach 68.4% by 2050, with above one billion residents living in cities suffering from water shortage (He et al., 2021 ; McDonald et al., 2011).

The city of Al-Madinah is the fourth largest urban agglomerations, by population, in the Kingdom of Saudi Arabia (UN-HABITAT, 2019a), with a population of 1.278 million and a population density of around 5000 km² (UN-HABITAT, 2019a, 2018). The population growth rate in 2016 was nearly 4.5% (UN-HABITAT, 2019a, 2018). In addition, its religious importance in the Islamic world, means that many religious occasions occur annually, including the pilgrimages, Umrah and Ramadan, where it hosts over 8 million visitors per year (UN-HABITAT, 2019a). These put additional stress on natural water resources.

Water resources are considered scarce not only in Al-Madinah city but also in the whole of the Kingdom of Saudi Arabia (KSA). KSA is deemed to be one of the largest dry areas in the Middle East, with scant rainfall (Al-Ibrahim, 1991). It is devoid of permanent watercourses and freshwater sources such as rivers and lakes (Al-Ibrahim, 1991 ; Amin et al., 2016). This highly causes the challenges of current water deficiency and meeting growing water demand in the future. Consequently, seawater desalination and groundwater exploitation are the main solutions for water supply in many large cities and in arid countries, such as Al-Madinah (He et al., 2021). However, the desalination process is costly, energy intensive and may have impacts on the marine environment (Almutaz et al., 2012 ; He et al., 2021). The overexploitation of groundwater could lead to depletion and deterioration of water quality (El Maghraby, 2014b).

Therefore, sustainable management to mitigate such pressure is considered the best solution to avoid any potential future water demand issues or scarcity problems (Cosgrove and Loucks, 2015). This requires an understanding of future water demand in cities under changing demographic and socio-economic factors (Johannsen et al., 2016). This is critical to establishing adequate planning and improving water conservation measures (Babel et al., 2006). Moreover, identifying such factors contributing to increasing water demands or those causing supply-demand imbalances is considered the cornerstone for sustainable management plan.

Accordingly, this study aims to understand water demand in Al-Madinah from 1990 to 2030 in the light of the city's future development plans, by identifying the fundamental driving forces and the most influential factors in water consumption. The IPAT model was adapted to facilitate predicting future water consumption trends under various demographic, economic and technological assumptions and predicting future water demands under the IPCC's_SSP scenarios.

We believe this to be the first use of the IPAT model in Saudi Arabia to predict the water demand in a major city, such as Al-Madinah. Additionally, the IPAT model has rarely been applied to the water demand domain, and this study would contribute to enriching the water research discipline.

6.2 Methodology

6.2.1 The IPAT model

the IPAT model or extended forms such as STIRPAT and Kaya have been widely used to measure human activities' environmental effects related to growth in carbon dioxide emissions, as well as to determine driving factors. The IPAT model was suggested by Ehrlich and Holdren (1971) for studying the relationship between environmental resources and economic growth (Ehrlich and Holdren, 1971). It seeks to understand the environmental impacts (I) (Ehrlich and Holdren, 1971) by changes in population (P), affluence (per capita GDP) (A), and technology (T) (Vélez-Henao et al., 2019; Jin et al., 2016).

$$I = P \times A \times T \qquad (1)$$

Waggoner and Ausubel in 2002 developed the IPAT identity as the ImPACT model by dividing the T factor into consumption per unit of GDP (C) and impact per unit of consumption (T) (York et al., 2003). The ImPACT model has targeted identifying the factors that could be changed to reduce impacts and the fundamental factors that affect each factor (York et al., 2003). The IPAT model has strength in defining the principal forces that influence environmental changes and showing their relationships, which are often interconnected and cannot operate individually in determining or accounting for environmental impacts (York et al., 2003 ; Uddin et al., 2016).

The IPAT formula assumes linearity between variables, which are often not linear relationships among them (Uddin et al., 2016 ; Vélez-Henao et al., 2019). Therefore, the IPAT model has been reformulated by Dietz and Rosa in 1997 (Vélez-Henao et al., 2019), and is named the STIRPAT that refer to STochastic Impacts by Regression on Population, Affluence, and Technology (Liang et al., 2020). STIRPAT is characterized by treating the links among drivers of impacts as hypotheses that could be tested rather than assume the causal relationship between them as well as to estimate the weights or importance of the factors econometrically (Vélez-Henao et al.,

2019 ; Aguir Bargaoui et al., 2014). Both of Liang et al. (2020); Jin et al. (2016); Uddin et al. (2016) have displayed that the reformalised model as follows:

$$Ii = aP_i^b A_i^c T_i^d e_i \quad (2)$$

Where: (P) population, affluence (A) and technology (T) as drivers of environment change (I); b, c, d = the exponents of P, A, T; e = the error term; i= individual observations in the study and a = The constant of the model. The logarithmic form of STIRPAT form is expressed as:

$$ln(I_i) = a + bln(P_i) + cln(A_i) + dln(T_i) + e_i \quad (3)$$

The STIRPAT model is based on the decomposition analysis approach that provides decomposing, combining or modifying the associated influencing factors (Feng, 2017). Therefore, in the present study the water demand issue could be decomposed into its different drivers. The IPAT identity has been modified slightly in the present study to be I=PAUT, where AL/GDP and W/BA represent the T (technology factors), while BA/AL describes the U (urbanisation) factor. The equation of the adapted IPAT or STIRPAT model for the present study is expressed as follows:

$$W = P * \frac{GDP}{P} * \frac{\mathrm{AL}}{GDP} * \frac{\mathrm{BA}}{\mathrm{AL}} * \frac{\mathrm{W}}{\mathrm{BA}} \quad (4)$$

Where P represents the population; GDP/P is Gross domestic product per capita; AL/GDP is the productivity of agricultural lands (AL); W/BA is the water intensity of built-up areas (W = water consumption and BA= built-up areas), and BA/AL is the ratio between built-up areas and agricultural land.

Water intensity of built-up areas (W/BA) represents the amount of water consumed per unit of built-up area. It directly links water consumption and urban development, also reflecting water use efficiency (or inefficiency) in urban areas. The ratio between built-up areas and agricultural land (BA/AL) allows for assessing the spatial relationship between urbanization (built-up areas) and agricultural land that can significantly alter water demand and availability. A higher ratio, for example, suggests increased urbanization, leading to higher water demand. By including , AL/GDP

, the model accounts for how efficiently and technologically advanced the land is used for agricultural production and how this efficiency impacts water consumption.

In the modified IPAT, one factor needs to be removed to run the regressions and to avoid the result being zero. The missing factor has been determined based on the residuals and examined the p-values of variables of coefficients of variables in the model. The ratio between water and built-up areas (W/BA) negatively affected the model with a Durbin-Watson d-statistic value of about .83 and chi is 3.44; thus, it has been excluded.

The linear logarithmic of IPAT or STIRPAT of the present study is expressed as follows:

$$In(W) = In(P) + In\left(\frac{GDP}{P}\right) + In\left(\frac{AL}{GDP}\right) + In\left(\frac{BA}{AL}\right) \qquad (5)$$

6.2.2 Ordinary least squares (OLS)

Several statistical models have been used in order to develop water demand future scenarios efficiently, whether they have applied individually or combined with further models such as time series approach. The regression analysis is the most commonly employed for linear forecast functions (Wang et al., 2017b).The multiple regression equation takes the form:

$$\mathrm{Y} = \mathrm{B}_0 + \mathrm{B}_1\mathcal{X}_1 + \mathrm{B}_2\mathcal{X}_2 + \epsilon_, \qquad (6)$$

Where: Y= dependent variable; $B_{0=}$ intercept; X= independent variables, and ε= random error with Eε= 0

Ordinary least squares (OLS) have been applied to conduct a regression analysis of the IPAT model, with examined the VIFs, Durbin Watson and Normality as well as multicollinearity and autocorrelation to employ the model in scenarios accurately. OLS has been implemented on time series water demand data in Al-Madinah City (1990-2020). Autocorrelation refers to correlation among the variables in two successive time intervals (Jin et al., 2016). Data unaffected by autocorrelation is considered one of the critical assumptions of regression analysis to avoid misleading predictions. This issue could be present in the time series. Outliers' observations could also significantly affect the model's coefficients, which often detected by examining residuals' graph of the OLS. Accordingly, the inclusion of a lagged value or dummy variable or standardizing

the values has been suggested to reduce such issues. Generally, the dummy variable in the quantitative analysis could be defined as a numeric substitute for a qualitative statement or a logical proposition, taking on values of either 1 or 0 (Garavaglia and Sharma, 1998).

6.2.3 Partial least squares regression (PLS-R)

Multicollinearity refers to correlation between two or more predictor variables; it is usually caused by using the same information in two or more predictor variables (Adnan et al., 2006 ; Jin et al., 2016). This problem could produce errors in the model and the parameter estimations, such as increasing the variance in estimations, which in turn influence the regression equation that would be inaccurate in predicting the future (Liang et al., 2020 ; Maitra and Yan, 2008). Various statistical methods have proven their effectiveness in eliminating the problem of multicollinearity among variables, such as Partial Least Squares Regression (PLSR), Ridge Regression (RR) and Principal Component Regression (PCR) (Irfan et al., 2013). Adnan et al. (2006), Maitra and Yan (2008), and Irfan et al. (2013) all have concluded that the PLS-R technique proved more efficient diminishing the multicollinearity issue. Therefore, the present study used the Partial Least Squares Regression (PLSR) to address the multicollinearity problem.

Partial least squares regression is a robust multivariate regression approach that provides a wide variety of analyses (Fang et al., 2015), which also is effective in eliminating multicollinearity by assuming dependency between the variables. The fundamental idea of PLSR is to maximize the covariance between X and y and compression of X into a few components (Ergon, 2005); the X and y data are generated by a few latent variables and formation its structures, as well as the maximizing covariance between extracted factors being by decomposing the matrices of x and y are into latent structures in an iterative process (Shawul et al., 2019 ; Fang et al., 2015). The decomposition carried out by PLS-R can be expressed as:

$$\begin{aligned} x &= t_1 P_1^T + t_2 P_2^T + \text{th}\, p_h^T + e_h \\ y &= U_1 q_1 + u_2 q_2 + u_h q_h + f_h \end{aligned} \qquad (7)$$

where,'' t_i and u_i (i = 1, 2, ...,h) are the latent variables extracted from the sample data of the explanatory variable X and the explained variable y respectively, pi is the loading vector or weights for X, and q_i (i = 1, 2, ...,h) is the loading value or weights for y, and eh and f_h are the residual vectors''(Chai et al., 2018)(pp219).

Generally, in the PLS-R model, the primary data X and Y, or sampled factors and responses are projected into T and U respectively, which are the latent variables, where the extracted factors T (X-scores) are utilised to predict U (Y-scores) (Tobias, 1996). The t1/t2 oval plot and the t1/u1 scatter plot are viewed as significant outputs that could be examined to establish the appropriateness PLS-R modelling of applying, where the t1/u1 scatter plot will determine the extent of the linear relationship between the variables whereas the t1/t2 oval plot (confidence ellipse) displays the range of homogeneity of the independent variables in the interpretation of the dependent variable, as the occupation of all variables within the boundaries of the ellipse indicates the possibility of reliance on the results of the model (Liang et al., 2020 ; Shawul et al., 2019 ; Li et al., 2015).

In order to implement these models (OLS and PLS-R) the Stata and XLSTAT software packages have been used. Furthermore, the OLS and PLS model projections for water demand in the study area will be compared with the local authority forecast presented by the Saudi National Water Company, which was mainly based on the population growth variable.

6.2.4 The variables' importance in the projection (VIP)

The variables' importance in the projection (VIP) has also been estimated by the PLS-R model, which identifies each explanatory variable's contribution in the projection model; generally, the average of the squared VIP-scores is 1, due to the total of the squares of VIP scores being equivalent for all the variables in X; therefore, if all variables would contribute with the same degree of importance in the produced model, the sum of the VIP would be 1, accordingly; if the value of a variable is more than 0.8, the variable will be considered important and has contributed enormously (Liu et al., 2020 ; Li et al., 2015 ; Mendez et al., 2020), the VIP is expressed as follows:

$$VIP_j = \sqrt{P \sum_{h=1}^{m} {}^{2}_{r_h}(Y; t_h) w_{h_j}^2 / \sum_{h=1}^{m} r_h^2(Y; t_h)} \quad (8)$$

Where p is the number of independent input variables; $w_{h_j}^2$ is the component of the j_{th} variable on the latent variable t_h , which is used to evaluate the marginal contribution of X_j to the construction of t_h latent variable; $r_h^2(Y; t_h)$ indicates the explanatory of all extracted components to Y (Liu et al., 2020 ; Li et al., 2015).

6.3 Materials and Data

6.3.1 The socio-economic development pathways (SSPs) scenarios

The socio-economic development pathways (SSPs) are scenarios for global socioeconomic changes projected until 2100 (IPCC, 2017) ,which have been used to generate greenhouse gas emissions scenarios with multiple climate strategies (Riahi et al., 2017). These SSPs involved the main elements represented in Gross Domestic Product (GDP), population (age, sex, education) and urbanization (Yang and Cui, 2019). Moreover, the SSPs were divided into five pathways or five storylines that consist of (SSP1) sustainability, (SSP2) middle of the road, (SSP3) fragmentation, (SSP4) inequality, and (SSP5) fossil-fuelled development, as shown in Table 6-1 (Chen et al., 2020 ; Riahi et al., 2017 ; Yang and Cui, 2019).

Table 6-1. The storylines of SSPs pathways scenarios

SSP element	Pathway Scenarios
SSP1	Is a sustainability pathway with diminishing the intensity and fossil fuel dependence and accelerated technology development with high investment. The population growth relatively low, and there is rapid urbanization, and land-use change is strongly regulated.
SSP2	Is Middle of the Road pathway with diminishing resource and energy intensity and gradually decreasing fossil fuel dependency. Technological development proceeds apace. The population growth is moderate, and per-capita income levels develop at a medium pace on the global average. The land-use change is in medium regulation with a continuation of historical patterns, including the slow decline in the rate of deforestation.

SSP element	Pathway Scenarios
SSP3	Is Fragmentation pathway that the world is separated into regions characterized by extreme poverty, moderate wealth in some countries whereas a bulk of countries struggle to maintain living standards where economic development is slow. The growth of resource intensity and fossil fuel dependency. There are low investments in technology development and education, which causes slow down economic increase. Population growth in this scenario is high in developing countries and low in industrialized. Inadequate regulation in land-use changes and continued deforestation, whereas the urbanization, follows the slow pathway due to slow economic growth.
SSP4	Is inequality pathway with highly unbalanced investments in human capital where the economic growth is moderate in industrialized and middle-income countries, while low-income countries default behind. The advancement of technology is high in the high-tech economy. Population growth is low in developed countries and relatively high in other countries. The moderate speed in urbanization expansion and the high-income countries will follow a central urbanization pathway. Land-use change is strongly regulated in high-income countries.
SSP5	Is fossil-fuel development pathway with energy demand is high, and most of this demand is satisfied with carbon-based fuels. Moreover, the accelerated technological progress and development of human capital, as well as the economic development is relatively rapid with slower population growth, leading to a less vulnerable world better able to adapt to climate impacts. In addition, the fast urbanization patterns occur in all countries under this scenario, while the land-use change is medium regulated with a slow decline in the rate of deforestation.

*Adapted from (O'Neill et al., 2017 ; Yang and Cui, 2019 ; Riahi et al., 2017 ; Abt et al., 2019 ; O'Neill et al., 2013 ; Van der Mensbrugghe, 2015)

The process of developing a scenarios model for the water demand requires preparing multiple data that is an effect on the accuracy of predictions results including Gross domestic product (GDP), population, Land Use/Land Cover, the productivity of agricultural lands (AL/GDP), the water intensity of built-up areas (W/BA) and the ratio between urban and agricultural land (BA/AL).

6.3.2 Population in Al-Madinah

The City of Al-Madinah is considered to be the fourth in terms of urban agglomeration and population size in the Kingdom of Saudi Arabia (UN-HABITAT, 2019a). According to the Saudi Central Department of Statistics and Information GaStat (2010) states that the total population of Al-Madinah was around 1,183,000 in 2010 and was counted by about 1,489,000 in 2020, with an average yearly increase of around 2.1%. In addition, Al-Madinah City experienced a notable growth rate of about 2.90% between 2004 and 2014, which also increased to 4.5% in 2016 with a population density of around 5000 persons per square kilometre (UN-HABITAT, 2019a, 2018). Al-Madinah is also expected to reach approximately 2,064,000 in 2030, as shown in Figure 6-1 , as a permanent residential population where an average annual growth rate over the period from 2020 to 2030 will reach about 6.5%, with almost 12 million visitors annually by 2040 (UN-HABITAT, 2019a).

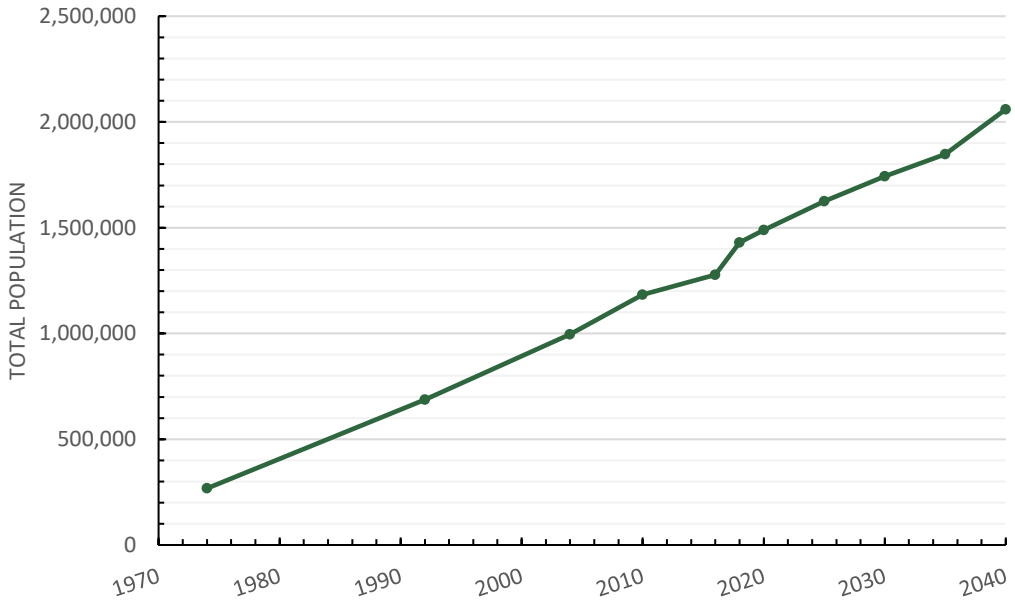

Source: GaStat (1974, 1992, 2004, 2010) and the population projections from (MOMRA,2019) and (UN, 2018)

Figure 6-1. Population in Al- Madinah city 1974-2040

Future projections of the Al-Madinah population (2020-2030) were unavailable under SSPs scenarios. Therefore, firstly, the relationship between the United Nations historical population data (1990-2019) and the country-scale SSPs data was established. A correlation of .98 was

obtained for the relationship, which indicates that the UN population data for Saudi Arabia would also represent Al-Madinah well. Secondly, to simulate SSPs scenarios of the population for Al-Madinah, the growth rate calculated between each scenario in the SSPs for Saudi Arabia was used to apply to the UN population projections data for the city to obtain the scenarios.

6.3.3 Gross domestic product (GDP)

The historical data and future GDP projections on the cities scale in Saudi Arabia are not available. The GDP and GDP per-capita data is available at the country level in Saudi Arabia rather than city scale ; therefore, such data has been taken into account in the present study, especially there are no substantial differences among Saudi cities in GDP per-capita. This could return to there are attempts to creating a more balanced develop economically and geographically between all Saudi cities (UN-Habitat, 2019b).

Estimating historical and future GDP for Al-Madinah city involved understanding the relationship between GDP and population. Thus, for the historical period (1990-2020), the GDP Per Capita data of country scale has been used to extract the total GDP for Al-Madinah city by multiplying the GDP_PC with the population numbers that were recorded in the official census. In the same approach, the future GDP (2021-2030) have been calculated by multiplying the estimation's GDP_PC of Saudi Arabia, which was developed by the International Institute for Applied Systems Analysis (IIASA) and is included under the SSPs scenarios database, with the population' of Al-Madinah that has been projected by United Nation.In terms of the future GDP projections, in Al-Madinah under the Shared Socioeconomic Pathways (SSPs) have indicated that the GDP will experience an increase after 2025 to 2030 under SSP 5 with a slight increase under SSP1 and SSP2 scenario whereas the GDP is predicted to be stable under SSP3 and SSP4, as shown in Figure 6-2.

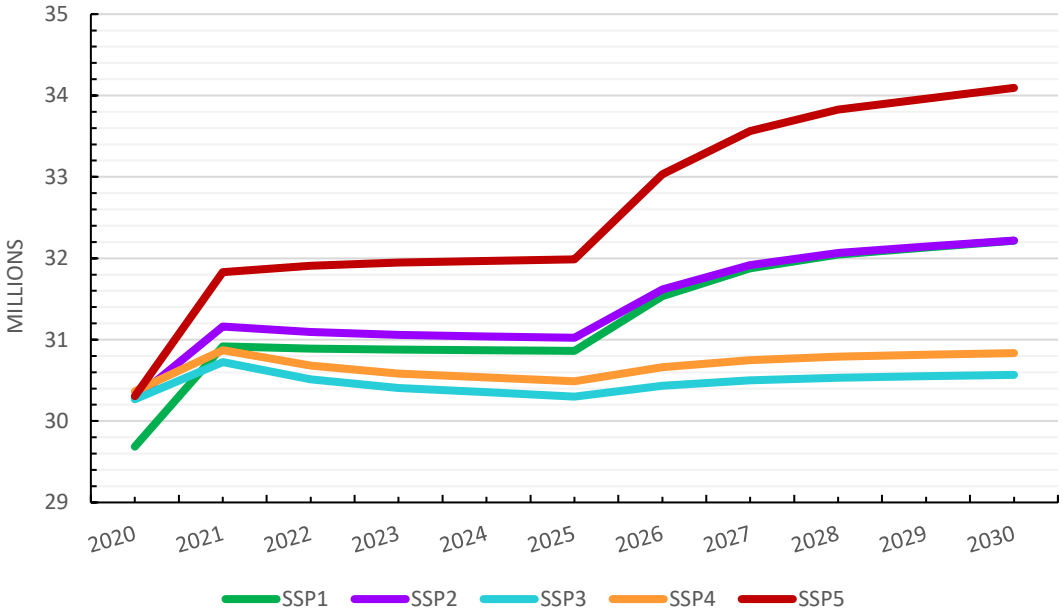

Figure 6-2. The future GDP projections under SSPs in Al-Madinah (2020-2030)

The present study used the population and GDP PC from the socio-economic determinants that have followed the five scenarios as showing in the Table 6-2 describes the population and GDP_PC variables under SSPs scenarios. The other factors' data were obtained for the same period from the relevant ministries in the Kingdom of Saudi Arabia, as listed in Table 6-3; all missing data then has been processed by the linear forecasting method to complete all the time.

Table 6-2.The SSPs scenarios descriptions of the Population and Gross domestic product per-capita (GDP_PC) variables.

SSP element	Population	Growth (GDP per capita)
SSP1	Low	Moderate
SSP2	Moderate	Moderate
SSP3	High	Low
SSP4	Moderate	Low
SSP5	Low	High

* Adapted from (O'Neill et al., 2017 ; Yang and Cui, 2019 ; Riahi et al., 2017 ; Abt et al., 2019 ; O'Neill et al., 2013 ; Van der Mensbrugghe, 2015)

Table 6-3. Description of the study variables

The variables	type	Unit of measurement	From – to	Source
dependent variable				
Water Consumption	Historical data	Thousand Cubic Meters	2003-2019	(MWE, 2014, 2013) and (MEWA, 2019)
	projection data		2020-2030	(SWPC, 2019)
independent variables				
Gross domestic product (GDP)	Historical data	USD per capita in current prices	1990	(World Bank, 2016b)
	projection data		1991-2020	(GaStat, 2020)
			2021-2030	(Cuaresma, 2017)
population	Historical data	Number of people	1974,1992, 2004, 2010	(GaStat, 2010)
	projection data		2020-2030	(UN, 2018), (MOMRA,2019)
Land Use/Land Cover (Built-up area, Agricultural lands)	Historical data	Square kilometers	1990, 2000, 2020	Extracted from Landsat images
	projection data		2030	(MOMRA, 2020)

In summary, the present study used the variables of water consumption as the dependent variable, and both population, Gross domestic product (GDP), built-up area and agricultural lands as independent variables, three relations models have been extracted from these variables, which included the relationship between agricultural lands and the GDP to determine the amount of agricultural land contribution, the second model between urban areas and agricultural lands, and the third represented the relationship between water consumption and urban areas.

6.4 The results

6.4.1 Determination of Influencing Factors under IPAUT model

The growth trends, as displayed in Figure 6-3, and using Pearson bivariate correlation analysis of the influencing factors, (see Figure S6-1 in appendix 3). And Table 6-4, the variable water consumption, population and GDP-PC showed steady growth over the years, where water consumption increased around six times and the population growth tripled from the baseline year 1990. Therefore, the correlation coefficients of the water consumption variable with population and GDP per capita are both above 0.9. In addition, the water consumption / urban areas relationship that indicates the extent of water consumption in urban areas appeared to

have changed little across the period. This relationship was weakly correlated with water consumption (P=.14). This relationship indicates water consumption intensity under technological change or advancements to implement water conservation measures or improve water management practices. However, it is expected that Al-Madinah city will have an increase in population and a massive expansion of built-up areas. Therefore, the water intensity of built-up areas (W/BA) decreases could mean that the water consumption within urban areas will not increase proportionally to the extent of urban development or the expansion of built-up areas, caused by, for example, limited investment in water infrastructure.

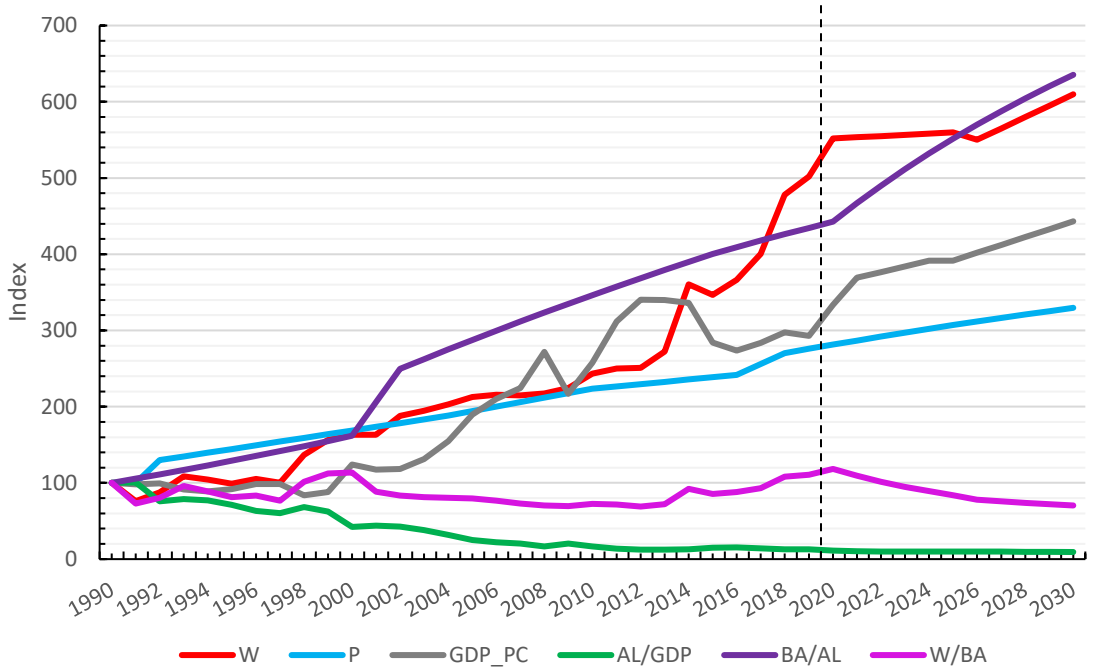

Figure 6-3. The growth trend of the variables and models in Al-Madinah in 1990–2030 (W- water consumption, P - population, GDP PC - Gross domestic product per capita, AL/GDP represent agricultural lands/ GDP, BA/AL represent built-up area/ agricultural lands and W/BA represent water consumption/ built-up area).

The relationship between agricultural lands /GDP measuring the agriculture sector's contribution to the GDP, showed that the economic growth of Al-Madinah is developing faster than agricultural lands, which do not contribute meaningfully to GDP. Thus, water consumption correlated strongly and negatively (-0.78) with the model of agricultural lands / GDP. To clarify, when using the agricultural land to GDP ratio to represent the technology factor (T) in the IPAT model, a low contribution of agricultural land to GDP suggests that agricultural advancements may not keep pace with economic growth, leading to a declining share of agricultural land in GDP. This could also indicate a need for more investment and innovation in agricultural technologies to improve efficiency and reduce water demand, as well as imply that other factors, such as population growth, changes in consumption patterns, or policies, are playing a more significant role in driving water demand.

Table 6-4. The Pearson correlation between variables

Variables	W/BA	W	P	BA/AL	GDP_PC	AL/GDP
W	0.137	**1**	**0.969**	**0.956**	**0.923**	**-0.781**
P	-0.018	**0.969**	**1**	**0.987**	**0.956**	**-0.888**
GDP_PC	-0.133	**0.923**	**0.956**	**0.970**	**1**	**-0.860**
BA/AL	-0.120	**0.956**	**0.987**	**1**	**0.970**	**-0.874**
AL/GDP	0.110	**-0.781**	**-0.888**	**-0.874**	**-0.860**	**1**
W/BA	**1**	0.137	-0.018	-0.120	-0.133	0.110

Values in bold are different from 0 with a significance level alpha=0.05

Furthermore, the relationship between built-up and agricultural lands detected the efficiency aspect of consuming water. Urban areas in Al-Madinah city expanded faster than agricultural areas, with an expectation of that an increase will continue. The BA/AL model showed a significantly positive correlation with water consumption by (P= .95). Overall, water consumption / urban areas rate variable has the weakest correlation with other variables. Water consumption has the highest correlation with the built-up areas/agricultural lands and the population variable, respectively.

6.4.2 Autocorrelation and Multicollinearity Diagnostic

Ordinary least squares (OLS) have applied to conduct a regression analysis of the IPAT model, Table 6-5 displays the OLS regression results. Autocorrelation and multicollinearity have been examined to employ the model in scenarios accurately. Firstly, the examined residuals' graph of the OLS model showed that there are outliers' observations in the dependent values that correspond to 2014, 1993 and 1997, respectively, which could have a significant effect on the model's coefficients. Accordingly, the dummy variable has been included in the independent variables for 2014 data due to being the most irregular year among serial data. Moreover, the Durbin-Watson statistic is used to test for autocorrelation degree. The estimated regression equation is considered free of autocorrelation if the DW value is close to 2, while the value close to 4 indicates a positive autocorrelation, in contrast, a DW value nearby to zero means a negative autocorrelation (Razak et al., 2013). The DW value of the present model is .986, which indicates the existence of positive autocorrelation that needs to be improved. Consequently, a Lag variable (Lag_W) of the dependent variable water consumption (W) by one slow period for one year (1990), has been placed within the independent variables, as well as creating one column for dummy data represent the year 2014, which was the most irregular year among serial data. The result showed a satisfactory DW value of 1.93 through an examination of the autocorrelation of variables.

Secondly, Selecting the appropriate regression analysis approach is usually based on measuring and determining the multicollinearity among all variables (Ma et al., 2017). The variance inflation factor (VIF) is considered as the common technique to estimate multicollinearity where values more than 10 indicates to existing critical multicollinearity among the independent variables, which often means the ordinary least squares (OLS) regression is not an accurate approach for analysing such data because it will not reflect the actual relationship among factors and its coefficients could be not reliable (Ma et al., 2017 ; Uddin et al., 2016 ; Li et al., 2015) . VIF values, as shown in VIF values, as shown in Table 6-5, indicate a high level of collinearity between most of the independent variables, especially those related to GDP_PC and agricultural lands/ GDP_PC factors. Therefore, Partial least squares (PLS) regression is considered one of the most efficacious approaches that have been applied to avoid the multicollinearity problems (Liang et al., 2020 ; Li

et al., 2015). As shown in the Figure 6-4 of t1/u1 scatter plot, the PLS results presented that the relationship was almost linear, indicating such findings could be accepted for addressing issues such as water consumption (Li et al., 2015).

Moreover, the correlation between t1/t2 as displayed in Figure 6-5, revealed that the variables used have distributed within the oval plot where no points were outside the shape, which evidence that the PLS results were consistent and reliable utilising. Accordingly, the regression equation that extracted using the partial least squares and could be employed in prediction scenarios.

Table 6-5. OLS Regression results including the VIFs, Durbin Watson and Normality

Model	Unstandardized Coefficients		Standardized Coefficients	t	Sig	Tolerance	VIF
	B	Std. Error	Beta				
Model_OLS							
(Constant)	-11.6270	4.963		-2.34	0.027		
P	3.975	.7602	1.999	5.23	.000	0.013	79.151
GDP_PC	2.591	.616	2.480	4.20	.000	0.005	188.823
AL/GDP	2.990	.7126	4.099	4.20	.000	0.002	516.831
BA/AL	.753	.252	0.703	2.99	0.006	0.033	29.989
Model_OLS_L.W.Dummy							
(Constant)	-11.627	2.892	-11.406	-3.944	0.001		
L.W	0.619	0.106	0.597	5.821	0.0001	0.056	17.906
P	1.996	0.538	0.935	3.713	0.001	0.01	107.912
GDP_PC	0.672	0.429	0.649	1.569	0.13	0.004	291.608
AL/GDP	0.955	0.487	1.284	0.687	0.499	0.002	731.519
BA/AL	0.116	0.169	0.105	1.96	0.062	0.026	39.86
Dummy	0.239	0.075	0.081	3.164	0.004	0.907	1.104
Autocorrelation:	time variable: year, 1990 to 2020 delta: 1 unit						
Durbin Watson-OLS:	.9869556						
Durbin Watson OLS _L.W _dummy:	1.93						
Heteroscedasticiy:	Breusch-Pagan / Cook-Weisberg test for heteroskedasticity Ho: Constant variance Variables: fitted values of W chi2(1) = 4.71 Prob > chi2 = 0.0300						

Skewness / Kurtosis test for noemality				joint	
Variable	Obs	Pr(Skewness)	Pr(Kurtosis)	Adj chi2(2)	Prob>chi2
U	30	0.2202	0.1534	3.82	0.1479

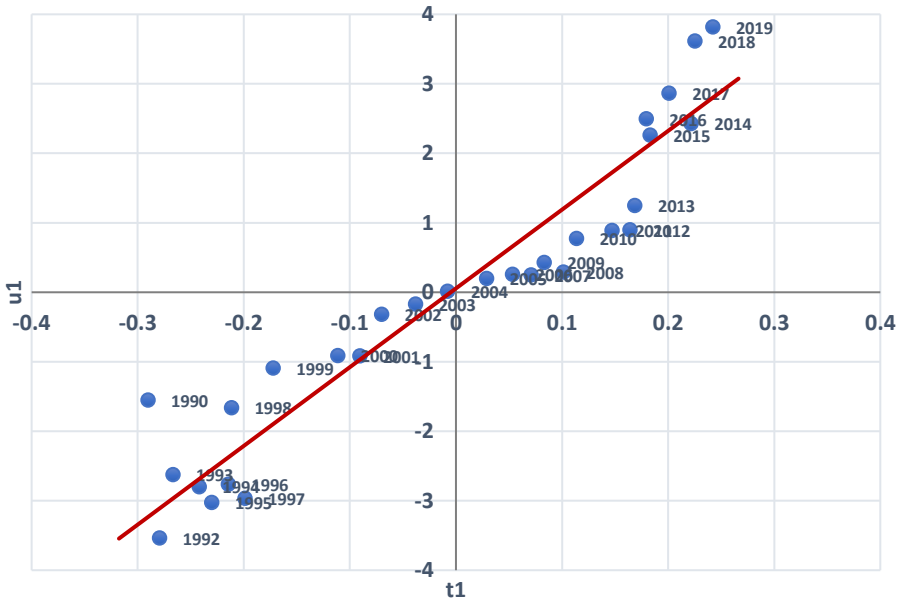

Figure 6-4. Scatter plot *of t1 (x) /u1 (y)*.

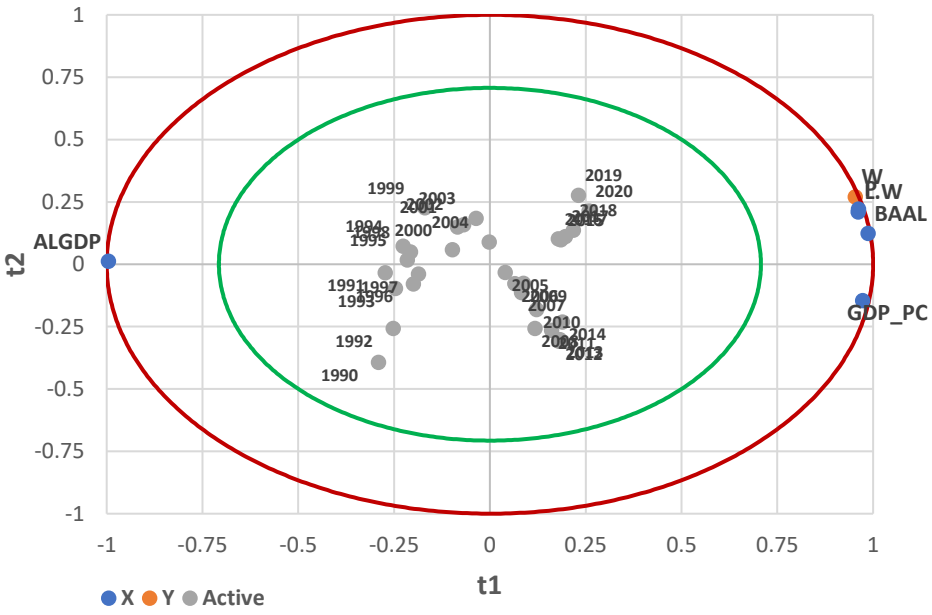

Figure 6-5. t1(x) / t2(y) oval plot. X = predictor variables, Y = dependent variables.

The PLS-R regression revealed that the variable of the Al/GDP has become negatively associated with a low impact. It was also evident from the coefficients in Table 6-6 that the population and the built-up areas/agriculture rate were the essential variables in explaining water consumption trends in Al-Madinah city with VIP more than 0.8 scores. In contrast, the GDP_PC was the lowest variable in interpreting or less important by 1.02 as VIP value.

Table 6-6. PLS Coefficients and Variable Importance in the Projection (VIP)

Variable	Coefficient	Std. deviation	VIP	Standard deviation
Intercept	-2.444	2.863		
P	0.525	0.310	1.102	0.024
GDP_PC	0.031	0.193	1.026	0.02
BA/AL	0.198	0.032	1.098	0.019
AL/GDP	-0.072	0.070	1.077	0.017
R^2	0.944			
Std. deviation	0.137			
MSE	0.017			
RMSE	0.130			
Cumulative Q^2 quality	0.913			

6.4.3 Scenario analysis and prediction of water demand in Al-Madinah

This study attempted to apply SSPs scenarios for water demand in Al-Madinah using two types of regression models represented in OLS and PLS. The water demand will continue to grow by a rate of 11% according to the projection of local authority, as shown in Figure 6-6, whereas the results revealed that all the SSPs scenarios expect that water consumption rate will increase by the total average 17% and 28% under OLS and PLS models respectively, which is considered almost

two times higher than local authority projection, as displayed in Table 6-7 and Figure 6-7 Generally, it can be evidently observed that the predictions of the OLS model were almost closer to the local authority's estimations than the PLS model.

The water demand scenarios in the present study based on that the variables of built-up areas and agricultural lands would be in high growth as have been established by the developments plans of the city 2030 Vision, As discussed in Chapter 5, whereas the determinants of population and GDP will be changed according to the SSPs predictions.

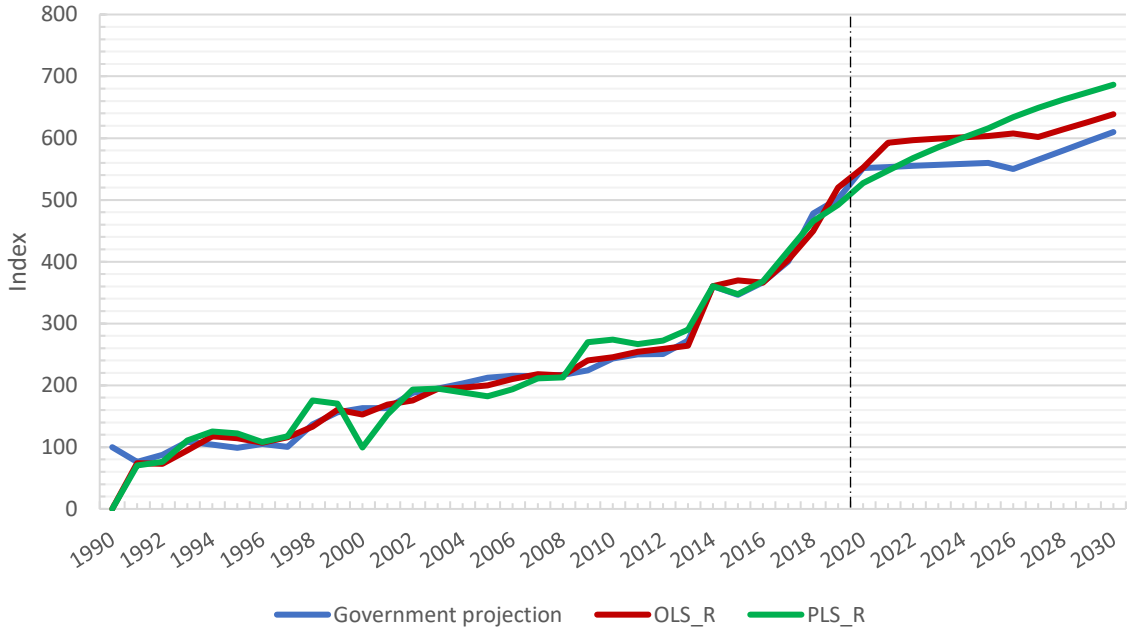

Figure 6-6. The water consumption scenarios in Al-Madinah under OLS and PLS regression

Table 6-7. The water consumption in Al-Madinah under SSPs scenarios

Water demand	Government projection	OLS _R	PLS_R
	11%		
SSP1		16%	24%
SSP2		18%	29%
SSP3		19%	31%
SSP4		20%	32%
SSP5		13%	21%

The SSP1 represent assumptions of low population and moderate GDP that will lead to growth in water demand for Al-Madinah of 16% and 24% under OLS and PLS models, respectively. The SSP2 will experience a moderate increase in population and GDP, leading to a rise in the

water demand of 18% and 29% under OLS and PLS models, respectively. Furthermore, SSP3 (high population growth, lower GDP) and SSP4 (declining population, high GDP growth) were predicted to present major challenges by raising the water demand by 19% to 20% and 31% to 32%, under the OLS and the PLS models respectively.

The results of the assumptions of low population rates with high GDP that were set in SSP5 for Al-Madinah predicted that the water demand would increase by 13% and 21% in all SSP scenarios, as shown in Figure 6-7.

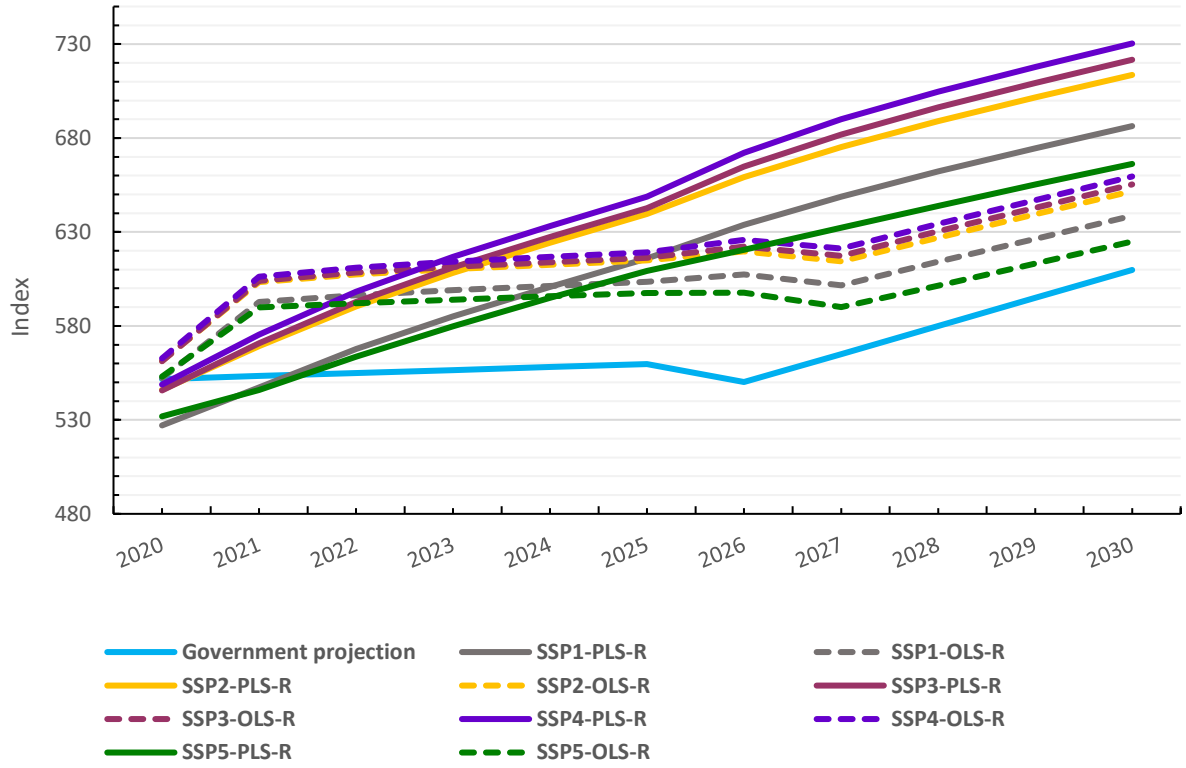

Figure 6-7. The effect of population and GDP changes under SSPs scenarios on water demand in Al-Madinah (2020 -2030)

6.5 Discussion

Water availability and supply-demand imbalances are complex issues affected by various interfered factors represented in the changing socioeconomics, such as the population, urbanisation, GDP per capita, and technological level, as well as climatic factors. Therefore, a deep understanding of water demand requires analysing the water situation under potential driving factors (Zhao et al., 2014) These needs to be examined and analysed by a method that has the capability to quantify such variables' impact as driving forces on water demand.

The IPAT is considered an effective model to examine and extract the driving forces and identify the relationship between them and their impacts (Zhao et al., 2014 ; York et al., 2003). Accordingly, the adapted IPAT model in the present study helped effectively analyse and identify the fundamental driving forces in water demand in Al-Madinah despite the fact that the IPAT model was not designed originally for application in water resources issues. Generally, this finding is consistent with the few previous studies that applied the IPAT model in the water field, such as Quéfélec and Allal (2014) and Jin et al. (2016), who have indicated the IPAT model capability in examining the driving forces to identify their impacts whether under different assumptions or for quantifying water footprint for water demand.

The IPAT model was adapted in the current study to be IPUAT and expanded to include additional factors: agricultural land/GDP and water consumption/built-up area that represent the technology's factors, and built-up area/agricultural land describes the urbanisation factor alongside population and GDP variables. These as well as the standard IPAT variables were found to be influential. All variables used have a VIP value of more than 0.8 scores; hence, no element could be neglected as one of the influence drivers on water demand. The variables' importance in the projection (VIP) based on the IPUAT model has indicated that the population variable had a positive influence, and it was the most essential factor in explaining water demand trends in Al-Madinah city. This finding aligns with the estimate provided by Hanasaki et al. (2012b) that increasing water stress and demand would be driven as a direct result of population growth. It is also predicted that from 2071 to 2100, about 39% and 55% of global residents will experience high stress on water due to population increase (Hanasaki et al., 2012b). In the present study, when the population increases by one per cent, water demand grows by about 0.52% based on the PLS-R coefficient.

Moreover, the effective usage variable of water was measured by the rate between built-up areas and agricultural lands. It is considered the second most influential factor in water consumption. However, it also had a positive effect under the PLS-R coefficient, which indicated that if water consumption for urban area activities increases by 1%, water needs in Al-Madinah will grow by around 0.19% on the efficiency scale. This could be returned to urban expansion in Al-Madinah that shows a faster growth trend than the agricultural areas; hence, a development strategy would be required to reduce such negative situations and manage water consumption sustainably. In contrast, the technology factors, represented by the

agricultural land/GDP rate, had a negative relationship. The Al/GDP coefficient reveals that with every 1 % increase in the technology factor represented in the productivity of agricultural lands (Al/GDP) variable, water demand is expected to decrease by not exceeding about -0.07 %. This minor influence could be attributed to the economic development trend of Al-Madinah, which indicates that the other sectors are improving more rapidly than the agricultural sector that does not contribute meaningfully to GDP. According to the MCCI (2017), about 33% of the total Gross domestic product of Al-Madinah is obtained from the industry sector, while just about 2% is from the agricultural sector.

In addition, both Alcamo et al. (2007) and Li et al. (2017) have found that increasing income and GDP_PC were the more critical influences on increasing the water demands. However, the situation was different in Al-Madinah, where the GDP_PC was the least variable in explaining water needs. The VIP value was around 1.02, and the PLS_R coefficient also showed that every increase of 1 % in GDP_PC will only lead to an addition of about 0.03 % in water demand. This low influence might be caused by the low water prices for municipal and residential use in Saudi Arabia that ranged from 0.10 Halala for consuming 50 cubic meters to 6.00 SAR for 300 cubic meters or more per month. These prices are the equivalent of about 0.019 and 6.00 British Pounds. Recently, these prices have been raised by the National Water Company (NWC) in an attempt to rationalize the growing consumption of water; the prices have become 0.10 Halala for consuming 15 cubic meters or less and 6.00 SAR for 60 cubic meters or more water consumption per month (NWC, 2015 ; MEWA, 2018b). Accordingly, it is possible with these new policies that the GDP will have more impact on water demand in the future.

Furthermore, in reviewing the development plans for Al Madinah under Vision 2030, the current and future status of water demand might be affected by an increase in built-up areas. These will amount to around 745.95 square kilometres with low-density about 28.2 people/ha, which indicates that the urban area in Al- Madinah will increase by almost 54%. Moreover, it has been proposed to increase the cultivation lands by adding about 91.08 km², which would be an approximate 29% increases in 2020. These development plans are accompanied by exaggerated expectations for population numbers, rising to 2,064,000 by the year 2030, an estimated growth rate of 2.9% per year. Therefore, the water demand would be affected given that the Saudi National Water Company expect demand will increase by

11% by 2030. However, this prediction might not reflect the actual needs because population growth for a few years was the only variable considered in the water demand assessment. It also disregards any future land use or agricultural development plans and GDP. On the contrary, the expectation of water demand under models OLS and PLS that included these variables was almost two times higher than the local authority projection by an average of 17% and 28%, respectively.

According to the expectation of The Saudi Water Partnership Company SWPC (2020), the supply deficit might range from 21.3% in 2022 to 24.2% in 2026 under current, and future development capacities of desalination plants, the principal water source . Thus, to satisfy the water shortage by operating the Yanbu 4 desalination plant that is planned enter into force in 2023, with a capacity of up to 450,000 m^3/d. About 70% of its production capacity could cover the city's water needs (SWPC, 2020).

Therefore, as a result of identifying the socioeconomic variables as crucial driving forces of water demand changes (Graham et al., 2018), developing the future water needs scenarios under such factors would assist in the investigation and detection of any potential future challenges. Although the Shared Socioeconomic Pathways (SSPs) have been generated without definite assumptions related to the future of water (Graham et al., 2018), the socioeconomic factors could be adapted to use in the water sector. Thus, population and GDP determinants from SSPs storylines have been applied to produce the water demand scenarios in Al-Madinah. These two factors were selected because the population was the most important factor in directing water demand according to the result of the IPUAT model, whereas the GDP represented the main factor that would be affected by the local authority plan that relied on rationalizing water consumption by raising prices.

The effect of population and GDP changes under SSP scenarios on water demand in Al-Madinah (2020 -2030) showed that the water demand would increase within all scenarios. The water consumption under the SSP3 and SSP4, that experience higher growth in population than GDP are projected to increase using both OLS and PLS models. This result confirms what was also reported by Wada et al. (2016), who predicted that the domestic water withdrawals in Saudi Arabia would experience a continued increase of about 100–200% until 2050 because of population growth. In comparison, this study estimated that an increase in water demand in Al-Madinah will range between (SSP3 =19% to 20%) and (SSP4 = 31% to

32%) by the end of 2030. This outcome is also consistent with that of Mazzoni et al. (2018), who expected that the SSP3 scenario would be characterised by a scarcer water supply in the MENA region caused by not only the dry climate predictions but also the increasing water requirements for the population and irrigation sector by 2050. In the same context, it has been estimated that Saudi Arabia will experience the most substantial deficit level in 2050, which represents about 20% of the total available freshwater, as well as the shortage of water budget in the MENA region mainly caused by anthropogenic drivers more than it is associated with climatic elements (Mazzoni et al., 2018). Graham et al. (2018) also indicated that the expected growing global water demand in 2100 might be generated by slow technological and efficiency progress that may lead to more water withdrawals, which is accompanied in SSP3 by high population growth.

Furthermore, the increase in water needs would be relatively less under the SSP1 and SSP5, which have a higher GDP growth than population growth that might be attributed to the assumptions of enhanced education and employment opportunities for women presumed in these SSPs (Storylines, 2018).This reduction might be caused by developing highly efficient and economic water-saving technologies under SSP1 and SSP5 (Graham et al., 2018 ; Mazzoni et al., 2018). There are similarities between these findings and those described by Mazzoni et al. (2018) that the MENA region's population is expected to decline significantly after 2050 with a high economic development, especially in the SSP1 that also be accompanied by wet climatic conditions contribute to reducing the demand for water for irrigation purposes. Moreover, the percentage of decline in water demand estimated in the study area under SSP1 and SSP5 ranges from an average of 8% to 11% compared to the SSP3 and SSP4 scenarios by 2030. The present result could almost accord with a previous study by Graham et al. (2018), which expected a global decrease in the water withdrawal trend after 2050, estimated at 32% by 2100 under SSP5. This decline might be associated with an improvement in irrigation operations resulting from the technological development in the water sector, mainly because an increase in income has characterised these scenarios (Graham et al., 2018).

In SSP2, the Middle of the Road or Current Trends Continues, the population and GDP growth would be moderate. In Al-Madinah, an increase is expected of around 18% and 29% under OLS and PLS models, respectively. These projected rates are considered in line with the highest growth water demand scenarios SSP3 and SSP4 of the study area. However,

assumptions of the SSP2 scenario represented in the current trends may indicate an increase in water consumption, thus increasing demand and water pressure in many regions globally (Hanasaki et al., 2012b). Therefore, according to this assumption, the study area could also suffer if water consumption continues under current conditions and rates. Generally, SSPs 1 and 5 envision relatively optimistic trajectories for human development, whereas SSPs 3 and 4 outline more pessimistic development trend scenarios (O'Neill et al., 2016). The reduction in water demand observed in Al-Madinah under the SSP5 scenario could be primarily attributed to factors unrelated to climate policies, such as changes in population and economic growth (GDP), which may not necessarily reflect substantial climate mitigation measures emphasis. Mainly, the SSP5 scenario involved a continuous dependence on fossil fuels while implementing only limited climate procedures. Conversely, the SSP1 is featured by robust global collaboration, sustainability-driven practices, and commitment to efficient resource usage.

Overall, water demand is driven not only by the growth in population numbers but also by GDP-PC, agricultural lands, and built-up areas explanation. Consequently, water request predictions under all these changing variables are critical for developing the efficient of future water preservation and resource sustainability, as well as to achieving the proposed vision for Al-Madinah.

The modified IPAT model provided a comprehensive framework incorporating important factors affecting water consumption beyond the traditional population and affluence measures. This approach allowed for a more detailed water demand analysis with the interplay between economic development, agricultural efficiency and urbanization that is essential to manage water resources. However, the IPAT model might have limitations in this study when using "BA/AL" as the urbanization factor. The model may not fully capture scenarios where both built-up area (BA) and agricultural land (AL) increase simultaneously, leading to a substantial increase in water demand. This could return to the IPAT model in its traditional form, assuming a static relationship between population, affluence, technology, and environmental impact. It does not explicitly account for dynamic changes in land use patterns and interrelationships between factors such as simultaneous increases in built-up area (urbanization) and agricultural land and interrelationships between factors. Recognizing this limitation is crucial when using the IPAT model to inform decision-making and consider

multiple factors beyond the model's scope, such as land use planning, water management strategies, and sustainable development goals.

Moreover, the limitations that are represented in limited available data related to some variables of study such as built-up area and agricultural lands where this obstacle has been overcome not only by using statistical methods for predicting the missing values for complete the time series data, but also applied advanced methods in extracting data from satellite images that helped to update LULC maps for the study area. In addition, the lack of GDP data and the SSPs assumptions on the Al-Madinah city scale, where such data is just available on the country scale. Nevertheless, statistical approaches assisted in estimating GDP for Al-Madinah and examining to ensure that the study area was adequately represented. Consequently, all these techniques and methods have done has helped to limit shortcomings and improve simulated data to avoid and minimize uncertainties that could produce when generating scenarios, which might affect in terms of overestimating or miscalculating results. Furthermore, arising such limitations related to data availability in the current study might draw the attention of the local authorities to the necessity of developing statistical data for Al-Madinah as well as updating it periodically and making it available for future research purposes.

6.6 Conclusion

This study shows that the future socio-economic scenarios predict an increase in water demand twice that which is expected by the local authority. Scenarios that assume the growth of population would be higher than growth in the GDP (SSP3 and SSP4) are projected to lead to greater increase in water demands than scenarios where GDP is assumed to increase more quickly than the population (SSP1 and SSP5). This implies that the population factor was the most influential in the increase in water demand in the study area. Predictions indicate higher population growth and increasing demand for residential water use without corresponding GDP growth. Thus, there may be insufficient financial resources to implement the necessary measures to address this increased demand.

These findings have significant implications for developing water management in Al-Madinah. They should be a helpful guide to the interested local authorities in reviewing the measures

taken and management policies options towards reducing the increase in demand for water mitigating any potential adverse effects of the water shortage in the city.

This study also contributes to enriching the water management research field. By applying the modified IPAT model, the methodology presented could assist arid countries to improve water management policies and strategies to face the scarcity of water resources and increased demand in the context of socioeconomic changes. The proposed model could be applied in accordance with the countries' conditions by accommodating any number of extra variables. Further research is needed to evaluate water demand in Saudi Arabia using improved and more comprehensive socioeconomic data including, for example, investigating the current policies pursued of changing water prices and how its effectiveness in diminishing water consumption.

Chapter 7 General discussion and conclusion

Groundwater is considered one of the essential natural resources globally, where it has been estimated that approximately one-third of the world population has become entirely dependent on groundwater as a primary source of fresh water as an alternate for deficiency of surface water as well as meeting demand caused by an increasing population (Rahmati et al., 2018 ; Mogaji and Lim, 2017). In addition, the nature of the groundwater as a hidden resource might have constructed the perception that it is a vulnerable source and has low priority; hence, it may be easily be disregarded from development plans of water resources (Smith et al., 2016). Moreover, according to Jakeman et al. (2016), integrated groundwater management is often associated with many challenges due to requiring multiple substantial dimensions to be considered, such as natural and human settings, interrelating with various disciplines, uncertainty and technical methods available. However, addressing some of these dimensions will contribute to developing sustainable management of groundwater resources, especially in arid and semiarid countries with freshwater scarcity.

This chapter will discuss the main results in light of the thesis objectives and questions. It also highlights the relationships and effects of the developed models on the water resources landscape in arid regions such as Al-Madinah City. This thesis's methodological contributions will also be highlighted, and some suggestions that need more analysis in the future will be identified.

7.1 Research questions and summary of key findings.

The main aims of the present thesis were to develop models in the three dimensions represented in the integration of novel, sophisticated technologies with varied data formats for mapping potential groundwater zones, highlighting the potential implications of climate change and analysing future water demand patterns under socio-economic scenarios. Integrating these aspects in arid regions is required to achieve sustainable water resource management and develop effective strategies that manage the challenges imposed by altering ecological, hydrologic, and socio-economic conditions. The involved relationships could be shown by accurate and detailed groundwater mapping delineating the spatial distribution of aquifers to understand the potential groundwater zones. These maps are

capable of integrating with climate change data under potential future pathways for the concentrations of greenhouse gases (RCP scenarios), allowing projection and conception of how expected climatic variations in moderate (RCP4.5) and high (RCP8.5) scenarios conditions might influence the groundwater distribution zones over time. Water resources are also affected and interrelated with human factors or economic development, which are often measured by GDP and population, which are interlinked with processes, such as urbanisation, agricultural intensification, and industrialisation, all of without any planned mitigation, are likely to lead to increased water consumption and needs. The response to these challenges caused by the interplay of such factors could also be highly different across arid countries, even though they may have climate change challenges. Therefore, this thesis answered the following research questions:

Questions1 and 2: Where are the potential groundwater zones located in Al-Madinah region? and Which factors have the most impact on the determining potential groundwater locations?

These questions have been answered in Chapter 3. The results indicated that under the Fuzzy Gamma 0.97 and logistic regression models, the spatial distribution of very high potential groundwater areas in Al-Madinah is primarily compatible with volcanic lava areas. These areas mainly cover the central and northwestern areas of Al-Madinah province. These areas include stream valleys and the volcanic hills in the south and east of Al-Madinah city, extending north to Khaybar city.

Moreover, the comparison of the two models applied showed some similarities regarding the most important factors in determining the potential zones, including soil units, drainage density, slope aspects and fault density. In contrast, altitude contributed more to the fuzzy logic-frequency ratio model, while TWI_rainfall factors were more important in the logistic regression model. This inconsistent pattern might return to the mechanism of data analysis methods utilised.

Questions 3: How could climate change impact on these potential groundwater zones?

This question has been answered in Chapter 4. The results revealed that the temperature and ET0 variables have demonstrated a consistent increasing trend in the past period, which is predicted to continue in the future. Despite a slight rise in rainfall, estimated at 20.49% or

25mm, with a total of 147mm by the end of the century (2081-2100), along with an increase in water accumulation potential forecasted also between 2081-2100 under RCP8.5, the overall effect on groundwater availability might be insignificant. This is due to the projected temperature increase of approximately 2°C, coupled with higher ET0 levels (Average: 182.47 mm/month; Total: 2189 mm/year) during the same period. These changes in climatic conditions are expected to impact the suitability of potential groundwater zone sites. According to projections, these sites showed more stability and less variability across all future periods under the Fuzzy-Gamma 0.97 model than the logistic regression model that revealed larger changes in the potential zones compared to the baseline period.

Generally, under both models, the greatest gain in potential groundwater zones is expected between 2081-2100 under the RCP8.5 scenarios. Conversely, the most notable losses in suitable areas are predicted during the mid-century period (2061-2080) under the RCP4.5 scenario.

Questions 4: What are the possible effects of population and GDP on water demand?

This question has been answered in Chapter 6. The results confirm that population was the most important factor in explaining water consumption trends, and the GDP had a low influence on water demand in Al-Madinah. Therefore, the scenarios that consider the growth of population to be higher than the GDP (SSP3 and SSP4) are projected to experience a greater increase in water demands than scenarios where GDP develop more than the population (SSP1 and SSP5).

7.2 GIS-Mapping and Geospatial Analysis for Water Resource Management

Mapping potential groundwater zones could help develop the sustainable management of groundwater resources that have become necessary to minimise undesirable consequences such as overuse and groundwater depletion risk. It also lends understanding to where water is available and how it would best be conserved. Moreover, insufficient or absence of information and maps related to the potential groundwater, especially in arid regions, could significantly raise concerns for authorities responsible for water management. Therefore, by developing a methodological framework based on GIS techniques, the water resource mapping in the present study answered the questions related to determining the locations and the factors that most influenced the occurrence of potential groundwater areas. Mapping

water resources would contribute to developing proactive measures to respond to changing climate conditions, reducing the risk of water needs.

Applying suitability models in GIS for water resources typically involves defining modelling and analysis techniques as well as identifying factors influencing potential locations. The reviewed literature revealed that about 21 methods had been applied in mapping groundwater. This multiplicity of approaches might be caused by the expansion of new technologies, such as GIS techniques and RS data, that have facilitated the integration of various data types and easy analysis to develop prediction models and accurately map spatial phenomena (Roy et al., 2019 ; Aouragh et al., 2016). This also allowed the employment and examination of various approaches to produce potential groundwater maps, including multicriteria decision-making, bivariate and multivariate statistics, and data mining/machine learning. Nevertheless, there was no consensus about the most appropriate technique(Chen et al., 2018 ; Arabameri et al., 2019a). In addition, the accuracy of one approach could vary from being highly effective in certain regions to being considered satisfactory in others, such as the frequency ratio method that ranged under from AUC of 68% (in Goyang-si, South Korea) to 90% (in Konya, Turkey) (Lee et al., 2019 ; Ozdemir, 2011a). This disagreement can be attributed to the user's proficiency and experience, the quality and availability of input data, the complexity of the model used and the inherent strengths and limitations of the selected methods.

In the present study, it has been revealed that the integrated Fuzzy Logic-Frequency Ratio method is absent in the groundwater mapping field, although it was successfully used in other fields. This is in contrast to logistic regression that was broadly applied in groundwater mapping. A possible cause for this might be that the Fuzzy Logic method involves many phases and requires defining appropriate membership functions that sometimes need experience, while the logistic regression is characterised by being straightforward in application. The findings revealed the high prediction capability of the hybrid method of Fuzzy logic and Frequency ratio in identifying potential groundwater zones. This result supports previous studies into enhancing prediction accuracy by applying combined models. The combined approach often helps to diminish the overall error in predictions or the generalization error, which implies the prediction would be more accurate (Kotu and Deshpande, 2018). This finding is consistent with that of Razavi-Termeh et al. (2019); Naghibi et al. (2017a) and Miraki

et al. (2018) , who confirmed the ensemble methods could improve the effectiveness of the model's projections.

Selecting influential factors for mapping groundwater, whether within geographic information systems (GIS) or spatial analysis models, generally involves identifying and considering a range of relevant factors. Reviewing the literature is crucial for identifying these factors; it provides a broad understanding of various factors contributing to groundwater dynamics. Therefore, eleven influential criteria on potential groundwater occurrence in the study area have been selected, which were soil types, fault density, lithology categories, rainfall, Topographic Wetness Index (TWI), stream power index (SPI), drainage density, slope degree, slope aspect, plan curvature and altitude.

The present study determined these factors because geological formation, topography factors, and hydrological characteristics are generally considered more influential on groundwater dynamics. Geological formation dictates the subsurface properties crucial for groundwater storage and water transmission. Simultaneously, topography controls surface water flow, accumulation, and recharge sites that capture and direct limited precipitation in arid regions into the ground. Hydrological conditions comprise a broader understanding of surface runoff and water movement. However, certain influential factors prominently featured in the literature, such as Land Use and Land Cover (LULC), might not inherently perform as direct determinants of groundwater formation and may have limitations in their applicability. Therefore, testing the impact of LULC on the prediction models' accuracy before they are included would be important. The testing of the LULC factor showed a high relation with groundwater potential sites that were mostly within the current built-up zone because most of the groundwater wells used in the model are located in urban areas. This could negatively impact the prediction model by excluding or neglecting areas with a high probability of groundwater formations located out of urban areas, which could have a high possibility of promising new agricultural lands and residential areas due to potential groundwater availability. Accordingly, the LULC was excluded from this study.

Furthermore, the study area is generally characterised by low rainfall, where the annual average does not exceed 122 mm/y and is primarily concentrated in the highlands, which are considered not appropriate areas physically for groundwater formation and could also negatively affect prediction models. Therefore, the topographic wetness index (TWI) was

weighted by the precipitation variable to be more helpful in defining areas where water could accumulate based on the rainfall amount that is the primary recharging source. Employing the TWI-Rainfall factor is considered novel in mapping groundwater.

Although it has been found that the two models applied in this study had similarities in the most important factors: soil type, fault density, drainage density and slope aspect, and they differed in the factors of (altitudes contributing to the Fuzzy-Frequency ratio model) and (TWI-Rainfall contributing to the logistic regression model), the geographic analysis of the topographic gradients of Al-Madinah has shown a great influence not only on the spatial layout of urban areas and settlement patterns but also the distribution of groundwater possibility zones. Accordingly, the very high potential zones mostly occupied the valley beds and lava covers with low altitudes and terrain, with the near-zero aspect of flat areas, which hydrologically increases the opportunity for the water table to be closer to the surface when drilling wells for groundwater extraction. These areas were also categorized with more appropriate conditions to accumulate water and improve replenishment and groundwater recharge (Al-Abadi et al., 2016 ; Mahmoud and Alazba, 2016b).They could also influence the amount of solar radiation, evaporation, and soil moisture or water content, thus; groundwater recharging capacities (Elnaker and Zaleski, 2021).

7.3 Climate-Driven Water Challenges and Shaping Future Water Demand Scenarios

Based on the outcomes of the modelling under both methods, Al-Madinah would have limited availability of suitable areas for establishing groundwater wells, which might be affected not only by the geological, hydrological, and topographic complexities of the area but also by the potential ramifications of climate change and the impacts of human activities.

In recent decades, climate change has obviously affected surface and groundwater resources globally (Green, 2016). The expected changes in the frequency and intensity of precipitation, temperature and ET0 would have consequences on water resources in arid-semi arid regions, which could present, for example, according to Abderrahman and Al-Harazin, (2008) as cited in Alsarhan et al. (2016) ; Tarawneh and Chowdhury (2018) estimated that the surface runoff in Saudi Arabia could reduce by 115 to to184 MCM/ year with an increase in temperature by

one-degree Celsius and increase ET0 of 2.3%; this diminishing runoff could be as large as 600-960 MCM /year if temperature increased to five-degree Celsius and an ET0 to 12%. They also estimated the consequences on recharge groundwater aquifers, where the potential of recharge water losses might reach about 91.4 MCM/year (an increase of 1˚C, and ET0 about 2.3%), and 475 MCM/ year (an increase of 5 ˚C, ET0 about 12%) (Alsarhan et al., 2016 ; Tarawneh and Chowdhury, 2018).

In Al-Madinah, although the end-century 2081-2100 under RCP8.5 will experience a slight increase in rainfall of 1.73% (1.5 mm) and higher accumulation opportunity compared to other periods, such an increase might not have a pronounced effect on enhancing the availability of groundwater and surface water due to raising the temperature that is projected to be around two degrees celsius in the most months with an average ET0 about 182.47 mm/month (Total: 2189 mm/year with total increasing amount of about: 359.70 mm) in the same period. These results seem to be consistent with Ajjur and Al-Ghamdi (2021), who found that most of the MENA region is positively exposed to a scarcity of water availability due to high temperatures and expected drought rates that exceed precipitation rates under the SSP5-8.5 scenario. Moreover, by 2100, the annual reduction of water availability in MENA has been estimated to be 26 and 62 mm under SSP2-4.5 and SSP5-8.5, respectively, compared to the historical period (1981–2010) (Ajjur and Al-Ghamdi, 2021).

In the context of climate situations, Sultan et al. (2015) have projected that there will be no significant difference in the Red Sea Coastal Aquifer from 2013 to 2100, including watersheds of Al-Madinah. Sultan et al. (2015) also expected the rainfall to grow in Wadi Al-Hamd by 85mm at the end of the century, coinciding with increased initial losses of rains by more than 58% as well as evapotranspiration with decreasing runoff rates. These results seem consistent with the present study, which confirmed that Wadi Al-Hamd will experience a continuing rise in temperatures accompanied by an increased evaporation rate.

Despite the expected small increase of rainfall in Al-Madinah, the periods of rainfall or sporadic wet seasons, such as winter and autumn rains, could hold significant value to water resources through water storage techniques, including dams, which could be applied in arid regions as one of the adaptation strategies to cope with climate change effects, to provide a more stable water supply during drier times for agriculture, industry, and domestic use. or for recharging groundwater aquifer. The government constructed about 14 dams in Al-Madinah

to recharge groundwater to support water conservation measures in the region and minimise surface water losses that might result from evaporation. These dams are expected to recharge the potential groundwater zones under both models while also playing a pivotal role in supporting and optimising irrigation approaches in the study area.

The spatial variability was more prominent under the logistic regression model when compared to the Fuzzy Gamma 0.97 model. However, the high-potential groundwater zones are expected to experience changes spatially although by quantitatively small amounts under the climate future scenarios (RCP4.5 and RCP8.5). These slight changes do not indicate that climate change is an unimportant or ineffectual factor; on the contrary, the continuation of arid weather conditions represented in low precipitation rates, steadily rising temperatures with evapotranspiration, along with potential extreme events such as drought in the future all highly alert us to the need to take preventive measures that help to preserve the limited suitable zones of groundwater formation as well as adapting sustainable management practices and utilization of water resources.

However, these slight changes show that some places within the current urban area in the city's centre will shift into unsuitable locations for direct groundwater infiltration that also shows a low rainfall accumulation rate with a high estimated ET0 rate, especially at the end of the century under RCP8.5. One unexpected finding was that some lava grounds in the southeast and east of Al-Madinah city are projected to shift into unsuitable groundwater locations, even though these lands are typically associated with unique geological features and characteristics for storing groundwater. This shift might be attributed to the combination of reduced groundwater recharge due to climate change (lower precipitation and higher evapotranspiration) and urbanisation, which causes altered natural drainage patterns, leading to increased runoff and reduced infiltration, hence limiting groundwater recharge. Accordingly, although these areas may have historically been favourable for groundwater storage, shifts in hydrological patterns due to external factors can alter their suitability over time. Therefore, this finding needs more investigation by conducting field studies and analysing geological, ecological, and hydrological data. In comparison, the new suitable areas for groundwater are projected to form near the sites that have been planned to be urban areas or agricultural lands by 2030, such as expected in the northwestern and northeastern parts of Al-Madinah city.

The environmental and climate change impacts could be exacerbated by increasing population growth, urbanization and alterations in LULC. These effects would pose additional challenges in arid regions by leading, for example, to water stress or demand. Thus, identifying the key drivers of water demand and incorporating the future scenarios of climate change and socioeconomic factors to assess potential water availability and demand trends would be an effective tool for sustainable water management and evaluating mitigation and adaptation strategies, particularly in situations where uncertainty is inherent such as in the complex interplay between human activities and environmental systems (O'Neill et al., 2020). Accordingly, the future water resources of Al-Madinah are projected to experience additional stress until and probably beyond 2030, when water consumption is expected to increase around six times compared to the baseline year 1990.

From the main driving forces within the IPUAT model, population growth was the most influential variable in explaining water demand patterns, which is predicted to increase steadily. In Al-Madinah, the Per Capita water consumption increased by about 34.63% between 2015 and 2021, from 231 L/d to 311 L/d (MEWA, 2018a ; MEWA, 2021). This contradicted the Saudi Vision 2030, which aims to reduce the consumption Per Capita to 200 liters by 2020 and 150 liters by 2030 (MEWA, 2020). Thus, to meet these increasing water demands, Saudi Arabia is heavily depended on seawater desalination, considering using renewable sources could reduce carbon emissions, improve efficiency, and promote environmental sustainability. However, managing water demand will be of extreme important to address the issue, beyond increasing water supply (Biswas and Tortajada, 2022). Accordingly, new policies related to increased water prices were introduced to reduce wastage, household and municipal consumption and sustainably manage demand. This implies more weight for the impact of GDP variables on the water demand patterns in Al-Madinah.

Generally, the Al-Madinah development plan is working to develop an additional 746 km² of built-up area alongside adding about 91 km² of cultivation lands by the end of 2030 (UN-HABITAT, 2019a). Spatially, these proposed lands are in areas ranging from high to very high potential for groundwater formation based on the maps generated for the present study. Accordingly, developing more agricultural lands in arid and semi-arid cities such as Al-Madinah would be very likely to place additional stress on limited irrigation water resources,

mainly to be satisfied from existing groundwater wells. This would be more problematic by mid-century and end-century, if adaptation measures for water conservation have not been improved it is projected that Al-Madinah could face some drought conditions under the expectations of increasing temperatures and only small growth in precipitation quantity. These climate stressors would highly challenge the sustainability of agricultural systems. For instance, the increasing evapotranspiration trend under climate change is expected to cause soil moisture to decline by 0.81 m/year in Saudi Arabia by 2050, leading to the growing amount of irrigation water needed (Graham et al., 2020 ; El-Rawy et al., 2023 ; Chowdhury and Al-Zahrani, 2013b), especially if combined with a lack of investment in water-efficient technologies.

Furthermore, climate change's impacts could extend beyond climate-related components to the gross domestic product (GDP); as estimated by Kompas et al. (2018), the GDP of Saudi Arabia will decrease by 2100 by about 1.6% to 7.7% under increases of temperature of 1◦C to 4◦C, respectively. According to the World Bank (2016a), Middle Eastern countries are projected to have an economic decline ranging from 6% to 14% of GDP by 2050 caused by climate change that leads to water scarcity; these adversely affect agriculture, the public and incomes.

Such changes and rapid expansion of urbanisation would exert additional pressure on water resources. Water needs are expected to increase under urban development, which will continue to grow faster than the expansion predicted for agricultural lands. This assessment was derived from the effective usage index represented in urbanisation (the built-up area/agricultural lands) under the IPUAT model. These land use and cover changes would significantly impact groundwater resources, whether on recharge systems and quality or growth in local water demand (Barreteau et al., 2016). Moreover, this urbanization, on such a scale, would not be reasonable and sustainable for water supply and quality. It will probably cause water supply challenges for Al-Madinah that could involve not only straining existing water resources and declining water availability for irrigation but also an additional financial burden in developing infrastructure for new urban areas to provide desalination water for drinking purposes. This rapid urban expansion can also intensify local climate conditions. It exacerbates the urban heat island (UHI) influence, which leads to increased water demands

for cooling purposes, reduced water availability due to raised temperatures and ET0 rates (Uddin et al., 2021), as well as water quality deterioration (Vujovic et al., 2021).

Technological advancements are essential in managing and optimizing water resources for agricultural purposes. These advancements play a crucial role in accommodating the expansion of agricultural land and adapting to the expectations within the study area concerning changing climatic conditions. However, the technology variable in Al-Madinah, represented in the relationship between agricultural lands/Gross domestic product (GDP), showed no improvement, indicating inefficient water consumption practices, as well as a need for more investment and innovation in agricultural technologies to improve usage efficiency. For example, irrigation efficiency in Saudi Arabia was 53% in 2017, and it planned to develop up to 75% by 2030 (MEWA, 2017b). This improvement in water use efficiency was expected to be achieved by implementing agriculture and irrigation techniques to optimize water usage and reduce the cultivation of water-intensive crops such as date palms, which are considered a paramount part of agriculture in the Al-Madinah region (MEWA, 2017b). These measures would positively enhance the technological aspect mainly under the study area, which relies more on pumping from the groundwater wells for irrigation purposes than surface water availability. Furthermore, approximately 33% of the total GDP of Al-Madinah is obtained from the industry sector, while just about 2% is from the agricultural sector (MCCI, 2017). This often could lead to increased water demand for industrial purposes, and so establishing treatment plants to reclaim industrial wastewater in the industrial area in Al-Madinah would help to re-use water much more efficiently.

However, water reclamation technology for industrial purposes, or irrigation by the groundwater, requires significant energy that often raises greenhouse gas emissions levels. According to the World Bank (2016a), extracting groundwater demands about 30% more energy than utilising surface water for irrigation. Thus, technological improvements alone might not be sufficient to address water challenges completely (World Bank, 2016a). Accordingly, reducing water demand by improving consumption efficiency measures in all sectors would mitigate the adverse consequences of using power.

Accordingly, a higher contribution from the industrial sector to GDP might be associated with urbanization and population growth, which may involve changes in the water demand patterns of Al-Madinah. Population and GDP alteration are interdependent factors that could

highly influence the overall socio-economic context. Therefore, under the SSPs scenarios, the SSP3 and SSP4 are expected to have the largest water demand in Al-Madinah, because of the high population growth rate. According to water use scenarios produced by Hanasaki et al. (2013), the largest increase in per capita water use will be in the SSP3, which is characterized by high population growth rates; thus, water consumption for domestic and municipal usage is predicted to rise. Mazzoni et al. (2018) also confirmed that anthropogenic drivers such as population growth, agricultural expansion and urbanization development are expected to contribute more to water demand and groundwater depletion, specifically in the MENA region, than changes in climate, especially rainfall attributes in the next decades.

Moreover, increased water withdrawal in SSP3 could be attributed to slow technological progress and low-efficiency irrigation (Hanasaki et al., 2012b ; Graham et al., 2018) , which could place additional pressure on limited water resources in arid regions. Generally, moderate to high population growth combined with limited economic development in the SSP3 and SSP4 scenarios could be environmental sustainability challenges and increased resource requests, especially in arid regions. These conditions may lead to higher emissions that are often related to rising energy demands and could also be associated with a lack of emission management, competition, and pressure on limited local resources, such as water.

Overall, the development policies and planning in Al-Madinah should consistently monitor the effects of land use and land cover decisions on water resources, as well as revise regulations and practices based on new evaluations and changes in water resource conditions. For example, due to groundwater over-extraction in Saudi Arabia, especially for agricultural purposes, the government has recently implemented policies that include permits for groundwater well extraction and allowable withdrawal rates and volumes (MEWA, 2023). This measure would be a good step toward emphasising the necessity of sustainable water management practices.

These challenges also should be integrated under more comprehensive plans local to global scales that work to diminish extreme climate change events resulting from increasing greenhouse gas emissions. In this context, on a short-term plan, the Saudi National Water Strategy 2030 aims under The Water Act not only to address the water availability issues under the sustainable water sector and regulate and protect them but also to enhance the principle of transparency related to the right to access and exchange water information,

which helps decision-making and sustainable water management practices, as well as reducing the per capita daily consumption of water (MEWA, 2018b). This will be a good step towards improving water security for the country.

In the broader context, the Saudi Arabian government recognizes the potential risks of climate change and is engaged in implementing measures to mitigate and adapt to these challenges. This includes an updated goal of diminishing greenhouse gas emissions by 278 million tons per annum (mtpa) by 2030, which represents more than double the target submitted in 2015 to the UNFCCC (Al-Sarihi, 2021 ; SEC, 2021) , as well as working to a net zero target by 2060 (SEC, 2021). In addition, there are active investments in renewable energy sources and energy efficiency technologies (UNFCCC, 2022). The government also enhances water management techniques and promotes sustainable agricultural practices (UNFCCC, 2022). These initiatives reflect Saudi Arabia's commitment to addressing the challenges of climate change. According to Du et al. (2021), despite the high likelihood of water stress in Saudi Arabia due to the impact of climate change by the 2050s, mitigation measures will be implemented to alleviate this situation. The government has begun implementing these measures to address water scarcity and promote sustainable use. For example, invest in advanced wastewater treatment facilities to produce reclaimed water for industrial, agricultural, and other non-potable uses, such as in the industrial city of Al-Madinah. They have also Implemented increasing water pricing, encouraging conservation among high-volume users.

7.4 Potential groundwater zones and the future development plan, recommendations to policymakers

Al-Madinah development plan is developing an additional 746 km² of built-up area and adding about 91 km² of cultivation lands by the end of 2030, along with future development zones of about 3436 km² (UN-HABITAT, 2019a). Spatially, these proposed lands, as shown in Figure 7-1, are in areas ranging from high to very high potential for groundwater formation based on the maps results of the present study.

Location numbers 1 and 2, as shown in Figure **7-1**, are the main areas included in developing new agricultural lands. Developing new agricultural lands in the area (1) in the east of Al-Medinah would present an opportunity to expand agricultural production and increase food

production, mainly since it is located in a high potential area of groundwater as well as near the Wadi Huzuaza dam, which offers a high possibility to recharge these shallow groundwater zones. Moreover, the area (2) northwest of Al-Madinah will experience developing lands for agricultural activities simultaneously with establishing a small urban area. This urban area was classified on the 2020 map as a small residential area and planned to expand to a small city by 2030. Such developments would cause increased water demand and lead to higher groundwater extraction rates, potentially exceeding the limited natural recharge rates. Therefore, constructing a new dam near these areas in the upper region of Wadi Al-Hamed, characterized by high accumulation possibility, can enhance water storage availability, as shown in Figure 7-1. However, developing more agricultural lands without careful water management strategies can lead to long-term sustainability challenges, including groundwater depletion, land degradation, and reduced agricultural productivity.

The geographical features such as high elevation and slope restricted the direction and pattern of urban expansion in Al-Madinah and forced development to occur within existing urbanised areas or in valleys and plains where the terrain is more conducive to construction. This study indicated, many of these areas have high groundwater potential, such as areas in the location number (3) in Figure 7-1 that have most of the proposed built-up areas by 2030. Despite the fact that developments within current urban areas or in the same direction would allow for the optimisation and expansion of existing infrastructure networks and reduce the need for costly new infrastructure, the limited groundwater should be prioritised and under consideration in any urban planning processes. In addition, developing new built-up areas on such a scale (around 746 km² by 2030) would not be reasonable and sustainable for water supply and quality, and the local authority should review the urban development plan to guide expansion away from possible recharge locations and towards more sustainable urban growth corridors. The present study maps could help design groundwater protection zones and implement zoning regulations to restrict incompatible land uses in sensitive areas. This would protect valuable groundwater resources for future generations.

Furthermore, about 3436 km² in Al-Madinah city are allocated for future development zones, as displayed in Figure 7-1. These zones might be for infrastructure and utilities, recreational and green spaces, nature reserves, or other activities, not built-up areas, or agricultural lands. However, this study revealed that these zones are located in the valley-beds north, west, and

east. These locations offer promising conditions for the current potential of groundwater formation, as well as Western places are expected to shift into new suitable areas for groundwater, especially at the end of the century under RCP8.5 as shown in the location (4-b) in Figure 7-1. Therefore, improving the groundwater monitoring program within and around future development zones to track changes in groundwater levels and quality over time would be required. Regular monitoring can detect early signs of groundwater depletion or contamination, allowing for timely intervention. By incorporating these strategies into the planning and development of future zones, policymakers can effectively protect areas of high potential for groundwater while promoting sustainable urban growth and development.

Overall, mapping allowed for the visualisation of areas with high potential for groundwater resources in Al-Madinah, as well as identifying some areas where development activities may conflict with groundwater protection goals by overlaying this information with the future development plan (2030). This map provides a basis for long-term planning and adaptive management strategies by identifying critical zones and assessing the potential risks associated with various development activities concerning groundwater resources. This would allow planners and decision-makers to determine areas where certain activities, such as urban or agricultural practices, may pose a higher risk of groundwater contamination or depletion. Thus, the policies should be adjusted as needed to achieve sustainable development goals and protect limited groundwater resources in the face of evolving challenges.

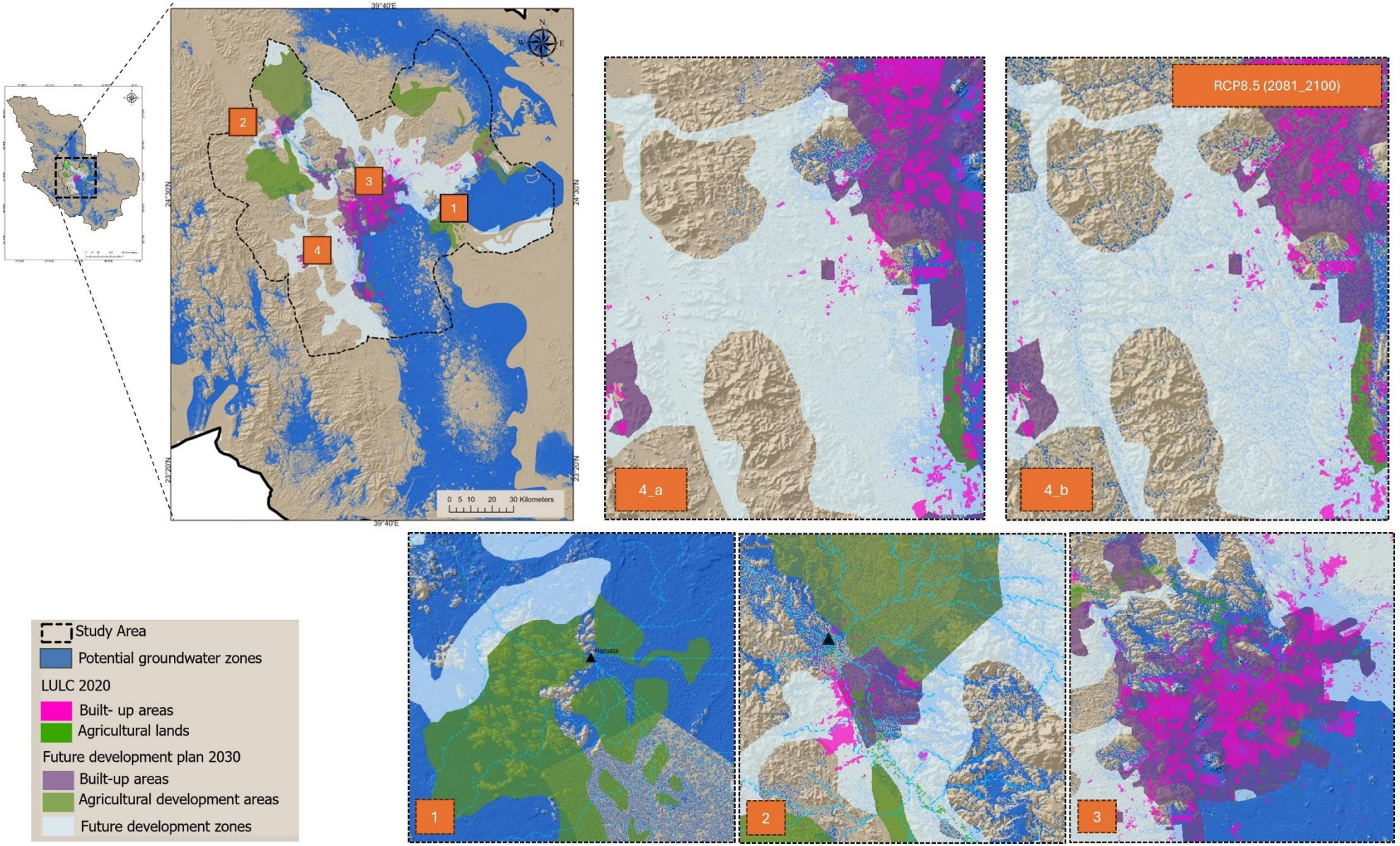

Figure 7-1 . Spatial overlay and distribution of potential groundwater zones and future development plan of Al-Madinah (2030). The figure illustrates the distribution of potential groundwater zones under urbanization and agriculture plans and future development zones.

7.5 Thesis contribution

Methodologically, this thesis introduces some important contributions to applying advanced modelling techniques in the water field. The critical review of the literature revealed an increasing trend of research efforts mapping the potential groundwater zones by applying a wide range of data mining or machine learning techniques and statistical models. The blending approach of the fuzzy logic (FL) model with frequency ratio (FR) to delineate the potential groundwater zones was absent in the groundwater field. This offers a chance to conduct scientific research to address the identified gap, which was introduced in Chapter 3.

The Fuzzy-Frequency method included the most relevant control factors and influence on groundwater formation and storage, including the Topographical wetness index (TWI) weighted by present and future rainfall under RCP scenarios considered as a novel method in mapping groundwater, which was introduced in Chapter 4.

This thesis also adopts an innovative approach by adapting the IPAT model to be IPAUT (Impact of Population, Affluence, Urbanization and Technology) and applying it to water resources to provide a comprehensive understanding of the driving factors for water demand under the main socio-economic scenarios, as shown in Chapter 6. The knowledge generated in Chapter 6 helps develop the application of such a framework to analyse factors that could impact water resources with the capability to expand and involve more elements. The IPAT also offered implementable frameworks in other arid regions that are suffering from data limitations.

Spatially, Al-Madinah City is a good location for applying such advanced modelling techniques where it has yet to be employed. This thesis also presents the first-time estimation of the reference evapotranspiration in the present and future periods (1970-2100) under representative concentration pathways (RCPs) scenarios, as well as the standardised precipitation evapotranspiration index (SPEI) in Al-Madinah City, which has shown in Chapter 4, this knowledge help to sustainable resource management and water availability assessment.

Moreover, updating LULC maps of the Al-Madinah City-Region scale was required; using the Random Forest Algorithm on Landsat Imagery created new maps covering three decades that were analysed in Chapter 5. The knowledge from Chapter Five would be highly of interest to the local authorities in the study area in formulating adaptive strategies and ensuring

sustainable land use practices in the face of altering environmental and societal conditions in arid regions. These maps show the spatial distribution of general types of water consumers, such as residential areas and agricultural lands, which is essential for managing water demand.

For future research, improving groundwater level records and gathering additional data, such as soil moisture content, would enrich the predictive capacity of models used as well as contribute to a more comprehensive understanding of the factors influencing groundwater availability. Integrating a broader set of impacting aspects on water needs, such as human activities simultaneously with climate changes, would also help prioritise adaptation strategies and resource allocation under a more holistic view of water resource dynamics. Groundwater recharge estimates could also enhance overall water balance assessments in such arid environments; for example, the good-resolution LULC maps generated in this study could be integrated with hydrological models for the simulation of runoff processes to improve the accuracy of runoff predictions and then recharge estimations. These improvements would help to establish a long-term monitoring program to continuously track changes in water availability, climate conditions, and socio-economic factors. This will enable the assessment of the effectiveness of adaptation measures over time and improve the strategies to address water security in arid regions.

Moreover, evaluating and analysing consumption patterns in arid regions with detailed water footprints for different sectors, including households, agriculture, and industry needs, is highly required to improve water use efficiency and introduce technologies and sustainable practices. Mapping future water demand is also needed. This map should combine population density, GDP distribution, and other relevant socio-economic indicators to create comprehensive maps spotlighting areas of water demand spatially, providing a roadmap for stakeholders and planners to establish sustainable water resource management.

7.6 Limitations and implications of the thesis

Water resources research often requires consideration of the geographical characteristics and integration of various knowledge bases and interdisciplinary science, such as hydrology and climatology, as well as socioeconomic variables, which might lead to some challenges associated with collecting data and also selecting methods that effectively incorporate and analyse these data. The main limitations and challenges of this study are represented by the

data gaps and accessibility, which are related to the lack of groundwater wells data for the wells' depth and the monitoring records, runoff data, as well as historical and present land use and land cover estimations of Al-Madinah on the city-region scale. However, managing these limitations has led to the adoption of several approaches for helping answers to thesis questions. Remote sensing and GIS technologies have been crucial in modelling different water resource management aspects of this thesis.

The combined method of predicting future precipitation patterns with the topographic wetness index (TWI) was highly effective in mapping groundwater's spatial distribution and detecting potential temporal and spatial changes in groundwater locations over future periods under RCP4.5 and RCP5.8 scenarios. This approach successfully surpassed the topography complexity of the study area, represented in the positive correlation between the concentration of rainfall and highland terrains, which are topographies considered low suitability for groundwater formation or as settlement residences. Because of the short length of rainfall and runoff records, it was difficult to detect trends in rainfall-runoff patterns and opportunities for recharge replenishment under climate changes. Thus, TWI-Rainfall measures overcame some of these problems of short hydrological data records in the study area. This method provided valuable insights into potential groundwater alterations, as shown in Chapter 4. It would also be beneficial and increase its reliability if applied in other arid regions with limited data accessibility.

Moreover, land use and land cover data are essential in studies of water supply and demand in arid regions. In the present study, the IPUAT model is based on the time series, the period from 1990 to 2020, for the variables such as the built-up areas and agricultural lands. However, some LULC (Land Use/Land Cover) data have been absent, including maps or estimations, for example, the start year 1990 or data over a longer time period for Al-Madinah. These available data also only had partial coverage of the study area caused by the administrative boundary changes suggested in the 2030 Vision of the Kingdom of Saudi Arabia (KSA), where the prioritizing development projects and plans became on the Al-Madinah City-region scale. To overcome these challenges and provide comprehensive insights into water demand changes using The IPUAT model, there was a pressing need for more detailed LULC data at this regional scale across historical periods. Therefore, Landsat satellite image classifications over three decades provided the classes needed. This data facilitated the

generation of time series data necessary for modelling future scenarios and studying water demand changes.

Geographic Information Systems (GIS) and remote sensing have facilitated the process of updating LULC maps in good resolution and enabled the extraction of the quantitative information for LULC categories over time. These classes are included in the IPUAT model that indicated should consider other variables such as GDP, urban area, and agricultural lands along with the population in prediction of future water demand. These generated maps would also benefit further research in natural resource management and climate change studies, as well as support urban and regional planning for the study area.

In addition, adaptable research methods such as the IPAT model provide more flexibility for including variables based on evolving research questions and the study area characteristics, improving the comprehensive understanding of various aspects of the issue analysed. The findings of the applied modified IPAT model in this thesis would encourage using it more in the water field, leading to continuous improvement and refinement of research methodologies and achieving more reliability.

Implementing a comprehensive study of water resources comprising the three interconnected aspects, as in this thesis, represented in mapping, climate change impacts, and future demand trends, would offer theoretical elements that contribute to the exploration of the natural and human-induced influential factors, as well as drawing a good framework that supports to understand groundwater resource dynamics in arid regions, such as Al-Madinah. These studies would also provide an important integrated perspective for managing the complex challenges associated with water resources in arid regions. Some novel and adaptable methodologies applied in this thesis could offer applicable insights to effective management in regions needing more data or data consistency. These are essential in guiding practical decisions, shaping policies, and developing strategies that can be applied in the real world. For example, the spatial understanding of groundwater resources always facilitates informed decision-making in allocating resources and planning LULC. This will also be enhanced by including considerations related to climate change, which allows for evaluating risks and formulating adaptive strategies to manage potential hydrological pattern alterations. Analysing future water demand allows to assess that the current resource management strategies are efficient and anticipate society's changing conditions and needs.

7.7 The Conclusion

The limited availability of suitable sites for groundwater resources in Al-Madinah could be a significant challenge, especially considering it is located in an arid semi-arid region. This challenge can be attributed mainly to the rise in demand caused by population growth and urbanization, more than being directly associated with climate change. Climate change effects on water availability, especially the invisible resources such as groundwater, often work in complex operations involving the local hydrological and geological features on varying scale. In contrast, socioeconomic factors such as population growth usually impact directly and are easily observed in the context of the immediate consequences of increased water demand or deficiency.

The interactive relationship between climate change and water demand requires coordinated efforts and proactive solutions in arid and semi-arid regions. Employing geospatial data analysis by modelling and visualising the potential water resources could be considered a first step towards enhancing water management practices. Mapping water resources provides several benefits for a city's future plans; it allows city decision-makers and planners to understand the locations and distribution of potential water sources. It also assists in identifying suitable urban growth areas and other activity zones that could involve threats to water sources' quality or quantity.

Finally, the results of this study are beneficial on the scale of arid and semi-arid areas that may suffer, such as Al-Madinah, not only from the lack of groundwater potential and the increasing water demand but also the limited access to historical observational runoff data and the groundwater level monitoring records of long-term periods that generally hamper quantitative water availability prediction. The findings from the models developed to detecting potential groundwater zones have been linked to the potential effects of future rainfall patterns changes under climate change scenarios and have identified the driving factors for increasing the water demand. Therefore, these models can be adapted and applied easily in any arid and semi-arid regions.

Appendices

Appendix 1

Table S3-1. Multicollinearity analysis among conditioning factors

Affecting factors	*GVIF	Df	*GVIF^(1/(2*Df))
Soil	1.99	5	1.07
Lithology	1.68	4	1.06
Faults Density	1.11	1	1.05
TWI- Rainfall	1.06	1	1.03
Drainage Density	1.20	1	1.09
SPI index	1.13	1	1.06
Plan Curvature	1.06	1	1.03
Slope degree	1.25	1	1.12
Altitudes	1.59	1	1.26
Slope aspect	1.26	8	1.01

*GVIF is the Generalized Variance Inflation Factor that is an indicator and a measure of the extent to which the multicollinearity contributes to an increase in the variance of the estimated regression coefficients in a logistic regression model. This factor is computed individually for each predictor variable within the model, providing insight into the impact of multicollinearity on the precision of the coefficient estimates (Nahhas, 2023). GVIF raised to the power of degrees of freedom. This indicator is often used as a more conservative version of the GVIF, considering the degrees of freedom associated with each variable. This adjusted GVIF is helpful for models with limited observations and adjusts for the potential overestimation of multicollinearity (Nahhas, 2023). In both indicators, values greater than 2 or 2.5 are indicative of a multicollinearity problem that may be of concern, whereas values above 5 or 10 reveal a big multicollinearity problem (Nahhas, 2023).

Appendix 2

Table S3-2. Values of AUC curves for the success rate of all models.

Test Result Variable(s)	Area	Std. Error[a]	Asymptotic 95% Confidence Interval	
			Lower Bound	Upper Bound
Fuzzy_Gamma_0.99	.951	.006	.939	.962
Fuzzy_Gamma_0.98	.947	.006	.935	.959
Fuzzy_Gamma_0.97	**.963**	.005	.953	.972
Fuzzy_Gamma_0.95	.955	.005	.945	.966
Fuzzy_Gamma_0.90	.950	.006	.938	.962
Fuzzy_Gamma_0.80	.950	.006	.939	.962
Fuzzy_Gamma_0.70	.948	.006	.936	.960
Fuzzy_Gamma_0.60	.949	.006	.937	.960
Fuzzy_Gamma_0.50	.946	.006	.934	.958
Fuzzy_And	.917	.008	.901	.933
Fuzzy_Or	.559	.016	.528	.590
Fuzzy_Sum	.569	.016	.538	.600
Fuzzy_Product	.950	.006	.938	.961

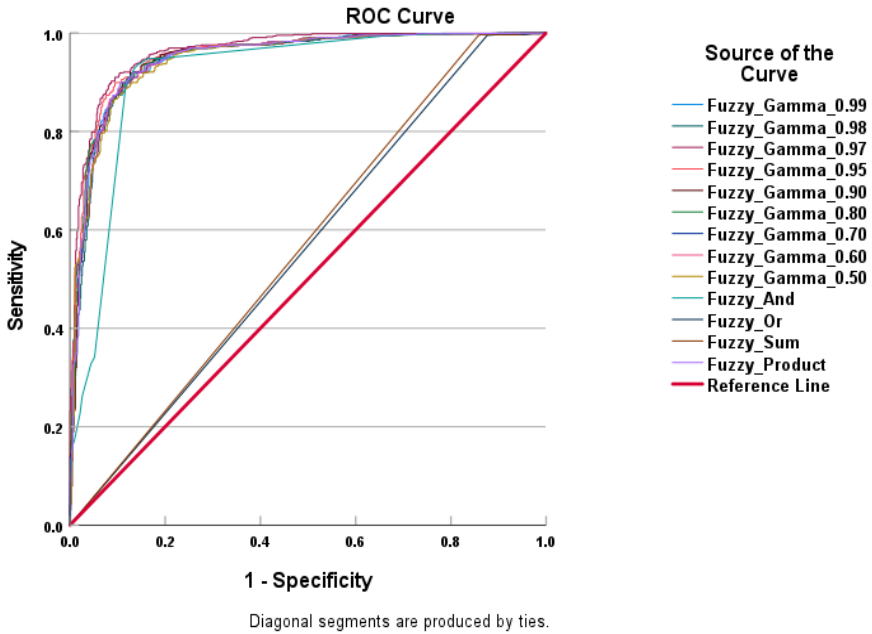

Figure S3-1. AUC curves for the success rate (training data) of all models.

Table S3-3. Values of AUC curves for the predictive rate of all models

Test Result Variable(s)	Area	Std. Error[a]	Asymptotic 95% Confidence Interval	
			Lower Bound	Upper Bound
Fuzzy_Gamma_0.99	.935	.011	.915	.956
Fuzzy_Gamma_0.98	.941	.010	.921	.961
Fuzzy_Gamma_0.97	.943	.010	.923	.962
Fuzzy_Gamma_0.95	.937	.011	.916	.958
Fuzzy_Gamma_0.90	.939	.010	.919	.959
Fuzzy_Gamma_0.80	.934	.011	.912	.955
Fuzzy_Gamma_0.70	.934	.011	.912	.955
Fuzzy_Gamma_0.60	.933	.011	.911	.954
Fuzzy_Gamma_0.50	.931	.011	.909	.952
Fuzzy_And	.884	.015	.854	.914
Fuzzy_Or	.555	.024	.508	.603
Fuzzy_Sum	.553	.024	.506	.601
Fuzzy_Product	.937	.010	.916	.957

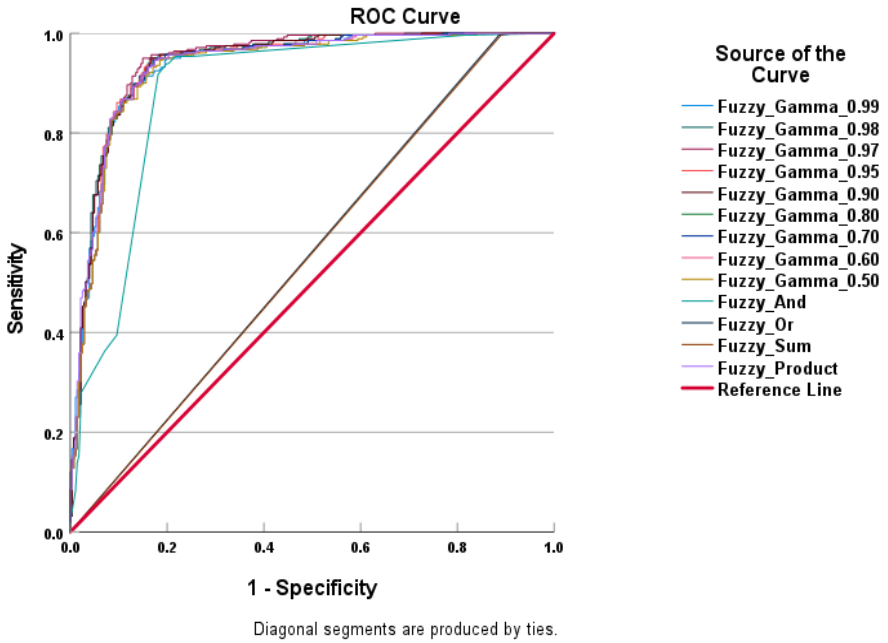

Figure S3-2. AUC curves for the predictive rate (test data) of all models.

Tables S3-2 and S3-3 and Figures S3-1 and S3-2 show the accuracy assessment of GWPZ maps under the ROC-AUC Curve computed the success and prediction rates. The Gamma operator's fuzzy overlay had a high ROC-AUC Curve value, while the Fuzzy_Or and Fuzzy_Sum models had the lowest success and prediction capability.

Appendix 3

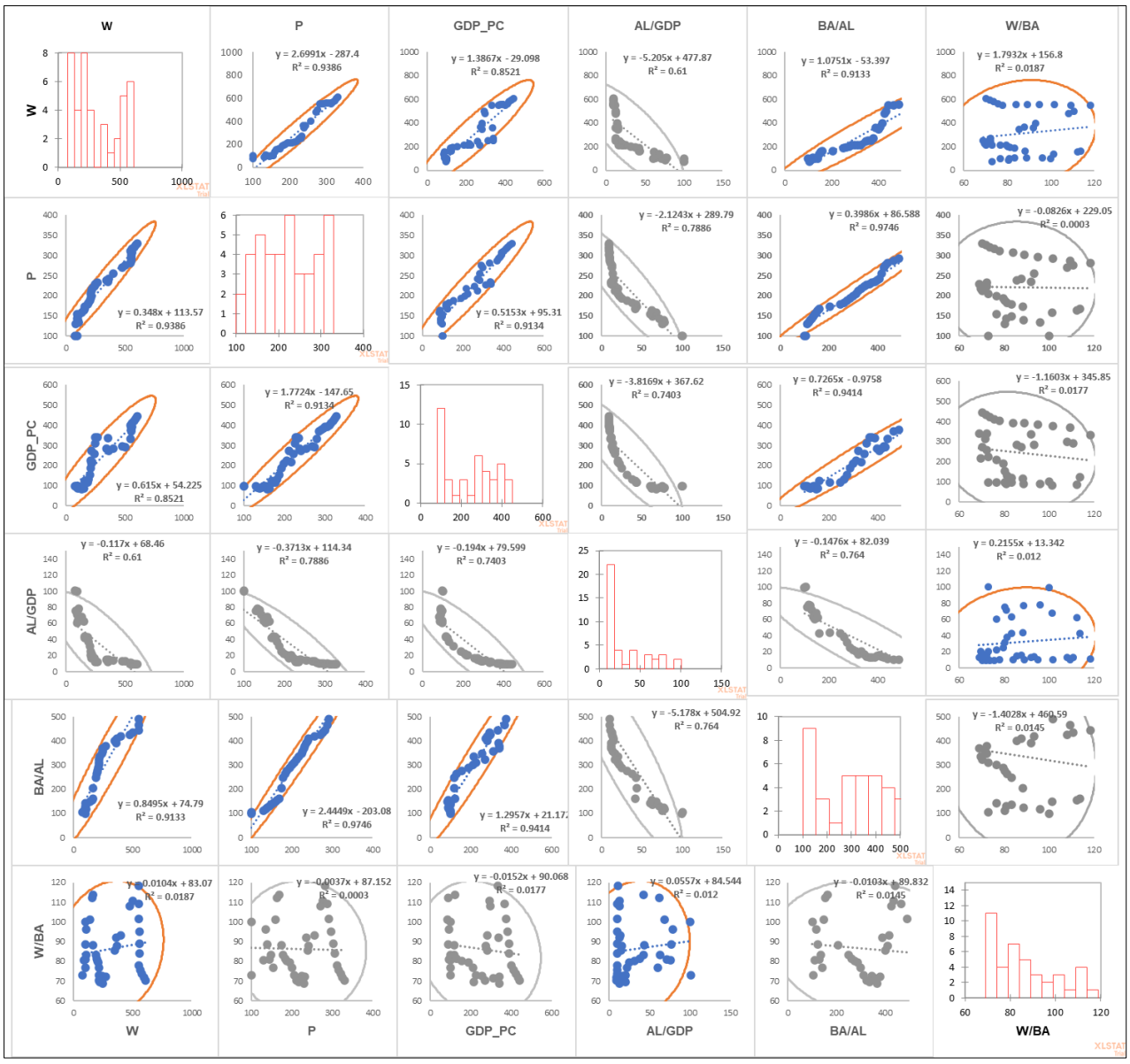

Figure S6-1. The scatter plot and correlations between study's variables

The Figure S6-1 shows the output of the correlation test by XLSTAT software. The histogram was displayed for each variable (diagonal), and a scatter plot was used for all combinations of variables. The red colour of the data points in the scatter plots revealed a positive correlation, and the grey colour is a negative one.

References

ABBAS, A. A. A. 2013. *Implications of climate change on crop water requirements in Saudi Arabia.* Master, King Fahd University of Petroleum & Minerals.

ABDEKAREEM, M., ABDALLA, F., AL-ARIFI, N., BAMOUSA, A. O. & EL-BAZ, F. 2023. Using Remote Sensing and GIS-Based Frequency Ratio Technique for Revealing Groundwater Prospective Areas at Wadi Al Hamdh Watershed, Saudi Arabia. *Water,* 15.

ABDERRAHMAN, W. A. 2000. Water Demand Management and Islamic Water Management Principles: A Case Study. *International Journal of Water Resources Development,* 16**,** 465-473.

ABDERRAHMAN, W. A. 2002. Should intensive use of non-renewable groundwater resources always be rejected? Intensive Use of Groundwater. Balkema Publishers. Lisse, Germany. .

ABDI, A. M. 2019. Land cover and land use classification performance of machine learning algorithms in a boreal landscape using Sentinel-2 data. *GIScience & Remote Sensing,* 57**,** 1-20.

ABDULLAH, H. M. Standardized precipitation evapotranspiration index (SPEI) based drought assessment in Bangladesh. Proceedings of 5th International Conference on Environmental Aspects of Bangladesh, 2014. ICEAB 2014.

ABT, R. C., PRESTEMON, J. P., FORSELL, N., BAKER, J. S., KOROSUO, A., JOHNSTON, C. & DAIGNEAULT, A. 2019. Developing Detailed Shared Socioeconomic Pathway (SSP) Narratives for the Global Forest Sector. *Journal of Forest Economics,* 34**,** 7-45.

ADIAT, K. A. N., NAWAWI, M. N. M. & ABDULLAH, K. 2012. Assessing the accuracy of GIS-based elementary multi criteria decision analysis as a spatial prediction tool – A case of predicting potential zones of sustainable groundwater resources. *Journal of Hydrology,* 440-441**,** 75-89.

ADNAN, N., AHMAD, M. H. & ADNAN, R. 2006. A Comparative Study On Some Methods For Handling Multicollinearity Problems. *MATEMATIKA,* 22**,** 109–119.

AGUIR BARGAOUI, S., LIOUANE, N. & NOURI, F. Z. 2014. Environmental Impact Determinants: An Empirical Analysis based on the STIRPAT Model. *Procedia - Social and Behavioral Sciences,* 109**,** 449-458.

AHMED, K., SACHINDRA, D. A., SHAHID, S., IQBAL, Z., NAWAZ, N. & KHAN, N. 2020. Multi-model ensemble predictions of precipitation and temperature using machine learning algorithms. *Atmospheric Research,* 236.

AJJUR, S. B. & AL-GHAMDI, S. G. 2021. Evapotranspiration and water availability response to climate change in the Middle East and North Africa. *Climatic Change,* 166.

AKGUN, A., SEZER, E. A., NEFESLIOGLU, H. A., GOKCEOGLU, C. & PRADHAN, B. 2012. An easy-to-use MATLAB program (MamLand) for the assessment of landslide susceptibility using a Mamdani fuzzy algorithm. *Computers & Geosciences,* 38**,** 23-34.

AL-ABADI, A. M. 2015. Groundwater potential mapping at northeastern Wasit and Missan governorates, Iraq using a data-driven weights of evidence technique in framework of GIS. *Environmental Earth Sciences,* 74**,** 1109-1124.

AL-ABADI, A. M., AL-TEMMEME, A. A. & AL-GHANIMY, M. A. 2016. A GIS-based combining of frequency ratio and index of entropy approaches for mapping groundwater availability zones at Badra–Al Al-Gharbi–Teeb areas, Iraq. *Sustainable Water Resources Management,* 2**,** 265-283.

AL-ABADI, A. M. & SHAHID, S. 2015. A comparison between index of entropy and catastrophe theory methods for mapping groundwater potential in an arid region. *Environ Monit Assess,* 187**,** 576.

AL-AHMADI, M. E. & EL-FIKY, A. A. 2009. Hydrogeochemical evaluation of shallow alluvial aquifer of Wadi Marwani, western Saudi Arabia. *Journal of King Saud University - Science,* 21**,** 179-190.

AL-IBRAHIM, A. A. 1991. Excessive Use of Groundwater Resources in Saudi Arabia: Impacts and Policy Options. *Springer on behalf of Royal Swedish Academy of Sciences,* 20**,** 34-37.

AL-RASHED, M. F. & SHERIF, M. M. 2000. Water Resources in the GCC Countries: An Overview. *Water Resources Management,* 14**,** 59–75.

AL-REFEAI, T. & AL-GHAMDY, D. 1994. Geological and geotechnical aspects of Saudi Arabia. *Geotechnieal and Geological Engineering,* 12**,** 253-276.

AL-RUZOUQ, R., SHANABLEH, A., MERABTENE, T., SIDDIQUE, M., KHALIL, M. A., IDRIS, A. & ALMULLA, E. 2019. Potential groundwater zone mapping based on geo-hydrological considerations and multi-criteria spatial analysis: North UAE. *Catena,* 173**,** 511-524.

AL-SARIHI, A. 2021. Saudi Arabia and the Paris climate agreement. *KFCRIS Commentaries. Retrieved December,* 8**,** 2021.

AL-SHAIBANI, A., LLOYD, J. W., ABOKHODAIR, A. & AL-AHMARI, A. 2007. A Hydrogeological and Quantitative Groundwater Assessment of the Basaltic Aquifer, Northern Harrat Rahat, Saudi Arabia. *Arab Gulf Journal of Scientific Research,* 25**,** 39-49.

AL-TURKI, S. 1995. *Water Resources in Saudi Arabia with Particular Reference to Tihama Asir Province.* Doctor of Philosophy, University of Durham.

AL-ZAHRANI, M. A. & ABO-MONASAR, A. 2015. Urban Residential Water Demand Prediction Based on Artificial Neural Networks and Time Series Models. *Water Resources Management,* 29**,** 3651-3662.

ALAHMADI, F. S. 2019. Groundwater Aquifer Delineation by Spatial Cluster Modeling in Madinah, Western Kingdom of Saudi Arabia. *American Journal of Geographic Information System,* 8(3)**,** 126-130.

ALAMRI, Y. & REED, M. 2019. Estimating Virtual Water Trade in Crops for Saudi Arabia. *American Journal of Water Resources,* 7**,** 16-22.

ALAVIPOOR, F. S., KARIMI, S., BALIST, J. & KHAKIAN, A. H. 2016. A geographic information system for gas power plant location using analytical hierarchy process and fuzzy logic. *Global J. Environ. Sci. Manage,* 2**,** 197- 207.

ALAWAD, M. N. J. 2018. Artificial Recharge (AR) of Groundwater Aquifers in Saudi Arabia. *ICEWES***,** 13-15.

ALCAMO, J., FLÖRKE, M. & MÄRKER, M. 2007. Future long-term changes in global water resources driven by socio-economic and climatic changes. *Hydrological Sciences–Journal–des Sciences Hydrologiques,* 52**,** 247–275.

ALDHARAB, H. S., ALI, S. A. & GHAREB, J. I. S. A. 2019. Analysis of Basin Geometry in Ataq Region, Part of Shabwah Yemen: Using Remote Sensing and Geographic Information System Techniques. *Bulletin of Pure & Applied Sciences- Geology,* 38f.

ALEMU, Z. A. & DIOHA, M. O. 2020. Modelling scenarios for sustainable water supply and demand in Addis Ababa city, Ethiopia. *Environmental Systems Research,* 9.

ALGHAMDI, A. G., ALY, A. A., ALDHUMRI, S. A. & AL-BARAKAHA, F. N. 2020. Hydrochemical and Quality Assessment of Groundwater Resources in Al-Madinah City, Western Saudi Arabia. *Sustainability,* 12.

ALHARBI, H. 2018. *Gentrification in the Central Zone of Medina, Saudi Arabia.* Doctor of Philosophy, University of Leicester.

ALMAZROUI, M. 2013. Simulation of present and future climate of Saudi Arabia using a regional climate model (PRECIS). *International Journal of Climatology,* 33**,** 2247-2259.

ALMAZROUI, M. 2019. Assessment of meteorological droughts over Saudi Arabia using surface rainfall observations during the period 1978–2017. *Arabian Journal of Geosciences,* 12.

ALMAZROUI, M., ISLAM, M. N., SAEED, S., SAEED, F. & ISMAIL, M. 2020. Future Changes in Climate over the Arabian Peninsula based on CMIP6 Multimodel Simulations. *Earth Systems and Environment,* 4**,** 611-630.

ALMOSLUT, M. 2015. *A Systems Approach to Groundwater Extension, Management and Replacement in Saudi Arabia.* Master of Science, Loyola Marymount University.

ALMUTAZ, I., AJBAR, A. H. & ALI, E. 2012. Determinants of residential water demand in an arid and oil rich country: A case study of Riyadh city in Saudi Arabia. *International Journal of Physical Sciences,* 7**,** 5787-5796.

ALNAJDI, O., CALAUTIT, J. K. & WU, Y. 2019. Development of a multi-criteria decision making approach for sustainable seawater desalination technologies of medium and large-scale plants: a case study for Saudi Arabia's vision 2030. *Energy Procedia,* 158**,** 4274-4279.

ALSARHAN, A., ZATARI, T., AL-ASALY, M., MIRZA, K., HARTHI, A., OTHMAN, M., BABIKER, M., KHAN, A., ALJABR, A., ALBUQAMI, F., AL-KHELAIFI, A., HAMZA, A., SAKKAL, M., AL-SHAIKH, M., HUSAIN,

T., KHAN, R., RAHMAN, S. M., KHONDAKER, A., BUKHARI, A. & AL-SHAMSI, M. 2016. *Third National Communication of the Kingdom of Saudi Arabia (Submitted to UNFCCC)*, Ministry of Energy, Industry and Mineral Resources.

AMANA 2009. Indicators of local development for the Al- Madinah region. Madinah Municipality - Kingdom of Saudi Arabia.

AMIN, A., IQBAL, J., ASGHAR, A. & RIBBE, L. 2018. Analysis of Current and Future Water Demands in the Upper Indus Basin under IPCC Climate and Socio-Economic Scenarios Using a Hydro-Economic WEAP Model. *Water,* 10.

AMIN, M. T., MAHMOUD, S. H. & ALAZBA, A. A. 2016. Observations, projections and impacts of climate change on water resources in Arabian Peninsula: current and future scenarios. *Environmental Earth Sciences,* 75.

ANBALAGAN, R., KUMAR, R., LAKSHMANAN, K., PARIDA, S. & NEETHU, S. 2015. Landslide hazard zonation mapping using frequency ratio and fuzzy logic approach, a case study of Lachung Valley, Sikkim. *Geoenvironmental Disasters,* 2.

ANTHONY J. VIERA, M. J. M. G. 2005. Understanding Interobserver Agreement: The Kappa Statistic. *Family Medicine,* 37.

AOURAGH, M. H., ESSAHLAOUI, A., EL OUALI, A., EL HMAIDI, A. & KAMEL, S. 2016. Groundwater potential of Middle Atlas plateaus, Morocco, using fuzzy logic approach, GIS and remote sensing. *Geomatics, Natural Hazards and Risk,* 8**,** 194-206.

ARABAMERI, A., REZAEI, K., CERDA, A., LOMBARDO, L. & RODRIGO-COMINO, J. 2019a. GIS-based groundwater potential mapping in Shahroud plain, Iran. A comparison among statistical (bivariate and multivariate), data mining and MCDM approaches. *Sci Total Environ,* 658**,** 160-177.

ARABAMERI, A., ROY, J., SAHA, S., BLASCHKE, T., GHORBANZADEH, O. & TIEN BUI, D. 2019b. Application of Probabilistic and Machine Learning Models for Groundwater Potentiality Mapping in Damghan Sedimentary Plain, Iran. *Remote Sensing,* 11.

ARABIA, S. First national communication. Kingdom Of Saudi Arabia, Submitted To The United Nations Framework Convention On Climate Change,(UNFCCC), 2005.

ARNOUS, M. O. 2016. Groundwater potentiality mapping of hard-rock terrain in arid regions using geospatial modelling: example from Wadi Feiran basin, South Sinai, Egypt. *Hydrogeology Journal,* 24**,** 1375-1392.

AYALEW, L. & YAMAGISHI, H. 2005. The application of GIS-based logistic regression for landslide susceptibility mapping in the Kakuda-Yahiko Mountains, Central Japan. *Geomorphology,* 65**,** 15-31.

AYESHA, S., HANIF, M. K. & TALIB, R. 2020. Overview and comparative study of dimensionality reduction techniques for high dimensional data. *Information Fusion,* 59**,** 44-58.

AYT OUGOUGDAL, H., YACOUBI KHEBIZA, M., MESSOULI, M. & LACHIR, A. 2020. Assessment of Future Water Demand and Supply under IPCC Climate Change and Socio-Economic Scenarios, Using a Combination of Models in Ourika Watershed, High Atlas, Morocco. *Water,* 12.

B RIADI, B. B., WIDIATMAKA, M J P YANUAR, B PRAMUDYA 2018. Identification and delineation of areas flood hazard using high accuracy of DEM data. *IOP Conference Series: Earth and Environmental Science.*

BABEL, M. S., GUPTA, A. D. & PRADHAN, P. 2006. A multivariate econometric approach for domestic water demand modeling: An application to Kathmandu, Nepal. *Water Resources Management,* 21**,** 573-589.

BALIOTI, V., TZIMOPOULOS, C. & EVANGELIDES, C. 2018. Multi-Criteria Decision Making Using TOPSIS Method Under Fuzzy Environment. Application in Spillway Selection. *Proceedings,* 2.

BAMOUSA, A. O., MATAR, S. S., DAOUDI, M. & AL-DOAAN, M. I. 2012. Structural and geomorphic features accommodating groundwater of Al-Madinah City, Saudi Arabia. *Arabian Journal of Geosciences,* 6**,** 3127-3132.

BARRETEAU, O., CABALLERO, Y., HAMILTON, S., JAKEMAN, A. J. & RINAUDO, J.-D. 2016. Disentangling the complexity of groundwater dependent social-ecological systems. *Integrated groundwater management: concepts, approaches and challenges***,** 49-73.

BATES, B., KUNDZEWICZ, Z. & WU, S. 2008. *Climate change and water*, Intergovernmental Panel on Climate Change Secretariat.

BENJMEL, K., AMRAOUI, F., BOUTALEB, S., OUCHCHEN, M., TAHIRI, A. & TOUAB, A. 2020. Mapping of Groundwater Potential Zones in Crystalline Terrain Using Remote Sensing, GIS Techniques, and Multicriteria Data Analysis (Case of the Ighrem Region, Western Anti-Atlas, Morocco). *Water,* 12.

BISWAS, A. K. & TORTAJADA, C. 2022. Future of desalination in the context of water security. *International Journal of Water Resources Development,* 38**,** 921-927.

BOB, M., ABD RAHMAN, N., TAHER, S. & ELAMIN, A. 2014. Multi-objective Assessment of Groundwater Quality in Madinah City, Saudi Arabia. *Water Quality, Exposure and Health,* 7**,** 53-66.

BOUROUBA, M. 2016. Geomorphological properties of Al Aqiq Watershed in Al Madinah Munawarah Area. *Journal of Arabic and Human Sciences* 19**,** 1331-1391.

BUCKLEY, J. J. 1984. The multiple judge, multiple criteria ranking problem: a fuzzy set approach. *Fuzzy Sets and Systems,* 13**,** 25 -37.

ČADRO, S., UZUNOVIĆ, M., ŽUROVEC, J. & ŽUROVEC, O. 2017. Validation and calibration of various reference evapotranspiration alternative methods under the climate conditions of Bosnia and Herzegovina. *International Soil and Water Conservation Research,* 5**,** 309-324.

CARVER, S. J. 1991. Integrating multi-criteria evaluation with geographical information systems. *International journal of geographical information systems,* 5**,** 321-339.

CHAI, J., LIANG, T., LAI, K. K., ZHANG, Z. G. & WANG, S. 2018. The future natural gas consumption in China: Based on the LMDI-STIRPAT-PLSR framework and scenario analysis. *Energy Policy,* 119**,** 215-225.

CHEN, H., MATSUHASHI, K., TAKAHASHI, K., FUJIMORI, S., HONJO, K. & GOMI, K. 2020. Adapting global shared socio-economic pathways for national scenarios in Japan. *Sustainability Science,* 15**,** 985-1000.

CHEN, W., LI, H., HOU, E., WANG, S., WANG, G., PANAHI, M., LI, T., PENG, T., GUO, C., NIU, C., XIAO, L., WANG, J., XIE, X. & AHMAD, B. B. 2018. GIS-based groundwater potential analysis using novel ensemble weights-of-evidence with logistic regression and functional tree models. *Sci Total Environ,* 634**,** 853-867.

CHEN, W., TSANGARATOS, P., ILIA, I., DUAN, Z. & CHEN, X. 2019. Groundwater spring potential mapping using population-based evolutionary algorithms and data mining methods. *Sci Total Environ,* 684**,** 31-49.

CHOWDHURY, S. & AL-ZAHRANI, M. 2013a. Characterizing water resources and trends of sector wise water consumptions in Saudi Arabia. *Journal of King Saud University - Engineering Sciences,* 27**,** 68-82.

CHOWDHURY, S. & AL-ZAHRANI, M. 2013b. Implications of Climate Change on Water Resources in Saudi Arabia. *Arabian Journal for Science and Engineering,* 38**,** 1959-1971.

CHUNG, C. & FABBRI, A. 2003. Validation of spatial prediction models for landslide hazard mapping. *Natural Hazards,* 30**,** 451–472.

CLOSAS, A. & MOLLE, F. 2016. Groundwater governance in the Middle East and North Africa.[Project report of the Groundwater Governance in the Arab World-Taking Stock and Addressing the Challenges].

COHEN, W. B. & GOWARD, S. N. 2004. Landsat's role in ecological applications of remote sensing. *Bioscience,* 54**,** 535-545.

COSGROVE, W. J. & LOUCKS, D. P. 2015. Water management: Current and future challenges and research directions. *Water Resources Research,* 51**,** 4823-4839.

CUARESMA, J. C. 2017. Income projections for climate change research: A framework based on human capital dynamics, Global Environmental Change. https://tntcat.iiasa.ac.at/SspDb/dsd?Action=htmlpage&page=30.

CZOGAŁA, E. & ŁĘSKI, J. 2000. Classical sets and fuzzy sets Basic definitions and terminology. *Fuzzy and Neuro-Fuzzy Intelligent Systems.* Heidelberg: Physica-Verlag HD,10.1007/978-3-7908-1853-6_1.

DAQAMSEH, S. 2017. Land Use Land Cover of an Urban Area using Remote Sensing (Texture Analysis Applications) and GIS - A Case Study of Central Region of Almadinah Almunawarah, Saudi Arabia. *International Journal of Advanced Remote Sensing and GIS,* 6**,** 2114-2123.

DE PAUW, E. 2002. *An archeological exploration of Arabian Peninsula,* Aleppo, Syria, ICARDA, International Center for Agricultural Research in the Dry Areas.

DERNONCOURT, F. 2013. Introduction to fuzzy logic. *Massachusetts Institute of Technology*.

DRIOUECH, F., ELRHAZ, K., MOUFOUMA-OKIA, W., ARJDAL, K. & BALHANE, S. 2020. Assessing Future Changes of Climate Extreme Events in the CORDEX-MENA Region Using Regional Climate Model ALADIN-Climate. *Earth Systems and Environment,* 4**,** 477-492.

DU, G.-L., ZHANG, Y.-S., IQBAL, J., YANG, Z.-H. & YAO, X. 2017. Landslide susceptibility mapping using an integrated model of information value method and logistic regression in the Bailongjiang watershed, Gansu Province, China. *Journal of Mountain Science,* 14**,** 249-268.

DU, P., XU, M. & LI, R. 2021. Impacts of climate change on water resources in the major countries along the Belt and Road. *PeerJ,* 9**,** e12201.

DYMOVA, L., KACZMAREK, K., SEVASTJANOV, P. & KULAWIK, J. 2021. A Fuzzy Multiple Criteria Decision Making Approach with a Complete User Friendly Computer Implementation. *Entropy (Basel),* 23.

EL-RAWY, M., BATELAAN, O., AL-ARIFI, N., ALOTAIBI, A., ABDALLA, F. & GABR, M. 2023. Climate Change Impacts on Water Resources in Arid and Semi-Arid Regions: A Case Study in Saudi Arabia. *Water,* 15.

EL MAGHRABY, M. 2014a. Groundwater Chemistry in an Area Covered by Lava Flows, Aqool Area, Eastern Al Madinah Al Munawarah City, Saudi Arabia. *European academic research,* 1.

EL MAGHRABY, M. M. S. 2014b. Hydrogeochemical characterization of groundwater aquifer in Al-Madinah Al-Munawarah City, Saudi Arabia. *Arabian Journal of Geosciences,* 8**,** 4191-4206.

EL MAGHRABY, M. M. S. 2015. Hydrogeochemical characterization of groundwater aquifer in Al-Madinah Al-Munawarah City, Saudi Arabia. *Arabian Journal of Geosciences,* 8**,** 4191-4206.

ELEWA, H. H. & QADDAH, A. A. 2011. Groundwater potentiality mapping in the Sinai Peninsula, Egypt, using remote sensing and GIS-watershed-based modeling. *Hydrogeology Journal,* 19**,** 613-628.

ELMAHDY, S. I. & MOHAMED, M. M. 2014. Probabilistic frequency ratio model for groundwater potential mapping in Al Jaww plain, UAE. *Arabian Journal of Geosciences,* 8**,** 2405-2416.

ELNAKER, N. & ZALESKI, T. The impact of slope aspect on soil temperature and water content. Proceesings of International symposium on soil science and plant nutrition. Samsun, Turkey, 2021. 156-163.

ELNESR, M. & ALAZB, A. 2013. Effect of Climate Change on Spatio-Temporal Variability and Trends of Evapotranspiration, and Its Impact on Water Resources Management in The Kingdom of Saudi Arabia. *Climate Change - Realities, Impacts Over Ice Cap, Sea Level and Risks.* 10.5772/54832.

ELNESR, M., ALAZBA, A. & ABU-ZREIG, M. 2010. Spatio-Temporal Variability of Evapotranspiration over the Kingdom of Saudi Arabia. *Applied Engineering in Agriculture,* 26**,** 833-842.

ERGON, R. 2005. Informative PLS score-loading plots for process understanding and monitoring. *Modeling, Identification and Control: A Norwegian Research Bulletin,* 26**,** 23-37.

ESRI. 2011. *ArcGIS Desktop Help - curvature* [Online]. Available: http://webhelp.esri.com/arcgisdesktop/9.3/index.cfm?TopicName=curvature [Accessed].

ESRI. 2016a. How Fuzzy Overlay works. Available from: https://pro.arcgis.com/en/pro-app/latest/tool-reference/spatial-analyst/how-fuzzy-overlay-works.htm.

ESRI. 2020. *Train Random Trees Classifier (Spatial Analyst)* [Online]. Environmental Systems Research Institute. Available: https://pro.arcgis.com/en/pro-app/latest/tool-reference/spatial-analyst/train-random-trees-classifier.htm [Accessed 30/08 2020].

ESRI. 2021. *Data classification methods* [Online]. Available: https://pro.arcgis.com/en/pro-app/latest/help/mapping/layer-properties/data-classification-methods.htm [Accessed].

ESRI. 2022a. *Accuracy Assessment* [Online]. Environmental Systems Research Institute. Available: https://pro.arcgis.com/en/pro-app/latest/help/analysis/image-analyst/accuracy-assessment.htm [Accessed 30/08 2020].

ESRI. 2022b. *How Line Density works* [Online]. Available: https://pro.arcgis.com/en/pro-app/latest/tool-reference/spatial-analyst/how-line-density-works.htm [Accessed].
ESRI, E. S. R. I. 2016b. *Applying fuzzy logic to overlay rasters* [Online]. Available: https://desktop.arcgis.com/en/arcmap/10.3/tools/spatial-analyst-toolbox/applying-fuzzy-logic-to-overlay-rasters.htm [Accessed].
FALLATAH, O. A. 2019. Groundwater Quality Patterns and Spatiotemporal Change in Depletion in the Regions of the Arabian Shield and Arabian Shelf. *Arabian Journal for Science and Engineering,* 45**,** 341-350.
FAN, F. & LEI, Y. 2015. Decomposition analysis of energy-related carbon emissions from the transportation sector in Beijing. *Transp Res D Transp Environ,* 42**,** 135-145.
FANG, N., SHI, Z., CHEN, F. & WANG, Y. 2015. Partial Least Squares Regression for Determining the Control Factors for Runoff and Suspended Sediment Yield during Rainfall Events. *Water,* 7**,** 3925-3942.
FAO 2007. Coping with water scarcity: challenge of the twenty-first century. United Nations Food and Agriculture Organization Rome, Italy.
FAYE, C., MANUELA GRIPPA & WOOD, S. 2019. Use of the Standardized Precipitation and Evapotranspiration Index (SPEI) from 1950 to 2018 to determine drought trends in the Senegalese territory. *Climate Change,,* 5(20)**,** 327-341.
FENG, G., JENKINS, J. N., ADELI, A., OUYANG, Y., FISHER, D. K., ABDO, Z. & COBB, S. 2016. Trend Analysis and Forecast of Precipitation, Reference Evapotranspiration, and Rainfall Deficit in the Blackland Prairie of Eastern Mississippi. *Journal of Applied Meteorology and Climatology,* 55**,** 1425-1439.
FENG, S. 2017. The Driving Factor Analysis of China's CO₂ Emissions Based on the STIRPAT Model. *Open Journal of Social Sciences,* 05**,** 49-58.
FEROZUR, R. M., JAHAN, C. S., AREFIN, R. & MAZUMDER, Q. H. 2019. Groundwater potentiality study in drought prone barind tract, NW Bangladesh using remote sensing and GIS. *Groundwater for Sustainable Development,* 8**,** 205-215.
FICK, S. E. & HIJMANS, R. J. 2017. WorldClim 2: new 1-km spatial resolution climate surfaces for global land areas. *International journal of climatology,* 37**,** 4302-4315.
FISHER, D. K. & PRINGLE III, H. C. 2013. Evaluation of alternative methods for estimating reference evapotranspiration. *Agricultural Sciences,* 04**,** 51-60.
FULAZZAKY, M. 2014. Challenges of Integrated Water Resources Management in Indonesia. *Water,* 6**,** 2000-2020.
GAO, C. K., WANG, D., CAI, J. J. & ZHU, W. G. 2010. Scenario analysis on economic growth and environmental load in China. *Procedia Environmental Sciences,* 2**,** 1335-1343.
GARAVAGLIA, S. & SHARMA, A. A smart guide to dummy variables: Four applications and a macro. Proceedings of the northeast SAS users group conference, 1998. Citeseer.
GASTAT 2010. Population and Housing Census. Saudi Central Department of Statistics and Information.
GASTAT 2017. Detailed results of the Agriculture Census. General Authority for Statistics, Saudi Arabia
GASTAT 2018a. Percentage of desalinated water to total freshwater available for municipal use in Saudi Arabia during the period 2010-2018. General Authority for Statistics, Saudi Arabia.
GASTAT 2018b. Percentage Of Non-Renewable Groundwater To Fresh Water Consumption By Sector (Municipal And Agricultural) In Saudi Arabia During The Period 2014-2018. General Authority for Statistics, Saudi Arabia.
GASTAT 2020. Gross Domestic Product. General Authority for Statistics in Saudi Arabia
GASTAT 2022. Population and Housing Census. Saudi Central Department of Statistics and Information.
GEMITZI, A., THRACE, G. F., ESKIOGLOU, P. & PETALAS, C. 2011. Evaluating landslide susceptibility using environmental factors, fuzzy membership functions and GIS. *Global NEST Journal,* 13**,** pp 28-40.

GHANIM, A. A. 2019. Water Resources Crisis in Saudi Arabia, Challenges and Possible Management Options: An Analytic Review. *International Journal of Environmental and Ecological Engineering,* 13.

GHARBIA, S. S., SMULLEN, T., GILL, L., JOHNSTON, P. & PILLA, F. 2018. Spatially distributed potential evapotranspiration modeling and climate projections. *Sci Total Environ,* 633**,** 571-592.

GHIASSI, M., ZIMBRA, D. K. & SAIDANE, H. 2008. Urban Water Demand Forecasting with a Dynamic Artificial Neural Network Model. *Journal of Water Resources Planning and Management,* 134**,** 138-146.

GHOLAMI, M., GHACHKANLU, E. N., KHOSRAVI, K. & PIRASTEH, S. 2019. Landslide prediction capability by comparison of frequency ratio, fuzzy gamma and landslide index method. *Journal of Earth System Science,* 128.

GHOSH, B. 2021. Spatial mapping of groundwater potential using data-driven evidential belief function, knowledge-based analytic hierarchy process and an ensemble approach. *Environmental Earth Sciences,* 80.

GIDEY, E., DIKINYA, O., SEBEGO, R., SEGOSEBE, E. & ZENEBE, A. 2017. Cellular automata and Markov Chain (CA_Markov) model-based predictions of future land use and land cover scenarios (2015–2033) in Raya, northern Ethiopia. *Modeling Earth Systems and Environment,* 3**,** 1245-1262.

GRABS, T., SEIBERT, J., BISHOP, K. & LAUDON, H. 2009. Modeling spatial patterns of saturated areas: A comparison of the topographic wetness index and a dynamic distributed model. *Journal of Hydrology,* 373**,** 15-23.

GRAHAM, N. T., DAVIES, E. G. R., HEJAZI, M. I., CALVIN, K., KIM, S. H., HELINSKI, L., MIRALLES-WILHELM, F. R., CLARKE, L., KYLE, P., PATEL, P., WISE, M. A. & VERNON, C. R. 2018. Water Sector Assumptions for the Shared Socioeconomic Pathways in an Integrated Modeling Framework. *Water Resources Research,* 54**,** 6423-6440.

GRAHAM, N. T., HEJAZI, M. I., CHEN, M., DAVIES, E. G. R., EDMONDS, J. A., KIM, S. H., TURNER, S. W. D., LI, X., VERNON, C. R., CALVIN, K., MIRALLES-WILHELM, F., CLARKE, L., KYLE, P., LINK, R., PATEL, P., SNYDER, A. C. & WISE, M. A. 2020. Humans drive future water scarcity changes across all Shared Socioeconomic Pathways. *Environmental Research Letters,* 15.

GREEN, T. R. 2016. Linking climate change and groundwater. *In:* JAKEMAN, A. J., BARRETEAU, O., HUNT, R. J., RINAUDO, J.-D. & ROSS, A. (eds.) *Integrated groundwater management: Concepts, approaches and challenges.* Cham: Springer International Publishing,10.1007/978-3-319-23576-9_5.

GUAN, D., LI, H., INOHAE, T., SU, W., NAGAIE, T. & HOKAO, K. 2011. Modeling urban land use change by the integration of cellular automaton and Markov model. *Ecological Modelling,* 222**,** 3761-3772.

GUPTA, M. & SRIVASTAVA, P. K. 2010. Integrating GIS and remote sensing for identification of groundwater potential zones in the hilly terrain of Pavagarh, Gujarat, India. *Water International,* 35**,** 233-245.

GURUVAYUR, S. R. & SUCHITHRA, R. A detailed study on machine learning techniques for data mining. 2017 International Conference on Trends in Electronics and Informatics (ICEI), 2017. IEEE, 1187-1192.

GUTUB, S. A. 2013. A Case Study of Al-Madinah's Water Resources and Reclaimed Wastewater Reuse Perspective. *International Journal of Civil & Environmental Engineering IJCEE-IJENS,* 13.

HAFEZ, M. A.-S. & MIRAJ, N. M. 2013. Al-Madinah from a Climate perspective. *Geography and the Gulf Cooperation Council: Prospects and Concerns.* Gulf Geographical Society - King Abdul Aziz Darah.

HAJKOWICZ, S. & COLLINS, K. 2006. A Review of Multiple Criteria Analysis for Water Resource Planning and Management. *Water Resources Management,* 21**,** 1553-1566.

HALDER, S., ROY, M. B. & ROY, P. K. 2020. Fuzzy logic algorithm based analytic hierarchy process for delineation of groundwater potential zones in complex topography. *Arabian Journal of Geosciences,* 13.

HALMY, M. W. A., GESSLER, P. E., HICKE, J. A. & SALEM, B. B. 2015. Land use/land cover change detection and prediction in the north-western coastal desert of Egypt using Markov-CA. *Applied Geography,* 63**,** 101-112.

HANASAKI, N., FUJIMORI, S., YAMAMOTO, T., YOSHIKAWA, S., MASAKI, Y., HIJIOKA, Y., KAINUMA, M., KANAMORI, Y., MASUI, T., TAKAHASHI, K. & KANAE, S. 2012a. A global water scarcity assessment under shared socio-economic pathways – Part 2: Water availability and scarcity. *Hydrology and Earth System Sciences,* 17**,** 2393–2413.

HANASAKI, N., FUJIMORI, S., YAMAMOTO, T., YOSHIKAWA, S., MASAKI, Y., HIJIOKA, Y., KAINUMA, M., KANAMORI, Y., MASUI, T., TAKAHASHI, K. & KANAE, S. 2012b. A global water scarcity assessment under shared socio-economic pathways – Part 2: Water availability and scarcity. *Hydrology and Earth System Sciences,* 17**,** 2393–2413.

HANASAKI, N., FUJIMORI, S., YAMAMOTO, T., YOSHIKAWA, S., MASAKI, Y., HIJIOKA, Y., KAINUMA, M., KANAMORI, Y., MASUI, T., TAKAHASHI, K. & KANAE, S. 2013. A global water scarcity assessment under Shared Socio-economic Pathways – Part 1: Water use. *Hydrology and Earth System Sciences,* 17**,** 2375-2391.

HARRIS, I., JONES, P. D., OSBORN, T. J. & LISTER, D. H. 2014. Updated high-resolution grids of monthly climatic observations–the CRU TS3. 10 Dataset. *International journal of climatology,* 34**,** 623-642.

HASTIE, T., TIBSHIRANI, R. & FRIEDMAN, J. 2009. *The Elements of Statistical Second Edition Learning Data Mining, Inference, and Prediction,* New York, Springer Series in Statistics.

HE, C., LIU, Z., WU, J., PAN, X., FANG, Z., LI, J. & BRYAN, B. A. 2021. Future global urban water scarcity and potential solutions. *Nat Commun,* 12**,** 4667.

HERMAS, E. S., EL-BARODI, M. & AL-GHAMDI, K. 2015. Integration of Point and Remote Sensing Data for Monitoring Surface Runoff around Madinah City, Saudi Arabia. *Advances in Remote Sensing,* 04**,** 287-302.

HILBE, J. M. 2016. *Practical guide to logistic regression*, crc Press.

HOCINE KINIOUAR, AZZEDINE HANI & KAPELAN., Z. 2017. Water Demand Assessment of the Upper Semi-arid Sub-catchment of a Mediterranean Basin. *Energy Procedia,* 119**,** 870-882.

HUANG, F., ZHANG, D. & CHEN, X. 2019. Vegetation Response to Groundwater Variation in Arid Environments: Visualization of Research Evolution, Synthesis of Response Types, and Estimation of Groundwater Threshold. *Int J Environ Res Public Health,* 16.

HÜLLERMEIER, E. 2005. Fuzzy methods in machine learning and data mining: Status and prospects. *Fuzzy Sets and Systems,* 156**,** 387-406.

HÜLLERMEIER, E. 2011. Fuzzy sets in machine learning and data mining. *Applied Soft Computing,* 11**,** 1493-1505.

IPCC 2017. IPCC Fifth Assessment Report (AR5) Observed Climate Change Impacts Database, Version 2.01. Palisades, NY: NASA Socioeconomic Data and Applications Center (SEDAC).

IRFAN, M., JAVED, M. & RAZA, M. A. 2013. Comparison of Shrinkage Regression Methods for Remedy of Multicollinearity Problem. *Middle-East Journal of Scientific Research,* 14 (4)**,** 570-579.

JAAFARI, A., MAFI-GHOLAMI, D., THAI PHAM, B. & TIEN BUI, D. 2019. Wildfire Probability Mapping: Bivariate vs. Multivariate Statistics. *Remote Sensing,* 11.

JAAFARZADEH, M. S., TAHMASEBIPOUR, N., HAGHIZADEH, A., POURGHASEMI, H. R. & ROUHANI, H. 2021. Groundwater recharge potential zonation using an ensemble of machine learning and bivariate statistical models. *Sci Rep,* 11**,** 5587.

JAHN, R., BLUME, H., ASIO, V., SPAARGAREN, O. & SCHAD, P. 2006. *Guidelines for soil description*, FAO.

JAIN, A. & SHARMA, A. 2020. Membership function formulation methods for fuzzy logic systems: a comprehensive review. *Journal of Critical Reviews,* 7.

JAKEMAN, A. J., BARRETEAU, O., HUNT, R. J., RINAUDO, J.-D., ROSS, A., ARSHAD, M. & HAMILTON, S. 2016. Integrated groundwater management: an overview of concepts and challenges. *Integrated groundwater management: Concepts, approaches and challenges***,** 3-20.

JANG, J. S. R. & CHUEN-TSAI, S. 1995. Neuro-fuzzy modeling and control. *Proceedings of the IEEE,* 83**,** 378-406.

JEBUR, M. N., PRADHAN, B., SHAFRI, H. Z. M., YUSOFF, Z. M. & TEHRANY, M. S. 2015. An integrated user-friendly ArcMAP tool for bivariate statistical modelling in geoscience applications. *Geoscientific Model Development,* 8**,** 881-891.

JIA, G., SHEVLIAKOVA, E., ARTAXO, P., DE-DOCOUDRÉ, N., HOUGHTON, R., HOUSE, J., KITAJIMA, K., LENNARD, C., POPP, A. & SIRIN, A. 2019. Land–climate interactions. *Special Report on Climate Change and Land: An IPCC Special Report on climate change, desertification, land degradation, sustainable land management, food security, and greenhouse gas fluxes in terrestrial ecosystems.* IPCC.

JIMÉNEZ, B., OKI, T., ARNELL, N., BENITO, G., COGLEY, J. G., DOELL, P., JIANG, T. & MWAKALILA, S. S. 2014. Freshwater resources. 10.1017/CBO9781107415379.008.

JIN, C., HUANG, K., YU, Y. & ZHANG, Y. 2016. Analysis of Influencing Factors of Water Footprint Based on the STIRPAT Model: Evidence from the Beijing Agricultural Sector. *Water,* 8.

JOHANNSEN, I., HENGST, J., GOLL, A., HÖLLERMANN, B. & DIEKKRÜGER, B. 2016. Future of Water Supply and Demand in the Middle Drâa Valley, Morocco, under Climate and Land Use Change. *Water,* 8.

JOHNSON, P. R. 2006. Explanatory notes to the map of Proterozoic geology of western Saudi Arabia. Saudi Geological Survey Technical Report SGS-TR-2006-4.

JOSE, D. M., VINCENT, A. M. & DWARAKISH, G. S. 2022. Improving multiple model ensemble predictions of daily precipitation and temperature through machine learning techniques. *Sci Rep,* 12**,** 4678.

KAHSAY, K. D., PINGALE, S. M. & HATIYE, S. D. 2018. Impact of climate change on groundwater recharge and base flow in the sub-catchment of Tekeze basin, Ethiopia. *Groundwater for Sustainable Development,* 6**,** 121-133.

KAMIS, A. S. 2012. Future Domestic Water Demand for Jeddah City. *Journal of King Abdulaziz University-Meteorology, Environment and Arid Land Agriculture Sciences,* 23**,** 137-146.

KHASHOGJI, M. S. & EL MAGHRABY, M. M. S. 2012. Evaluation of groundwater resources for drinking and agricultural purposes, Abar Al Mashi area, south Al Madinah Al Munawarah City, Saudi Arabia. *Arabian Journal of Geosciences,* 6**,** 3929-3942.

KHOSHTINAT, S., AMINNEJAD, B., HASSANZADEH, Y. & AHMADI, H. 2019. Application of GIS-based models of weights of evidence, weighting factor, and statistical index in spatial modeling of groundwater. *Journal of Hydroinformatics,* 21**,** 745-760.

KIM, J., CHOI, J., CHOI, C. & PARK, S. 2013. Impacts of changes in climate and land use/land cover under IPCC RCP scenarios on streamflow in the Hoeya River Basin, Korea. *Sci Total Environ,* 452-453**,** 181-95.

KLEINBAUM, D. G. & KLEIN, M. 2010. Introduction to Logistic Regression. *Logistic Regression.* 10.1007/978-1-4419-1742-3_1.

KOMPAS, T., PHAM, V. H. & CHE, T. N. 2018. The Effects of Climate Change on GDP by Country and the Global Economic Gains From Complying With the Paris Climate Accord. *Earth's Future,* 6**,** 1153-1173.

KOTU, V. & DESHPANDE, B. 2018. *Data science: concepts and practice*, Morgan Kaufmann.

KRITIKOS, T., ROBINSON, T. R. & DAVIES, T. R. H. 2015. Regional coseismic landslide hazard assessment without historical landslide inventories: A new approach. *Journal of Geophysical Research: Earth Surface,* 120**,** 711-729.

KUMAR, P., HERATH, S., AVTAR, R. & TAKEUCHI, K. 2016. Mapping of groundwater potential zones in Killinochi area, Sri Lanka, using GIS and remote sensing techniques. *Sustainable Water Resources Management,* 2**,** 419-430.

KUMAR, R. & ANBALAGAN, R. 2015. Landslide susceptibility zonation in part of Tehri reservoir region using frequency ratio, fuzzy logic and GIS. *Journal of Earth System Science,* 124**,** 431-448.

LAMICHHANE & SHAKYA 2019a. Integrated Assessment of Climate Change and Land Use Change Impacts on Hydrology in the Kathmandu Valley Watershed, Central Nepal. *Water,* 11.

LAMICHHANE, S. & SHAKYA, N. M. 2019b. Alteration of groundwater recharge areas due to land use/cover change in Kathmandu Valley, Nepal. *Journal of Hydrology: Regional Studies,* 26.

LEE, S., HYUN, Y. & LEE, M.-J. 2019. Groundwater Potential Mapping Using Data Mining Models of Big Data Analysis in Goyang-si, South Korea. *Sustainability,* 11.

LI, B., LIU, X. & LI, Z. 2015. Using the STIRPAT model to explore the factors driving regional CO2 emissions: a case of Tianjin, China. *Natural Hazards,* 76**,** 1667-1685.

LI, M., FINLAYSON, B., WEBBER, M., BARNETT, J., WEBBER, S., ROGERS, S., CHEN, Z., WEI, T., CHEN, J., WU, X. & WANG, M. 2017. Estimating urban water demand under conditions of rapid growth: the case of Shanghai. *Regional Environmental Change,* 17**,** 1153-1161.

LI, T., LÓPEZ VALENCIA, O. M., JOHANSEN, K. & MCCABE, M. F. 2023. A Retrospective Analysis of National-Scale Agricultural Development in Saudi Arabia from 1990 to 2021. *Remote Sensing,* 15.

LIANG, X., GONG, Q., ZHENG, H. & XU, J. 2020. Examining the impact factors of the water environment using the extended STIRPAT model: A Case Study in Sichuan. *Environ Sci Pollut Res Int,* 27**,** 12942-12952.

LIN, B. & LI, Z. 2020. Spatial analysis of mainland cities' carbon emissions of and around Guangdong-Hong Kong-Macao Greater Bay area. *Sustainable Cities and Society,* 61.

LIU, X., YANG, X. & GUO, R. 2020. Regional Differences in Fossil Energy-Related Carbon Emissions in China's Eight Economic Regions: Based on the Theil Index and PLS-VIP Method. *Sustainability,* 12.

LLAMAS, M. R., MARTINEZ-SANTOS, P. & HERA, A. D. L. 2006. The Manifold Dimensions of Groundwater Sustainability: An Overview. *The global importance of groundwater in the 21st century : proceedings of the International Symposium on Groundwater Sustainability.* Alicante, Spain.

LOPEZ-RUIZ, H., BLAZQUEZ, J. & HASANOV, F. 2019. Estimating Saudi Arabia's Regional GDP Using Satellite Nighttime Light Images. The King Abdullah Petroleum Studies and Research Center (KAPSARC).

MA, M., PAN, T. & MA, Z. 2017. Examining the Driving Factors of Chinese Commercial Building Energy Consumption from 2000 to 2015: A STIRPAT Model Approach. *Journal of Engineering Science and Technology Review,* 10**,** 28-38.

MAHMOUD, S. H. & ALAZBA, A. A. 2016a. A coupled remote sensing and the Surface Energy Balance based algorithms to estimate actual evapotranspiration over the western and southern regions of Saudi Arabia. *Journal of Asian Earth Sciences,* 124**,** 269-283.

MAHMOUD, S. H. & ALAZBA, A. A. 2016b. Integrated remote sensing and GIS-based approach for deciphering groundwater potential zones in the central region of Saudi Arabia. *Environmental Earth Sciences,* 75.

MAHMOUD, S. H. & GAN, T. Y. 2019. Irrigation water management in arid regions of Middle East: Assessing spatio-temporal variation of actual evapotranspiration through remote sensing techniques and meteorological data. *Agricultural Water Management,* 212**,** 35-47.

MAITRA, S. & YAN, J. 2008. Principle Component Analysis and Partial Least Squares: Two Dimension Reduction Techniques for Regression. *Casualty Actuarial Society Discussion Paper Program***,** 79-90.

MAJEED, M. T., KHAN, S. & TAHIR, T. 2020. Analytical tool for unpacking the driving forces of environmental impact: an IPAT analysis of Pakistan. *GeoJournal*.

MALIEHE, M. & MULUNGU, D. M. M. 2017. Assessment of water availability for competing uses using SWAT and WEAP in South Phuthiatsana catchment, Lesotho. *Physics and Chemistry of the Earth, Parts A/B/C,* 100**,** 305-316.

MALLICK, J., KHAN, R. A., AHMED, M., ALQADHI, S. D., ALSUBIH, M., FALQI, I. & HASAN, M. A. 2019. Modeling Groundwater Potential Zone in a Semi-Arid Region of Aseer Using Fuzzy-AHP and Geoinformation Techniques. *Water,* 11.

MANAP, M. A., NAMPAK, H., PRADHAN, B., LEE, S., SULAIMAN, W. N. A. & RAMLI, M. F. 2012. Application of probabilistic-based frequency ratio model in groundwater potential mapping using remote sensing data and GIS. *Arabian Journal of Geosciences,* 7**,** 711-724.

MANSOURI, R. W., AL-SHAIBANI, A. M., MAKKAWI, M. H. & TAWABINI, B. S. 2022. Groundwater quality assessment of northern Harrat Rahat Aquifer, Saudi Arabia. *Hydrogeology Journal*.

MARGAT, J. & VAN DER GUN, J. 2013. *Groundwater around the world: a geographic synopsis*, Crc Press,https://doi.org/10.1111/gwat.12072.
MATABADAL, A. 2012. Country report SAUDI ARABIA. Economic Research Department.
MAW 1984. Water Atlas of Saudi Arabia. . Riyadh, Saudi Arabia.: Ministry of Agriculture and Water.
MAW 1985. Soil Atlas of Saudi Arabia. Riyadh, Saudi Arabia.: Ministry of Agriculture and Water.
MAZZONI, A., HEGGY, E. & SCABBIA, G. 2018. Forecasting water budget deficits and groundwater depletion in the main fossil aquifer systems in North Africa and the Arabian Peninsula. *Global Environmental Change,* 53**,** 157-173.
MCCI 2017. Features of Al-Madinah region. Al-Madinah Chamber of Commerce & Industry.
MCDONALD, R. I., GREEN, P., BALK, D., FEKETE, B. M., REVENGA, C., TODD, M. & MONTGOMERY, M. 2011. Urban growth, climate change, and freshwater availability. *Proc Natl Acad Sci U S A,* 108**,** 6312-7.
MCKEE, T. B., DOESKEN, N. J. & KLEIST, J. 1993. The relationship of drought frequency and duration to time scales. *8th Conference on Applied Climatology.* Anaheim.
MCSWEENEY, C. F., JONES, R. G., LEE, R. W. & ROWELL, D. P. 2014. Selecting CMIP5 GCMs for downscaling over multiple regions. *Climate Dynamics,* 44**,** 3237-3260.
MEDASANI, S., KIM U, J. & KRISHNAPURAM, R. 1998. An overview of membership function generation techniques for pattern recognition. *International Journal of Approximate Reasoning***,** 391-417.
MEIMR 2018. Saudi Arabia's first BUR prepared, submitted to UNFCCC the United Nations Framework Convention on Climate Change: Ministry of Energy, Industry and Mineral Resources Saudi Arabia.
MENDEZ, K. M., BROADHURST, D. I. & REINKE, S. N. 2020. Migrating from partial least squares discriminant analysis to artificial neural networks: a comparison of functionally equivalent visualisation and feature contribution tools using jupyter notebooks. *Metabolomics,* 16**,** 17.
MENEZES, M. D. D., OWENS, P. R., SILVA, S. H. G. & CURI, N. 2013. digital soil mapping approach based on fuzzy logic and field expert knowledge. *Ciênc. agrotec., Lavras***,** 287 - 298.
MENNIS, J. & GUO, D. 2009. Spatial data mining and geographic knowledge discovery—An introduction. *Computers, Environment and Urban Systems,* 33**,** 403-408.
MEP 2014. Ninth Development Plan -Water And Sanitation. Ministry of Economy and Planning.
METWALY, M., ABDALLA, F. & TAHA, A. I. 2021. Hydrogeophysical Study of Sub-Basaltic Alluvial Aquifer in the Southern Part of Al-Madinah Al-Munawarah, Saudi Arabia. *Sustainability,* 13.
MEWA 2017a. Annual Report. Ministry of Environment ,Water and Agriculture of Saudi Arabia.
MEWA 2017b. National Agriculture Strategy and Executive Summary 2030. Ministry of Environment, Water and Agriculture. Saudi Arabia.
MEWA 2018a. Annual Report. Ministry of Environment ,Water and Agriculture of Saudi Arabia.
MEWA 2018b. National Water Strategy 2030. Ministry of Environment, Water and Agriculture. Saudi Arabia.
MEWA 2019. Annual Report. Ministry of Environment ,Water and Agriculture of Saudi Arabia.
MEWA. 2020. *General reports and indicators* [Online]. Ministry of Environment, Water and Agriculture. Saudi Arabia 2020 Available: https://www.mewa.gov.sa/ar/Pages/default.aspx [Accessed].
MEWA 2022. Daily Dams Report (2018_2021). Ministry of Environment ,Water and Agriculture of Saudi Arabia.
MEWA 2023. Well license issuing terms and conditions. Ministry of Environment ,Water and Agriculture of Saudi Arabia.
MEWA, M. O. E. W. A. A. 2021. Annual Report.

: Ministry of Environment ,Water and Agriculture of Saudi Arabia.
MIRAKI, S., ZANGANEH, S. H., CHAPI, K., SINGH, V. P., SHIRZADI, A., SHAHABI, H. & PHAM, B. T. 2018. Mapping Groundwater Potential Using a Novel Hybrid Intelligence Approach. *Water Resources Management,* 33**,** 281-302.

MIRONOVA, Y. N. 2018. Use of fuzzy sets in modeling of GIS objects. *International Conference Information Technologies in Business and Industry 2018.* Journal of Physics: Conference Series 1015.
MITCHELL, A. & MINAMI, M. 1999. *The ESRI guide to GIS analysis: geographic patterns & relationships*, ESRI, Inc.
MMDA, A.-M. R. D. A. 2020. Soil map. Al-Madinah Region Development Authority.
MODON 2016. Annual Report,MODON. The Saudi Authority for Industrial Cities and Technology Zones.
MODON 2017. Annual Report, MODON. The Saudi Authority for Industrial Cities and Technology Zones.
MODON 2019. Annual Report, MODON. The Saudi Authority for Industrial Cities and Technology Zones.
MOGAJI, K. A. & LIM, H. S. 2017. Application of a GIS-/remote sensing-based approach for predicting groundwater potential zones using a multi-criteria data mining methodology. *Environ Monit Assess,* 189**,** 321.
MOGHADDAM, D. D., REZAEI, M., POURGHASEMI, H. R., POURTAGHIE, Z. S. & PRADHAN, B. 2015. Groundwater spring potential mapping using bivariate statistical model and GIS in the Taleghan Watershed, Iran. *Arabian Journal of Geosciences,* 8**,** 913-929.
MOHAMED, M. M. & ELMAHDY, S. I. 2016. Fuzzy logic and multi-criteria methods for groundwater potentiality mapping at Al Fo'ah area, the United Arab Emirates (UAE): an integrated approach. *Geocarto International,* 32**,** 1120-1138.
MOHAMMADY, M., MORADI, H. R., ZEINIVAND, H. & TEMME, A. J. A. M. 2014. A comparison of supervised, unsupervised and synthetic land use classification methods in the north of Iran. *International Journal of Environmental Science and Technology,* 12**,** 1515-1526.
MOHAMMED, W. E. & ALGARNI, S. 2020. A remote sensing study of spatiotemporal variations in drought conditions in northern Asir, Saudi Arabia. *Environmental Monitoring and Assessment,* 192.
MOMRA 2016. MADINA CPI PROFILE. Ministry of Municipal and Rural Affairs in the Kingdom of Saudi Arabia.
MOMRA 2020. The proposed land uses for Al-Madinah project. the Ministry of Municipal and Rural Affairs.
MOORE, I. D., GRAYSON, R. B. & LADSON, A. R. 1991. Digital terrain modelling: a review of hydrological, geomorphological, and biological applications. *Hydrological processes,* 5**,** 3-30.
MOORE, J. M. 1979. Primary and secondary faulting in the Najd fault system, Kingdom of Saudi Arabia.
MORRISON, A. M. 2005. Receiver operating characteristic (ROC) curve preparation: A tutorial. *Report ENQUAD 2005-20.* Boston, Massachusetts Water Resources Authority.
MUHAMEDYEV , R. 2015. Machine learning methods An overview. *Computer Modeling and New Technologies,* 19**,** 14-29.
MWE 2012. NOMINATION OF Ministry of Water & Electricity Kingdom of Saudi Arabia. King Hassan II Great World Water Prize.
MWE 2013. Water Consumption and Number of Subscribers, by city.: Ministry of Water and Electricity.
MWE. 2014. *Annual report 2014* [Online]. Ministry of Water and Electricity Kingdom of Saudi Arabia. Available: https://www.mewa.gov.sa/ar/InformationCenter/DocsCenter/YearlyReport/Pages/default.aspx [Accessed 2021].
MWE 2015. Annual report 2015. Ministry of Water and Electricity Kingdom of Saudi Arabia.
NADZRI, I. F. M., KHALID, N., WAHAB, W. A. & HASHIM, N. Analyzing the Effectiveness of Support Vector Machine and Random Forest Classifiers in Delineating the Green Area. IOP Conference Series: Earth and Environmental Science, 2023. IOP Publishing, 012032.
NAGHIBI, S. A., AHMADI, K. & DANESHI, A. 2017a. Application of Support Vector Machine, Random Forest, and Genetic Algorithm Optimized Random Forest Models in Groundwater Potential Mapping. *Water Resources Management,* 31**,** 2761-2775.

NAGHIBI, S. A. & DASHTPAGERDI, M. M. 2017. Evaluation of four supervised learning methods for groundwater spring potential mapping in Khalkhal region (Iran) using GIS-based features. *Hydrogeology Journal,* 25**,** 169-189.

NAGHIBI, S. A., MOGHADDAM, D. D., KALANTAR, B., PRADHAN, B. & KISI, O. 2017b. A comparative assessment of GIS-based data mining models and a novel ensemble model in groundwater well potential mapping. *Journal of Hydrology,* 548**,** 471-483.

NAGHIBI, S. A. & POURGHASEMI, H. R. 2015. A Comparative Assessment Between Three Machine Learning Models and Their Performance Comparison by Bivariate and Multivariate Statistical Methods in Groundwater Potential Mapping. *Water Resources Management,* 29**,** 5217-5236.

NAGHIBI, S. A., POURGHASEMI, H. R. & ABBASPOUR, K. 2017c. A comparison between ten advanced and soft computing models for groundwater qanat potential assessment in Iran using R and GIS. *Theoretical and Applied Climatology,* 131**,** 967-984.

NAGHIBI, S. A., POURGHASEMI, H. R. & DIXON, B. 2015. GIS-based groundwater potential mapping using boosted regression tree, classification and regression tree, and random forest machine learning models in Iran. *Environ Monit Assess,* 188**,** 44.

NAHHAS, R. 2023. Introduction to Regression Methods for Public Health Using R. Hentet fra https://bookdown. org/rwnahhas/RMPH.

NAMPAK, H., PRADHAN, B. & MANAP, M. A. 2014. Application of GIS based data driven evidential belief function model to predict groundwater potential zonation. *Journal of Hydrology,* 513**,** 283-300.

NASIR, M. J., KHAN, S., ZAHID, H. & KHAN, A. 2018. Delineation of groundwater potential zones using GIS and multi influence factor (MIF) techniques: a study of district Swat, Khyber Pakhtunkhwa, Pakistan. *Environmental Earth Sciences,* 77.

NATIONS, U. 2015. Climate Projections and Extreme Climate Indices for the Arab Region.

NAVANE, V. S. & SAHOO, S. N. 2017. A review of integrated RS and GIS technique in groundwater potential zone mapping. *Hydro- International, L.D***,** 1-10.

NCM. 2019. *Drought Status Analysis* [Online]. The National Centre of meteorology in Saudi Arabia. Available: https://ncm.gov.sa/Ar/Climate/DroughtMonitoring/Pages/Drought-situational-Analysis.aspx [Accessed].

NEGNEVITSKY, M. 2005. *Artificial Intelligence: A Guide to Intelligent Systems,* Harlow, England ; New York, Addison-Wesley.

NITHYA, C. N., SRINIVAS, Y., MAGESH, N. S. & KALIRAJ, S. 2019. Assessment of groundwater potential zones in Chittar basin, Southern India using GIS based AHP technique. *Remote Sensing Applications: Society and Environment,* 15.

NIYAZI, B. A., AHMED, M., MASOUD, M. Z., RASHED, M. A. & BASAHI, J. M. 2019. Sustainable and resilient management scenarios for groundwater resources of the Red Sea coastal aquifers. *Sci Total Environ,* 690**,** 1310-1320.

NOLAN, B. T., FIENEN, M. N. & LORENZ, D. L. 2015. A statistical learning framework for groundwater nitrate models of the Central Valley, California, USA. *Journal of Hydrology,* 531**,** 902-911.

NURFADILA, J. S., BAJA, S., NESWATI, R., RUKMANA, D. & ZYLSHAL4, Z. 2019. Initial Results on Landuse/Landcover Classification Using Pixel-Based Random Forest Algorithm on Sentinel-2 Imagery over Enrekang Region. *The 4th International Conference of Indonesian Society for Remote Sensing.* IOP Conf. Series: Earth and Environmental Science 280 (2019) 012036.

NWC. 2015. *The new water tariff* [Online]. National Water Company, Saudi Arabia Available: https://www.nwc.com.sa/Arabic/Pages/NewTarrifCalculator.aspx [Accessed 2021].

NYIMBILI, P. H. & ERDEN, T. A combined model of GIS and Fuzzy Logic evaluation for locating emergency facilities: a case study of Istanbul. 8th International Conference on Cartography and GIS, 2020. Eds: Bandrova T., Konečný M., Marinova S.

O'NEILL, B. C., TEBALDI, C., VAN VUUREN, D. P., EYRING, V., FRIEDLINGSTEIN, P., HURTT, G., KNUTTI, R., KRIEGLER, E., LAMARQUE, J.-F., LOWE, J., MEEHL, G. A., MOSS, R., RIAHI, K. & SANDERSON, B. M. 2016. The Scenario Model Intercomparison Project (ScenarioMIP) for CMIP6. *Geoscientific Model Development,* 9**,** 3461-3482.

O'NEILL, B. C., CARTER, T. R., EBI, K., HARRISON, P. A., KEMP-BENEDICT, E., KOK, K., KRIEGLER, E., PRESTON, B. L., RIAHI, K., SILLMANN, J., VAN RUIJVEN, B. J., VAN VUUREN, D., CARLISLE, D., CONDE, C., FUGLESTVEDT, J., GREEN, C., HASEGAWA, T., LEININGER, J., MONTEITH, S. & PICHS-MADRUGA, R. 2020. Achievements and needs for the climate change scenario framework. *Nature Climate Change,* 10**,** 1074-1084.

O'NEILL, B. C., KRIEGLER, E., EBI, K. L., KEMP-BENEDICT, E., RIAHI, K., ROTHMAN, D. S., VAN RUIJVEN, B. J., VAN VUUREN, D. P., BIRKMANN, J., KOK, K., LEVY, M. & SOLECKI, W. 2017. The roads ahead: Narratives for shared socioeconomic pathways describing world futures in the 21st century. *Global Environmental Change,* 42**,** 169-180.

O'NEILL, B. C., KRIEGLER, E., RIAHI, K., EBI, K. L., HALLEGATTE, S., CARTER, T. R., MATHUR, R. & VAN VUUREN, D. P. 2013. A new scenario framework for climate change research: the concept of shared socioeconomic pathways. *Climatic Change,* 122**,** 387-400.

ODHIAMBO, G. O. 2016. Water scarcity in the Arabian Peninsula and socio-economic implications. *Applied Water Science,* 7**,** 2479-2492.

OGUZTIMUR, S. 2011. Why approach the fuzzy hierarchical analytical process to transportation problems? *European Regional Science Association.*

OH, H.-J., AHN, S.-C., CHOI, J.-K. & LEE, S. 2010. Sensitivity analysis for the GIS-based mapping of the ground subsidence hazard near abandoned underground coal mines. *Environmental Earth Sciences,* 64**,** 347-358.

OH, H.-J., KIM, Y.-S., CHOI, J.-K., PARK, E. & LEE, S. 2011. GIS mapping of regional probabilistic groundwater potential in the area of Pohang City, Korea. *Journal of Hydrology,* 399**,** 158-172.

OLADIPUPO, T. 2010. Types of Machine Learning Algorithms. *New Advances in Machine Learning.* 10.5772/9385.

OSBORNE, J. W. 2019. Bringing balance and technical accuracy to reporting odds ratios and the results of logistic regression analyses. *Practical Assessment, Research, and Evaluation,* 11.

OUDA, O. K. M. 2013. Water demand versus supply in Saudi Arabia: current and future challenges. *International Journal of Water Resources Development,* 30**,** 335-344.

OZDEMIR, A. 2011a. GIS-based groundwater spring potential mapping in the Sultan Mountains (Konya, Turkey) using frequency ratio, weights of evidence and logistic regression methods and their comparison. *Journal of Hydrology,* 411**,** 290-308.

OZDEMIR, A. 2011b. Using a binary logistic regression method and GIS for evaluating and mapping the groundwater spring potential in the Sultan Mountains (Aksehir, Turkey). *Journal of Hydrology,* 405**,** 123-136.

OZDEMIR, A. & ALTURAL, T. 2013. A comparative study of frequency ratio, weights of evidence and logistic regression methods for landslide susceptibility mapping: Sultan Mountains, SW Turkey. *Journal of Asian Earth Sciences,* 64**,** 180-197.

PANDE, C. B., MOHARIR, K. N., KHADRI, S. F. R. & PATIL, S. 2018. Study of land use classification in an arid region using multispectral satellite images. *Applied Water Science,* 8.

PARIZI, E., HOSSEINI, S. M., ATAIE-ASHTIANI, B. & SIMMONS, C. T. 2020. Normalized difference vegetation index as the dominant predicting factor of groundwater recharge in phreatic aquifers: case studies across Iran. *Sci Rep,* 10**,** 17473.

PARK, S., HAMM, S.-Y., JEON, H.-T. & KIM, J. 2017. Evaluation of Logistic Regression and Multivariate Adaptive Regression Spline Models for Groundwater Potential Mapping Using R and GIS. *Sustainability,* 9.

PEI, Z., FANG, S., WANG, L. & YANG, W. 2020. Comparative Analysis of Drought Indicated by the SPI and SPEI at Various Timescales in Inner Mongolia, China. *Water,* 12.

PINTO, D., SHRESTHA, S., BABEL, M. S. & NINSAWAT, S. 2015. Delineation of groundwater potential zones in the Comoro watershed, Timor Leste using GIS, remote sensing and analytic hierarchy process (AHP) technique. *Applied Water Science,* 7**,** 503-519.

PORTMANN, F. T., DÖLL, P., EISNER, S. & FLÖRKE, M. 2013. Impact of climate change on renewable groundwater resources: assessing the benefits of avoided greenhouse gas emissions using selected CMIP5 climate projections. *Environmental Research Letters,* 8**,** 024023.

POURGHASEMI, H. R. & BEHESHTIRAD, M. 2014. Assessment of a data-driven evidential belief function model and GIS for groundwater potential mapping in the Koohrang Watershed, Iran. *Geocarto International,* 30**,** 662-685.

POURTAGHI, Z. S. & POURGHASEMI, H. R. 2014. GIS-based groundwater spring potential assessment and mapping in the Birjand Township, southern Khorasan Province, Iran. *Hydrogeology Journal,* 22**,** 643-662.

POWERS, R., RAMIREZ, L., REDMOND, C. & ELBERG, E. 1966. Geology of the Arabian Peninsula—Sedimentary Geology of Saudi Arabia: USG Survey Professional Paper, 560-D. Washington.

PRADHAN, A. M. S. & KIM, Y.-T. 2014. Relative effect method of landslide susceptibility zonation in weathered granite soil: a case study in Deokjeok-ri Creek, South Korea. *Natural Hazards,* 72**,** 1189-1217.

QAISRANI, Z. N., NUTHAMMACHOT, N., TECHATO, K. & ASADULLAH 2021. Drought monitoring based on Standardized Precipitation Index and Standardized Precipitation Evapotranspiration Index in the arid zone of Balochistan province, Pakistan. *Arabian Journal of Geosciences,* 14.

QI, C. & CHANG, N. B. 2011. System dynamics modeling for municipal water demand estimation in an urban region under uncertain economic impacts. *J Environ Manage,* 92**,** 1628-41.

QIN, J., TAO, H., ZHAN, M., MUNIR, Q., BRINDHA, K. & MU, G. 2019. Scenario Analysis of Carbon Emissions in the Energy Base, Xinjiang Autonomous Region, China. *Sustainability,* 11.

QUÉFÉLEC, S. & ALLAL, S. 2014. Development, water and energy in the context of climate change in North Africa. *Regional Environmental Change,* 15**,** 1611-1625.

RAHMATI, O., NAGHIBI, S. A., SHAHABI, H., BUI, D. T., PRADHAN, B., AZAREH, A., RAFIEI-SARDOOI, E., SAMANI, A. N. & MELESSE, A. M. 2018. Groundwater spring potential modelling: Comprising the capability and robustness of three different modeling approaches. *Journal of Hydrology,* 565**,** 248-261.

RAHMATI, O., NAZARI SAMANI, A., MAHDAVI, M., POURGHASEMI, H. R. & ZEINIVAND, H. 2014. Groundwater potential mapping at Kurdistan region of Iran using analytic hierarchy process and GIS. *Arabian Journal of Geosciences,* 8**,** 7059-7071.

RAHMATI, O., POURGHASEMI, H. R. & MELESSE, A. M. 2016. Application of GIS-based data driven random forest and maximum entropy models for groundwater potential mapping: A case study at Mehran Region, Iran. *Catena,* 137**,** 360-372.

RAJASEKHAR, M., SUDARSANA RAJU, G., SREENIVASULU, Y. & SIDDI RAJU, R. 2019. Delineation of groundwater potential zones in semi-arid region of Jilledubanderu river basin, Anantapur District, Andhra Pradesh, India using fuzzy logic, AHP and integrated fuzzy-AHP approaches. *HydroResearch,* 2**,** 97-108.

RAVILIOUS, C., DE LAMO, X., JUFFE BIGNOLI, D., SALVATERRA, T., MCDERMOTT LONG, O., ARNELL, A., GOSLING, J. & MILES, L. 2020. How to Present Complex Data on Maps and other Visuals for Effective Policy Communication: Using visual tools and spatial information to support decisions for REDD+ implementation. *Prepared on behalf of the UN-REDD Programme. UN Environment Programme World Conservation Monitoring Centre, Cambridge, UK*.

RAZAK, M., AHMAD, I., BUJANG, I., TALIB, A. H. & IBRAHIM, Z. 2013. IPAT-fuzzy model in measuring air pollution: evidence from Malaysia. *American International Journal of Contemporary Research,* 3**,** 62-69.

RAZANDI, Y., POURGHASEMI, H. R., NEISANI, N. S. & RAHMATI, O. 2015. Application of analytical hierarchy process, frequency ratio, and certainty factor models for groundwater potential mapping using GIS. *Earth Science Informatics,* 8**,** 867-883.

RAZAVI-TERMEH, S. V., SADEGHI-NIARAKI, A. & CHOI, S.-M. 2019. Groundwater Potential Mapping Using an Integrated Ensemble of Three Bivariate Statistical Models with Random Forest and Logistic Model Tree Models. *Water,* 11.

REGMI, A. D., DEVKOTA, K. C., YOSHIDA, K., PRADHAN, B., POURGHASEMI, H. R., KUMAMOTO, T. & AKGUN, A. 2013. Application of frequency ratio, statistical index, and weights-of-evidence models and their comparison in landslide susceptibility mapping in Central Nepal Himalaya. *Arabian Journal of Geosciences,* 7**,** 725-742.

REJAUR RAHMAN, M. & SAHA, S. K. 2008. Multi-resolution segmentation for object-based classification and accuracy assessment of land use/land cover classification using remotely sensed data. *Journal of the Indian Society of Remote Sensing,* 36**,** 189-201.

RIAHI, K., VAN VUUREN, D. P., KRIEGLER, E., EDMONDS, J., O'NEILL, B. C., FUJIMORI, S., BAUER, N., CALVIN, K., DELLINK, R., FRICKO, O., LUTZ, W., POPP, A., CUARESMA, J. C., KC, S., LEIMBACH, M., JIANG, L., KRAM, T., RAO, S., EMMERLING, J., EBI, K., HASEGAWA, T., HAVLIK, P., HUMPENÖDER, F., DA SILVA, L. A., SMITH, S., STEHFEST, E., BOSETTI, V., EOM, J., GERNAAT, D., MASUI, T., ROGELJ, J., STREFLER, J., DROUET, L., KREY, V., LUDERER, G., HARMSEN, M., TAKAHASHI, K., BAUMSTARK, L., DOELMAN, J. C., KAINUMA, M., KLIMONT, Z., MARANGONI, G., LOTZE-CAMPEN, H., OBERSTEINER, M., TABEAU, A. & TAVONI, M. 2017. The Shared Socioeconomic Pathways and their energy, land use, and greenhouse gas emissions implications: An overview. *Global Environmental Change,* 42**,** 153-168.

ROY, A., KEESARI, T., SINHA, U. K. & SABARATHINAM, C. 2019. Delineating groundwater prospect zones in a region with extreme climatic conditions using GIS and remote sensing techniques: A case study from central India. *Journal of Earth System Science,* 128.

ROY, J. & SAHA, D. S. 2019. GIS-based Gully Erosion Susceptibility Evaluation Using Frequency Ratio, Cosine Amplitude and Logistic Regression Ensembled with fuzzy logic in Hinglo River Basin, India. *Remote Sensing Applications: Society and Environment,* 15.

ROY, P. K., BASAK, S. K., MOHINUDDIN, S., ROY, M. B., HALDER, S. & GHOSH, T. 2022. Modelling groundwater potential zone using fuzzy logic and geospatial technology of an deltaic island. *Modeling Earth Systems and Environment*.

RWANGA, S. S. & NDAMBUKI, J. M. 2017. Accuracy Assessment of Land Use/Land Cover Classification Using Remote Sensing and GIS. *International Journal of Geosciences,* 08**,** 611-622.

S. DHIMAN, H. & DEB, D. 2020. Multi-criteria Decision-Making: An Overview. *Decision and Control in Hybrid Wind Farms.* Singapore: Springer Singapore,10.1007/978-981-15-0275-0_2.

SADOLLAH, A. 2018. Introductory Chapter: Which Membership Function is Appropriate in Fuzzy System? *Fuzzy Logic Based in Optimization Methods and Control Systems and its Applications.* 10.5772/intechopen.79552.

SAGIA 2019. Saudi Arabia's Economic Cities. Economic Cities Agency, Saudi Arabian General Investment Authority

SAHANA, M. & PATEL, P. P. 2019. A comparison of frequency ratio and fuzzy logic models for flood susceptibility assessment of the lower Kosi River Basin in India. *Environmental Earth Sciences,* 78.

SAHOO, S., MUNUSAMY, S. B., DHAR, A., KAR, A. & RAM, P. 2017. Appraising the Accuracy of Multi-Class Frequency Ratio and Weights of Evidence Method for Delineation of Regional Groundwater Potential Zones in Canal Command System. *Water Resources Management,* 31**,** 4399-4413.

SAMA 2020. Gross Domestic Product - Annual Growth Rate. The Saudi Central Bank.

SEC, S. E. C. 2021. Environmental, Social and Governance (ESG) Report.

SEEYAN, S., MERKEL, B. & ABO, R. 2014. Investigation of the Relationship between Groundwater Level Fluctuation and Vegetation Cover by using NDVI for Shaqlawa Basin, Kurdistan Region – Iraq. *Journal of Geography and Geology,* 6.

SELVAM, S., MAGESH, N. S., SIVASUBRAMANIAN, P., SOUNDRANAYAGAM, J. P., MANIMARAN, G. & SESHUNARAYANA, T. 2014. Deciphering of Groundwater Potential Zones in Tuticorin, Tamil Nadu, Using Remote Sensing and GIS Techniques. *Journal Geological Society of India,* 84**,** 597–608.

SGS, S. G. S. 2017a. *Geological map of the Al-Madinah*.

SGS, S. G. S. 2017b. *Lithological units map*.

SGS, S. G. S. 2018. *Phanerozoic geology of Saudi Arabia* [Online]. Available: https://sgs.gov.sa/en [Accessed 15 NOV 2020].

SHAWUL, A. A., CHAKMA, S. & MELESSE, A. M. 2019. The response of water balance components to land cover change based on hydrologic modeling and partial least squares regression (PLSR) analysis in the Upper Awash Basin. *Journal of Hydrology: Regional Studies,* 26.

SHIMPI, S., ROKADE, V. M. & UPASANI, K. 2019. Application of Remote Sensing and GIS for Groundwater Potential Zonation: A Case Study of Bori-Chikli Watershed, Maharashtra, India. *Bulletin of Pure & Applied Sciences- Geology,* 38f.

SHRESTHA, S., BACH, T. V. & PANDEY, V. P. 2016. Climate change impacts on groundwater resources in Mekong Delta under representative concentration pathways (RCPs) scenarios. *Environmental Science & Policy,* 61**,** 1-13.

SIEBER, J. & PURKEY, D. 2015. *USER GUIDE for WEAP*, Stockholm Environment Institute, U.S. Center.

SMITH, M., CROSS, K., PADEN, M. & LABAN, P. 2016. *Spring Managing groundwater sustainably,* Gland, Switzerland, IUCN,http://dx.doi.org/10.2305/IUCN.CH.2016.WANI.8.en.

SMITHSON, M. & VERKUILEN, J. 2006. An overview of fuzzy set mathematics. In Fuzzy set theory. Thousand Oaks, California: SAGE Publications, Inc.

SOOFI, A. & AWAN, A. 2017. Classification Techniques in Machine Learning: Applications and Issues. *Journal of Basic & Applied Sciences,* 13**,** 459-465.

SØRENSEN, R., ZINKO, U. & SEIBERT, J. 2005. On the calculation of the topographic wetness index: evaluation of different methods based on field observations. *Hydrology and Earth System Sciences***,** 101–112.

SPENCER, M. 2013a. Extraterrestrial radiation dataset. *scottishsnow* [Online]. Available from: https://scottishsnow.wordpress.com/2013/05/20/ext-radiation/.

SPENCER, M. 2013b. GB potential evapotranspiration dataset. *scottishsnow* [Online]. Available from: https://scottishsnow.wordpress.com/2013/07/11/gb-pe/.

SRIVASTAVA, V., SRIVASTAVA, H. B. & LAKHERA, R. C. 2010. Fuzzy gamma based geomatic modelling for landslide hazard susceptibility in a part of Tons river valley, northwest Himalaya, India. *Geomatics, Natural Hazards and Risk,* 1**,** 225-242.

STORYLINES, S. 2018. Supplementary note for the SSP data sets.

STRAHLER, A. N. 1967. Quantitative analysis of watershed geomorphology. *Transactions,, American Geophysical Union,* 38**,** 913–920.

SUBYANI, A. M. & AL-AHMADI, F. S. 2011. Rainfall-runoff modeling in the Al-Madinah area of western Saudi Arabia. *Journal of environmental hydrology* 19.

SUI, D. Z. 1992. A fuzzy GIS modeling approach for urban land evaluation. *Cow., Environ. and Urban Systems,* 16**,** 101-115.

SULTAN, M., SEFRY, S. & ABUABDALLAH, M. 2015. Impacts of Climate Change on the Red Sea Region and its Watersheds, Saudi Arabia. *The Red Sea.* 10.1007/978-3-662-45201-1_22.

SWCC 2014. Anuual Report

SWCC 2019. Quantity of Water Desalinated, by Desalination plants (2007- 2018). Saline Water Conversion Corporation

SWPC 2019. SWPC 7 year statement - 2019 - 2025. Saudi Water Partnership Company.

SWPC 2020. SWPC-7-Year-planning Statement-2020-2026. Saudi Water Partnership Company.

TAHMASSEBIPOOR, N., RAHMATI, O., NOORMOHAMADI, F. & LEE, S. 2015. Spatial analysis of groundwater potential using weights-of-evidence and evidential belief function models and remote sensing. *Arabian Journal of Geosciences,* 9.

TALPUR, N., SALLEH, M. N. M. & HUSSAIN, K. 2017. An investigation of membership functions on performance of ANFIS for solving classification problems. *Materials Science and Engineering 226.* International Research and Innovation Summit.

TALUKDAR, S., SINGHA, P., MAHATO, S., SHAHFAHAD, PAL, S., LIOU, Y.-A. & RAHMAN, A. 2020. Land-Use Land-Cover Classification by Machine Learning Classifiers for Satellite Observations—A Review. *Remote Sensing,* 12.

TARAWNEH, Q. & CHOWDHURY, S. 2018. Trends of Climate Change in Saudi Arabia: Implications on Water Resources. *Climate,* 6.

THANH NOI, P. & KAPPAS, M. 2017. Comparison of Random Forest, k-Nearest Neighbor, and Support Vector Machine Classifiers for Land Cover Classification Using Sentinel-2 Imagery. *Sensors (Basel),* 18.

TIEN BUI, D., SHIRZADI, A., CHAPI, K., SHAHABI, H., PRADHAN, B., PHAM, B., SINGH, V., CHEN, W., KHOSRAVI, K., BIN AHMAD, B. & LEE, S. 2019. A Hybrid Computational Intelligence Approach to Groundwater Spring Potential Mapping. *Water,* 11.

TOBIAS, R. An Introduction to Partial Least Squares Regression. 1996.

UDDIN, A. S. M. S., KHAN, N., ISLAM, A. R. M. T., KAMRUZZAMAN, M. & SHAHID, S. 2021. Changes in urbanization and urban heat island effect in Dhaka city. *Theoretical and Applied Climatology,* 147**,** 891-907.

UDDIN, G. A., ALAM, K. & GOW, G. 2016. Estimating the Major Contributors to Environmental Impacts in Australia. *Ecological Economics and Statistics,* 37 (1)**,** 1-14.

UN-HABITAT. 2018. *Madinah CPI Profile* [Online]. Report jointly published by Future Saudi Cities Programmme, UN-Habitat Saudi Arabia, Ministry of Municipal and Rural Affairs. Available: https://unhabitat.org/cpi-profile-al-madinah-al-munawarah [Accessed 2021].

UN-HABITAT. 2019a. *Madinah City Profile* [Online]. Report jointly published by Future Saudi Cities Programmme, UN-Habitat Saudi Arabia, Ministry of Municipal and Rural Affairs. Available: https://unhabitat.org/sites/default/files/2020/04/madinah.pdf [Accessed 24/07 2020].

UN-HABITAT 2019b. Saudi Cities Report 2019. Nairobi, Kenya: United Nations.

UN 2018. Population Division (2018). United Nations, Department of Economic and Social Affairs, World Urbanization Prospects: The 2018 Revision.Online Edition.

UN 2019. World Population Prospects. United Nations.

UN 2022. The United Nations World Water Development Report 2022: Groundwater: Making the invisible visible. UNESCO, Paris.: UNESCO, Paris.

UNAL, I. 2017. Defining an optimal cut-point value in ROC analysis: an alternative approach. *Computational and mathematical methods in medicine,* 2017.

UNFCCC 2022. Updated first Nationally Determined Contribution (NDC),Saudi Arabia.

VAKHSHOORI, V. & ZARE, M. 2016. Landslide susceptibility mapping by comparing weight of evidence, fuzzy logic, and frequency ratio methods. *Geomatics, Natural Hazards and Risk,* 7**,** 1731-1752.

VALI, A., COMAI, S. & MATTEUCCI, M. 2020. Deep Learning for Land Use and Land Cover Classification Based on Hyperspectral and Multispectral Earth Observation Data: A Review. *Remote Sensing,* 12.

VAN DER GUN, J. 2012. Groundwater and global change: trends, opportunities and challenges.

VAN DER MENSBRUGGHE, D. 2015. Shared socio-economic pathways and global income distribution.

VÉLEZ-HENAO, J.-A., FONT VIVANCO, D. & HERNÁNDEZ-RIVEROS, J.-A. 2019. Technological change and the rebound effect in the STIRPAT model: A critical view. *Energy Policy,* 129**,** 1372-1381.

VELLIANGIRI, S., ALAGUMUTHUKRISHNAN, S. & JOSEPH.S., I. T. 2019. A Review of Dimensionality Reduction Techniques for Efficient Computation. *Procedia Computer Science.,* 165**,** 104-111.

VICENTE-SERRANO, S. M., BEGUERÍA, S. & LÓPEZ-MORENO, J. I. 2010. A Multiscalar Drought Index Sensitive to Global Warming: The Standardized Precipitation Evapotranspiration Index. *Journal of Climate,* 23**,** 1696-1718.

VIJITH, H. & DODGE-WAN, D. 2019. Modelling terrain erosion susceptibility of logged and regenerated forested region in northern Borneo through the Analytical Hierarchy Process (AHP) and GIS techniques. *Geoenvironmental Disasters,* 6.

VUJOVIC, S., HADDAD, B., KARAKY, H., SEBAIBI, N. & BOUTOUIL, M. 2021. Urban Heat Island: Causes, Consequences, and Mitigation Measures with Emphasis on Reflective and Permeable Pavements. *CivilEng,* 2**,** 459-484.

WADA, Y., FLÖRKE, M., HANASAKI, N., EISNER, S., FISCHER, G., TRAMBEREND, S., SATOH, Y., VAN VLIET, M. T. H., YILLIA, P., RINGLER, C., BUREK, P. & WIBERG, D. 2016. Modeling global water use for the 21st century: the Water Futures and Solutions (WFaS) initiative and its approaches. *Geoscientific Model Development,* 9**,** 175-222.

WANG, S., ZHAO, T., ZHENG, H. & HU, J. 2017a. The STIRPAT Analysis on Carbon Emission in Chinese Cities: An Asymmetric Laplace Distribution Mixture Model. *Sustainability,* 9.

WANG, X.-J., ZHANG, J.-Y., SHAHID, S., XIE, W., DU, C.-Y., SHANG, X.-C. & ZHANG, X. 2017b. Modeling domestic water demand in Huaihe River Basin of China under climate change and population dynamics. *Environment, Development and Sustainability,* 20**,** 911-924.

WORLD BANK 2016a. *High and dry: Climate change, water, and the economy*, The World Bank.
WORLD BANK. 2016b. *World development indicators* [Online]. Available: http://data.worldbank.org/country/saudiarabia [Accessed 19 February 2020].
WORLDCLIM. 2020. *Global climate and weather data* [Online]. Available: https://www.worldclim.org/data/index.html [Accessed 2020].
YAGOUB, M. M. & AL BIZREH, A. A. 2014. Prediction of Land Cover Change Using Markov and Cellular Automata Models: Case of Al-Ain, UAE, 1992-2030. *Journal of the Indian Society of Remote Sensing,* 42**,** 665-671.
YANG, S. & CUI, X. 2019. Building Regional Sustainable Development Scenarios with the SSP Framework. *Sustainability,* 11.
YORK, R., ROSA, E. A. & DIETZ, T. 2003. STIRPAT, IPAT and ImPACT: analytic tools for unpacking the driving forces of environmental impacts. *Ecological Economics,* 46**,** 351-365.
YOUSEFI, S., SADHASIVAM, N., POURGHASEMI, H. R., GHAFFARI NAZARLOU, H., GOLKAR, F., TAVANGAR, S. & SANTOSH, M. 2020. Groundwater spring potential assessment using new ensemble data mining techniques. *Measurement,* 157.
ZABIHI, M., POURGHASEMI, H. R., POURTAGHI, Z. S. & BEHZADFAR, M. 2016. GIS-based multivariate adaptive regression spline and random forest models for groundwater potential mapping in Iran. *Environmental Earth Sciences,* 75.
ZADEH, L. A. 1965. Fuzzy Sets. *Information and Control,* 8**,** 338--353.
ZADEH, L. A. 2008. Is there a need for fuzzy logic? *Information Sciences,* 178**,** 2751-2779.
ZAHARANI, K. H., AL-SHAYAA, M. S. & BAIG, M. B. 2011. Water Conservation in the Kingdom of Saudi Arabia for Better Environment: Implications for Extension and Education. *Bulgarian Journal of Agricultural Science,* 17**,** 389-395.
ZAIDI, F. K., NAZZAL, Y., AHMED, I., NAEEM, M. & JAFRI, M. K. 2015. Identification of potential artificial groundwater recharge zones in Northwestern Saudi Arabia using GIS and Boolean logic. *Journal of African Earth Sciences,* 111**,** 156-169.
ZAKARIA, MAJUMDER, A. K. & RAHMAN, M. 2016. Morphometric Analysis of Reju Khal Drainage Basin using Geographic Information System (GIS) and SRTM data. *International Journal of Scientific & Engineering Research,* 7.
ZHANG, L., NAN, Z., XU, Y. & LI, S. 2016. Hydrological Impacts of Land Use Change and Climate Variability in the Headwater Region of the Heihe River Basin, Northwest China. *PLoS One,* 11**,** e0158394.
ZHANG, X. M., HE, G. J., ZHANG, Z. M., PENG, Y. & LONG, T. F. 2017. Spectral-spatial multi-feature classification of remote sensing big data based on a random forest classifier for land cover mapping. *Cluster Computing,* 20**,** 2311-2321.
ZHAO, C., CHEN, B., HAYAT, T., ALSAEDI, A. & AHMAD, B. 2014. Driving force analysis of water footprint change based on extended STIRPAT model: Evidence from the Chinese agricultural sector. *Ecological Indicators,* 47**,** 43-49.
ZYOUD, S. H. & FUCHS-HANUSCH, D. 2016. Estimates of Arab world research productivity associated with groundwater: a bibliometric analysis. *Applied Water Science,* 7**,** 1255-1272.